Novel Thieno[3,4-*b*]pyrazine Based π-Conjugated Polymers For Optoelectronic Devices

Dissertation

Zur Erlangung des akademischen Grades
doctor rerum naturalium (Dr. rer. nat.)

vorgelegt dem Rat der Chemisch-Geowissenschaftlichen Fakultät
der Friedrich-Schiller-Universität Jena

von M.Sc. M.Phil Munazza Shahid
geboren am 26.01.1975 in Sargodha

Jena, August 2006

Gutachter:

1. Prof. Dr. E. Klemm

2. Prof. Dr. U. Scherf

Tag der öffentlichen Verteidigung: 25-10-2006

# Contents

1   Introduction

Conjugated polymers[1] have attracted considerable attention as a new class of electronic material, since the study of these systems has generated entirely new scientific concepts as well as potential for new technology. Conjugated polymers are organic semiconductors and as such important materials for applications in electronic and photonic devices. Prime examples are polymeric light-emitting diodes,[2] plastic lasers,[3] and polymer-based photovoltaic cells,[4] but at least in principle, conjugated polymers[5] should be able to pertain all of the functions an inorganic semiconductor displays, FETs,[6] and may lead in the future to "molecular electronics".[7] The primary advantage of organic polymers over their inorganic counterparts is their ease of processing by dip coating, spin casting, printing,[8] or use of doctor blade techniques. However, conjugated polymers are likewise important as sensory materials for water, organic vapors, and explosives either by fluorescence quenching or in artificial nose devices, which change their conductivity upon exposure to a suitable analyte.[9]

The goal with organics-based devices is not necessarily to attain or exceed the level of performance of inorganic semiconductor technologies (silicon is still the best at the many things that it does) but to benefit from a unique set of characteristics combining the electrical properties of (semi)conductors with the properties typical of plastics, that is, low cost, versatility of chemical synthesis, ease of processing, and flexibility. Interest in conjugated polymers picked up significantly after the 1976 discovery that they can be made highly electrically conducting following a redox chemical treatment.[10] This discovery led to the 2000 Nobel Prize in Chemistry awarded to Alan Heeger, Alan MacDiarmid, and Hideki Shirakawa. By the mid-eighties, many research teams in both academia and industry were investigating π-conjugated oligomers and polymers for their nonlinear optical properties or their semiconducting properties, paving the way to the emergence of the fields of plastic electronics and photonics.[1]

During the past 20 years these conjugated polymers have given rise to an enormous amount of experimental and theoretical work devoted to (i) the analysis of their structure and properties using a whole arsenal of physical techniques, (ii) the development of synthetic methods allowing a better control of their structure and electronic properties, (iii) the synthesis of functional polymers in which the electronic properties are associated with specific properties afforded by covalently attached prosthetic groups,[11-13] and (iv) the analysis of their multiple

technological applications extending from bulk utilizations such as antistatic coatings, energy storage, to highly sophisticated electronic, photonic, and bioelectronic devices.

The class of conjugated polymers which has found the most attention in the past is undoubtedly the poly(*p*-phenylenevinylene)s **(PPVs)** which "made it big" since Friend's 1990 report of organic polymeric LEDs.[2,14] Other well-established classes of conjugated polymers are the polydiacetylene **(PDA)**,[15] polyphenylene **(PPP)**,[16,17] and polyacetylene **(PA)**.[18]

PA   **PDA**   **PPV**   **PPP**   **PAE**
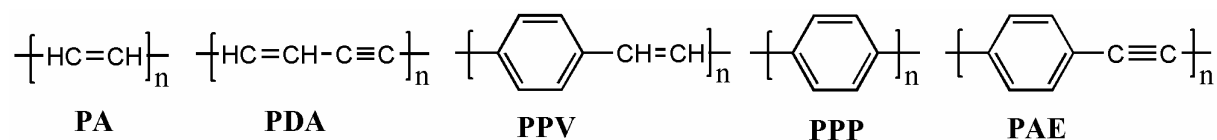
1.1   Motivation

The worldwide demand for energy has grown dramatically over the last century with an increase in the industrialization of the world. The need for energy is likely to grow even more in the 21st century with the improvements in living standards across the planet. This high demand of energy brings into question the energy sources currently used and the depletion of natural resources.

1.1.1   Fossil Fuels

Oil, coal, and natural gas are usually referred to as fossil fuels. The percentage of energy production that is from fossil fuels was more than 70 %. The combustion of fossil fuels is used to produce electric power and heat. The other renewable sources summarize geothermal, non-wood waste, solar, wind, wood and wood waste. The percent missing to add up to 100 % is due to rounding byproducts of this combustion process are carbon dioxide (CO_2) and sulfur compounds like SO_2. While the former is related to the greenhouse effect[19] leading to global warming and the rise in sea level, the latter is a cause of acid rain harming the environment. In addition to the catastrophic environmental consequences of using fossil fuels, the earth's resources of oil, coal, and natural gas are limited and will deplete sooner or later. Estimates suggest that within 20 years oil and natural gas production rates will start to decrease.[20,21] With these prospects, new sources of energy must be implemented that do not rely on depleting resources.

1.1.2   Renewable Energy

Renewable energy sources use natural resources without depleting them and with no harmful side effects for the environment. Examples include power plants that use wind energy; energy from water due to waves, tidal motion or potential energy (rivers); and solar energy. The energy provided by the sun can be used in solar collector systems to heat water or by direct conversion into electric energy in photovoltaic devices. Current renewable energy systems cannot produce energy at the low cost that conventional fossil fuel power plants can. For large-scale implementation of renewable energy power plants, it is therefore necessary to develop systems that can compete on an economic level with fossil fuel facilities, either by decreasing cost, increasing efficiency, or a combination of both.

1.1.3   Plastic Solar Cells

Photovoltaics are attractive renewable energy power sources. The sun supplies a peak intensity of about 1 kW/m2 on the surface of the earth. Of course, this intensity is reduced

when the sun is not at zenith due to location or time of day. The optical energy supplied by the sun can be converted into electric energy in a solar cell. Due to the rather high cost of Si solar cell systems today, they are mainly used in remote locations where there is no power line from a conventional power plant available. To make solar cell systems more competitive with fossil fuel power plants, a significant reduction in cost must be achieved.

A promising approach towards low cost photovoltaic devices is fabrication of solar cells based on organic materials.[22-27] In one class of these devices, Si or GaAs are replaced by semiconducting polymer materials in combination with fullerene materials as the active layer. These materials are usually soluble in common organic solvents. This solubility makes device production relatively easy. Thin films can be spin cast[28] or doctor bladed[29] from solution. Even screen printing and ink jet printing have been demonstrated.[30] Since thin organic films are flexible, they can also be applied to flexible plastic substrates making the whole device flexible and allowing for cheap roll-to-roll production methods.

Another unique characteristic of polymeric materials is that the optical and electrical properties can be changed by altering the molecular structure of the monomers. It is therefore possible to tune the optical and electrical properties of the polymer in order to optimize device performance.

Band gap engineering of such π-conjugated species play crucial roles in optimizing the performance of optoelectronic devices based on active organic components.[31-38]

The field of solar cells based on conjugated polymers is subject to intensive research. Several device architectures to incorporate the materials have been explored,[39-42] and those based on the bulk heterojunction concept are promising due to power conversion efficiencies up to 5% recently accomplished.[43,44]

Polymers with a high absorption coefficient and broad absorption spectra are required for efficient harvesting of the solar energy. Most conjugated polymers have a band gap >2 eV, and absorb only small part of solar photon flux spectrum, which ranges from 300 to 2500 nm with a maximum flux around 700 nm. Low band gap polymers (Eg ≤ 1.8 eV) are an approach for absorbing the solar spectrum on a broader range.[45,46]

Background on Polymer Photovoltaics

The discovery of conducting polymers in the mid 1970's has led to intense research of a whole new class of materials, showing that the electrical properties of polymers can range from insulating to semiconducting to conducting (conductivity >100,000 S/cm has been shown.[47] These new semiconducting and conducting materials combine the electrical and optical properties of inorganic semiconductors with the mechanical flexibility of polymers. While the

electrical and optical properties can be quite similar to inorganics, the charge carriers and charge transport mechanisms in semiconducting polymers are essentially different from their inorganic counterparts.

This part introduces, the charge carriers and excitation processes that are important for organic photovoltaic devices and a basic understanding of the most important characteristics of solar cells with a focus on organic devices.[48,49]

Charge Transport in Organic Materials

Semiconducting polymers can usually be described as quasi-one-dimensional semiconductors. Semiconducting and conducting polymers are conjugated polymers, which refers to the alternating single and double bonds between the carbon atoms on the polymer backbone. The double bonds result from the fact that, while carbon has four valence electrons, the carbon atoms in conjugated molecules bind to only three (or sometimes two) other atoms. The remaining electrons form π-electron bonds that are delocalized over the entire molecule. While the polymer chains can be very long (microns), the conjugation length along the chain can be interrupted (e.g. by foreign atoms, bending of the polymer chain, or crosslinks) and is typically less than 100 nm. The molecular levels are grouped in bands, and in the limit of very long conjugation length, the band structure picture associated with inorganic semiconductors can be applied to organic semiconductors. The band edge of the valence band is referred to as the "Highest Occupied Molecular Orbital" (HOMO) and the edge of the conduction band is called the "Lowest Unoccupied Molecular Orbital" (LUMO).

Photoexcitation in Polymers

The energy gap between the HOMO and LUMO level in conjugated polymers is typically within the range of visible photons. Upon absorption of an incoming photon, an electron is promoted into the LUMO level, leaving behind a hole in the HOMO level.

Donor-Acceptor Interface

In most conjugated polymers, the predominant excited species is the singlet exciton. At room temperature the electron and hole are bound to each other and there are no free charge carriers. An essential process for polymeric solar cells after photoexcitation is charge separation. Since the electron and hole are bound together, a mechanism must be found to efficiently separate electron and hole and to prevent recombination of the two. A possibility to achieve this charge separation is by introducing an electron acceptor that dissociates the exciton by transferring the electron from the polymer (therefore being the electron donor) to the electron acceptor material. As a result, the polymer is left with a P^+ polaron that can drift through the film to the anode while the electron is in the acceptor material and can be

transported to the cathode. The main condition for the exciton dissociation to occur is that the electron affinity of the acceptor is larger than the ionization potential of the donor.

A well-known acceptor material is the buckminsterfullerene C_{60}. Since the discovery of ultrafast charge transfer from conjugated polymers to C_{60},[50] its properties as an electron acceptor have been subject to intense research. The charge transfer typically occurs within the femtosecond time regime. An upper time limit was found to be 300 fs[51] which is three orders of magnitude faster than any electron-hole recombination process within the polymer. The charge transfer range is about 5-10 nm, which makes close proximity of C_{60} to the photoexcitation on the polymer essential. While the charge transfer range is similar in different models, the mechanism leading to the electron transfer from the polymer to the fullerene is a subject of controversy. Halls *et al.* suggest that the singlet excitons diffuse from the location of photoexcitation to the polymer-fullerene interface and are dissociated at the interface.[52] They studied the photovoltaic response in heterojunction devices prepared from poly(phenylenevinylene) (PPV) and C_{60}. In addition to experiments, they modeled the photocurrent spectra under the assumption that all absorbed photons create singlet excitons and all singlet excitons within the diffusion range of the interface are dissociated and contribute to the photocurrent. From the quantitative agreement of the modeled current spectra and the experimental spectra they deduce a diffusion range of 6-8 nm and conclude that the agreement is strong evidence for the diffusion model.

There are two general ways to create a donor-acceptor interface in organic devices. One is to bring two films in contact at the surface, which creates a heterojunction. In this case, only a fraction of the bulk of the materials (within ~10 nm of the interface) builds a donor-acceptor interface. The other is to blend the two materials to form one mixed layer. In this case, the whole bulk of the device has a donor-acceptor interface. These devices are called bulk-heterojunction devices. There are various methods to create a bulk-heterojunction including blending of the materials in a solution from which the film is cast, interdiffusion of the two materials into each other, or coevaporation of both materials.
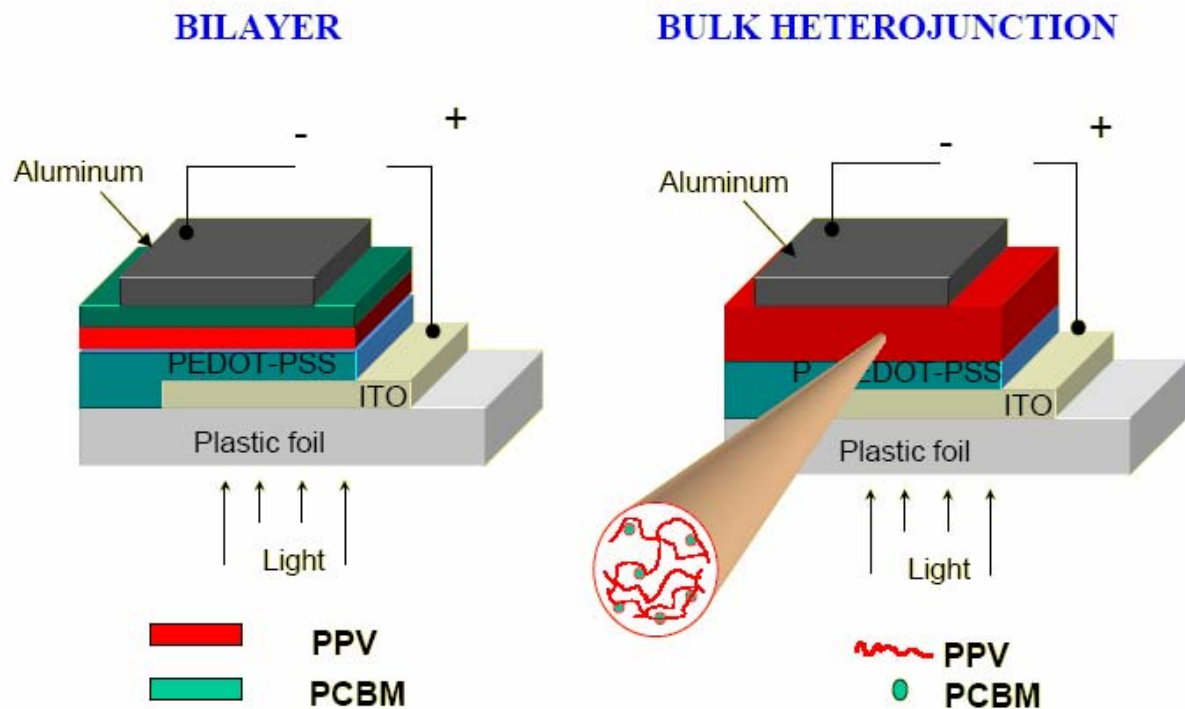
Figure 1.1. Schemetic diagram of organic solar cells.

Short Circuit Current , Open Circuit Voltage and Fill Factor[53]

The typical current–voltage characteristic of a solar cell is shown in Figure 1.2. A few important points on the curve that are used to determine the efficiency of solar cells and to compare different cells are labeled in the graph:
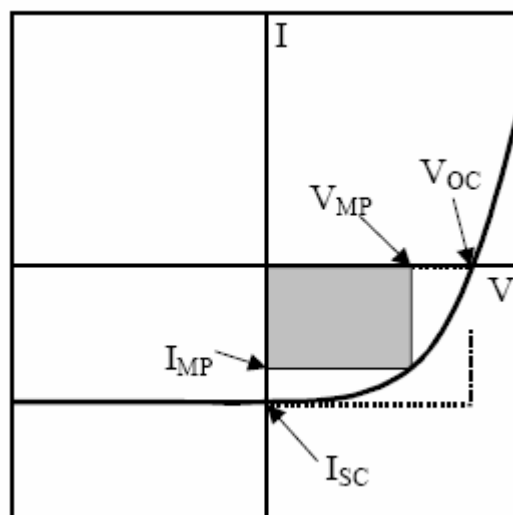
Figure 1.2. Current versus voltage characteristic of a solar cell under illumination.

• The intersection of the curve with the y-axis (current) is referred to as the short circuit current I_{SC}. I_{SC} is the maximum current the solar cell can put out under a given illumination

power without an external voltage source connected. It is measured by connecting both electrodes to an ammeter.

• The intersection with the x-axis (voltage) is called the open circuit voltage (V_{OC}). V_{OC} is the maximum voltage a solar cell can put out. It is measured by connecting the illuminated solar cell to a voltmeter.

• I_{MP} and V_{MP} are the current and voltage at the point of maximum power output of the solar cell. I_{MP} and V_{MP} can be determined by calculating the power output P of the solar cell ($P=I*V$) at each point between I_{SC} and V_{OC} and finding the maximum of P.

Out of these quantities, the fill factor FF can be calculated. FF is defined as

$$FF = \frac{P_{max}}{I_{SC} \cdot V_{OC}} = \frac{I_{MP} \cdot V_{MP}}{I_{SC} \cdot V_{OC}}$$

The fill factor is the ratio of the rectangles given by the maximum power point and I_{SC} and V_{OC} (see Figure 1.2). The fill factor therefore gives a measure of the quality of the I-V characteristic of the solar cell. Its theoretical limits are between 0.25 (ohmic nonrectifying behavior of the solar cell) and 1. In practice, FF can even drop below 0.25 when a blocking contact is formed at one of the electrodes.

In general, the overall efficiency of a solar cell is larger for larger FF. In the ideal limit of FF approaching 1 the solar cell puts out a constant maximum current at any voltage between 0 and V_{OC}.

1.1.4 Thieno[3,4-*b*]pyrazine, A promising material for optoelectronic devices

Thieno[3,4-*b*]pyrazines have been shown to be excellent precursors for the production of low band gap conjugated polymers.[54-57] Recently, photovoltaic devices consisting of thieno[3,4-*b*]pyrazines based low-band gap polymers[54-57] as hole-transporting materials have shown improved efficiencies.

Thieno[3,4-*b*]pyrazine is a polarized species[58] and lowers the bandgap dramatically when incorporated into a polymer backbone. Recent theoretical calculations suggested a lower band-gap for the poly(thieno[3,4-b]pyrazine) (0.70 eV) even lower than for poly(isothianaphthene) (0.80 eV).
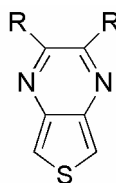
Thieno[3,4-*b*]pyrazine

However, for these compounds to be fully utilized in optoelectronic applications, a general synthetic route must be developed that allows access to a large number of different functionalities in the 2, 3, 5 and 7 positions. Such functionalities are necessary to tune and modulate the physical, electronic, and optical properties of the polymers.[54-57,59]
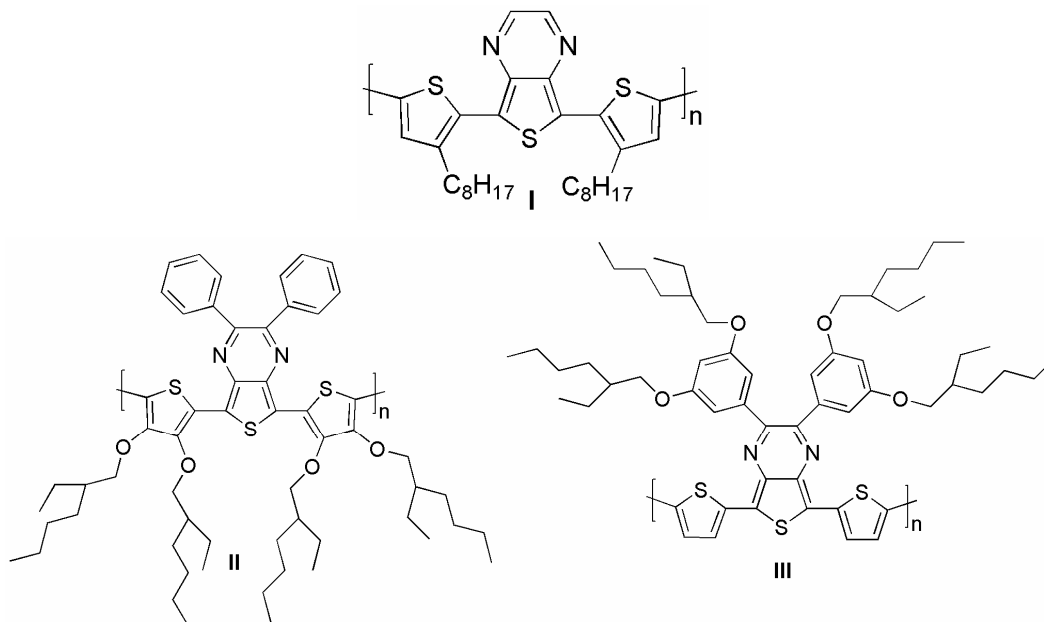
The goal of this research work was to synthesize thieno[3,4-*b*]pyrazine based polymers, belonging to the quinoid family of low band gap polymers. A new narrow band gap system was designed, symbolized as [-A-Q-A-]$_n$, where A is aromatic donor unit and Q is *o*-quinoid acceptor unit. The properties of polymers are considered to correlate straightforwardly to those of structurally defined monomers [A-Q-A]. Although donor-acceptor type polymers in

electrochemically generated systems have received much attention,[60] little work has been done on the synthesis of these polymers using chemically grown polymers which are soluble and processable. Moreover there are no previous studies on fully substituted conjugated poly(arylenevinylene)s which demonstrate the efficiency of this approach for band gap shortening. We have combined both tactics and prepared the novel poly(heteroarylenevinylene)s, with a new backbone architecture. However investigations of structure-property relationships of polymers are essential for a full understanding of the role of a particular n-type moiety.
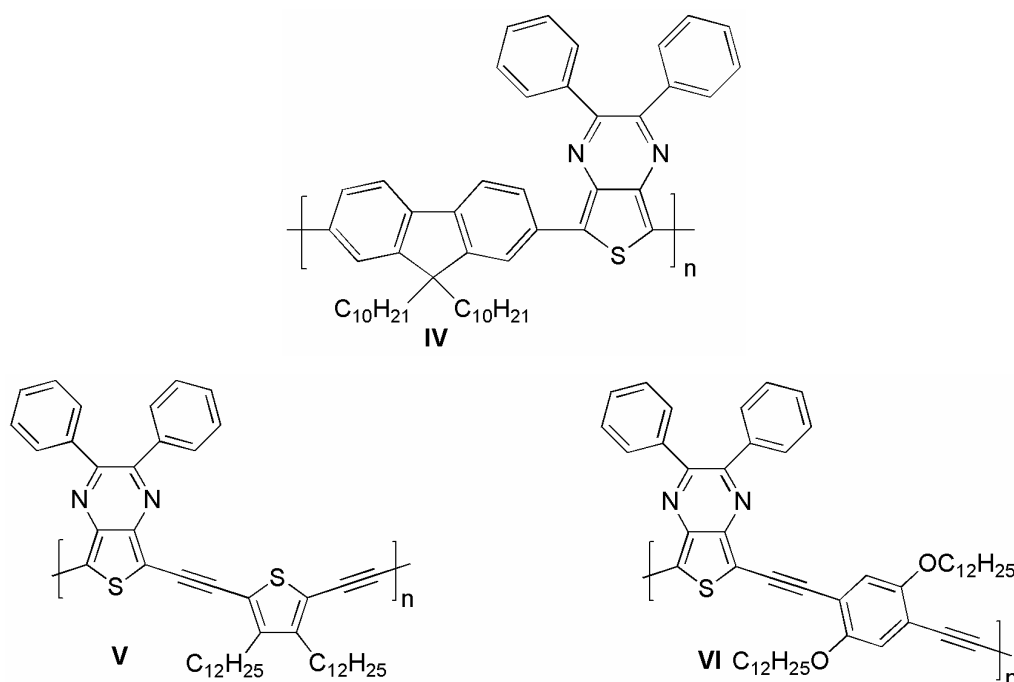
Our previous studies report the incorporation of thieno(3,4-*b*)pyrazine group into poly(arylene)s[61] and poly(aryleneethynylene)s[62] backbone that results in a remarkable increase in absorption maxima and lowering of band gap. There is no research on the characteristics of introducing the pendant thieno(3,4-*b*)pyrazine group into the poly(*p*-phenylenevinylene) and poly(arylene)s backbone. Second part of the work presents the synthesis, characterization of a series of new poly(*p*-phenylenevinylene)s and poly(arylene)s containing symmetrically 5,7-disubstituted pendant thieno(3,4-*b*)pyrazine group.

2   General Part

2.1 Horner–Wadsworth–Emmons reaction (HWE)

Wittig–Horner reaction or Horner–Wadsworth–Emmons reaction (HWE) is one of the most important reactions in organic synthesis used to form α,β-unsaturated ketones, α,β-unsaturated esters and other conjugated systems. The synthetic importance of the reaction is based on the fact that the new carbon–carbon double bond in the product molecule is generated at a fixed position. Other methods for the formation of carbon–carbon double bonds, e.g. elimination of water or HX, or pyrolytic procedures often lead to mixtures of isomers.[63] Olefin synthesis employing phosphonium ylides was introduced in 1953 by Witting and Geissler.[64] In 1958 Horner disclosed a modified Witting reaction employing phosphonate-stabilized carbanions;[65] the scope of the reaction was further defined by Wadsworth and Emmons.[66]

1-Overall Reaction

The chemical reaction of stabilized phosphonate carbanion with aldehyde (or ketones) produces predominantly E-alkenes.
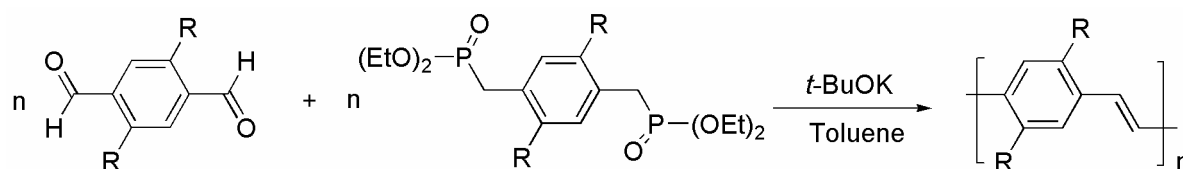
Scheme 2.1. PPV synthesis by Horner–Wadsworth–Emmons Polycondensation.

2- Reaction Mechanism

As first reported by Horner,[67] carbanionic phosphine oxides can be used; today carbanions from alkyl phosphonates are most often used. The latter are easily prepared by application of the *Arbuzov reaction*. The reactive carbanionic species is generated by treatment of the appropriate phosphonate with base, e.g. sodium hydride, n-butyllithium or potassium *t*-butoxide.
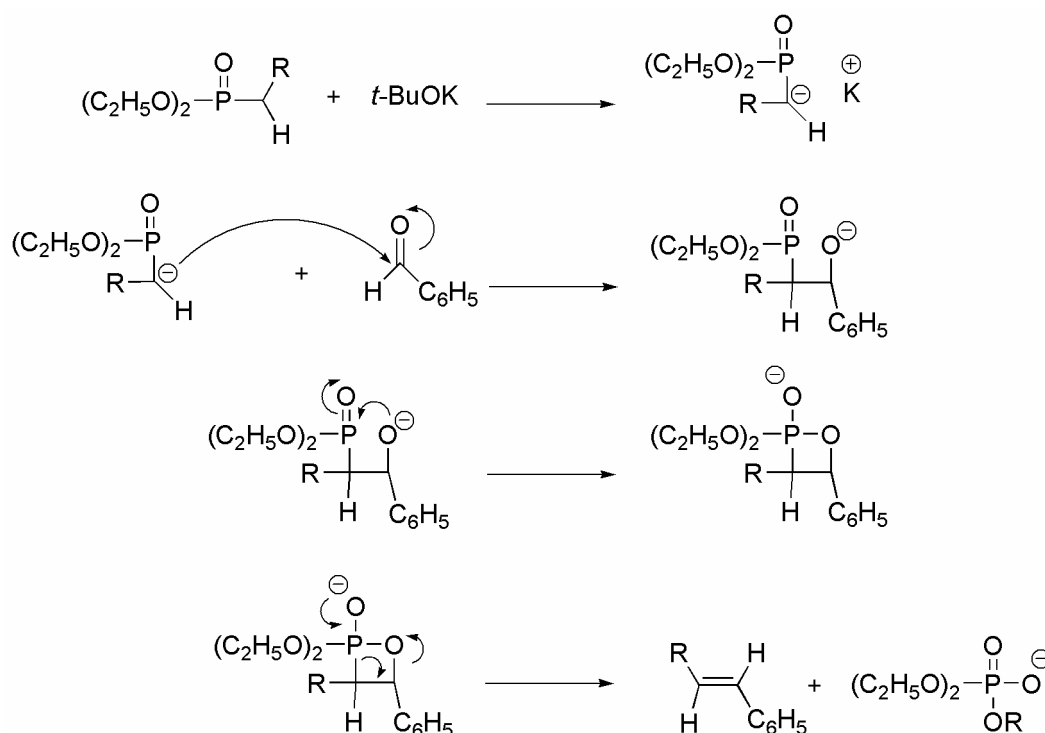
Scheme 2.2. Mechanism of Horner–Wadsworth–Emmons condensation.

Nucleophilic addition of phosphonate carbanion to the carbonyl is rate determining.[68] The four ring intermediate with P and O, called oxaphosphetane, is typical of the HWE reaction. The resulting phosphate byproduct is readily separated from the desired products by simply washing with water. The electron withdrawing group alpha to the phosphonate is necessary for the final elimination to occur. Absence of electron withdrawing group afford stable ß-hydroxyphosphonates.[69] Direct interconversion of intermediates is possible when R = H. The ratio of olefin isomers is dependent upon the stereochemical outcome of the initial addition and upon the ability of intermediates to equilibrate.[70] Thomson and Heathcock have performed a systematic study on the stereochemical outcome without modifying the structure of the phosphonate.[71] They found greater *E*-steroeselectivity with the following conditions:

- Increasing steric bulk of the aldehyde
- Higher reaction temperature
- Li> Na > K salts
- Using the solvent DME over THF

It was also found that bulky phosphonate and bulky electron withdrawing groups enhance *E*-alkene selectivity.
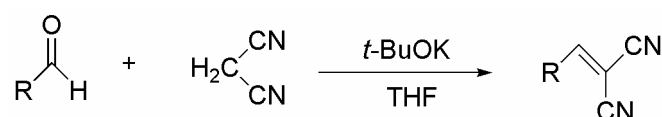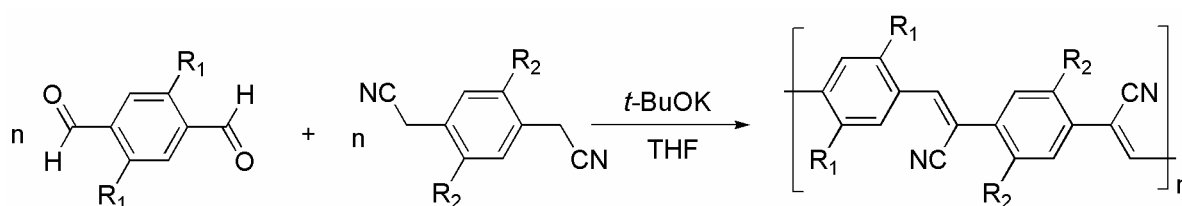
2.2   Knoevenagel condensation

The Knoevenagel condensation is an important carbon carbon bond-forming reaction in organic synthesis.[72] Ever since its discovery in 1894,[73] the Knoevenagel reaction has been widely used in organic synthesis to prepare coumarins and their derivatives, which are important intermediates in the synthesis of cosmetics, perfumes and pharmaceuticals.[74] In recent times, there has been a growing interest in Knoevenagel products not only because of their significant biological activities but also for the synthesis of new conducting materials, in particular for the synthesis of poly(phenylene cyanovinylene)s.[75] These materials have been shown to exhibit electroluminescence, that is, a light emission produced by the action of an electrical current.

The reaction involves the condensation of a carbonyl compound (aldehyde or ketone) with an active methylene compound of the type Z-CH$_2$-Z'. The Z groups are electron withdrawing groups, such as CHO, COR, COOH, COOR, CN, NO$_2$, SOR, SO$_2$R, SO$_2$OR or similar groups. This classical reaction is usually catalyzed by organic bases (primary, secondary and tertiary amines), ammonia and ammonium salts or by Lewis acids such as CuCl, ZnCl$_2$.

1-Overall Reaction

2- Knoevenagel polycondensation

Scheme 2.3. General PPV synthesis by Knoevenagel Polycondensation.

3-Mechanism of Knoevenagel condensation

The reaction belongs to a class of carbonyl reactions that are related to the aldol reaction. The mechanism[76] is formulated by analogy to the latter. The initial step is the deprotonation of the CH-acidic methylene compound. A catalytic amount of base can be used for this purpose. The corresponding anion formed by deprotonation subsequently adds to the carbonyl substrate to

give aldol type intermediate. Loss of water from intermediate leads to a primary α,β-unsaturated product.
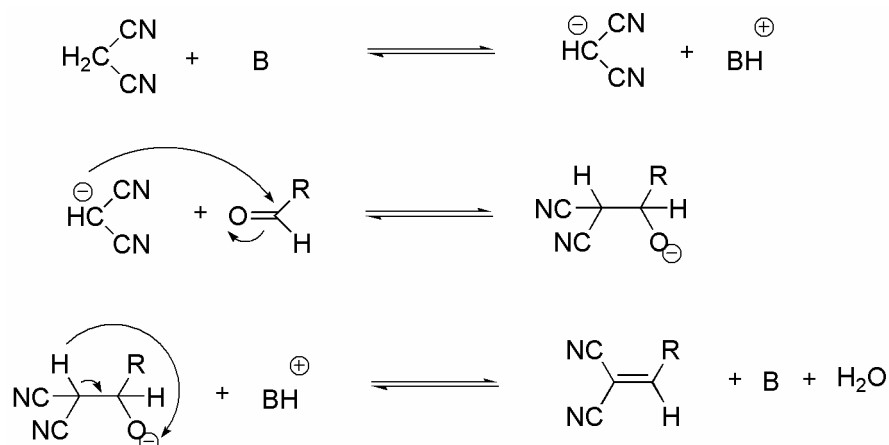
Scheme 2.4. Mechanism of Knoevenagel condensation.

Virtually any aldehyde or ketone and any CH-acidic methylene compound can be employed in the Knoevenagel reaction; however the reactivity may be limited due to steric effects. Some reactions may lead to unexpected products from side-reactions or from consecutive reactions of the initially formed Knoevenagel product. Suitable substituents X and Y that can activate the methylene group to become CH-acidic, are electron-withdrawing groups—e.g. carboxy, nitro, cyano and carbonyl groups. Malonic acid as well as cyano acetic acid and derivatives (ester, nitrile, and amide) are often used. In general two activating groups X and Y are required to achieve sufficient reactivity; malononitrile $CH_2(CN)_2$ is considered to be the most reactive methylene compound with respect to the Knoevenagel reaction. As would be expected, ketones are less reactive than aldehydes. In addition yield and rate of the condensation reaction are influenced by steric factors. Because of the mild reaction conditions, and its broad applicability, the Knoevenagel reaction is an important method for the synthesis of α,β-unsaturated carboxylic acids.[72] Comparable methods[77] are the *Reformatsky reaction*, the *Perkin reaction*, as well as the *Claisen ester condensation*. The Knoevenagel reaction is of greater versatility; however the Reformatsky reaction permits the preparation of α,β-unsaturated carboxylic acids that are branched in α-position.

2.3   Gilch Reaction

A useful synthetic route to PPVs is the polymerization of 1,4-bis(chloromethyl)arenas by treatment with about equiv. of potassium *tert*-butoxide in non alcoholic solvents like THF. The analogous reaction with 1,4-bis(bromomethyl)arenes can also be used. This methodology was used by Gilch and Wheelwright[78] as one of the more early PPV synthesis. Gilch polymerization has been widely preferred as it offers a number of important advantages for the introduction of vinylene units along the polymer backbone with high molecular weight, low polydispersity index and allows for easy purification.

1-Overall Reaction

1,4-dihalo-*p*-xylylenes are treated with excess of potassium *tert*-butoxide in organic solvents (e.g. THF), where polymerization is carried out either by the controlled addition of monomer to a solution of base or by the controlled addition of base to a solution of monomer.[79]
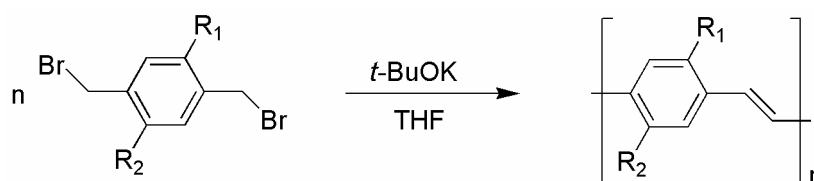
Scheme 2.5. PPV synthesis by Gilch Polymerization.

2-Mechanism of Gilch Polymerization

Even though this synthesis is currently being applied, the mechanism of the polymerization of the *p*-quinodimethane-based polymerization is still the subject of an ongoing discord. The two mechanistic possibilities -anionic or radical- have been hard to distinguish.

The mechanistic route involves *p*-quinodimethane system as actual monomer. The first step is a base-induced 1,6-elimination from a *p*-xylene derivative, leading to the in situ formation of the *p*-quinodimethane system. Second, this intermediate polymerizes spontaneously to the precursor polymer. The conjugated structure is obtained in a third step, directly or after thermal treatment depending on the specific chemical structure of the starting monomer and the polymerization conditions.
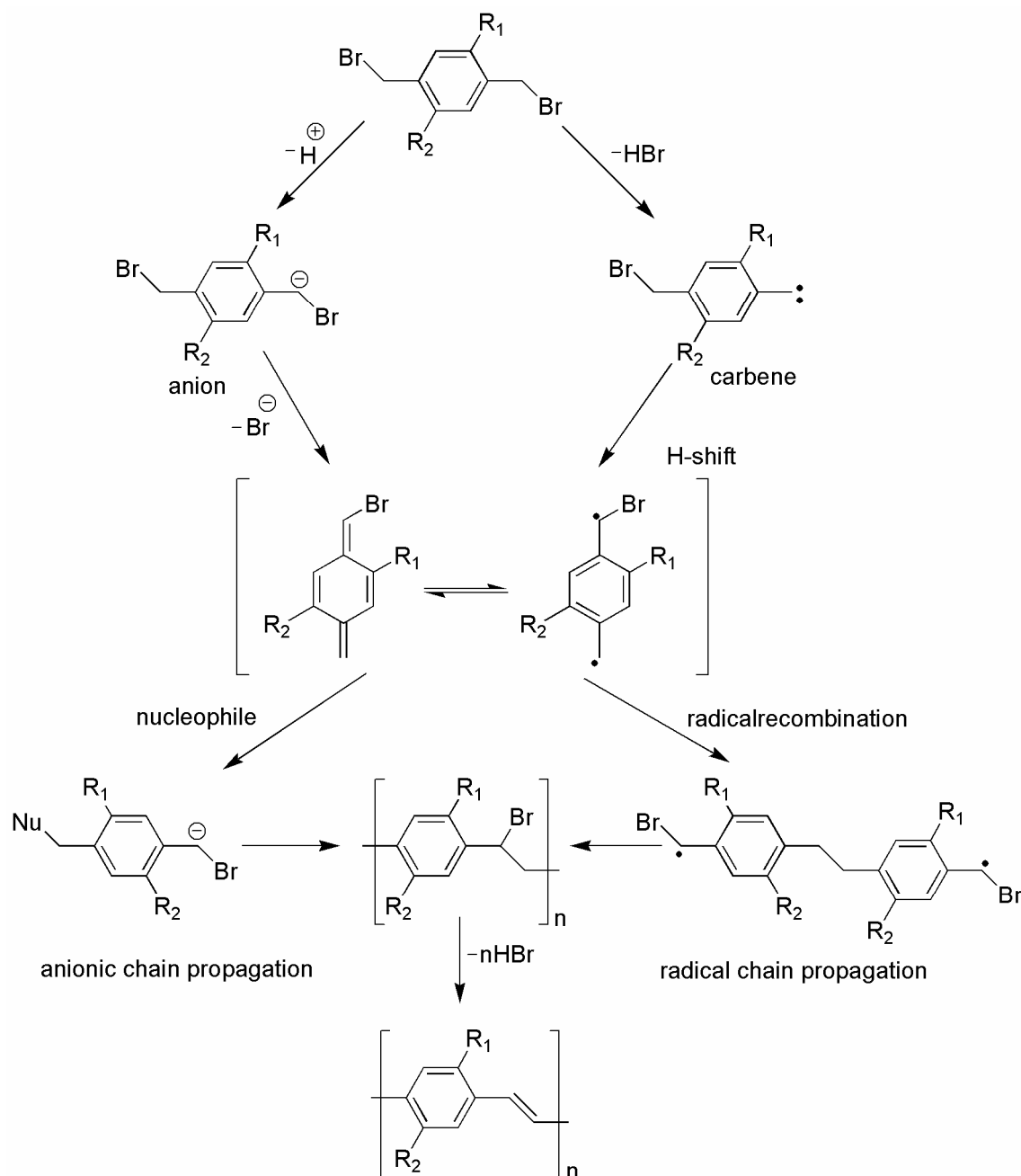
Scheme 2.6. Proposed mechanisms of Gilch Polymerization.

For the second step- the polymerization itself -there are two reasonable possibilities: (i) a free radical mechanism, which is claimed for precursor polymerization e.g. by Vanderzande[80] and Wessling,[81] or (ii) an anionic induced polymerization, which is described by Hsieh[82] for the chloro precursor route. It is even possible that these two pathways compete with each other, depending on the exact reaction conditions. Several recent publications on the Gilch route state or favor an anionic polymerization mechanism[83,84] while others argue that the route proceeds via a radical mechanism.[85,86]

2.4 Suzuki Cross-Coupling

The Pd-catalysed Suzuki–Miyaura (SM) coupling reaction[87] is one of the most efficient methods for the construction of C–C bonds. Although several other methods (e.g. Kharash coupling, Negishi coupling, Stille coupling, Himaya coupling, Liebeskind–Srogl coupling and Kumuda coupling) are available for this purpose, the SM cross-coupling reaction which produces biaryls has proven to be the most popular in recent times. The preference for the SM cross-coupling reaction above the other Pd-catalysed cross-coupling reactions is not incidental. The key advantages of the SM coupling are the mild reaction conditions and the commercial availability of the diverse boronic acids that are environmentally safer than the other organometallic reagents.[88-95] In addition, the handling and removal of boron-containing by-products is easy when compared to other organometallic reagents, especially in a large-scale synthesis.

1-Overall Reaction

R=Alkyl, Aryl, O-Alkyl

X= Br, I
R´=Acceptor (ester, nitril)
or Donor (OR, NR$_2$, alkyl)
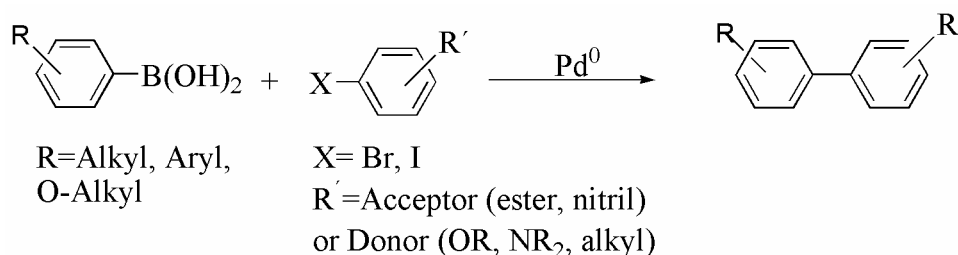
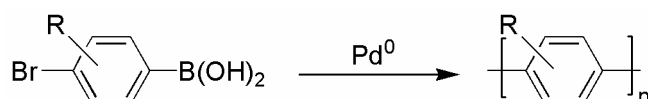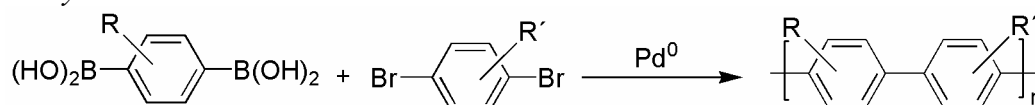**Scheme 2.7.**

SM cross-coupling reaction is also used for polycondensation and can proceed in two ways as shown in scheme 2.8. In AB type,[96] a bifunctional monomer leads to polycondsation, while AA/BB type polycondsation involves two types of monomers with different functionalities, yielding alternative copolymers.[97,98]

AB-Polycondensation

AA/BB-Polycondensation

Scheme 2.8.

2- Mechanism of Suzuki Cross-Coupling
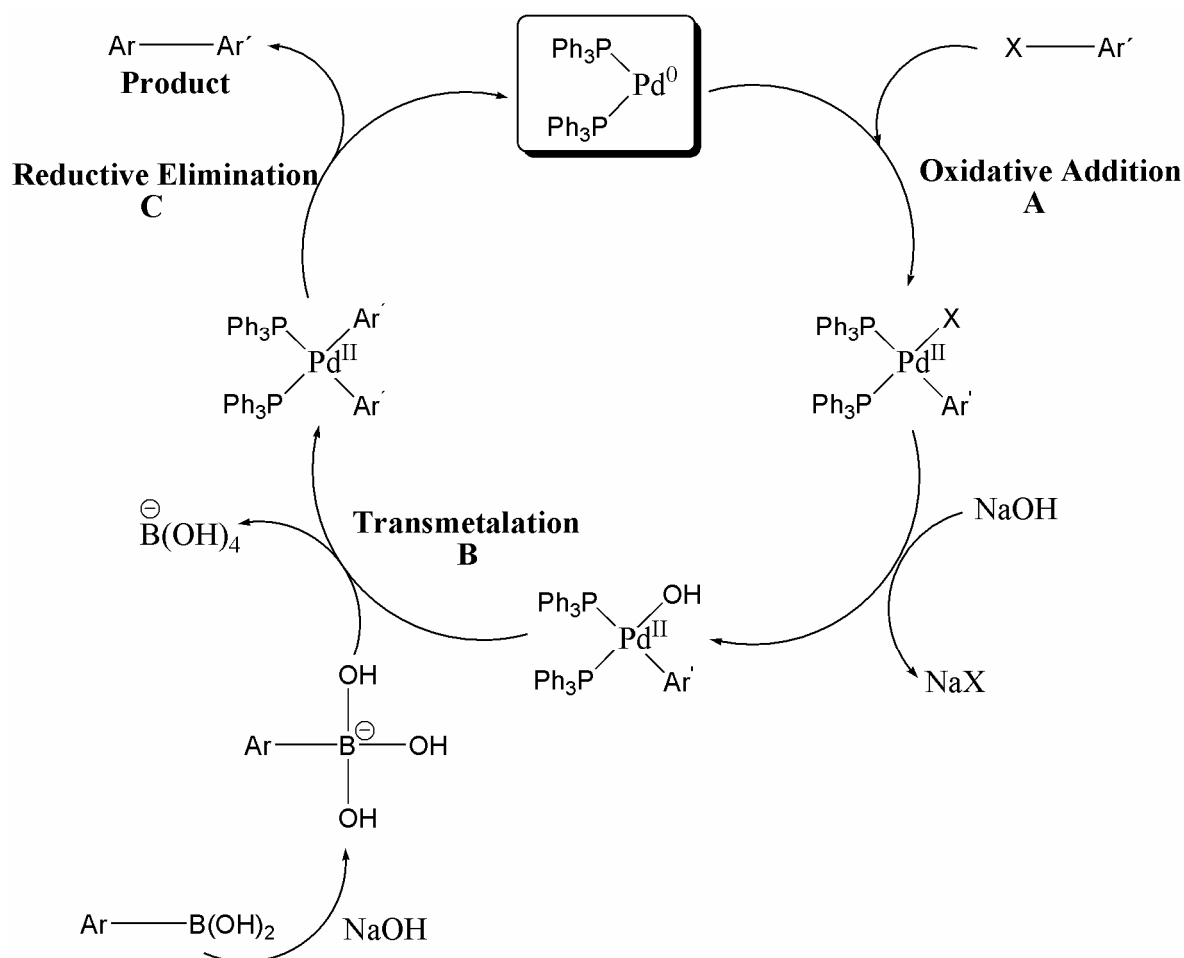
Scheme 2.9. Mechanism of Suzuki Coupling

The general catalytic cycle for the cross-coupling of organometallics with organic halides catalysed by transition metals, which involves (a) oxidative addition, (b) transmetallation, (c) reductive elimination sequences, is widely accepted. Although a similar catalytic cycle has also been suggested for the Suzuki reaction,[99] it differs in that two equivalent bases are required (Scheme 2.9). The coupling reaction of organic boron compounds proceeds only in the presence of bases. This is due to the fact that the organic group on boron is not nucleophilic enough for the transfer from the boron to the palladium in the transmetallation step because of the strong covalent character of the B-C bond in boron compounds. Therefore, it is necessary to increase the carbanion character of organic groups by the formation of an organoborate with a tetravalent boron atom, which utilizes base. Further, it is known that bases substitute for Pd-X to form Pd-OH (or Pd-OR) which has higher activity. Thus, the transmetallation reaction in the Suzuki reaction is favored by the formation of both four-coordinated boron compounds and Pd-OH (or Pd-OR).

Aryl halide and aryl triflate function as electrophiles whose reactivity order is Ar-I > Ar-Br > Ar-OTf >> Ar-Cl. Aryl chlorides are usually not reactive enough, with the exception of those having heteroaromatic rings and electron-withdrawing groups. This is because the oxidative addition of aryl chlorides to palladium complexes is too slow to develop the catalytic cycle. A recent paper showed that the use of nickel catalysts for the cross-coupling reaction with aryl chlorides obtained favorable results.[100] Although the most often used catalyst in the Suzuki reaction is $Pd(PPh_3)_4$, various palladium catalysts are also employed, such as $Pd(dppb)Cl_2$, $PdCl_2(PPh_3)_2$, $Pd(OAc)_2$ and $PdCl_2$ etc. $PPh_2(m\text{-}C_6H_4SO_3Na)$ is used as phosphine ligand when the reaction is carried out in aqueous solvent. For example, the cross coupling reaction using the water-soluble palladium complex $Pd[PPh_2(m\text{-}C_6H_4SO_3Na)]_3$ between sodium 4-bromobenzenesulfonate and 4-methylbenzeneboronic acid obtained the corresponding biaryl in good yield,[101] compared to using $Pd(PPh_3)_4$ in a two-phase organic solvent. Bases are always required in the Suzuki reaction as opposed to the coupling reaction using organotin or organozinc reagents. The best results are achieved with the use of a relatively weak base and Na_2CO_3 is a most frequently used. However, the strong bases such as $Ba(OH)_2$ and K_3PO_4 are efficient in reactions involving steric hindrances.

It is known that the base is involved in the coordination sphere of the palladium and the formation of the $Ar\text{-}PdL_2\text{–}OR$ from $Ar\text{-}PdL_2\text{–}X$ is known to accelerate the transmetalation step. There are some drawbacks with the Pd-mediated SM cross coupling reaction. Only aryl bromides and iodides can be used, as the chlorides only react slowly. Some of the recent results to overcome this problem are addressed by Kotha et al. in a review.[102] By-products such as self-coupling products, coupling products of phosphine-bound aryls, are often formed. The most frequently used catalyst, $Pd(PPh_3)_4$, suffers from this drawback and the phenyl group of the PPh_3 becomes incorporated in the products giving scrambled derivatives. A bulky phosphine ligand $(o\text{-}MeOC_6H_4)_3P$ is sufficient to retard this type of side-reactions and deliver high yields of the desired product. Under oxygen-free conditions, homocoupling products can be avoided and, in order to remove the dissolved oxygen, it is desirable to de-gas the solvents by a suitable method.

2.5   Basics of Polycondensation

The classical subdivision of polymers into two main groups was made around 1929 by W. H. Carothers, who proposed that a distinction be made between polymers prepared by the stepwise reaction of monomers (condensation polymers) and those formed by chain reactions (addition polymers).

One basic simplifying assumption proposed by Flory, was that all functional groups can be considered as being equally reactive. This implies that a monomer will react with either monomer or polymer species with equal ease.

Carothers Equation

W. H. Carothers, pioneer of step-growth reactions, proposed a simple equation relating number-average degree of polymerisation $\bar{P}_n$ to a quantity p describing the extent of the reaction for linear polycondensations or polyadditions.

If N_0 is the original number of molecules present in an A-B monomer system and N the number of all molecules remaining after time t, then the total number of the functional groups of either A or B which have reacted is $(N_0 - N)$. At that time t the extent of reactivity p is given by

$$P = (N_0 - N)/N_0 \qquad \text{or} \qquad N = N_0(1 - p)$$

If we remember that $\bar{P}_n = N_0/N$, a combination of expression gives the Carothers equation,

$$\bar{P}_n = 1/(1 - p) \tag{Eq. 2.1}$$

The Carothers equation is particularly enlightening when we examine the numerical relation between $\bar{P}_n$ and p; thus for $p = 95\%$, $\bar{P}_n = 20$ and when $p = 99\%$, then $\bar{P}_n = 100$. Graphically Carothers equation can be represented as mentioned below.
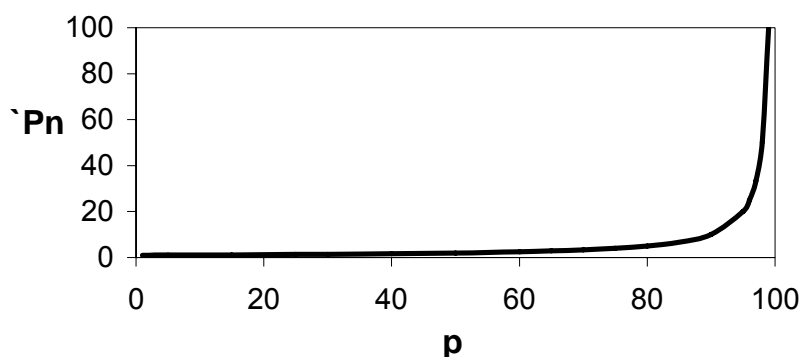
Figure 2.1. Graphical presentation of Carothers equation.

This equation is also valid for an A-A + B-B reaction when one considers that in this case there are initially $2N_0$ molecules. More usefully, a precisely controlled stoichiometry is

required and stoichiometric factor r can be added to Carothers equation and extended form can be expressed as

$$\bar{P}_n = (1 + r)/(1 + r - 2rp) ; \qquad\qquad r = n_A/n_B \leq 1 \qquad \textbf{(Eq. 2.2)}$$

where r is the ratio of the number of molecules of the reactants.[103]

3   Results and Discussion

3.1   Pi-conjugated polymers containing thieno[3,4-*b*]pyrazine unit incorporated in backbone chain.

### 3.1.1   Synthesis and Characterization of Monomers and Model Compounds

Starting from commercially available hydroquinone in four steps 4-formyl-2,5-bis(hexyloxy)phenylboronic acid (**5**) was obtained as illustrated in Scheme 3.1. The first three steps leading to 4-bromo-2,5- bis(hexyloxy)benzaldehyde (**3**) were carried out according to literature procedures.[104-106] The subsequent protection followed by the reaction of (**4**) with trimethylborate, n-BuLi in THF provided (**5**) in 76% yield after recrystallization.
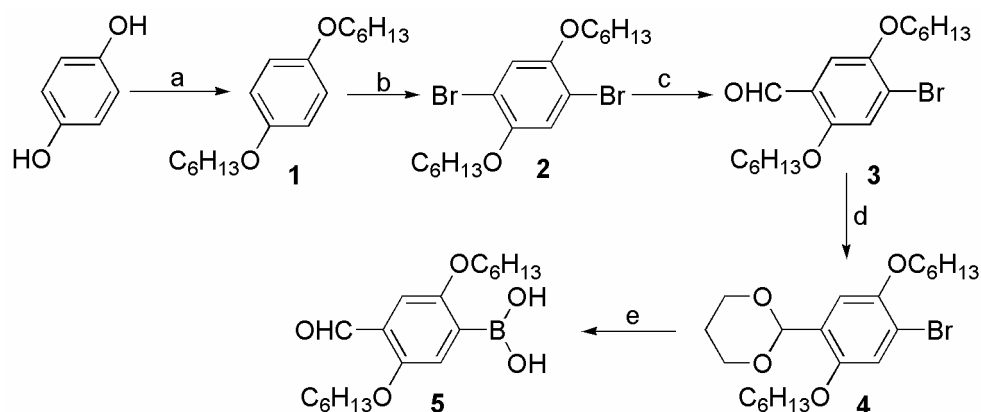
Reagents and conditions: (a) 1-bromohexane, DMSO, KOH, room temperature; (b) DMF, bromine, room temperature; (c) diethyl ether, BuLi, DMF, 10-15 ^{0}C; (d) toluene, 1,3-propandiol, BF$_3$.OEt$_2$, 6 h reflux; (e) i) THF, BuLi, trimethylborate, -78 ^{0}C to room temperature, ii) 1M HCl, room temperature, 24 h.

Scheme 3.1. Synthesis of Compound **5**.

Another four step synthesis resulting in the formation of 1,2-bis-[4-(2-ethyl-hexyloxy)-phenyl]-ethane-1,2-dione (**11**) was started with the alkylation of 4-bromophenol with ethylhexyloxy bromide in the presence of KOH in anhydrous dimethyl sulfoxide. By Sonogashira cross coupling reaction[107] of 1-(2-ethylhexyloxy)-4-bromobenzene (**7**) with trimethylsilylacetylene and deprotection in THF, methanol mixture using aq. KOH led to the formation of 1-(2-ethylhexyloxy)-4-ethynylbenzene (**9**). Compound (**9**) was coupled with (**7**) again by following Sonogashira reaction conditions to synthesize 1,1'-ethyne-1,2-diyl-bis[4-(2-ethyl-hexyloxy)benzene] (**10**) which was further oxidized by KMnO$_4$ in acetone and water at room temperature to give respective dione (**11**) in good yield.
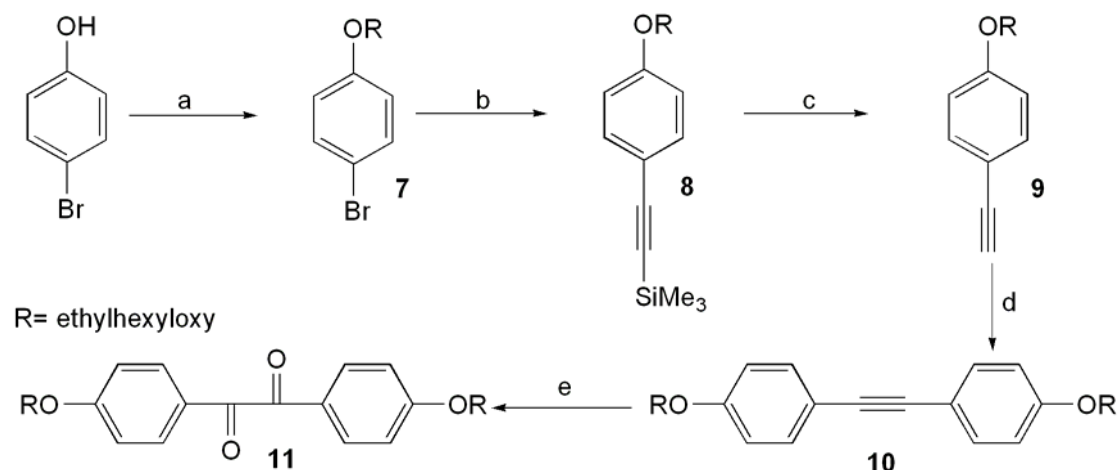
Reagents and conditions: (a) 1-bromoalkane, DMSO, KOH, room temperature; (b) trimethylsilylacetylene, diisopropylamine, Pd(PPh$_3$)$_2$Cl$_2$, CuI, 70 ^{0}C, 12 h; (c) THF, methanol, aq. KOH (2M), room temperature, 5 h; (d) **21**, diisopropylamine, Pd(PPh$_3$)$_4$, 80 ^{0}C, 12 h; (e) acetone, water, KMnO$_4$, room temperature, 4 h.

Scheme 3.2. Synthesis of Compound **11**.

Thieno[3,4-*b*]pyrazine and its 2,3-disubstituted analogues can be readily synthesized from thiophene as shown in Scheme 3.3.[108,109] Compound **13** was readily produced by the nitration of **12** via fuming HNO$_3$ and H$_2$SO$_4$. Without the use of the fuming acids, only the mononitro product was produced. Likewise, an extended 3h reaction time was required, as lesser times resulted in mixtures of mono- and dinitro- products. Treatment of **13** with Sn and HCl reduced both the NO$_2$ functionalities and removed the Br protecting groups. As the reduction was carried out under acidic conditions, the isolated precipitate is the diammonium salt (**14**). The isolated **3·2H$^+$** salt was purified by diethyl ether and acetonitrile washes.[109d] To obtain amine, the salt is taken in diethyl ether and water (1:1) at 0 ^{0}C and basify it with 4N Na$_2$CO$_3$. The amine is highly hygroscopic and has to be subsequently used in next step.
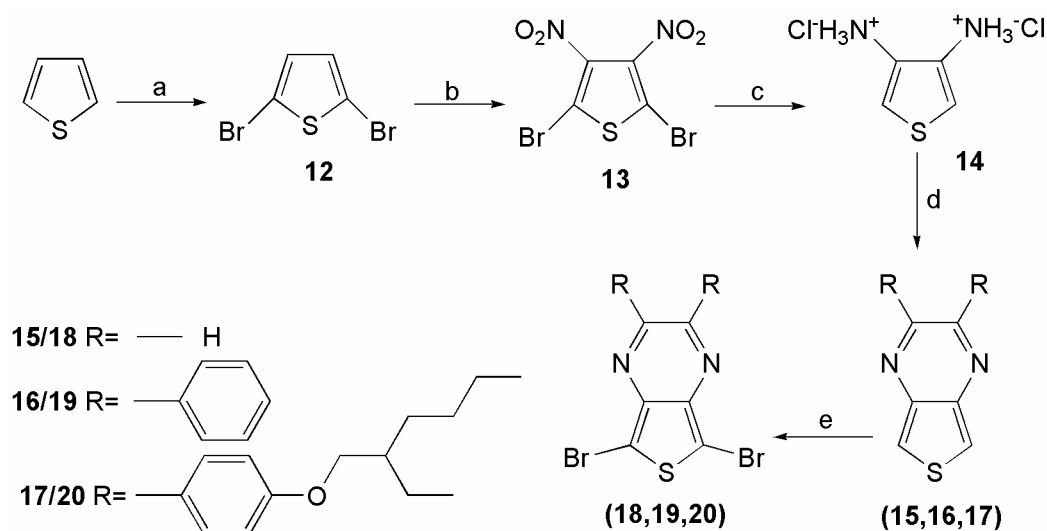
Reagents and conditions: (a) diethyl ether, aq. HBr, bromine, -10 ^{0}C, 15 min.; (b) conc. H_2SO_4, conc. HNO_3, fuming H_2SO_4, 20-25 ^{0}C, 3 h; (c) Sn, conc. HCl, room temperature, 24 h; (d) ethanol, α-diones, triethylamine, room temperature, 24 h; (e) $CHCl_3$, CH_3COOH, NBS, dark, room temperature.

Scheme 3.3. Synthesis of Compounds **18, 19** and **20**.

Due to instability of amine, we have treated the diammonium salt with α-diones (benzil, 2,3-butadione and **11**) in absolute ethanol for 24h and the thieno[3,4-*b*]pyrazines (**15, 16** and **17**) were recovered in relatively higher yields. The initially isolated products were all relatively free of impurities, and analytical samples could be prepared by either recrystallization or chromatography. The dibromo derivatives (**18** and **19**) were prepared by bromination of **15, 16** using NBS in a mixture of chloroform and acetic acid (1:1) in dark under argon. In case of **17** bromination was performed using NBS in DMF at –25 ^{0}C for 3h in dark under argon to obtain compound **20** in quantitative yield.

By Pd-catalyzed Suzuki cross coupling[91] of mono boronic acids (**5** and **6**) with respective 5,7-dibromo-2,3-disubsituted thieno[3,4-*b*]pyrazines (**18, 19, 20**), deep coloured products (**M-1-M-4**) were obtained in quantitative yields after chromatographic purification.
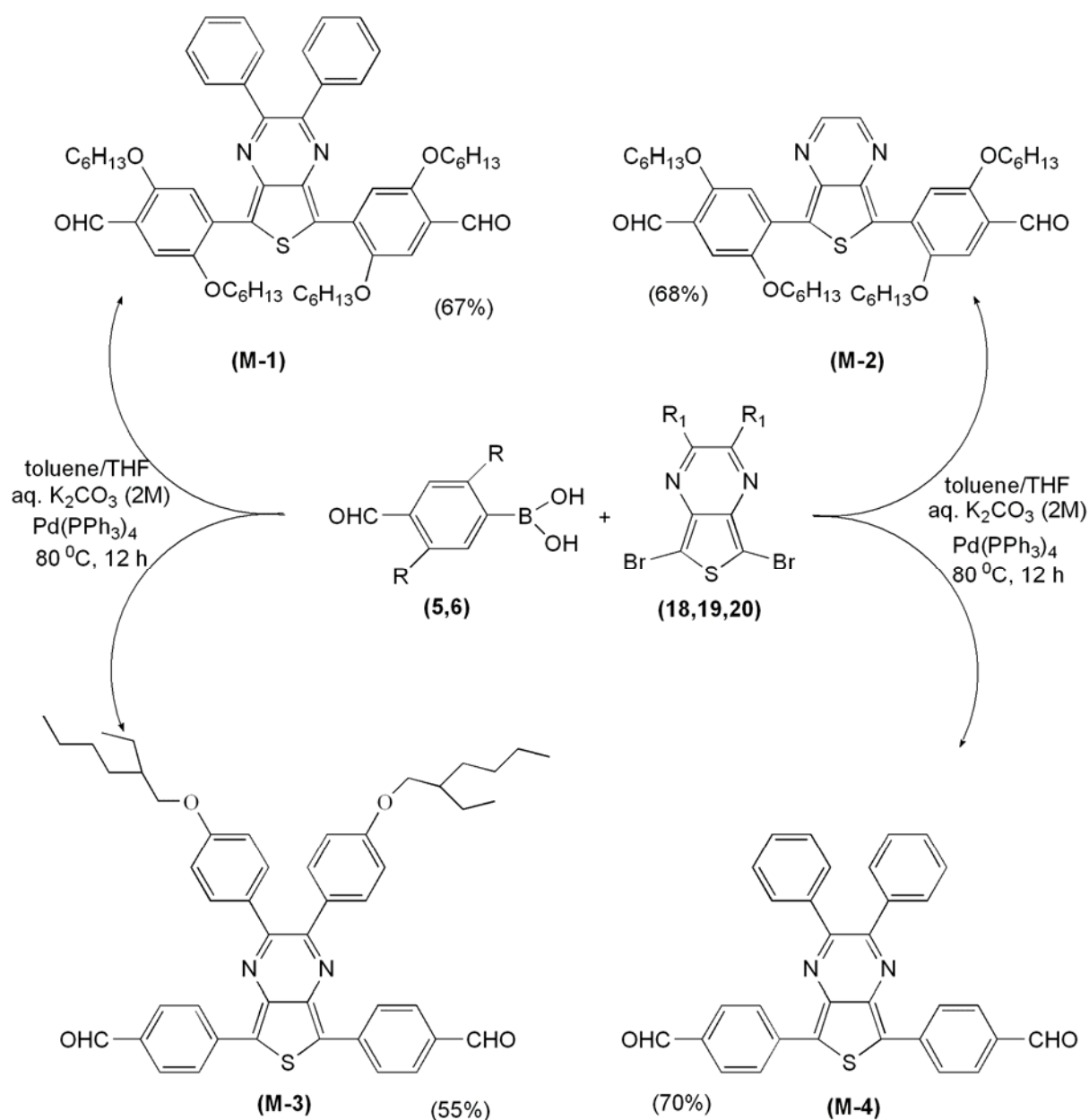
Scheme 3.4. Synthesis of Monomers **M1, M-2, M-3** and **M4**.

Monomers **(M-5, M-6** and **M-8)** were synthesized in high yields according to the known literature procedures.[104,110] 3,4-Dibromothiophene was converted to 3,4-dihexylthiophene **(21)** by Kumada coupling. Bisbromomethyl derivative of **(21)** was obtained in quantitative yield using HBr (30% in acetic acid) and paraformaldehyde in acetic acid. Compound **(22)** was finally converted to 3,4-dihexyl-2,5-bis(methylenediethylphosphate)-thiophene **(M-7)** by Michealis-Arbuzov reaction.
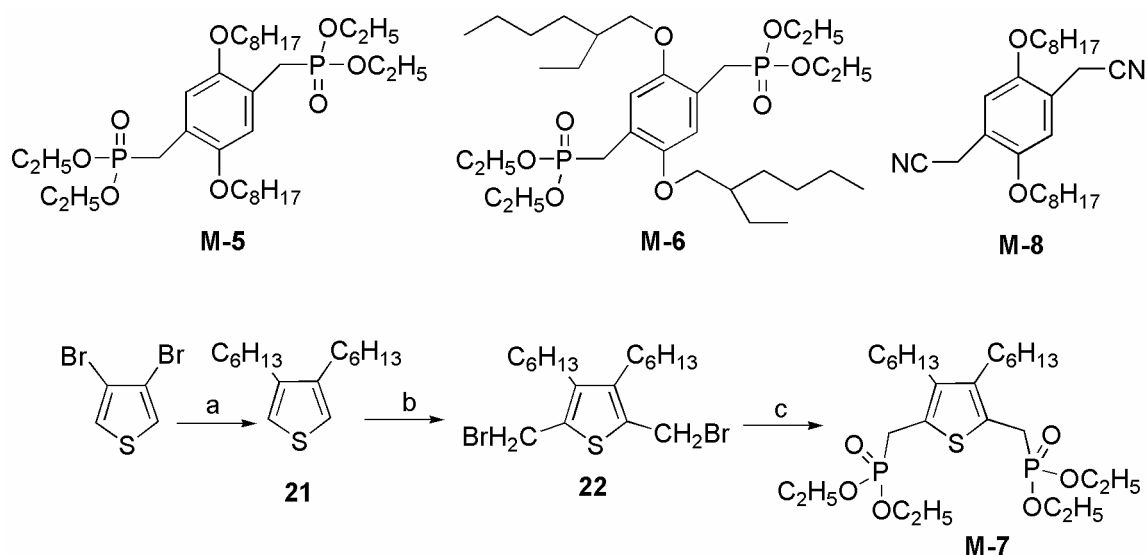
Reagents and conditions: (a) i) diethyl ether, Mg, 1-bromohexane, reflux, 2h, ii) Ni(dppp)Cl$_2$, 0 ^{0}C to reflux, 24h; (b) paraformaldehyde, HBr (30 % in acetic acid), glacial CH$_3$COOH, room temperature, 24 h. (c) triethyl phosphite, 160 ^{0}C, 4 h.

Scheme 3.5. Synthesis of Monomer **M-7**.

Diethyl(4-methyl-2,5-bis(octyloxy)phenyl)methylphosphonate **(25)** was synthesized by Michaelis Arbuzov reaction of the corresponding 1-(bromomethyl)-4-methyl-2,5-bis(octyloxy)benzene **(24)** following reported procedure.[111]
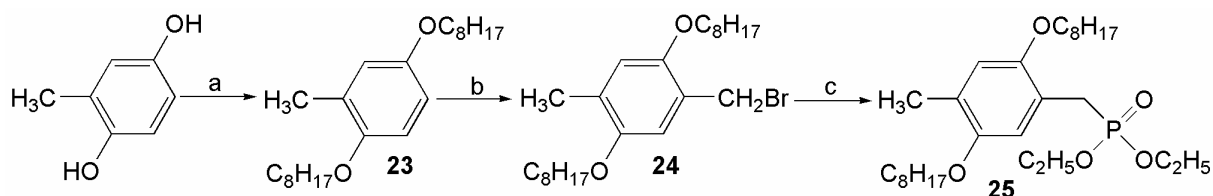
Reagents and conditions: (a) 1-bromoalkane, DMSO, KOH, room temperature; (b) formaldehyde, NaBr, conc. H$_2$SO$_4$, glacial CH$_3$COOH, 70 ^{0}C, 4h; (c) triethyl phosphite, 160 ^{0}C, 4 h.

Scheme 3.6. Synthesis of Compound **25**.

Synthesis of model compounds (**MD-1, MD-2**) was accomplished by Horner-Wadsworth-Emmons (HWE) olefination reaction of **M-1** with two equivalents of commercially available diethyl benzylphosphonate and mono phosphonate ester **(25)** respectively. While model compound (**MD-3**) is the Knoevenagel condensation product of M-**1** with phenyl acetonitrile. All the three model compounds were obtained in good yield after chromatographic purification and were soluble in common organic solvents. **MD-1** was dark violet in colour while **MD-1** and **MD-3** were green solids.
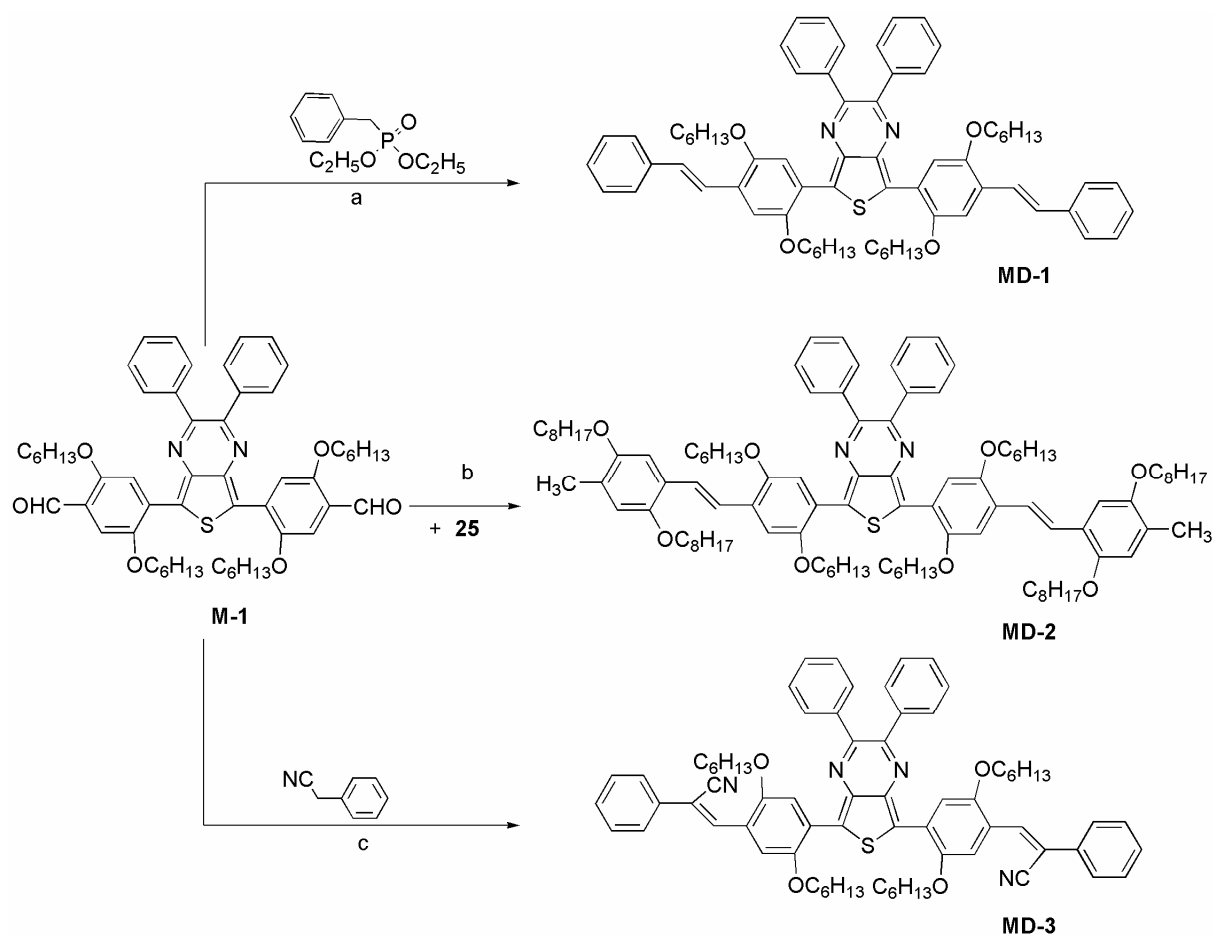
Reagents and conditions: (a) diethyl benzylphosphonate, THF, *t*-BuOK, 0 ^{0}C to room temperature 3 h; (b) 25, THF, *t*-BuOK, 0 ^{0}C to room temperature 3 h; (c) phenyl acetonitrile, THF, *t*-BuOK, *t*-BuOH, 40 ^{0}C, 4 h.

Scheme 3.7. Synthesis of Model Compounds **MD-1, MD-2** and **MD-3**.

The chemical structures of monomers (**M-1-M-8**) and 5,7-dibromo-2,3-disubsituted thieno[3,4-*b*]pyrazines (**18, 19, 20**) were confirmed by NMR, Mass and elemental analysis.

Figure 3.1 depicts the ^{1}HNMR of **M-1.** The peaks could be readily assigned to their respective protons. The spectrum showed aldehyde proton signals at 10.41 ppm, two protons of alkoxyphenylene adjacent to thienopyrazine moiety appeared at 9.20 ppm, while other two protons of alkoxy phenylene and phenyl rings protons appear between 7.60-7.26 ppm. The OCH$_2$ protons appeared between 4.20-3.9 ppm and other alkyl protons appeared upfield between 2.0-0.80 ppm.
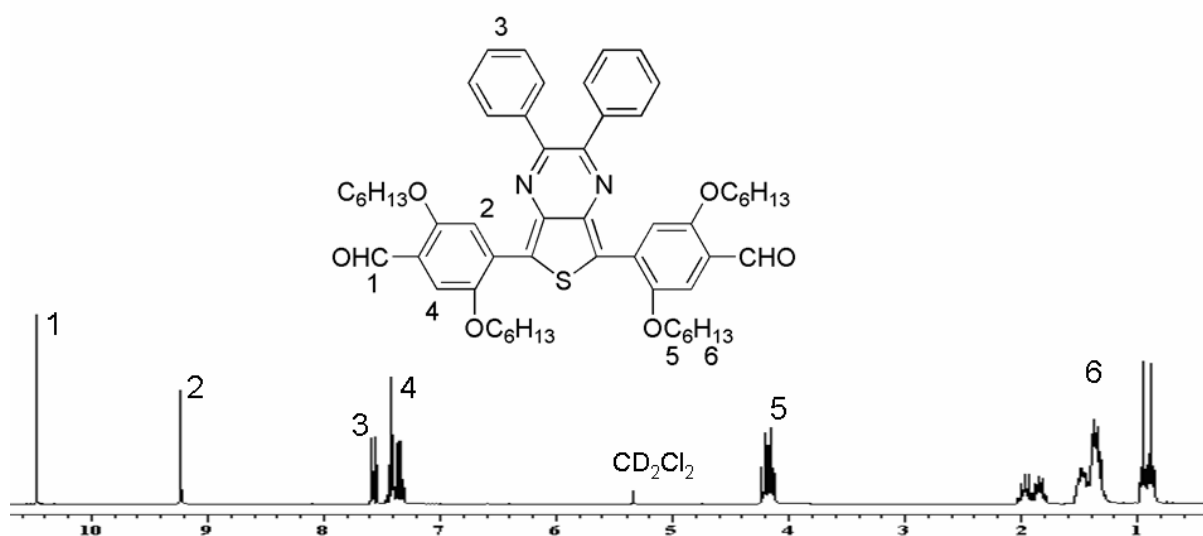
Figure 3.1. ^{1}HNMR of monomer **M-1**.

In ^{1}HNMR spectrum of monomer **M-2**, signals of two pyrazine protons (2,3-position) appeared along with phenyl protons adjacent to thienopyrazine at 8.57 ppm. The location of rest of protons signals similar to those of **M-1**.
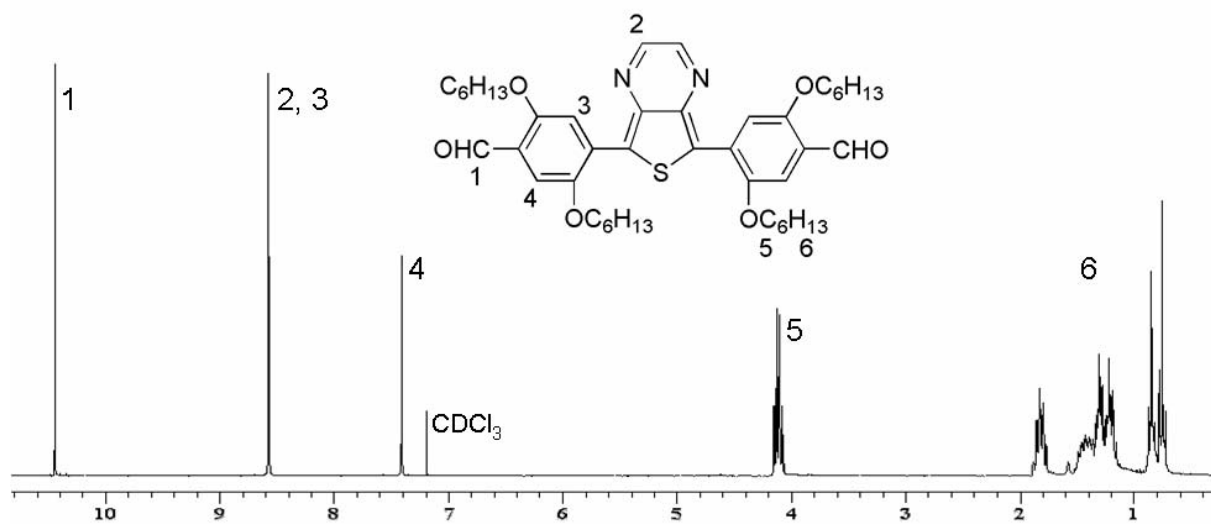
Figure 3.2. ^{1}HNMR of monomer **M-2**.

In case of **M-3** signals of phenyl protons adjacent to thiophene ring were detected at 8.51 ppm and those adjacent to aldehydic group were located at 7.55 ppm. The phenylene protons in the vicinity of pyrazine ring appeared downfield at around 7.98 ppm and the other phenylene protons close to alkoxy substituents appeared at 6.92 ppm respectively. Alkoxy protons were detected at 3.92 ppm and alky side chain protons were upfield between 1.78-0.86ppm.
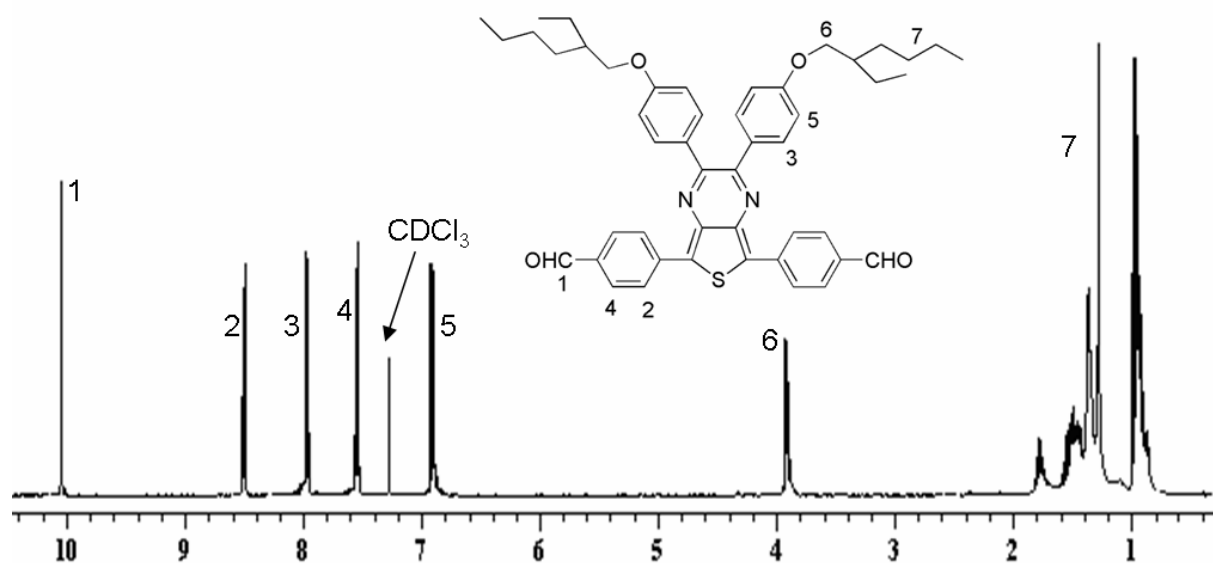
Figure 3.3. ^{1}HNMR of monomer **M-3**.

^{1}HNMR spectrum of monomer **M-4** showed phenyl protons adjacent to thiophene ring downfield at 8.52 and 8.00 ppm respectively. The protons of phenyl substituents at 2,3-position of pyrazine ring appeared between 7.58-7.34 ppm.
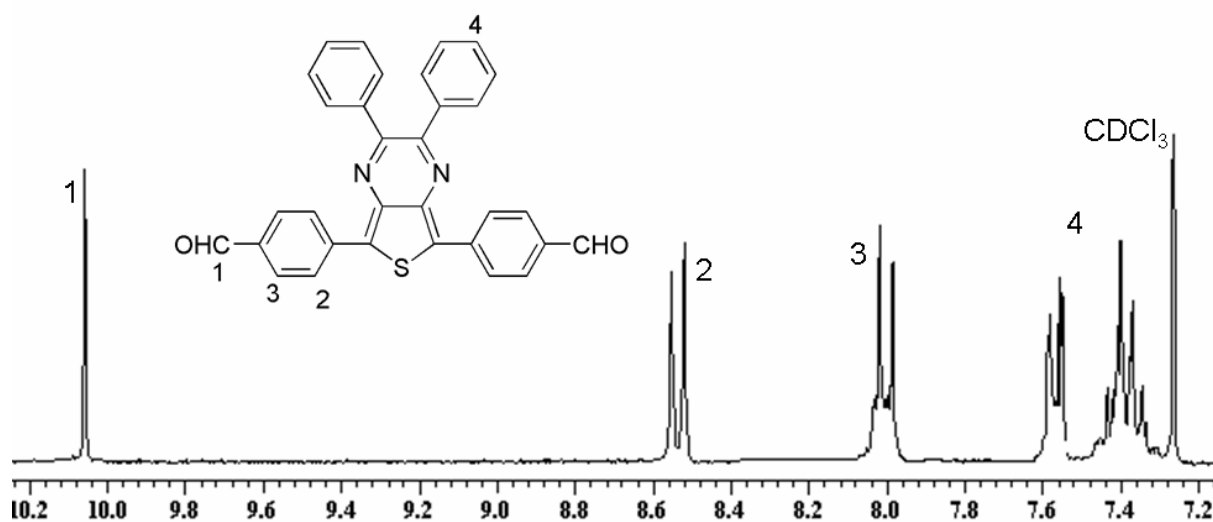
Figure 3.4. ^{1}HNMR of monomer **M-4**.
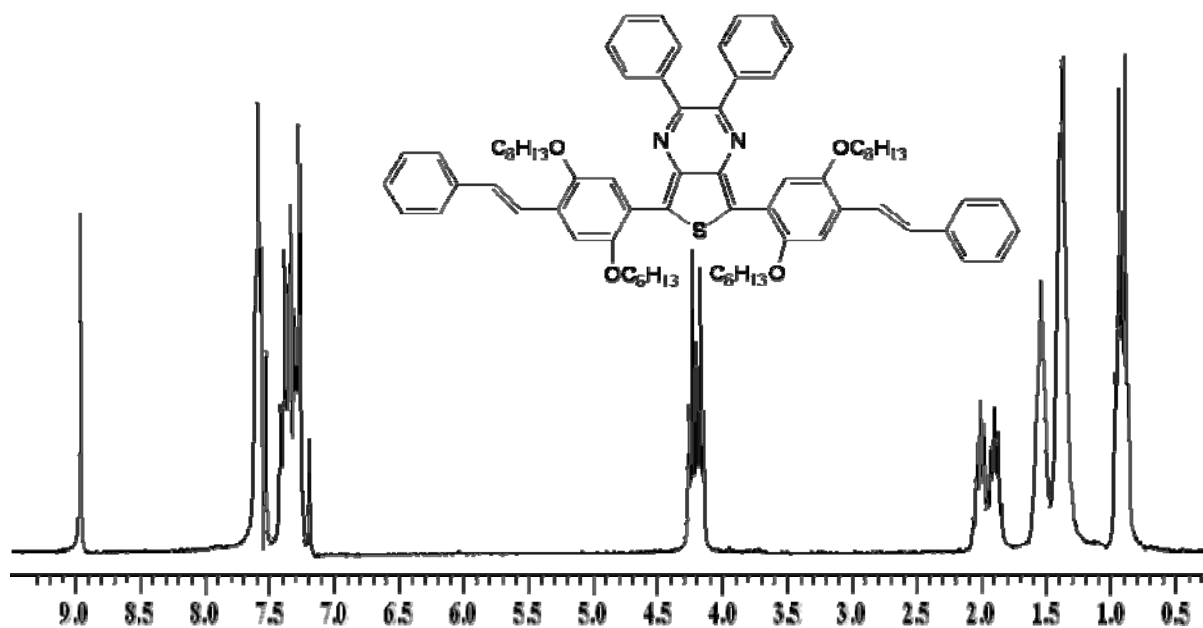
Figure 3.5. ^{1}HNMR of model compound **MD-1**.

^{1}HNMR spectra of model compounds **MD-1-MD-3** are depicted in Figures 3.5-3.7. All the upfield resonances could be readily assigned to side chains protons and those of down field resonances in aromatic region to the backbone protons.
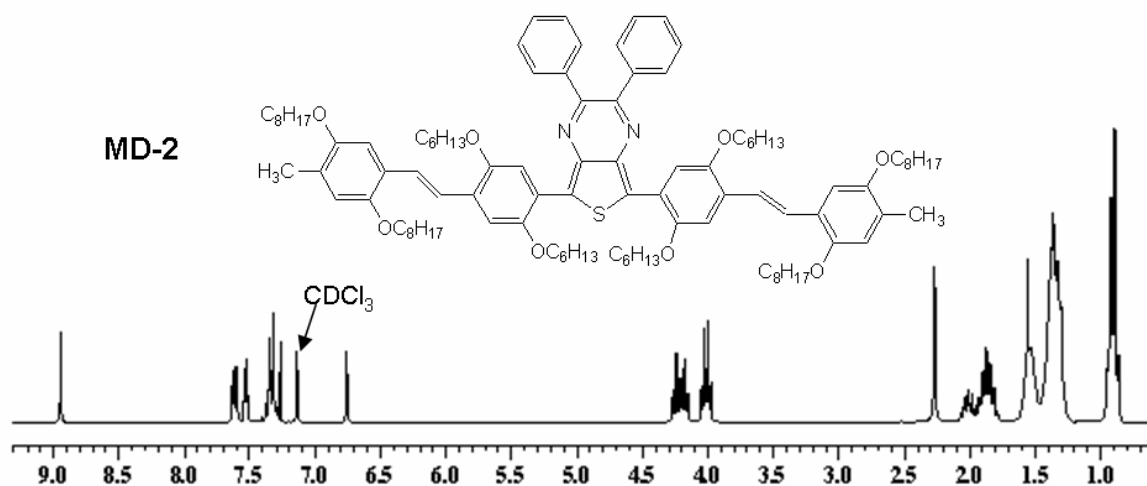
Figure 3.6. ^{1}HNMR of model compound **MD-2**.
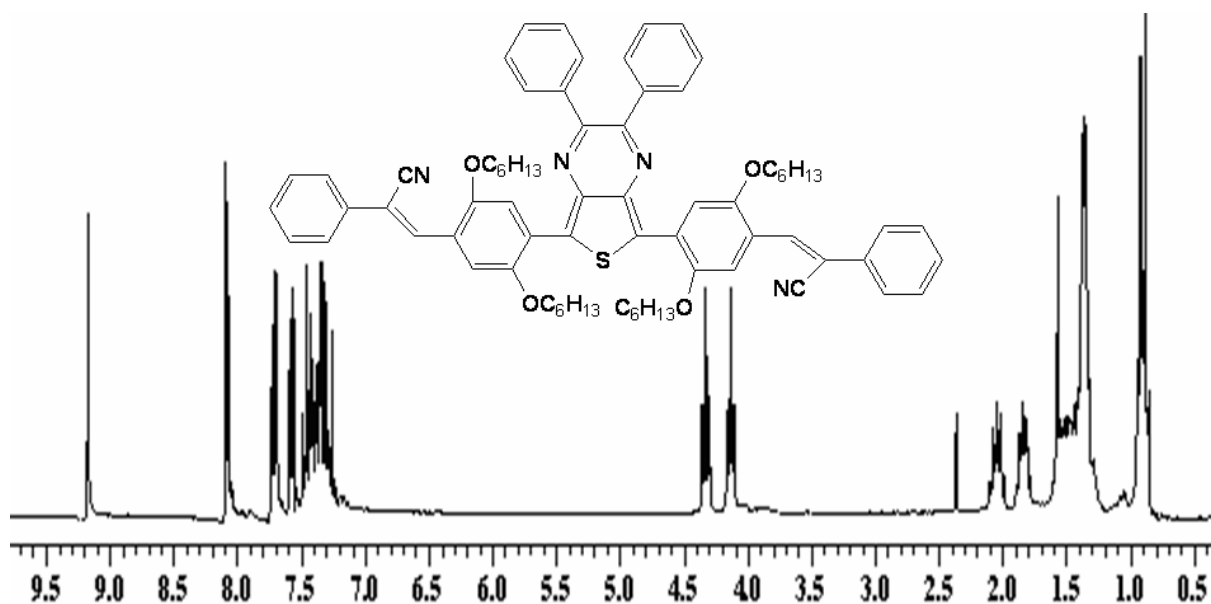
Figure 3.7. ^{1}HNMR of model compound **MD-3**.

3.1.2 Synthesis and Characterization of Polymers

The synthetic strategy employed for the synthesis of poly(heteroarylenevinylene)s (PHAVs) (**P-1-P-6**) was based on Horner polycondensation route,[112] and for Cyano-PHAVs (**P-7-P-9**) Knoevenagel polycondensation,[113] suitable for the synthesis of well-defined strictly alternating copolymers. The molecular structures of the PHAVs are shown in Scheme 3.8. With these synthetic routes, we obtained the PHAVs and CN-PHAVs polymers with high purity and good solubility. After purification and drying polymers were obtained as green solid.

P-5 R_1 = phenyl, R_2 = OC_6H_{13}, R_3 = OC_6H_{13}
P-6 R_1 = H, R_2 = OC_6H_{13}, R_3 = C_6H_{13}

P-7 R_1 = phenyl, R_2 = OC_6H_{13}, R_3 = OC_8H_{17}
P-8 R_1 = H, R_2 = OC_6H_{13}, R_3 = OC_8H_{17}
P-9 R_1 = ethylhexyloxy benzene, R_2 = H, R_3 = OC_8H_{17}
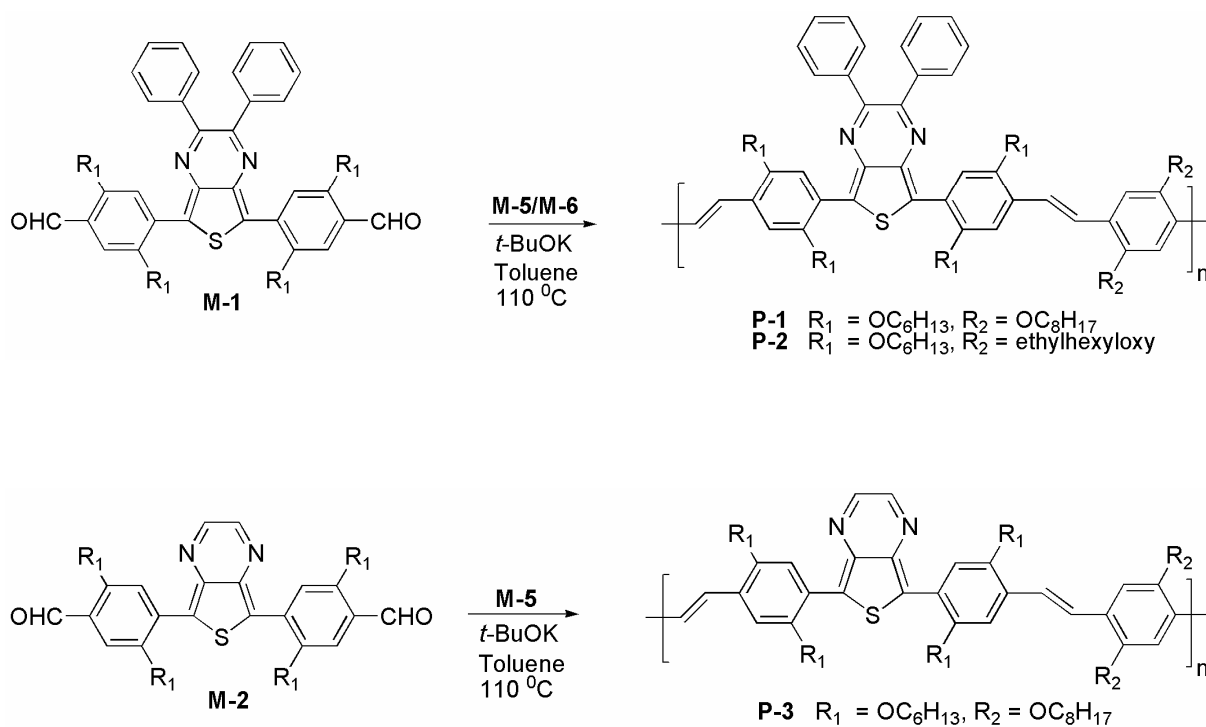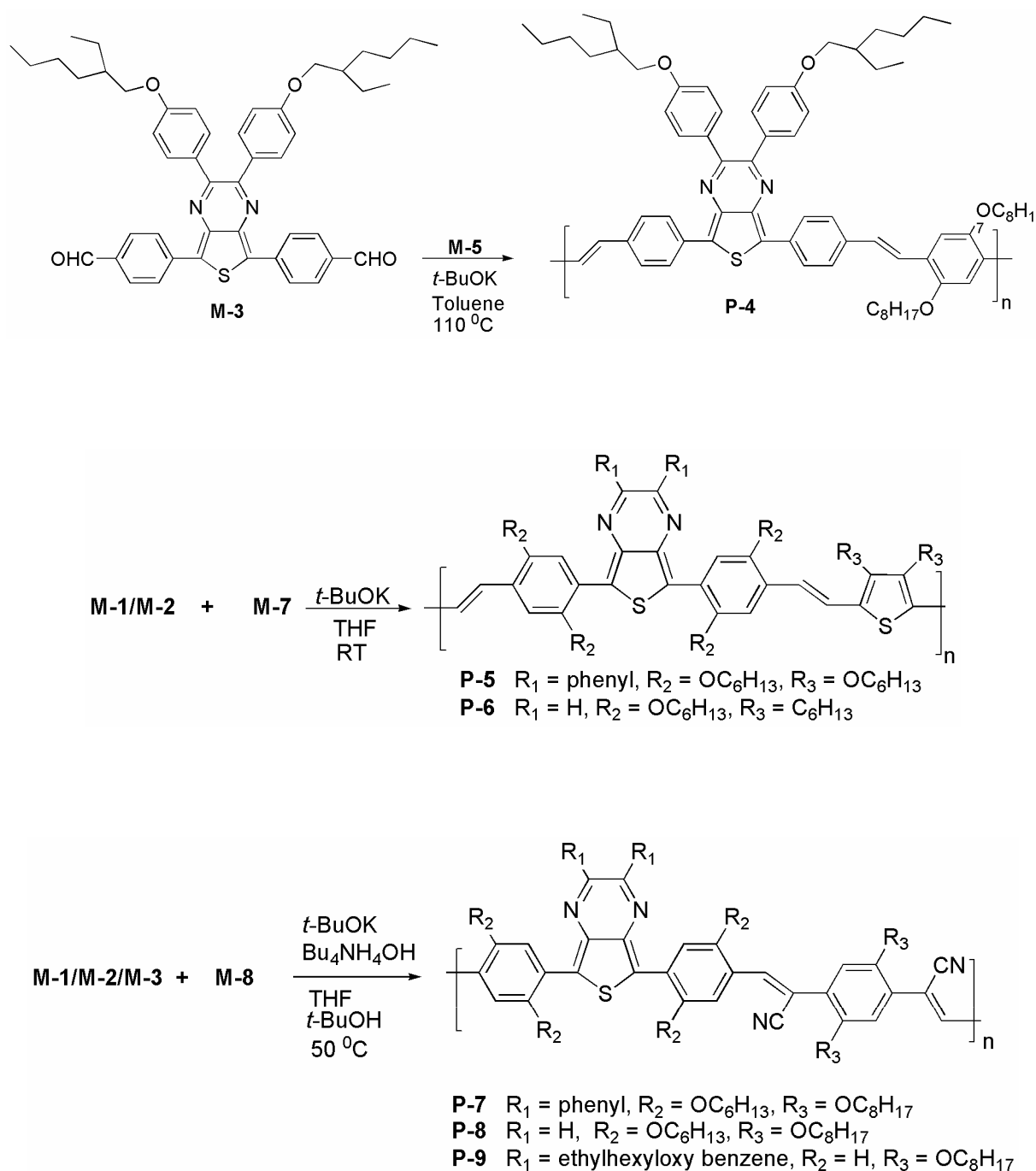
Scheme 3.8. Synthesis of Polymers P-1-P-9.

The chemical structure of the polymers (P-1-P-9) was confirmed by FTIR, ^{1}H, ^{13}C NMR and elemental analysis. ^{1}H NMR data were consistent with the proposed structure of the polymers. Compared with the ^{1}H NMR peaks of monomers, those of the polymers were broadened.
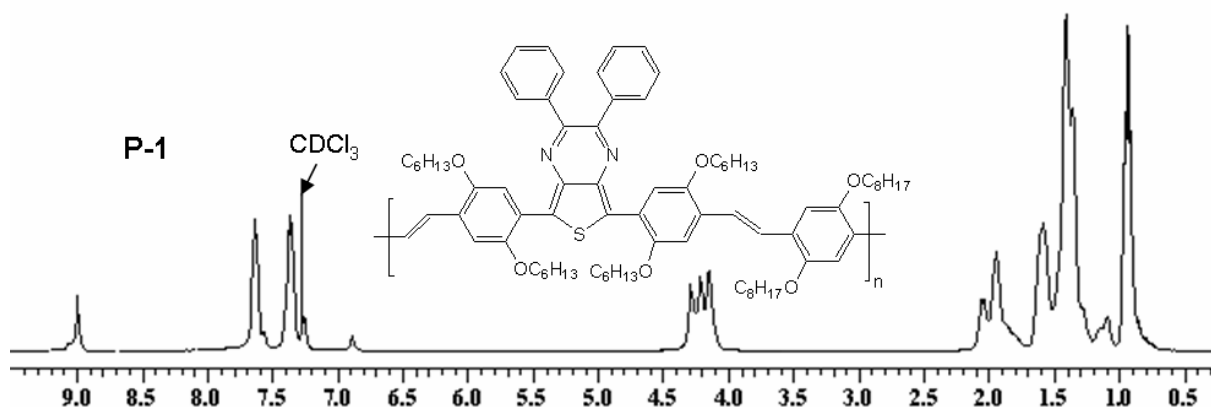
Figure 3.8. ^{1}HNMR of polymer **P-1**.

The ^{1}H NMR spectrum of **P-1** in CDCl$_3$ showed peaks indicating two protons of phenyl rings adjacent to thienopyrazine (5,7-position) at δ = 9.00, while protons of phenyl rings of thienopyrazine unit along two protons of phenyl rings adjacent to thienopyrazine moiety, vinylene and phenyl protons between δ = 7.63-7.26, and phenyl protons at δ = 6.89 ppm respectively. While that of –OCH$_2$ protons alkoxy side chain of phenyl units appeared between δ = 4.29-4.15 and other alkoxy side chain protons signals were present at δ = 2.06-0.93 ppm.
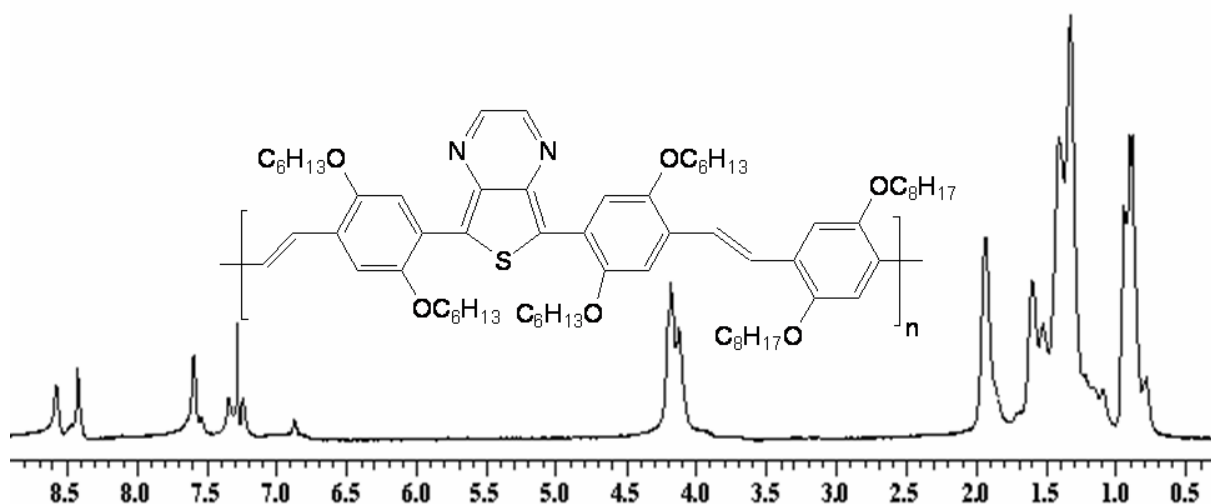
Figure 3.9. ^{1}HNMR of polymer **P-3**.

Similarly the ^{1}H NMR spectrum of **P-3** in CDCl$_3$ showed peaks indicating protons of thienopyrazine unit at δ = 8.57, phenyl rings adjacent to thienopyrazine at δ = 8.42, while other protons of phenyl rings adjacent to thienopyrazine moiety at δ = 7.59, vinylene and phenyl protons between δ = 7.34-6.87 ppm respectively. While that of –OCH$_2$ protons alkoxy

side chain of phenyl units appeared between δ = 4.20-4.12 and other alkoxy side chain protons signals were present at δ = 1.93-0.88 ppm.
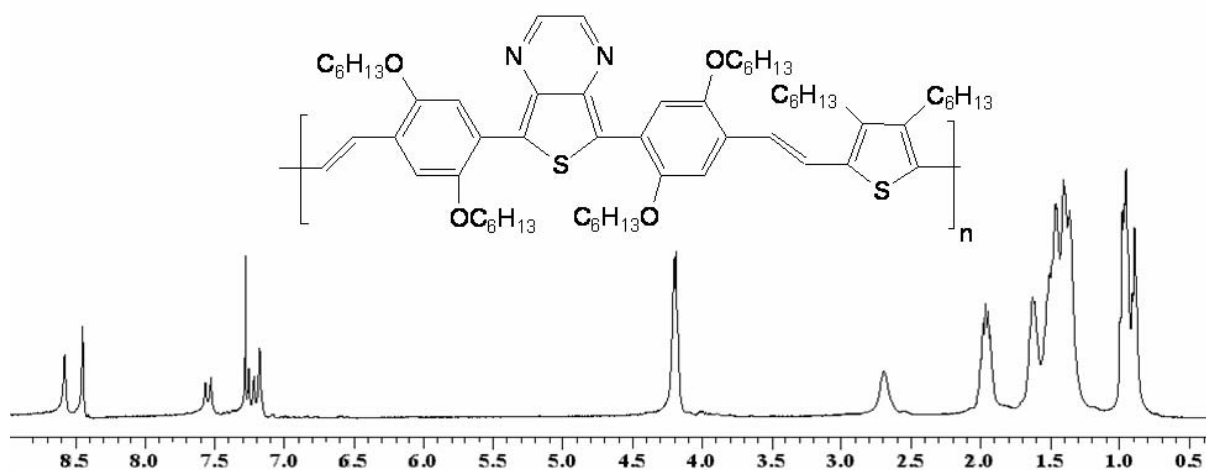
Figure 3.10. ^{1}HNMR of polymer **P-6**.

The ^{1}H NMR spectrum of **P-6** in $CDCl_3$ showed peaks indicating protons of thienopyrazine unit at δ = 8.57, phenyl rings adjacent to thienopyrazine at δ = 8.45, vinylene protons at δ = 7.56-7.52 and δ = 7.25-7.21, while other protons of phenyl rings adjacent to thienopyrazine moiety at δ = 7.17 ppm respectively. While that of –OCH$_2$ protons alkoxy side chain of phenyl units appeared at δ = 4.20, the –CH$_2$ protons of alkyl side chain of thiophene appeared at δ = 2.69 and other alkyl and alkoxy side chain protons signals were present at δ = 2.00-0.83 ppm. (For detailed NMR data of other polymers, see experimental, ^{1}H NMR and ^{13}C NMR spectra are present in appendix).

The average molecular weights of polymers were determined by gel permeation chromatography (GPC) with polystyrene as standards. THF served as eluting solvent. The number-average molecular weight $\overline{M}_n$, values of polymers (**P-1-P-9**) were between 50200-10000 g/mol, leading to degree of polymerisation between 39-9, (see Table 3.1).

Table 3.1. GPC data of polymers **P-1-P-9.**

Polymer	$\overline{M}$n (g/mol)	$\overline{M}$w (g/mol)	PDI	$\overline{P}$n	Yield (%)
P-1	32100	65100	2.0	26	55
P-2	33500	53100	1.5	27	70
P-3	29200	64600	2.2	27	63
P-4	10000	13300	1.5	09	51
P-5	13300	19200	1.4	13	67
P-6	15600	34200	2.1	14	55
P-7	50200	279000	5.0	39	55
P-8	42200	140000	3.3	37	55
P-9	10500	14000	1.9	09	50

Mn, GPC (polystyrene standards).
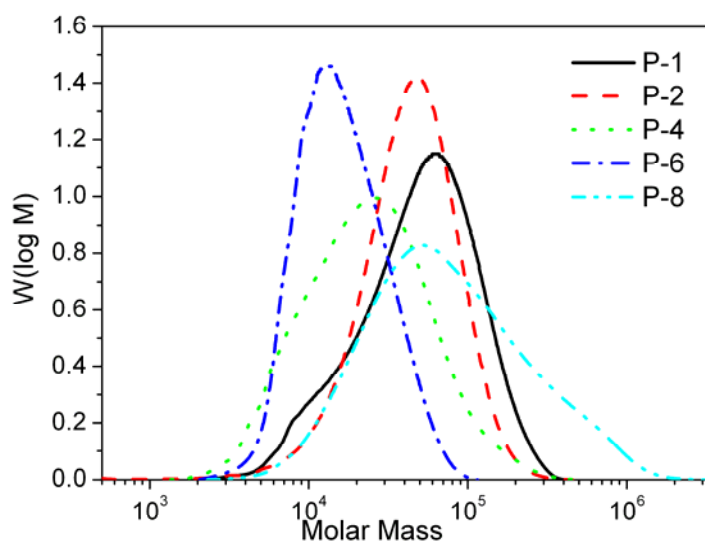
Figure 3.11. GPC curves of polymers **P-1, P-2, P-4, P-6** and **P-8**.

We investigated the thermal properties of these copolymers by thermogravimetric analysis (TGA) and differential scanning calorimetry (DSC) at a rate of 10 K/minute. All the polymers are thermally stable and have 5% weight loss temperatures in air >300 °C. We did not detect any possible phase transition signals during repeated heating/cooling DSC cycles for polymers (**P-1-P-9**). This observation probably results from the stiffness of the polymer's

chains. Obviously, the thermal stability of the PHAVs and CN-PHAVs is adequate for their applications in polymer solar cells and other optoelectronic devices.

3.1.3 Optical Properties of Monomers and Model Compounds

The photophysical characteristics of the new monomers and model compounds were investigated by UV-vis absorption and photoluminescence in dilute chloroform solution as well as in solid state. The optical data of monomers and model compounds are summarized in Table 3.2, namely the absorption peak maxima, λ_a, the absorption coefficients at the peak maxima, log ε, the optical band gap energy, E_g^{opt} (calculated from $\lambda_{10\%max}$, wavelength at which the absorption coefficient has dropped to 10% of the peak value),[114] the emission maxima λ_e, and the fluorescence quantum yields, Φ_{fl}. All emission data given here were obtained after exciting at the wavelength of the main absorption band. Figures 3.12, 3.13 and 3.14 show the absorption and emission spectra of monomers and model compounds.
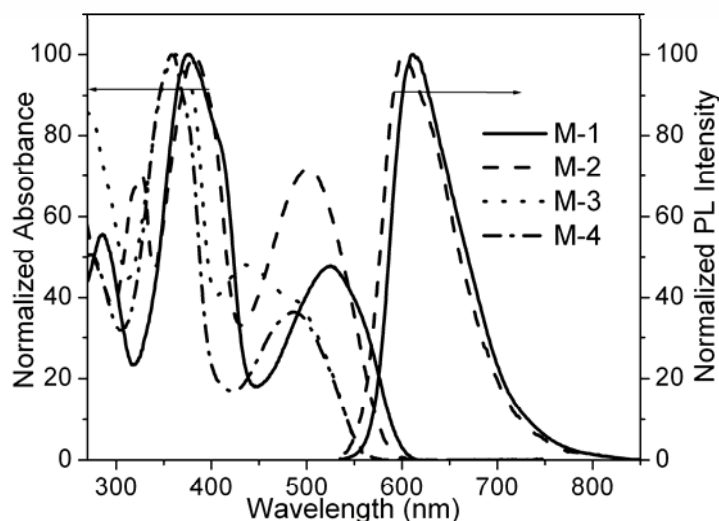
Figure 3.12. UV-vis spectra of **M-1**-**M-4** and emission spectra of **M-1** and **M-2** in solution (Toluene 10^{-7}mol).

The absorption spectra of the monomers (**M-1**-**M-4**) show two peaks located in the UV and visible region from ~358 to ~ 525 nm.The absorption maxima of monomers **M-1** and **M-2** are red shifted relative to **M-3** and **M-4**, due to presence of electron donor alkoxy phenylene adjacent to thienopyrazine moiety (see Figure 3.12). This indicates the substituent effect is more pronounced at 5 and 7 position of thieno[3,4-*b*]pyrazine. Presence of strong donor groups at these positions leads to a red shift in absorption spectra.

Table 3.2. Optical Data of Monomers (**M-1-M-4**) and Model Compounds (**MD-1-MD-3**) in Dilute Toluene Solution ($\sim 10^{-7}$ M) and in Solid State.[b]

Compound	UV-vis λ_{max}, nm				E_g opt. eV[c]		PL[d] λ_{em}, nm		% ϕ_{fl}
	Toluene (log ε)[a]	$\lambda_{0.1max}$ (nm)	film[b]	$\lambda_{0.1max}$ (nm)	Toluene	film	Toluene	film	Toluene
M-1	377, 525 (4.3)(4.3)	662	-		1.87		612		69
M-2	382, 499 (4.4)(4.5)	638	-		1.94		665		73
M-3	361, 436 (4.7)(4.3)	659	-		2.20	-	-	-	-
M-4	358, 487 (4.3)(4.3)	662	-		1.87	-	-	-	-
MD-1	399, 564 (4.7)(4.2)	660	325,545	596	1.87	2.08	684	634	20
MD-2	412, 575 (4.8)(4.4)	676	437,626	720	1.83	1.72	694	726	11
MD-3	433, 567 (4.7)(4.5)	650	449,597	692	1.90	1.79	668	697	30

[a]Molar absorption coefficient. Molarity is based on the repeating unit. [b]Spin coated from chlorobenzene solution. [c]$E_g^{opt} = hc / \lambda_{0.1max}$. [d]Photoluminescence data.
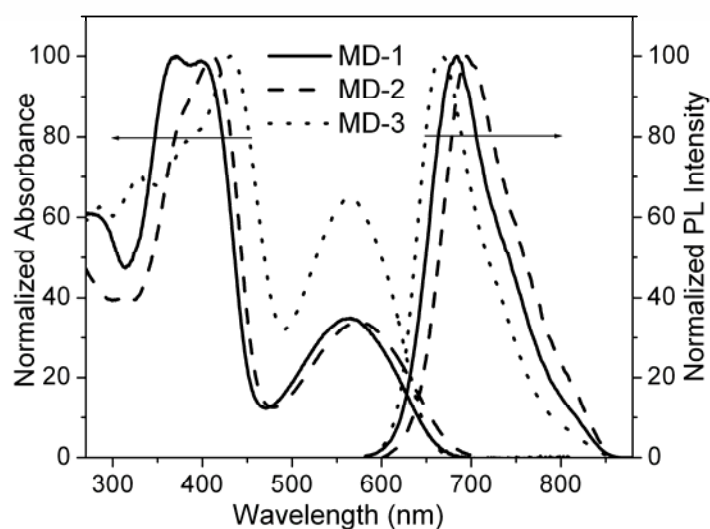
Figure 3.13. Normalized UV-vis and emission spectra of **MD-1**, **MD-2** and **MD-3** in solution (Toluene 10^{-7} mol).

The absorption maxima of model compounds **(MD-1-MD-3)** are red shifted relative to monomers (see Figures 3.13 and 3.14). Obviously, increase in conjugation length is the reason for this red shift.
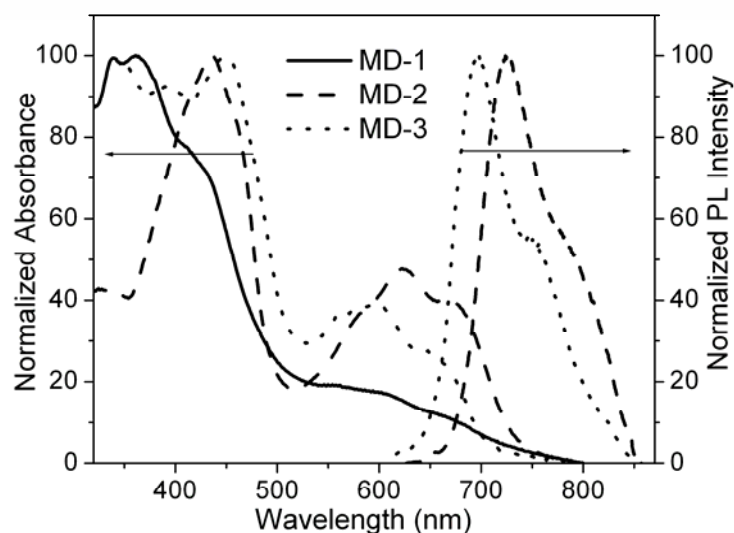
Figure 3.14. Normalized UV-vis of **MD-1**, **MD-2** and **MD-3** and emission spectra of **MD-2** and **MD-3** in solid state. (film from chlorobenzene)

3.1.4 Optical Properties of Polymers

In comparison to monomers and model compounds, the respective polymers (**P-1-P-9**)**,** show a red-shift in the UV absorption maxima (see Figure 3.15-3.20 and Tables 3.3-3.4). The differences in absorption can be probably due to higher number of repeating units of polymers **P-1-P-9** and hence an increase in effective conjugation length.[115]
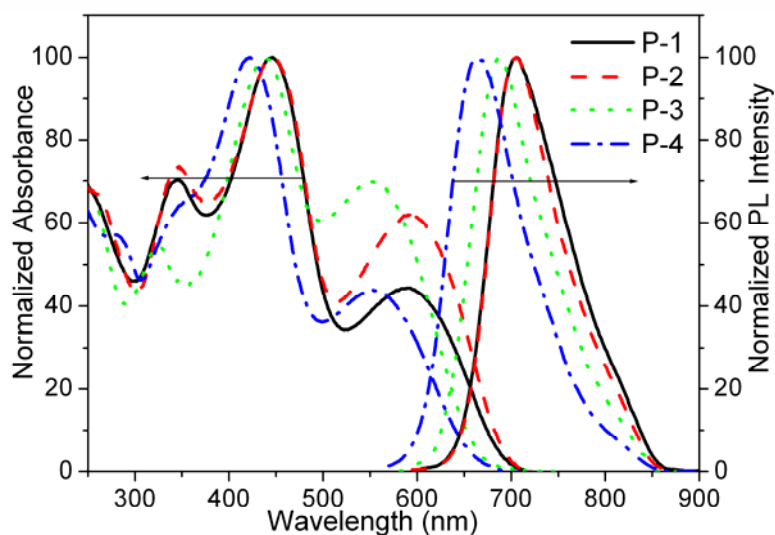
Figure 3.15. Normalized UV-vis and emission spectra of **P-1**, **P-2, P-3** and **P-4** in solution (Toluene 10^{-7}mol).

The copolymers, **P-5** and **P-6**, show the lowest energy absorption peak at a longer wavelength than the polymers (**P-1, P-2, P-3, P-4, P-7, P-8** and **P-9**) presumably owing to the presence of the strong electron donating alkyl thiophene units to give an enhanced intermolecular CT (charge transfer) interaction in these copolymers.
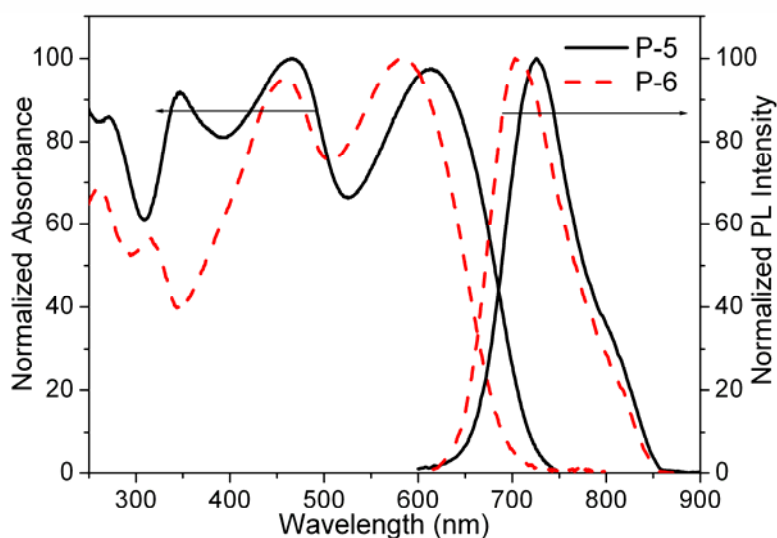
Figure 3.16. Normalized UV-vis and emission spectra of **P-5** and **P-6** in solution (Toluene 10^{-7}mol).

While, in case of polymers **P-4** and **P-9** due to presence of phenyl instead of alkoxy phenyl or alkylthiophene adjacent to thienopyrazine, a blue shift was observed relative to other polymers.
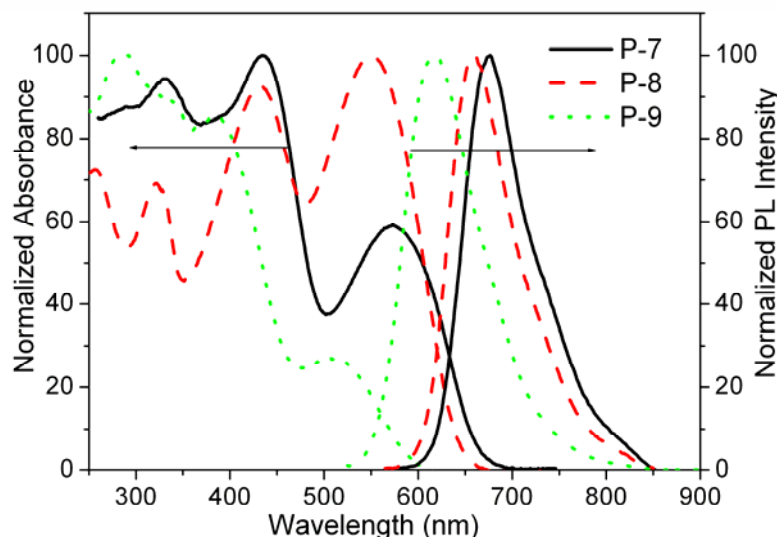
Figure 3.17. Normalized UV-vis and emission spectra of **P-7, P-8** and **P-9** in solution (Toluene 10^{-7}mol).

The polymers **P-1-P-9** show a strong red shift of λ_{max} (approximately 29-61 nm) when spin cast into thin films on quartz substrate from a chlorobenzene solution (see Figures 3.18-3.20).
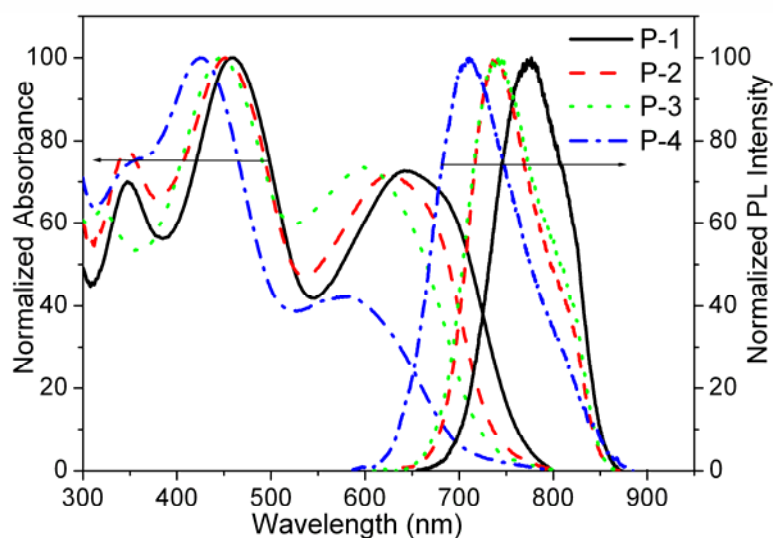
Figure 3.18. Normalized UV-vis and emission spectra of **P-1**, **P-2, P-3** and **P-4** in solid state. (film from chlorobenzene)

This indicates enhanced interchain interactions due to stacking of the polymers in the solid state, possibly assisted by planarization and with it an increase of conjugation length.[116] As anticipated, the alternation of electron-rich alkoxy phenylene/ alkyl thiophene and electron-deficient thienopyrazine units along conjugated backbone results in a low optical band gap (~1.56-2.08 eV).

Table 3.3. UV-Vis Data of polymers **P-1-P-9** in Dilute CHCl$_3$ Solution and in Solid State (Thin Films of 100-150 nm Thickness Spin-Casted from Chlorobenzene Solution).

Polymer	UV-vis $\lambda_{max,}$ nm				E_g opt. eV^c	
	Toluene (log ε)^a	$\lambda_{0.1max}$ (nm)	film^b	$\lambda_{0.1max}$ (nm)	Toluene	film
P-1	458, 589 (4.5)(4.2)	690	462, 650	750	1.80	1.65
P-2	446, 592 (4.6)(4.5)	689	450, 624	735	1.80	1.69
P-3	437, 552 (4.5)(4.4)	659	448, 608	721	1.88	1.72
P-4	422, 553 (4.7)(4.3)	659	428, 582	685	1.88	1.81
P-5	465, 615 (4.5)(4.5)	718	468, 650	790	1.72	1.57
P-6	458, 585 (4.5)(4.5)	689	467, 645	795	1.80	1.56
P-7	434, 573 (4.3)(4.3)	660	449, 614	721	1.87	1.72
P-8	432, 550 (4.4)(4.5)	676	435, 596	713	1.94	1.74
P-9	387, 511 (4.4)(3.9)	592	384, 518	596	2.09	2.08

^{a}Molar absorption coefficient. Molarity is based on the repeating unit. ^{b}Spin coated from chlorobenzene solution. ^{c}$E_g^{opt} = hc / \lambda_{0.1max}$. ^{d}Photoluminescence data.

The emission maxima of **P-1**, **P-2** and **P-6** in dilute chloroform solution are at $\lambda_{max,em} \sim 705$ nm, while the emission curves of **P-3, P-4** and **P-5**, showing their maxima at $\lambda_{max,em} = 690$, 665 and 726 nm, respectively. The fluorescence quantum yields were found to be around 03-33% for **P-1-P-9**.
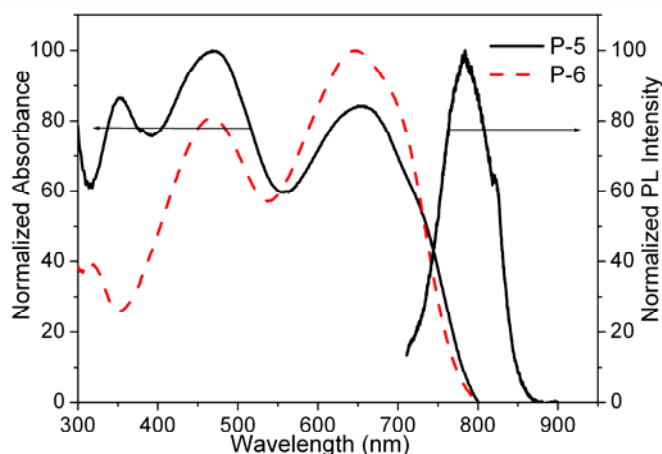
Figure 3.19. Normalized UV-vis of **P-5** and **P-6** and emission spectrum of **P-5** in solid state. (film from chlorobenzene)

The emission maxima of polymers (**P-1-P-9)** (except for **P-6**, no emission was observed) in solid film are red shifted than in solution, and a lower fluorescence quantum yield around 01-10% observed (Figures 3.18-3.20). We assumed, the reason for the low photoluminescence (PL) efficiency is a π-π stacking of the conjugated backbone cofacial to each other due to the favourable inter-chain π-π interactions, which lead to a self-quenching process of the excitons.[23-25]
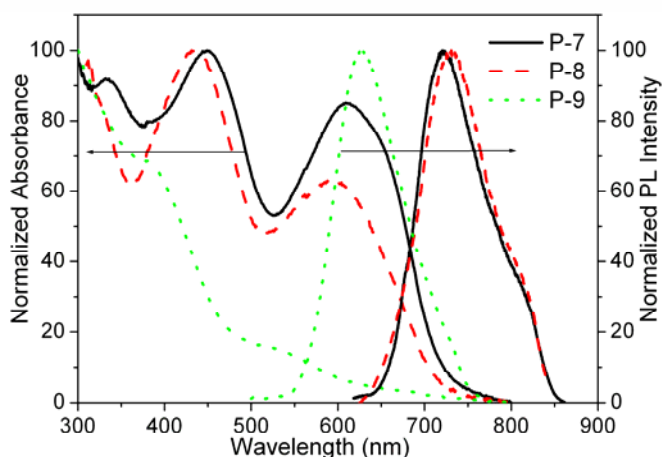
Figure 3.20. Normalized UV-vis and emission spectra of **P-7, P-8** and **P-9** in solid state. (film from chlorobenzene)

Table 3.4. Photoluminescence Data of **P-1-P-9** in Dilute Toluene Solution (~ 10^{-7} M) and in Solid State.[a]

Poly-mer	PL[b] $\lambda_{em,}$ nm		Stokes Shift		$\lambda_{0-0,}$ nm		E_g^{0-0}		% ϕ_{fl}	
	Toluene	film	Toluene	film	Toluene	film	Toluene	film	Toluene	film
P-1	706	772	117	122	658	725	1.88	1.71	07	1
P-2	705	738	113	114	662	698	1.87	1.77	09	1
P-3	690	742	138	134	636	693	1.94	1.78	07	1
P-4	665	713	112	131	615	652	2.01	1.90	17	1
P-5	726	785	111	135	686	745	1.80	1.66	03	0
P-6	703	000	118	-	664	-	1.86	-	03	0
P-7	677	722	104	108	634	684	1.95	1.81	07	5
P-8	658	682	108	86	620	674	2.00	1.83	20	5
P-9	619	627	108	109	561	565	2.21	2.19	33	10

[a]Spin coated from chlorobenzene solution. [b]Photoluminescence data.

The Stokes shifts between the absorption and emission of the polymers **P-1-P-9** are relatively large (between 104-138 nm in solution and 86-135 nm in film). Usually the Stokes shift comes from the two sources: emission either from the excited segments of a conjugated polymer undergoing deformation into more planar conformation along the chain or from the migrated excitons in other segments where ring rotations are not hindered.[117] The absence of substituents at 2,3-position of thienopyrazine moiety enable strong π-π interchain interaction, leading to the formation of excimers which provide radiationless decay channels for the excited states and hence resulting in larger Stokes shifts in case of polymer **P-3** and lower fluorescence quantum yields.[118-120] The presence of bulky substituents at 2,3-position of thienopyrazine moiety hinders strong π-π interchain interactions, less chances of excimer formation and hence relatively small Stokes shifts and better fluorescence quantum yields in case of polymers **P-7, P-8** and **P-9**.

3.1.5 Thermal Annealing Effect of P-1, P-2 and P-5 Films.

To get information about the molecular packing and effect of thermal annealing on polymer films, we performed thermal annealing of polymer films being prepared from a chlorobenzene

solution at different temperatures. At each temperature gradient the polymer film was annealed for 10 minutes, cooled to room temperature and UV absorption was measured.

As mentioned above, the visible absorption spectra of **P-1, P-2** and **P-5** films red-shifted obviously in comparison with their solution. The visible absorption peak of the polymer **P-1** film remain unchanged after the films were treated at 80, 100, 110, 125 and 150 °C for 10 min, as shown in Figure 3.21.
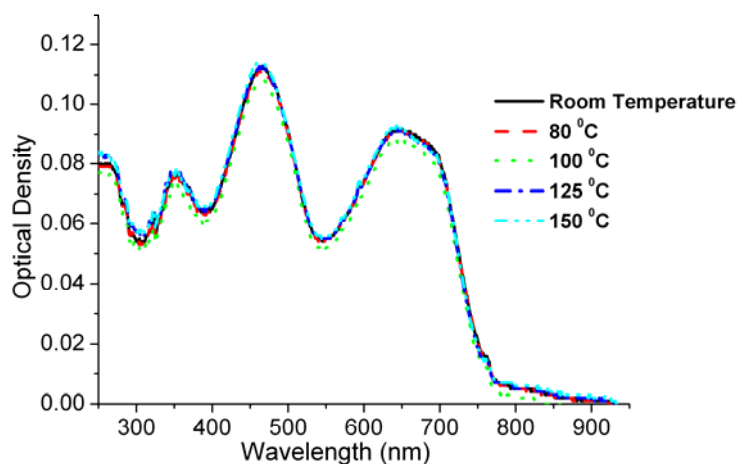
Figure 3.21. UV-vis spectra of **P-1** in solid state at different temperatures. (film from chlorobenzene)

In case of polymer **P-2**, the visible absorption peak was lowered in intensity by thermal annealing, and the second band almost disappear by annealing at 130 ^{0}C. The chromophore system is apparently destroyed.
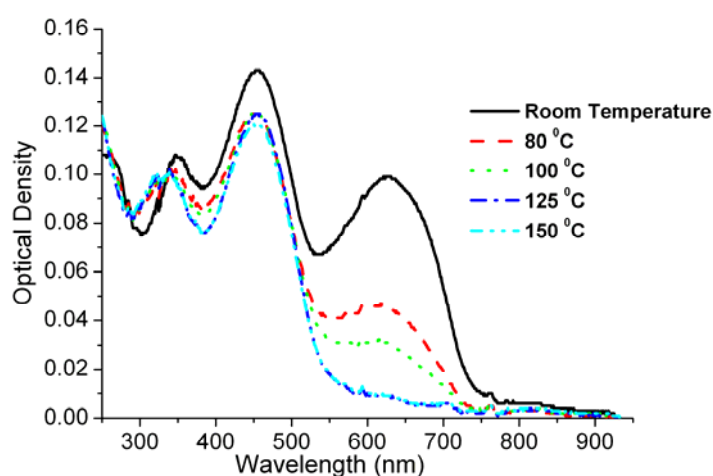
Figure 3.22. UV-vis spectra of **P-2** in solid state at different temperatures. (film from chlorobenzene)

In case of polymer **P-5**, the visible absorption peak was slightly red-shifted further to 675 nm after the films were treated at 130 °C for 10 min, as shown in Figure 3.23. After the thermal annealing, the band gap of the polymer calculated from the absorption edge is 1.53 eV. This phenomenon was also observed in some other polythiophene derivatives. For example, when the film of regioregular poly- [3-(4-octylphenyl)thiophene] (P3OPT) was thermally annealed or treated in chloroform vapor, its band gap reduced from 2.1 to 1.85 eV, along with significant increase of structure ordering.[121] When the film was thermally annealed, the macromolecular chains of the polymer could realign, and then the conjugation effect could be enhanced. So the band gap of the polymers, which determines the absorption of the π-π* transition of the main chain, could be decreased after the thermal annealing.
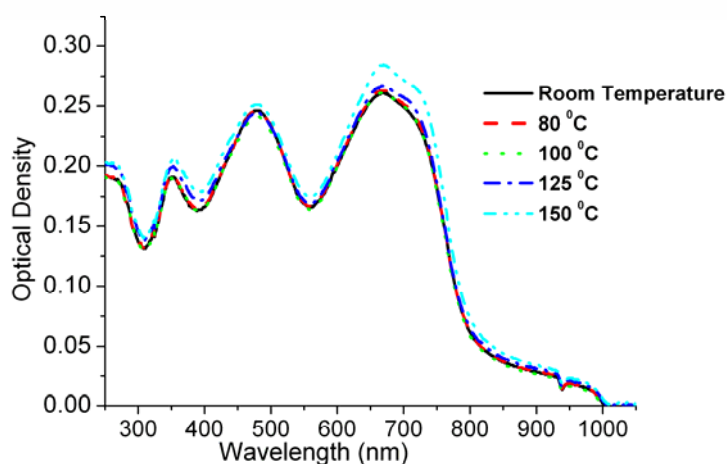
Figure 3.23. UV-vis spectra of **P-5** in solid state at different temperatures. (film from chlorobenzene)

3.1.6 Aggregate Formation in Solvent/Nonsolvent Solution

In order to obtain further information on the assumed self assembly of these polymers and aggregation, the absorption and emission spectra of polymers **P-1, P-2** and **P-8** in chloroform/methanol mixtures with different volume concentrations of methanol are shown in Figures 3.24, 3.25 and 3.26, respectively.
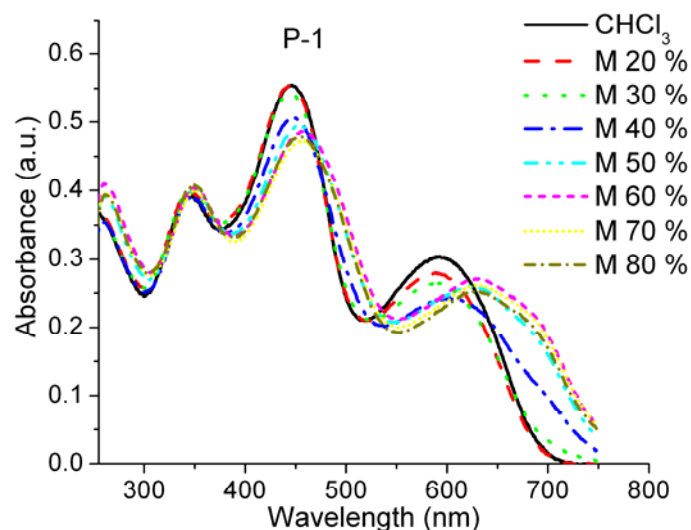
Figure 3.24. UV-vis spectra of **P-1** in CHCl$_3$ with different concentration of MeOH.

It should be noted here that in all cases the bulk solution maintains homogeneity. With an increase of methanol concentration, the second absorption band of these polymers is red shifted. Addition of methanol to the chloroform solution of **P-1, P-2** and **P-8** led to a change in the λ_{max} and above 50 % Vol. of methanol, a decrease in the intensity of the first band and a shift in second band at higher wavelength was observed. Clearly, the presence of significant amount of nonsolvent (methanol) in solution makes solute-solvent interaction energetically less favorable, thereby forcing polymer chain segments to approach each other for aggregate formation.
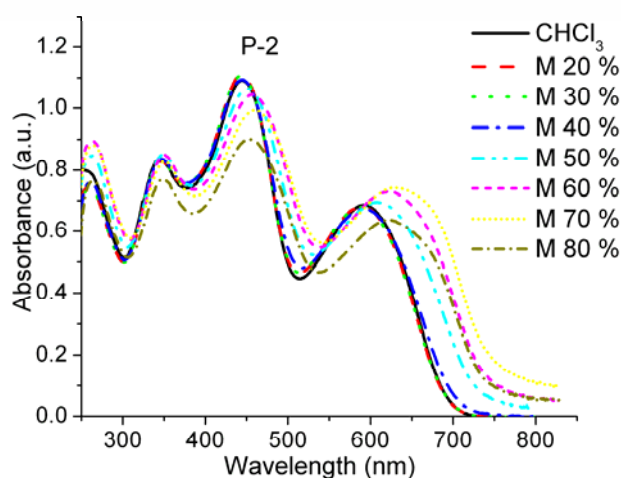
Figure 3.25. UV-vis spectra of **P-2** in CHCl$_3$ with different concentration of MeOH.

The aggregate band in solution occurred at nearly the same wavelength as that in the spin-cast film of these polymers, clearly showing that the aggregate structure retained in the film state once formed in solution. Similar phenomena were found in chloroform/methanol solutions of many conjugated polymers.[122]
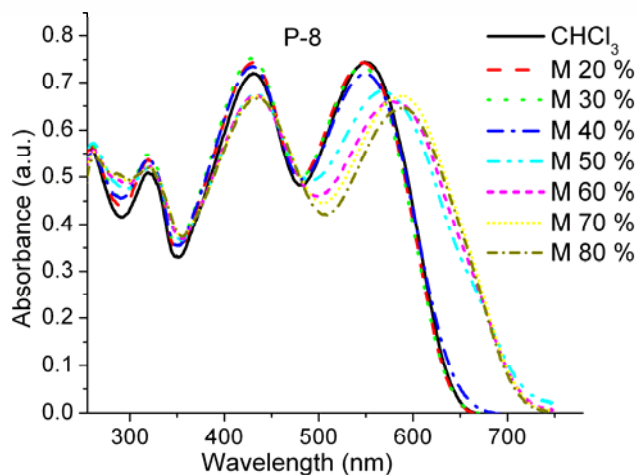
Figure 3.26. UV-vis spectra of **P-8** in $CHCl_3$ with different concentration of MeOH.

3.1.7 Electrochemical Studies of Model Compounds and Polymers

The cyclic and square-wave voltammetry were carried out using thin films of polymers prepared from dichloromethane(5 mg/mL) in acetonitrile at a potential scan rate of 15 mV/s. Ag/AgCl served as the reference electrode; it was calibrated with ferrocene ($E^{1/2}_{ferrocene} = 0.52$ V vs Ag/ AgCl). The supporting electrolyte was tetrabutylammonium hexafluorophosphate (n-Bu$_4$NPF$_6$) in anhydrous acetonitrile (0.1 M). The onset potentials are the values obtained from the intersection of the two tangents drawn at the rising current and the baseline charging current of the CV curves. Several ways to evaluate HOMO and LUMO energy levels from the onset potentials, $E^{ox/onset}$ and $E^{red/onset}$, have been proposed in the literature.[123-130] These were estimated here on the basis of the reference energy level of ferrocene (4.8 eV below the vacuum level)[126,127] according to the following equation:

$$E^{HOMO/LUMO} = [\text{-}(E_{onset\ (vs.\ Ag/AgCl)} - E_{onset\ (Fc/Fc+\ vs.\ Ag/AgCl)})] - 4.8\ eV.$$

The onset and the peak potentials, the electrochemical band gap energy, and the estimated position of the upper edge of the valence band (HOMO) and of the lower edge of conduction band (LUMO) are listed in Table 3.5.
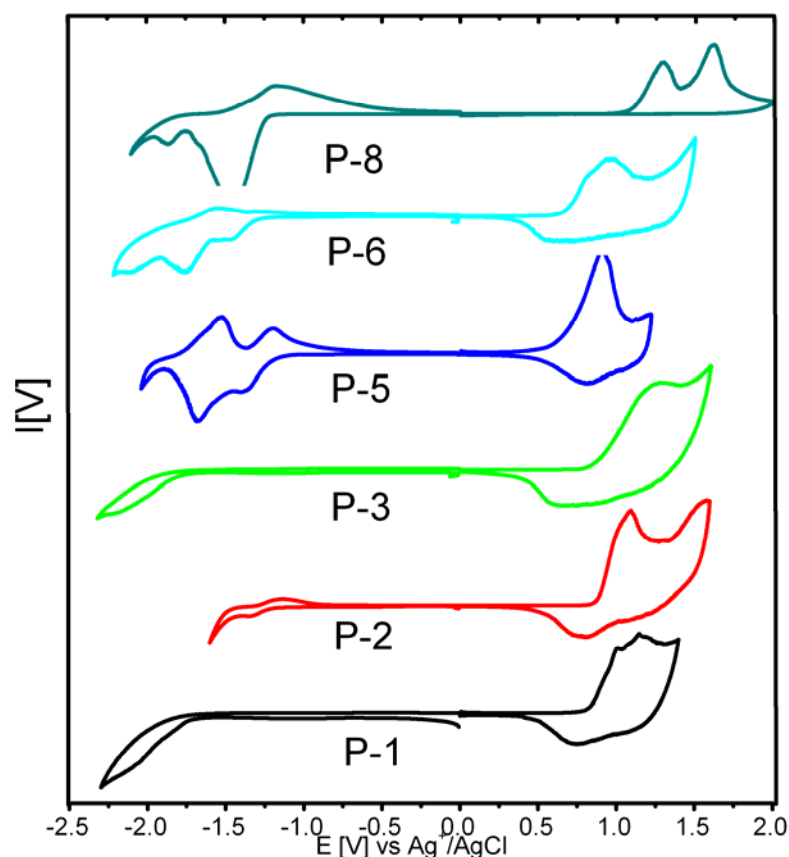
Figure 3.27. Cyclic voltammetry-curves of polymers (**P-1**-**P-6** and **P-8**) in 0.1M TBAPF$_6$/CH$_3$CN at 25 ^{0}C.

All the electrochemical data for the polymers (**P-1**, **P-2**, **P-3, P-5** and **P-6**) obtained from the films are listed in Table 3.5. As shown by the cyclic voltammograms in Figure 3.27, the electrochemical oxidation (or p-doping) of **P-1** starts at about 0.81 V Ag$^+$/Ag and gives p-doping peak at 1.04 V vs Ag$^+$/Ag, respectively. In a range from 0.0 to 2.0 V vs Ag$^+$/Ag, the film revealed stable in repeated scanning of CV, giving same CV curves. Similarly the oxidation of **P-2** and **P-3** starts at about 0.89 and 0.86 V Ag$^+$/Ag and gives p-doping peaks at 1.15 and 1.25 V Ag$^+$/Ag, respectively. However, oxidation of the polymers **P-5** and **P-6** starts at 0.64 and 0.70 V Ag$^+$/Ag and gives peaks at 0.83 and 0.93 V, respectively. Similarly the reduction of **P-2**, **P-3, P-5** and **P-6** starts at about -1.17, -0.91, -1.19 and -1.26 V Ag$^+$/Ag and gives n-doping peaks at –1.36, -1.09, -1.39 and –1.42 V Ag$^+$/Ag, respectively. In a range from 0.0 to -2.2 V vs Ag$^+$/Ag, the films revealed stable in repeated scanning of CV, giving same CV curves. However, we were not able to determine reduction in case of **P-1**. These moderately negative reduction potentials have been attributed to the electron withdrawing effects of thieno[3,4-*b*]pyrazine moiety.[60] The band gap energy directly measured from CV (*E*g$_{ec/onset}$ between 1.61-2.06 eV) and the optical band gap energy are close to each other. The discrepancy (ΔE_g) of both values lies within the range of error. From the onset potentials,

HOMO and LUMO energy levels were estimated. These values indicate these polymers can be good hole transporting materials making them suitable candidate for hole-injection and transport (Figure 3.28).
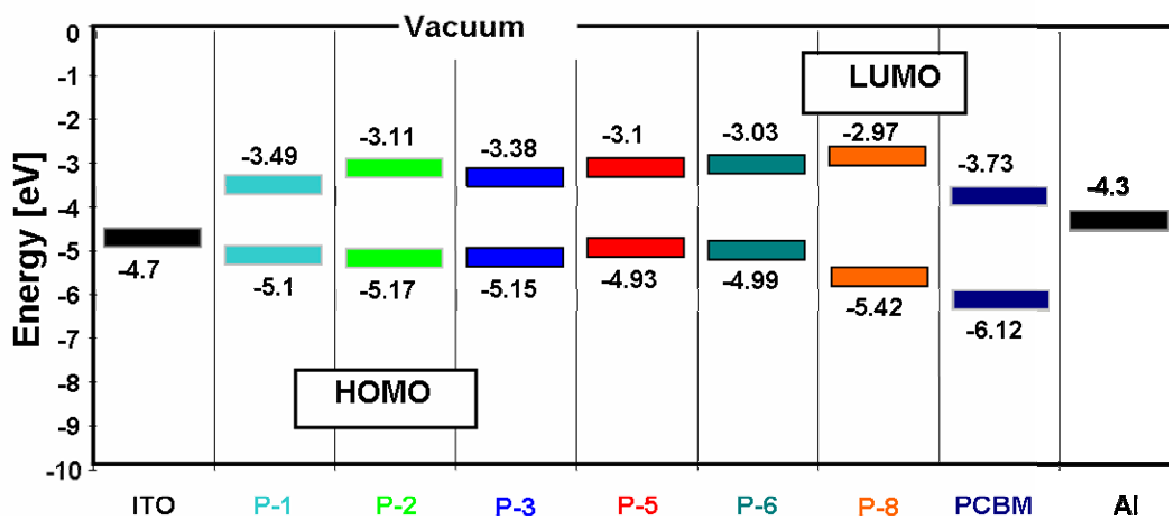
Figure 3.28. Energy Levels of the Polymers (**P-1-P-3, P-5, P-6** and **P-8**) and **PCBM**.

We have also measured the electrochemical data for model compounds in dichloromethane solution. All the three model compounds (**MD-1**, **MD-2** and **MD-3**) show reversible oxidation and reduction peaks (see Figure 3.29). The data is comparable to that of polymers. In Figures 3.27 and 3.29 there are reversible p-doping/dedoping (oxidation/rereduction) processes at positive potential range and n-doping/dedoping (reduction/reoxidation) processes at negative potential range for all the polymers. After repeated cycles of the potential scan, the reproducibility of the cyclic voltammograms is very good, which definitely verifies the reversibility of the p-doping/ dedoping and n-doping/dedoping processes. For the application of conjugated polymers and oligomers to electrochemical capacitors (ECCs), the reversible p-doping and n-doping processes are both needed. The reversible p-doping and n-doping properties of the polymers studied here indicate that these polymers and model compounds could also be promising materials for ECCs.
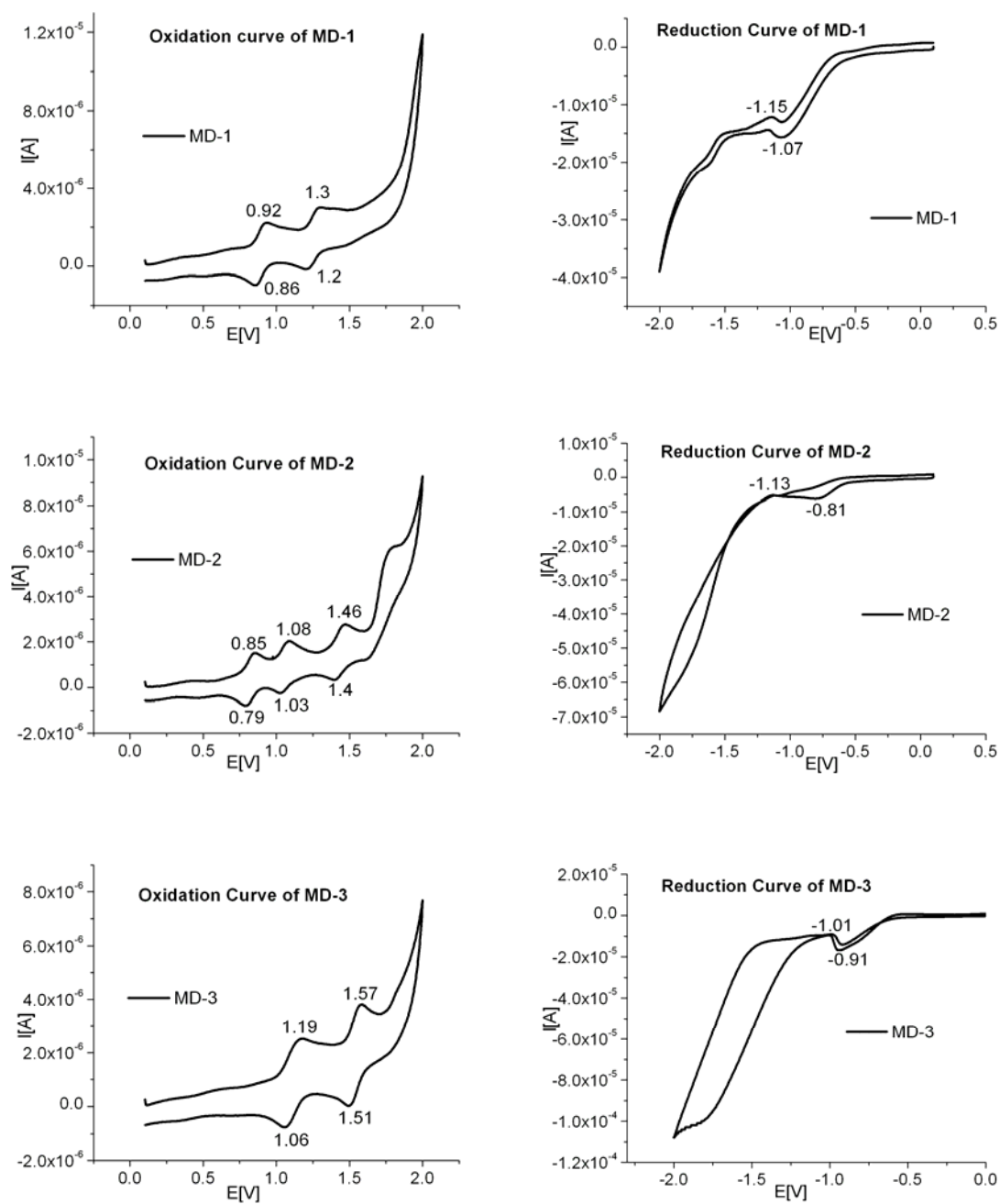
Figure 3.29. Cyclic voltammetry-curves of Model Compounds (**MD-1-MD-3**) in 0.1M TBAPF$_6$/CH$_3$CN at 25 ^{0}C.

Table 3.5. Electrochemical Potentials and Energy Levels of the Polymers **P-1, P-2, P-3, P-5, P-6, P-8** and Model Compounds (**MD-1-MD-3**).

Polymer	Oxidation Potential		Reduction Potential		Energy Levels[b]		Band Gap	
	E_{ox}^{a}	$E_{onset, Ox}$	E_{red}^{a}	$E_{onset, Red}$	HOMO	LUMO	E_g^{ec}	E_g^{opt}
	(V vs Ag/Ag$^+$)		(V vs Ag/Ag$^+$)		(eV)	(eV)		
P-1	1.04	0.81	----	----	-5.10	-3.49^a	1.61	1.61
P-2	1.15	0.89	-1.36	-1.17	-5.17	-3.11	2.06	1.68
P-3	1.25	0.86	-1.09	-0.91	-5.15	-3.38	1.77	1.72
P-5	0.83	0.64	-1.39	-1.19	-4.93	-3.10	1.83	1.55
P-6	0.93	0.70	-1.42	-1.26	-4.99	-3.03	1.96	1.56
P-8	1.31	1.13	-1.60	-1.32	-5.42	-2.97	2.45	1.72
MD-1	0.92	0.82	-1.07	-0.90	-5.11	-3.39	1.72	1.84
MD-2	0.85	0.78	-0.81	-0.73	-5.07	-3.56	1.51	1.72
MD-3	1.19	1.05	-0.91	-0.78	-5.34	-3.51	1.83	1.79

[a]Reduction and oxidation potential measured by cyclic voltammetry. [b]Calculated from the reduction and oxidation potentials assuming the absolute energy level of ferrocene/ferrocenium to be 4.8 eV below vacuum.

3.1.8 Photovoltaic Properties of Polymers P-1, P-2 and P-5

Thermal annealing of polymers and PCBM blends:

Blends of polymers **P-1**, **P-2** and **P-5** with well known acceptor **PCBM** (1:4) were spin coated from chlorobenzene solution on a quartz glass and thermally treated at different temperatures as shown in Figures 3.30-3.32.

In case of polymer **P-1:PCBM** (1:4) blend, there was no change in UV-absorption of film, when it was treated at 80 ^{0}C, 100 ^{0}C and 125 ^{0}C for 5 minutes at each temperature gradient. However, there is a slight change in absorption of film when it was thermally treated at 150 ^{0}C for 5 minutes. The intensity of band at ~ 440 nm is increased mainly due to formation of large aggregate or clusters of PCBM in blend. The colour of film was olive green before and after thermal annealing.
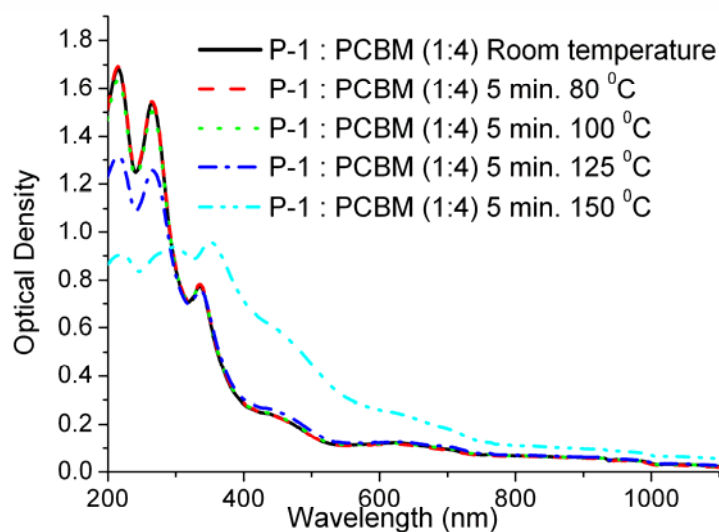
Figure 3.30. UV-vis spectra of **P-1:PCBM** (1:4) in solid state at different temperatures. (film from chlorobenzene)

Similarly in case of polymer **P-2:PCBM** (1:4) blend, there was no change in UV-absorption of film, when it was treated at 80 ^{0}C, 100 ^{0}C and 125 ^{0}C for 5 minutes at each temperature gradient. However, there is a slight change in absorption of film when it was thermally treated at 150 ^{0}C for 5 minutes. The intensity of band at ~ 440 nm is increased mainly due to formation of large aggregate or clusters of PCBM in blend. In case of polymer **P-2**, the colour of film was also olive green before and after thermal annealing.
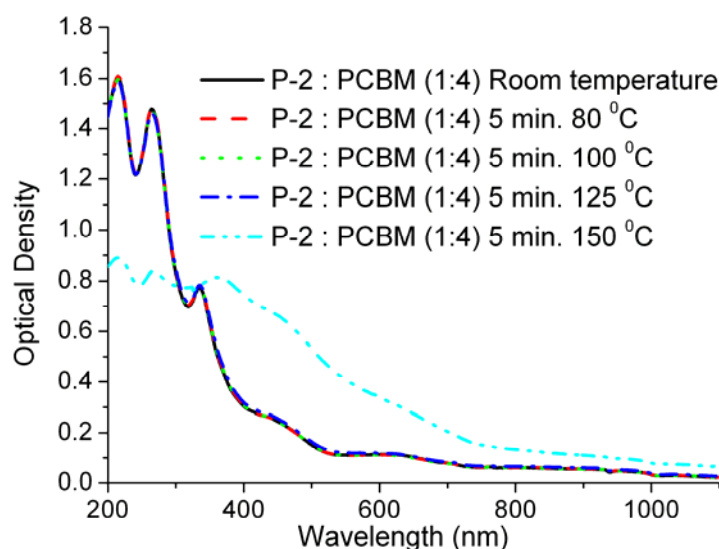
Figure 3.31. UV-vis spectra of **P-2:PCBM** (1:4) in solid state at different temperatures. (film from chlorobenzene)

Polymer **P-5:PCBM** (1:4) blend exhibit no change in UV-absorption of film, when it was treated at 80 ^{0}C, 100 ^{0}C and 125 ^{0}C for 5 minutes at each temperature gradient. However, there is a slight change in absorption of film when it was thermally treated at 150 ^{0}C for 5 minutes. The intensity of band at ~ 440 nm is increased but not as in case of polymer **P-1** and **P-2**, mainly due to formation of large aggregate or clusters of PCBM in blend. In case of polymer P-5, the colour of film was also olive green before and after thermal annealing.

Figure 3.32. UV-vis spectra of **P-5:PCBM** (1:4) in solid state at different temperatures. (film from chlorobenzene)

Figure 3.33. UV-vis spectra of polymer blends **P-1, P-2, P-5** with **PCBM** (1:4) in solid state at room temperature. (film from chlorobenzene)

Photovoltaic devices

For photovoltaic device preparation the substrates (polyester foil coated with indium tin oxide ITO, surface resistance of 60 Ω/square) were cleaned in an ultrasonic bath in methanol and isoprop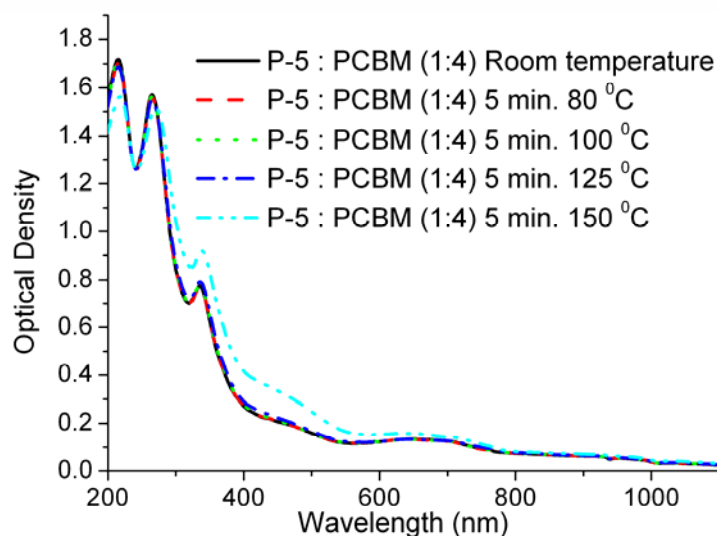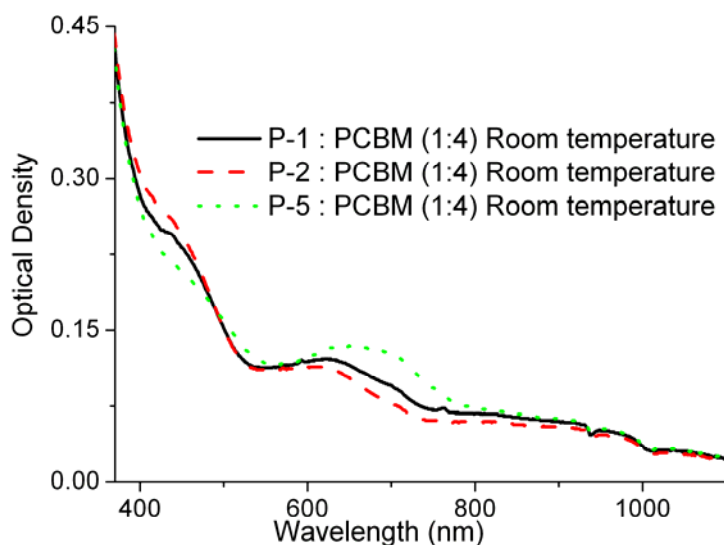anol. The area of the substrates was 5 cm x 5 cm. After drying the substrate a thin layer (~ 100 nm) of PEDOT:PSS (poly(3,4-ethylenedioxythiophene)-poly(styrenesulfonate) (Baytron P, Bayer AG/Germany) was spin-coated and dried. Subsequently, the photoactive layer was prepared by spin coating from composite solutions: **P-1** or **P-2** or **P-5**/ **PCBM** (1:4 weight ratio) in chlorobenzene on the top of the PEDOT:PSS layer. PCBM ([6,6]-phenyl-C_{61}-butanoic acid methyl ester) comes from the laboratory of *J. C. Hummelen* at the University of Groningen. The thickness of the photoactive layers was typically in the range of 100-150 nm. The aluminium cathode was thermally deposited (~ 80 nm) through a shadow mask, which defines a device area of 0.25 cm². I/V curves were recorded with a *Keithley* SMU 2400 Source Meter by illuminating the cells from the ITO side with 100 mW/cm² white light from a *Steuernagel* solar simulator to realise AM1.5 conditions. All cells were prepared and measured under ambient conditions.

Figures 3.34-3.36 show the *I-V* curves of the polymer solar cells under the illumination of AM 1.5, 100 mW/cm². The cell based on **P-1:PCBM** has an open-circuit voltage (Voc) of 678 mV, a short-circuit current (I_{SC}) of 3.48 mA/cm², a calculated fill factor (FF) of 0.46 and an AM1.5 power conversion efficiency of 1.10 %. The device parameters using **P-2:PCBM** were 4.31 mA/cm², 758 mV, 0.48 and 1.57 %. While in case of **P-5:PCBM,** device parameters were 3.81 mA/cm², 589 mV, 0.45 and 1.01 %.

The higher short circuit current and the open-circuit voltage of the **P-2:PCBM** cell compared with **P-1:PCBM** and **P5:PCBM** may be due to the somewhat lower HOMO level of **P-2** versus **P-1** and **P-5**, and presence of bulky ethylhexyloxy chains. In case of polymer **P-5**, the HOMO level (4.93 eV) is a bit higher than PEDOT:PSS (5.1 eV), this makes the potential barrier for the hole injection at the **P-5**/PEDOT:PSS interface slightly higher than that at **P-1** or **P-2**/PEDOT:PSS. Simultaneously the voltage influencing difference between the HOMO level of the donor polymer and the LUMO level of PCBM is slightly increased for **P-2:PCBM**.

These initial values for **P-2** are higher compared to the low band gap polymer diodes reported in the literature.[55,61] Nevertheless, these first devices are still not optimized. Further studies are underway to optimize devices based on these promising materials for photovoltaic devices.

For future advancement, the relatively high $V_{OC} = 0.758$ V at an optical band gap of $E_g = 1.69$ eV is encouraging, certainly in comparison with that of P3HT:PCBM devices where $V_{OC} = 0.63$ V and $E_g = 1.9$ eV.[44] On the other hand, the AM1.5 current density of $I_{SC} = 4.31$ mA/cm^2 is less than in P3HT:PCBM cells ($I_{SC} = 9.5$ mA/cm^2),[44] despite the extension of the spectral response to longer wavelengths. This can be attributed to a very low optical density of the 100 nm photoactive layer in optimized cells.
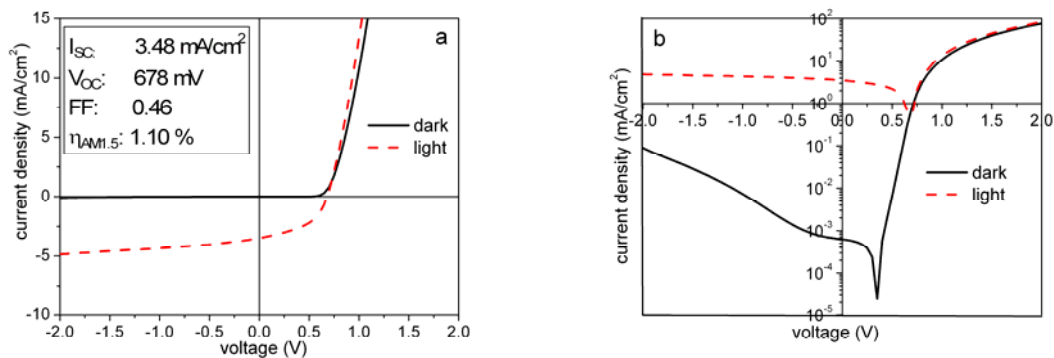
Figure 3.34. (a) *I-V* measurement of **P-1:PCBM 1:4** weight, solar cells measured in the dark and under illumination 100 mW/cm^2. (b) Shows the same data in a semi-logarithmic plot.
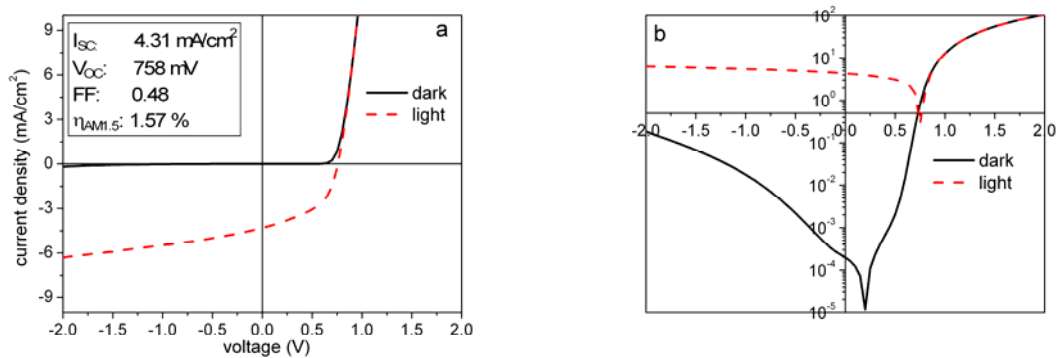
Figure 3.35. (a) *I-V* measurement of **P-2:PCBM 1:4** weight, solar cells measured in the dark and under illumination 100 mW/cm^2. (b) Shows the same data in a semi-logarithmic plot.
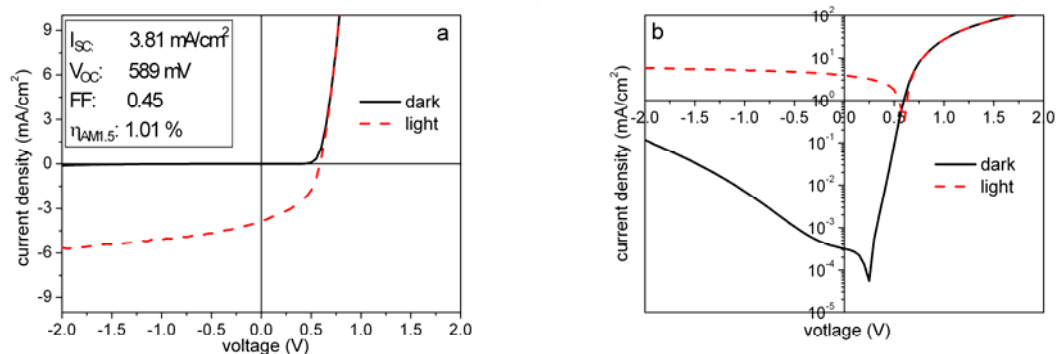
Figure 3.36. (a) *I-V* measurement of **P-5:PCBM 1:4** weight, solar cells measured in the dark and under illumination 100 mW/cm^2. (b) Shows the same data in a semi-logarithmic plot.

The slope of the *I–V* curves in reverse bias indicates that the charge carrier transport is highly field driven. We assume that this fact and the resulting modest fill factor of 0.48 are caused by a low hole mobility in these polymers as compared to the electron mobility in PCBM, creating a transport limitation. In addition, part of the charges may very well recombine to the polymer triplet state.[131] PIA measurements are in progress, but currently it is not clear to which extend this happens.

Table 3.6. Summary of photovoltaic properties of polymers **P-1, P-2** and **P-5**

Blend	I_{SC} mA/cm^2	V_{OC} Volts	Fill Factor %	PCE η %
P-1:PCBM 1:4	3.48	0.758	46	1.10
P-2:PCBM 1:4	4.31	0.678	48	1.57
P-5:PCBM 1:4	3.81	0.589	45	1.01

3.2   Pi- conjugated polymers containing thieno[3,4-*b*]pyrazine as pendant group

3.2.1   Synthesis and Characterization of Monomers and Model Compounds

The synthetic procedures used to prepare the monomers and model compounds are outlined in Schemes 3.9, 3.10 and 3.11. Monomers (**M-9-M-15** and **M-20**) were synthesized in multistep synthesis. Commercially available 4,4′-dimethylbenzil was brominated to its bromomethyl derivative (**27**)[132] by NBS-bromination. Similarly from commercially available 4-bromophenol in two steps 4-(2-ethylhexyloxy)phenyl boronic acid (**30**)[133] was obtained in good yield. By Suzuki coupling[91] of 2,5-dibromo-3,4-dinitro thiophene (**13**) with boronic acids (**29, 30**), compounds (**31**, **32**) were obtained in good yields. 2,5-disubstituted-3,4-dinitrothiophenes (**31**, **32**) were reduced to their respective diaminothiophenes (**33**, **34**) by tin chloride (anhydrous) in conc. HCl. The condensation[134] of (**33**, **34**) with commercially available 1,4-dibromo-butane-2,3-dione led to monomers (**M-9, M-10**) on one side and with 1,2-bis(4-(bromomethyl)phenyl)ethane-1,2-dione (**27**), monomers (**M-11, M-12**)   were obtained on the other side.
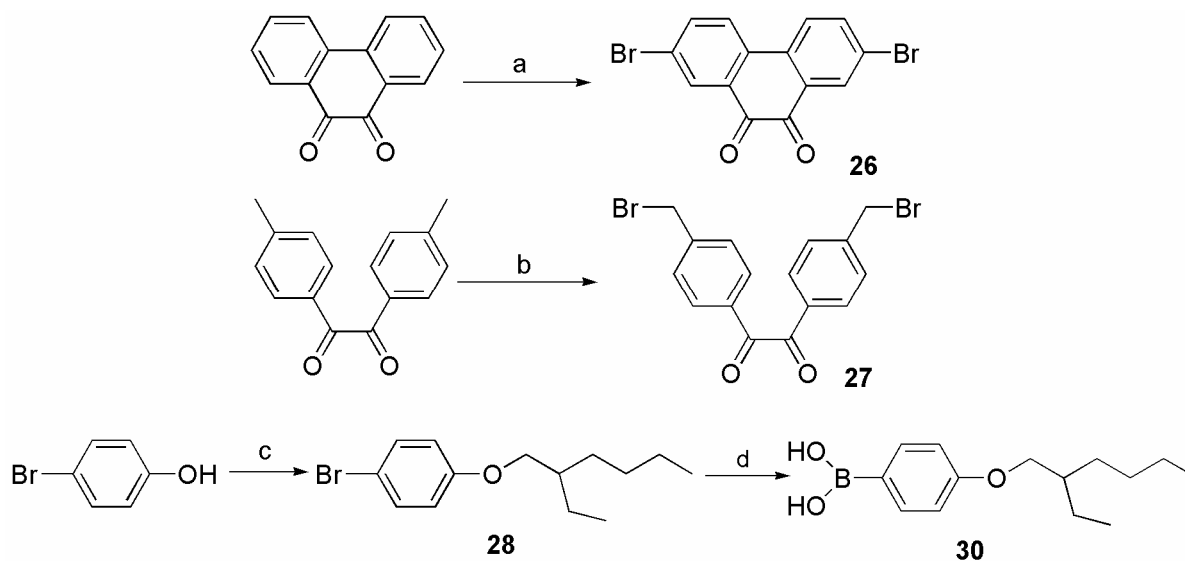
Reagents and conditions: (a) triflouromethanesulphonic acid, N-bromosuccinamide, room temperature, 3h; (b) CCl$_4$, NBS, reflux, 2h; (c) 1-bromo-2-ethylhexane, DMSO, KOH, room temperature; (d) THF, BuLi, trimethylborate, -78 ^{0}C to room temperature.

Scheme 3.9. Synthesis of Compounds **26, 27** and **30**.

Monomers (**M-9, M-11**) are deep red while (**M-10, M-12**) are violet in colour. Monomers (**M-9, M-10**) were further converted to their respective phosphonate esters (**M-13, M-14**) by

Michael Arbuzov reaction.[135] Commercially available 9,10-phenanthrenequinone was brominated by a reported procedure[136] to give bright orange crystals of 2,7-dibromophenanthrene-9,10-dione (**26**) in quantitative yield. The monomer (**M-15**) is the condensation product of compound (**26**) with (**34**). **M-15** is green in colour due to enhanced conjugation compared to other monomers (**M-9-M-12**). Despite of two bulky side chains, the solubility of **M-15** was relatively lower due to rigidity of the structure.
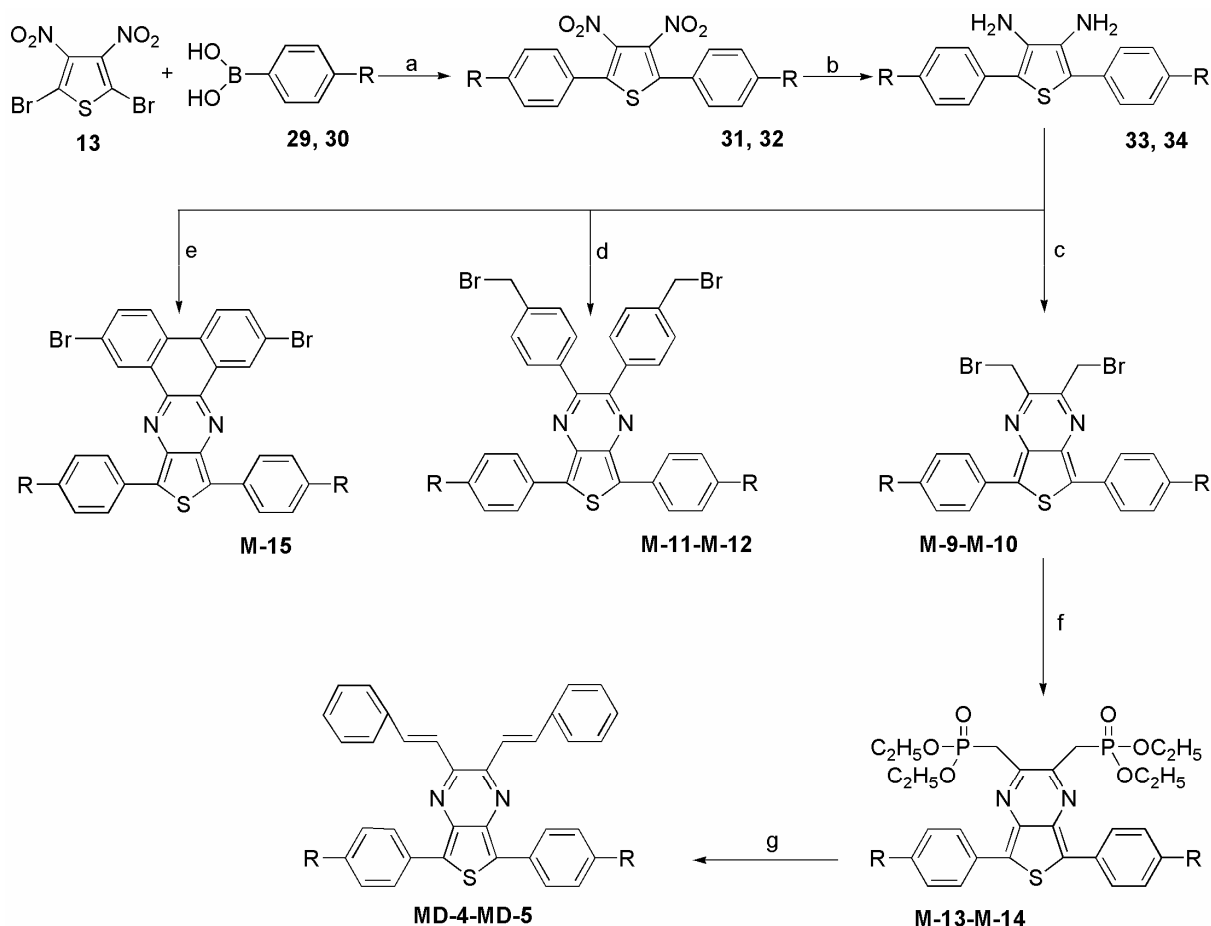
29, 31, 33, M-9,M-11, M-13, MD-4 R = Methyl
30, 32, 34, M-10, M-12 ,M-14, M-15, MD-5 R = Ethylhexyloxy

Reagents and conditions: (a) toluene, THF, aq. K_2CO_3 (2M), $Pd(PPh_3)_4$, 80 ^{0}C, 12 h; (b) ethanol, $SnCl_2$ (anhydrous), conc. HCl, reflux, overnight; (c) 1,4-dibrom-2,3-butandione, $CHCl_3$, p-toluenesulfonic acid, room temperature 12 h; (d) 1,2-bis(4-(bromomethyl)phenyl)ethane-1,2-dione, $CHCl_3$, p-toluenesulfonic acid, room temperature 12 h; (e) 2,7-dibromophenanthrene-9,10-dione, $CHCl_3$, p-toluenesulfonic acid, room temperature 12 h (f) triethyl phosphite, 160 ^{0}C, 4 h; (g) benzaldehyde, THF, *t*-BuOK, 0 ^{0}C to room temperature 3 h.

Scheme 3.10. Synthesis of Monomers **M9-M-15** and Model Compounds **MD-4-MD-5**.

From monomers (**M-13** and **M-14**) two model compounds (**MD-4** and **MD-5**) were synthesized according to the Horner-Wadsworth-Emmons olefination reaction.[137,138] The synthesis was carried out in THF at 0 ^{0}C in presence of strong base potassium *tert.* butoxide. Both model compounds were violet in colour and were obtained in good yields.
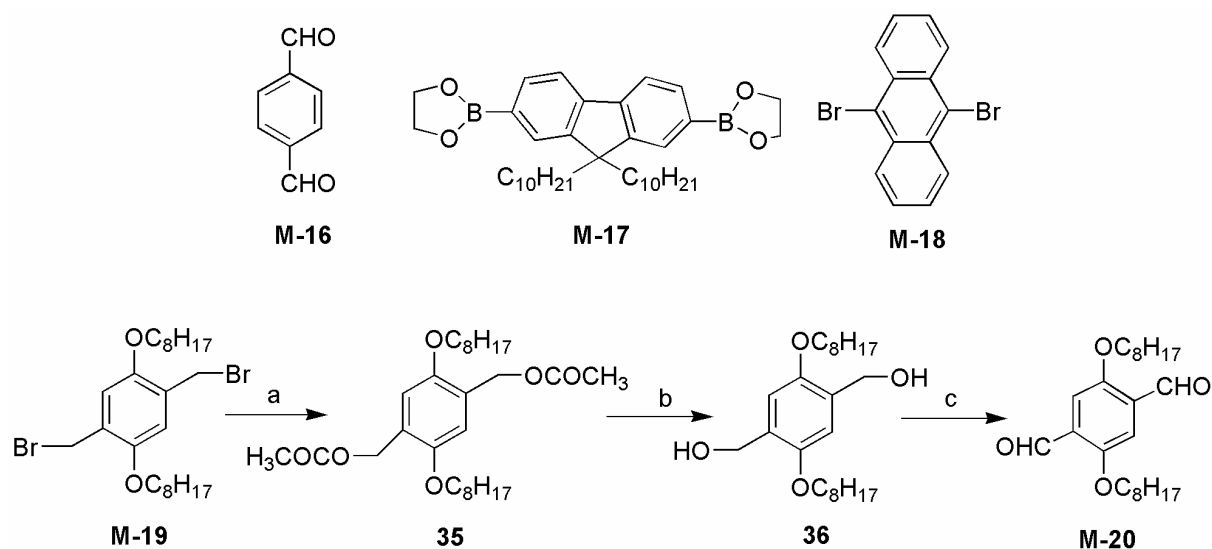
Reagents and conditions: (a) sodium iodide, sodium acetate (anhydrous), DMF, 140°; (b) ethanol, water, sodium hydroxide; (c) pyridium chlorochromate, molecular sieves, silica gel, CH_2Cl_2.
Scheme 3.11. Synthesis of Monomer **M-20**.

Monomers (**M-17**, **M-19** and **M-20**) containing alkyl and alkoxy chains in order to fulfill solubility requirement of designed polymers were also prepared as counter part of thieno[3,4-*b*]pyrazine containing monomers according to the procedures described in the literature.[104,139,140]
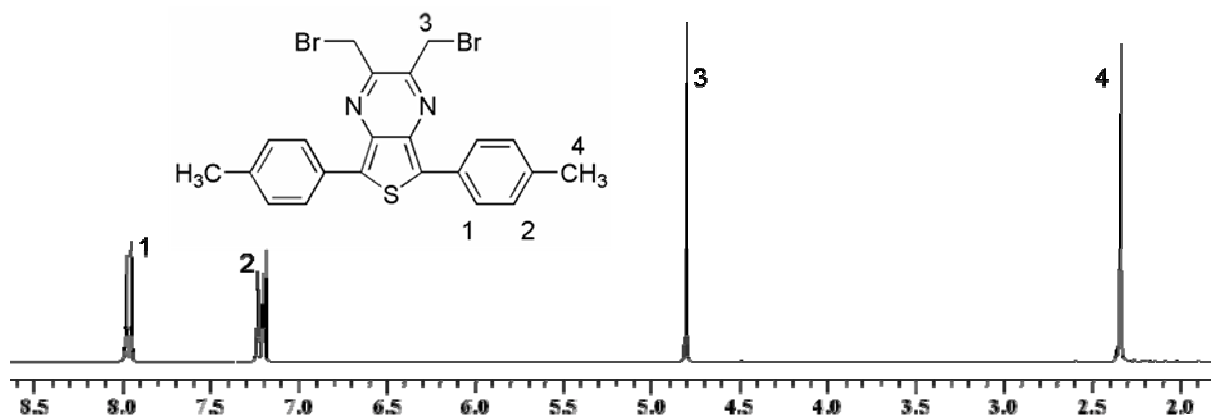
Figure 3.36. ^{1}HNMR of monomer **M-9**.

The chemical structures of monomers (**M-9-M-15, M-17, M-19, and M-20**) were confirmed by NMR, Mass and elemental analysis. ^{1}H and ^{13}C NMR spectra were in good agreement with the proposed structure of the monomers. The ^{1}H NMR spectrum of **M-9** in CDCl$_3$ showed peaks indicating four protons of phenyl rings adjacent to thienopyrazine (5,7-position) at δ = 7.98, while four protons of phenyl rings adjacent to methyl appeared at δ = 7.20, CH$_2$Br protons at δ = 4.80 and methyl protons signals were present at δ = 2.34 ppm.
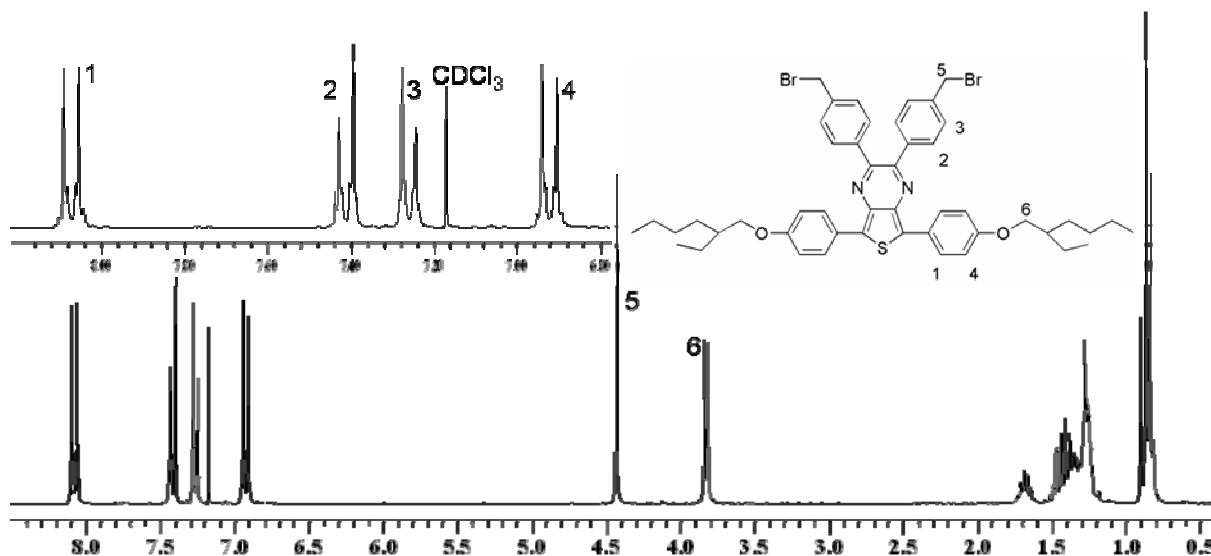
Figure 3.37. ^{1}HNMR of monomer **M-12**.

The ^{1}H NMR spectrum of **M-12** in CDCl$_3$ showed peaks indicating four protons of phenyl rings adjacent to thienopyrazine (5,7-position) at δ = 8.10, four protons of phenyl rings adjacent to pyrazine ring (2,3-position) at δ = 7.44, four protons of phenyl rings adjacent to CH$_2$Br (2,3-position) at δ = 7.28, while four protons of phenyl rings adjacent to ethylhexyloxy side chain (5,7-position) appeared at δ = 6.94, CH$_2$Br protons at δ = 4.43, OCH$_2$ protons at δ = 3.84 and alkyl protons appeared between δ = 1.17-0.81 ppm.
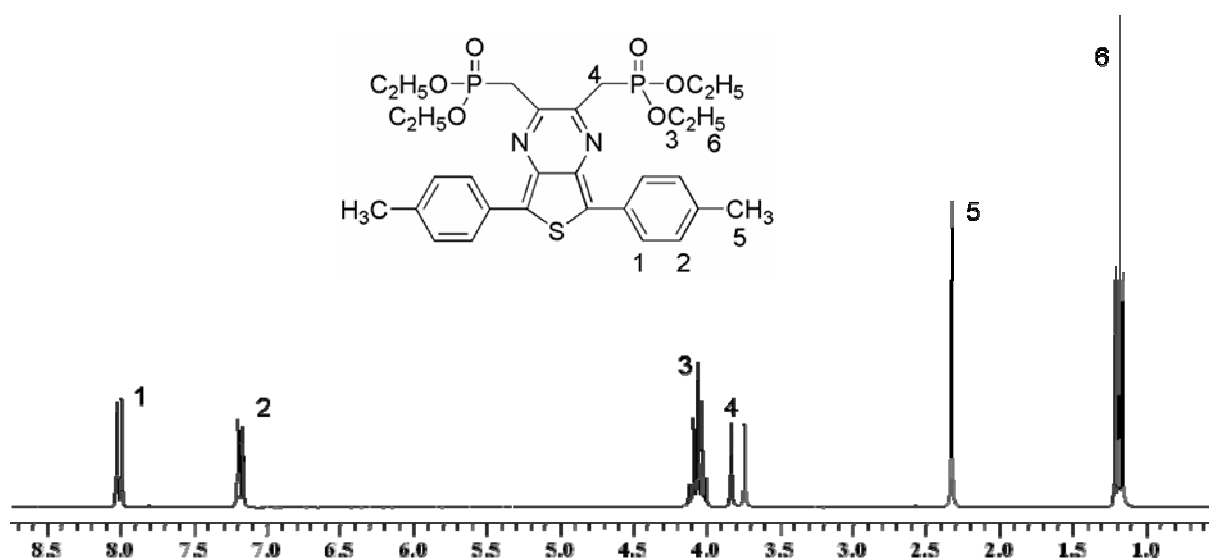
Figure 3.38. ^{1}HNMR of monomer **M-13**.

The ^{1}H NMR spectrum of **M-13** in CDCl$_3$ showed peaks indicating four protons of phenyl rings adjacent to thienopyrazine (5,7-position) at δ = 8.03, while four protons of phenyl rings adjacent to methyl appeared at δ = 7.20, OCH$_2$ protons at δ = 4.06, CH$_2$ protons adjacent to pyrazine ring (2,3-position) at δ = 3.83-3.74 and terminal methyl protons signals of tolyl were present at δ = 2.35 ppm while methyl protons of phosphonate ester appeared at-1.18 ppm.
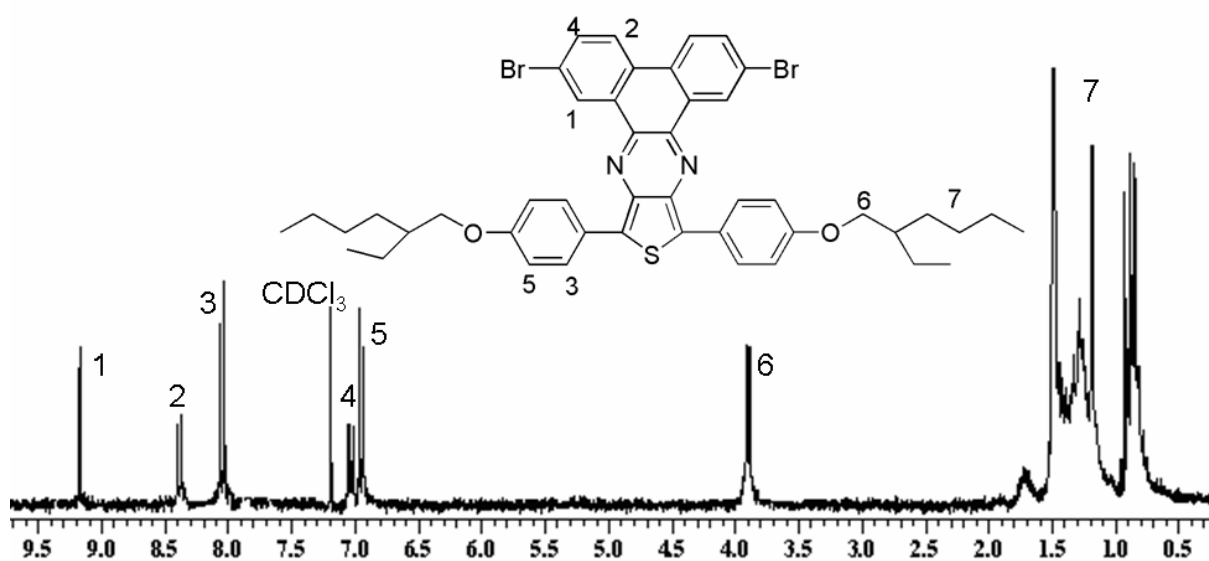
Figure 3.39. ^{1}HNMR of monomer **M-15**.

Similarly ^{1}H NMR spectrum of **M-15** in CDCl$_3$ showed peaks indicating two protons of phenazine at δ = 9.18, two more quinoxaline protons appeared at δ = 8.4, four protons of

phenyl rings adjacent to thienopyrazine (5,7-position) at δ = 8.06, remaining two protons of quinoxaline ring at δ = 7.03,   four protons of phenyl rings adjacent to ethylhexyloxy side chain (5,7-position) appeared at δ = 6.93,   four OCH$_2$ protons at δ = 3.91 and twenty six alkyl protons appeared between δ = 1.49-0.85 ppm.

The ^{1}H NMR spectrum of **MD-4** in CDCl$_3$ showed peaks indicating four protons of phenyl rings adjacent to thienopyrazine (5,7-position) at δ = 8.17, while four protons of vinylene bonds at δ = 7.90 and 7.64, protons of phenyl rings attached to vinylene bonds showed multiple signals between δ = 7.52-7.38, while four protons of phenyl rings adjacent to methyl appeared at δ = 7.29 and terminal methyl protons signals were present at δ = 2.44 ppm, respectively.
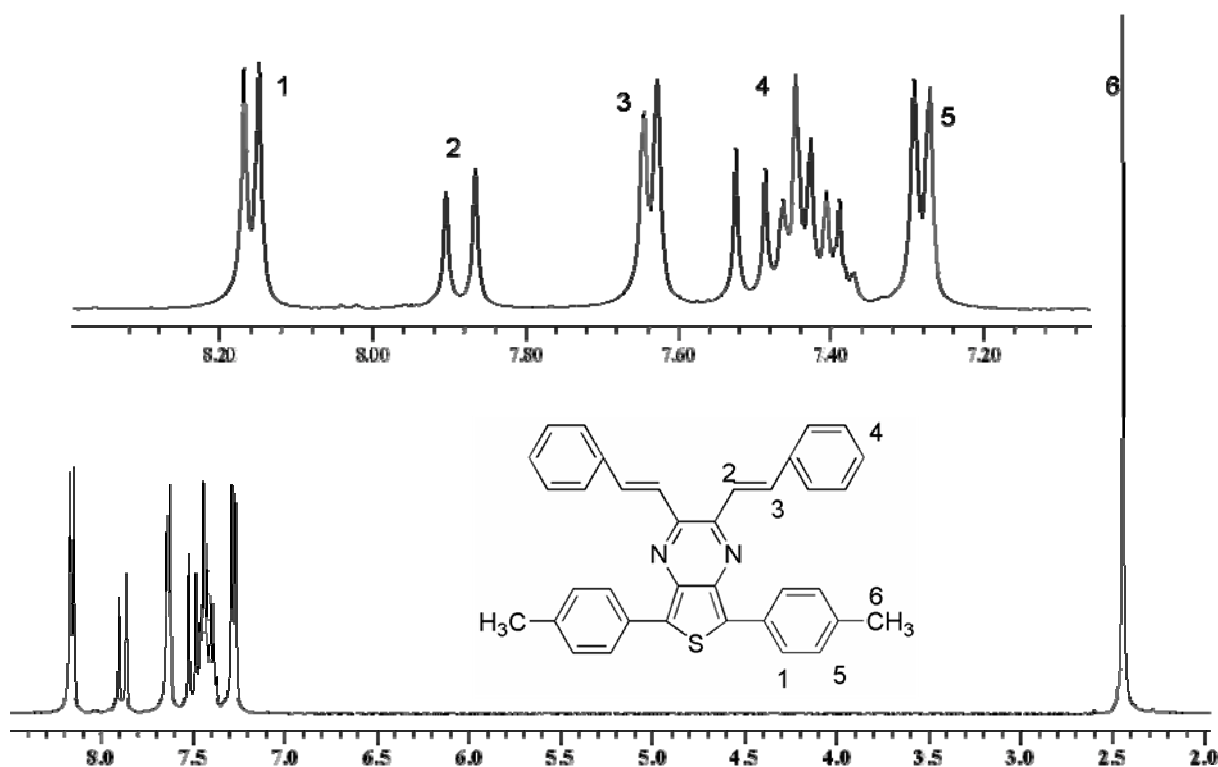
Figure 3.40. ^{1}HNMR of model compound **MD-4**.

3.2.2 Synthesis of Polymers

Poly(*p*-phenylenevinylene)s containing 5,7-disubstituted pendant thieno(3,4-b)pyrazine (**P-10,P-11,P-12**) were synthesized by **Horner-Wadsworth-Emmons polycondensation** route, suitable for the synthesis of well-defined strictly alternating copolymers. The polymers were reddish brown in colour and were soluble in common organic solvents such as chloroform, toluene and tetrahydrofuran (THF). The average molecular weights of polymers were determined by gel permeation chromatography (GPC) with polystyrene as standards. THF

served as eluting solvent. The number-average molecular weight $\overline{M}_n$ values of polymers (**P-10-P-12**) were between 8800-6000 g/mol, leading to degree of polymerisation between 13-7 with a polydispersity index of 1.7-1.3, (see Table 3.7).
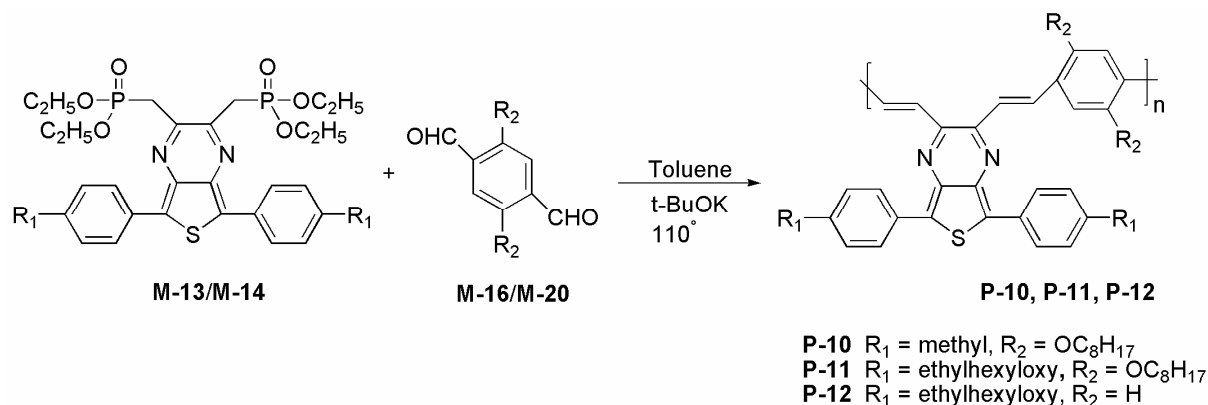
Scheme 3.12. Synthesis of Polymers **P-10-P-12**.

Copolymers (**P-13, P-14**) were synthesized via **Gilch polymerization**.[78] this method requires the use of excess strong alkali to ensure the formation of the fully eliminated structure. The polymerization route offers a number of important advantages for the introduction of vinylene units along the polymer backbone with high molecular weight, low polydispersity and allows for easy purification.The monomers are treated with potassium *tert*-butoxide in organic solvents (THF), where the polymerization is carried out either by the controlled addition of monomer to a solution of base or by the controlled addition of base to a solution of monomer. One of the major problems associated with the latter route is gel formation.[79] Indeed, if the rate of addition of monomer to base or base to monomer is not controlled precisely, the reaction typically leads to the formation of a gel, which limits the yield, molecular weight, polydispersity, solubility, and processability of the polymer. As an alternative approach, therefore, we have carried out the Gilch polymerization by first adding an equimolar amount of base into the reaction system. About 1 h later, the resultant solution was diluted with dry THF, to which an excess amount of the strong organic base was then added slowly. Most of the polymers with electron-withdrawing thieno(3,4-b)pyrazine units in side or main chains exhibit poor solubility that limits their application. In an attempt to improve the solubility, polymers (**P-13, P-14, P-15** and **P-16**) with longer flexible side chain were designed. These bulky side groups interrupt conjugation and interfere with the packing of the polymer chain, which results in the formation of amorphous PPVs.
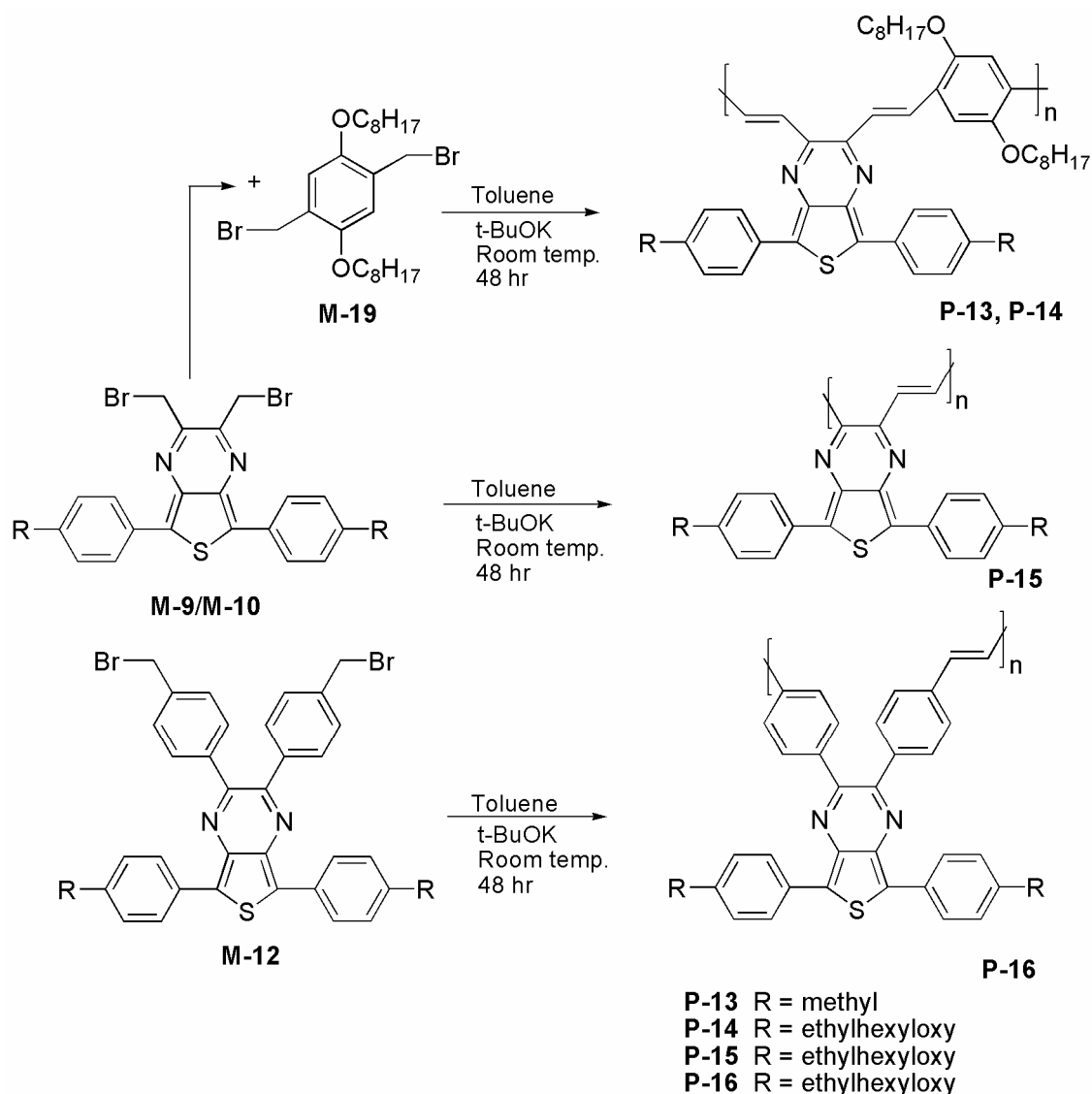
Scheme 3.13. Synthesis of Polymers **P-13-P-16**.

The number-average molecular weight $\overline{M}_n$, values of polymers (**P-13, P-14**) were between 11600-6100 g/mol, leading to degree of polymerisation between 13-9 with a polydispersity index of 6.1-4.2. High value of polydispersity index and low molecular weight of these polymers are possibly due to steric hinderance imposed by bulky substituents.

Two homopolymers (**P-15, P-16**) were also synthesized via Gilch polymerization. The number-average molecular weight $\overline{M}_n$, values of polymers (**P-15, P-16**) were between 11500-4200 g/mol, leading to degree of polymerisation between 16-7 with a polydispersity index of 1.7-1.2.

Random and alternating poly(9,9-didecylflourene-co-thienopyrazine) copolymers (**P-17**, **P-18, P-19**) were synthesized by **Suzuki coupling polymerization**. The polymers are green in colour. **P-17** and **P-18** were soluble in chloroform, toluene and tetrahydrofuran while **P-19**

showed solubility only on heating, low solubility of **P-19** can be attributed to its high molecular weight.
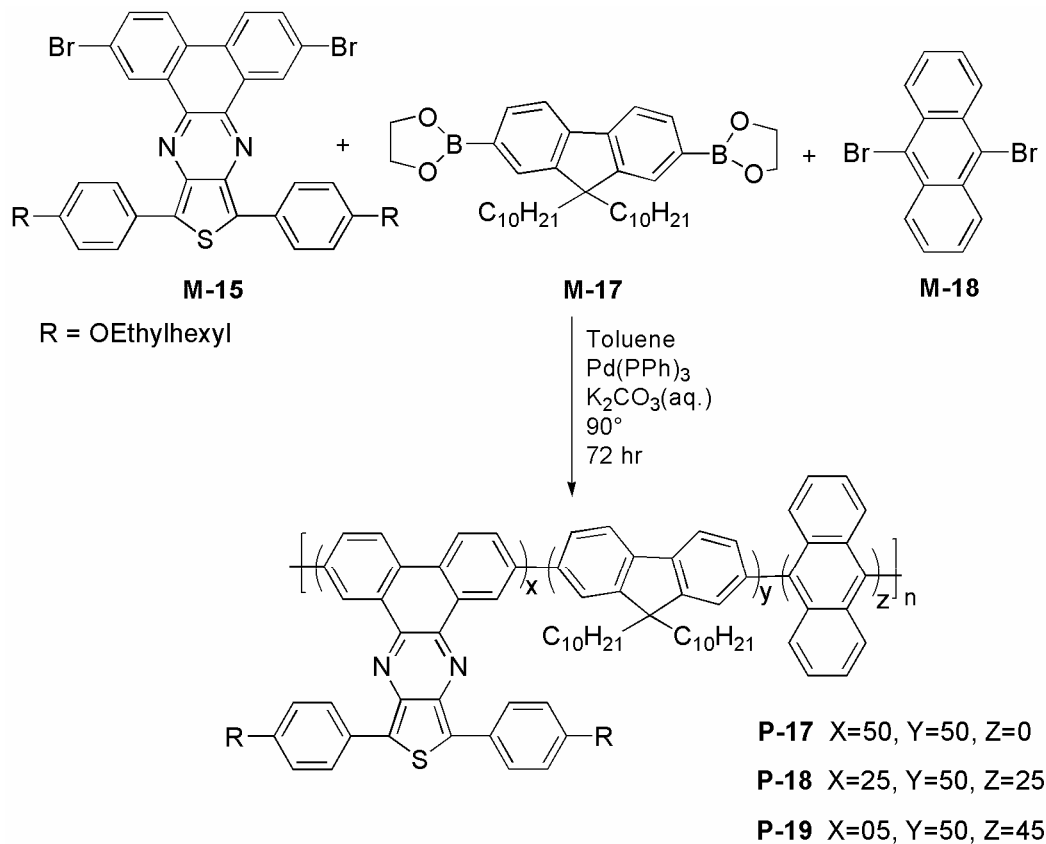
Scheme 3.14. Synthesis of Polymers **P-17-P-19**.
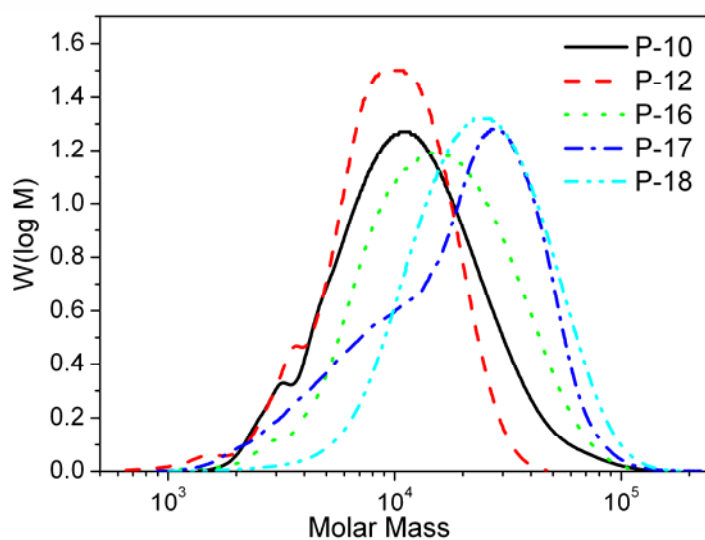
Figure 3.41. GPC curves of polymers **P-10, P-12, P-16, P-17** and **P-19**.

The number-average molecular weight $\bar{M}_n$, values of polymers (**P-17-P-19**) were between 18600-14000 g/mol, leading to degree of polymerisation between 54-12 with a polydispersity index of 1.8-1.5. (see Figure 3.41 and Table 3.7)

Table 3.7. GPC data of polymers **P-10-P-19.**

Polymer	$\bar{M}_n$ (g/mol)	$\bar{M}_w$ (g/mol)	PDI	$\bar{P}_n$	Yield (%)
P-10	8800	14800	1.68	13	72
P-11	5800	8400	1.46	07	65
P-12	7400	10900	1.46	11	64
P-13	6100	25200	4.2	09	70
P-14	11600	70500	6.05	13	58
P-15	4200	5000	1.2	07	67
P-16	11500	19400	1.7	16	69
P-17	14000	25500	1.8	12	71
P-18	18600	28800	1.5	42	73
P-19	18300	26800	1.5	54	67

M_n, GPC (polystyrene standards).

3.2.3 Characterization of Polymers

The chemical structures of the polymers (P-10-P-19) were verified by FTIR, ^{1}H, ^{13}C NMR and elemental analysis. The ^{1}H NMR spectra of the copolymers and homopolymers were consistent with the proposed structure of the polymers. Compared with the ^{1}H NMR peaks of monomers, those of the polymers were broadened. The ^{1}H NMR spectrum of **P-10** in CDCl$_3$ showed peaks indicating aromatic and vinylene protons between 8.26-7.25 ppm, -OCH$_2$ protons at 4.10 ppm, methyl protons of tolyl group at 2.47 ppm and remaining alkoxy side chain protons were present between 1.85-0.79 ppm, respectively.

Similarly ^{1}H NMR spectrum of **P-16** in CDCl$_3$ exhibited peaks indicating four protons of phenyl rings adjacent to thienopyrazine (5,7-position) at 8.22 ppm, while remaining phenyl and vinylene protons were present between 7.61-7.02 ppm. The -OCH$_2$ protons of ethylhexyloxy side chain appeared at 3.95 ppm and other alkyl protons were present upfield between 1.80-0.96 ppm. The signals of –CH$_2$Br end group can be seen at 4.53 ppm.
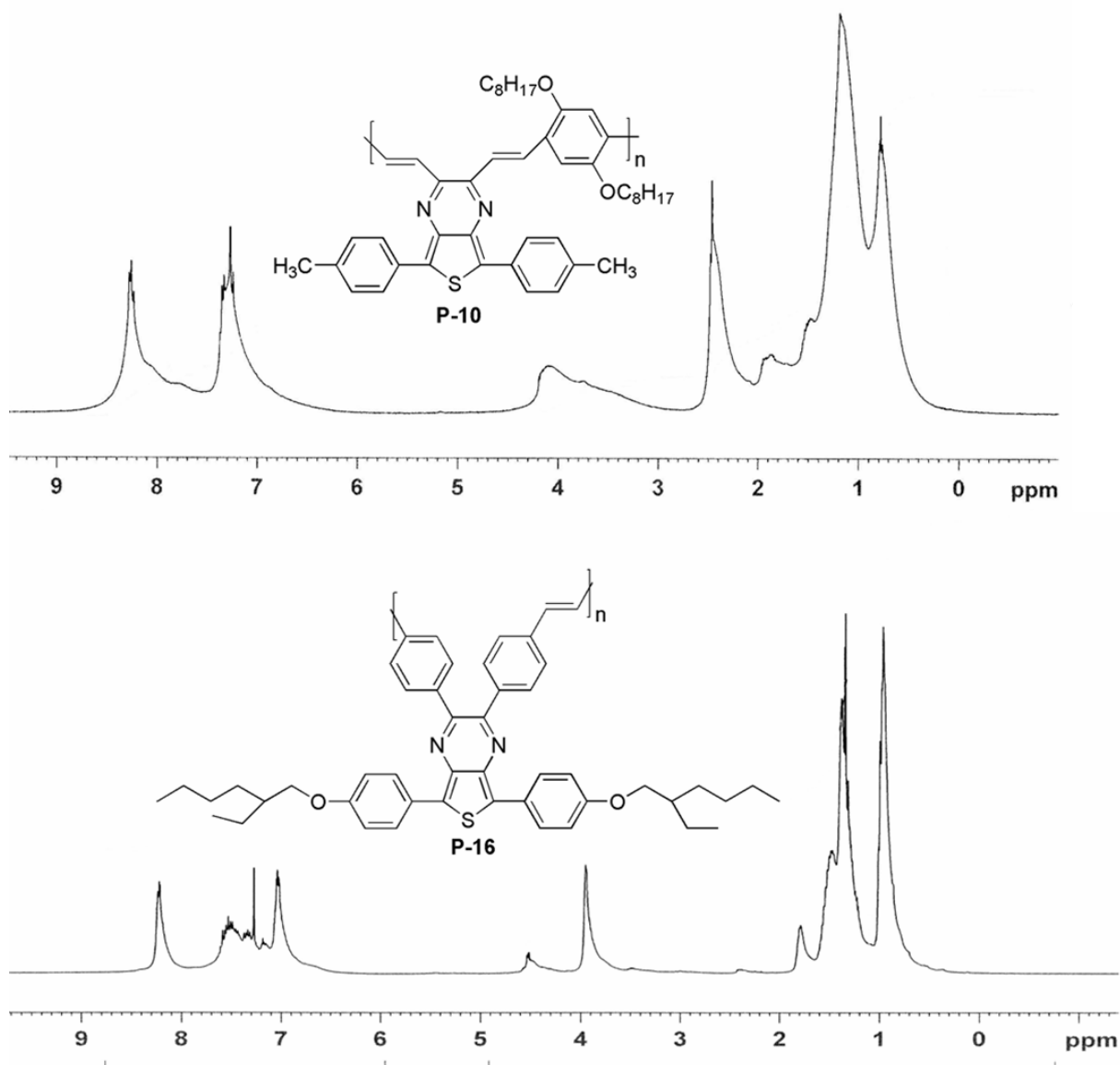
Figure 3.42. ^{1}HNMR of polymers **P-10** and **P-16**.

Figure 3.43 showed the ^{1}H NMR spectra of (**P-17, P-18** and **P-19**) in CDCl$_3$. In ^{1}H NMR spectra of all the three polymers, protons signals of quinoxaline ring were present at about 9.7 and 8.59 ppm, respectively. Remaining aromatic protons were present between 8.15-7.15 ppm. The –OCH$_2$ protons of ethylhexyloxy side chains can be seen at 4.05 ppm. While other alkyl side chain protons were present upfield between 2.37-0.84 ppm. The height of –OCH$_2$ protons signals in the three spectra is indicative of presence of monomer (**M-15**) in these polymers.
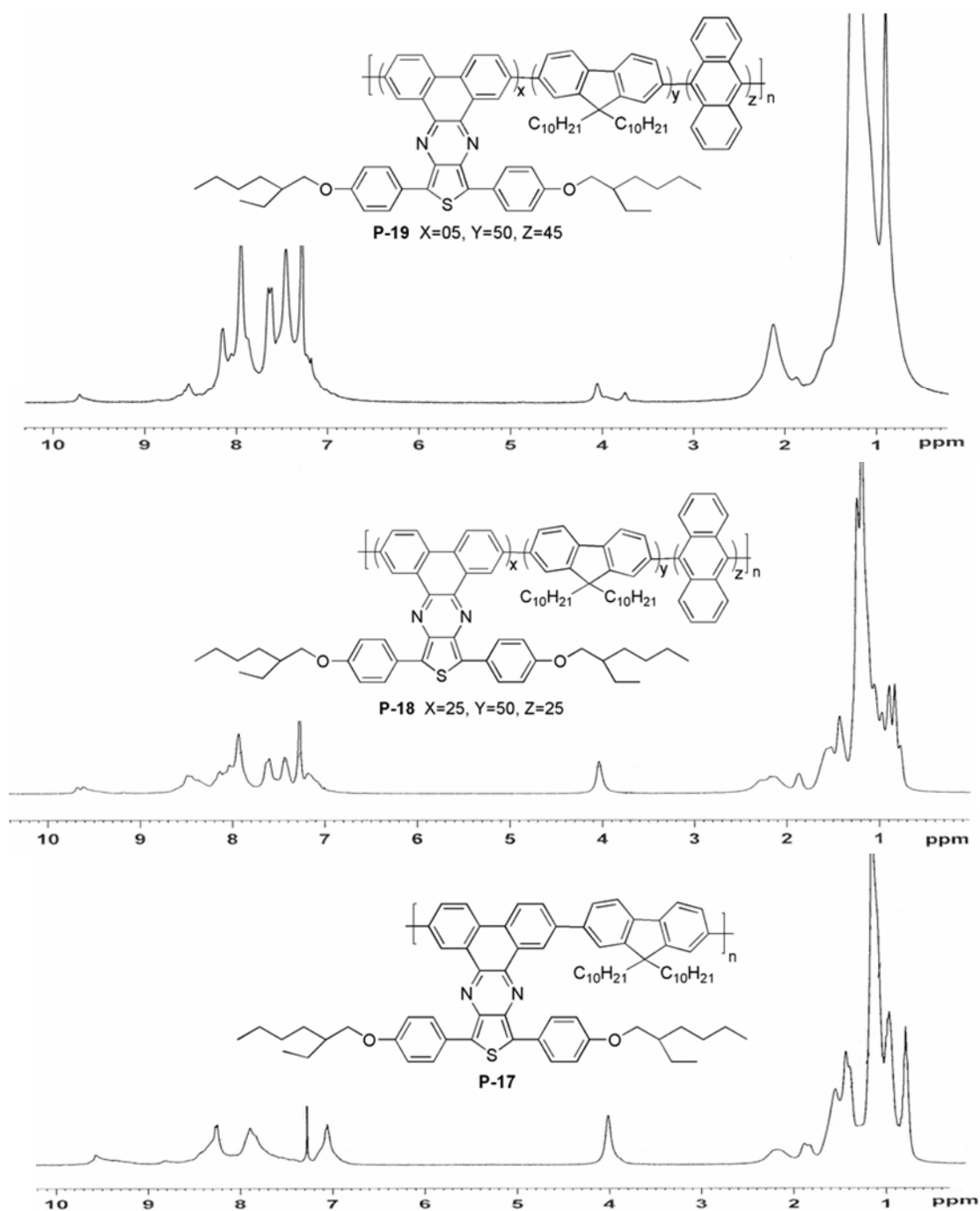
Figure 3.43. ^{1}HNMR of polymers **P-17, P-18** and **P-19**.

We investigated the thermal properties of these copolymers by thermogravimetric analysis (TGA) and differential scanning calorimetry (DSC) at a heating rate of 10 K/minute. All the polymers are thermally stable and thermal decomposition starts at >300 °C. We did not detect any possible phase transition signals during repeated heating/cooling DSC cycles for polymers (**P-10-P-19**) which indicate that the polymers have amorphous structures.

3.2.4 FT-IR Analysis

As the structure difference among **P10-P16** only lies in the different side chains attached to the phenylene rings, IR spectra of these polymers were similar to each other. It can be seen that the vibrational bands at 1607 and 1532 cm^{-1} in all the polymers (**P-10-P-16**) are due to stretching vibrations of the C=N group in the thienopyrazine ring. The polymers showed characteristic absorption bands at 2958, 2928, 2870 (C-H stretching of aliphatic segments); 1608, 1510, 1456 (aromatic); and 1242, 1176 (ether bond). The absorption bands at ~3056 and ~961 cm^{-1} are due to stretching modes for the vinylene C=C bond and C-H out-of-plane bending, respectively, of the trans configuration. The spectrum of model compounds   (**MD-4**, **MD-5**) were very similar but did not display any absorption at about ~ 965 cm^{-1} that was assigned to the out-of-plane deformation of the trans vinylene moiety.[141]
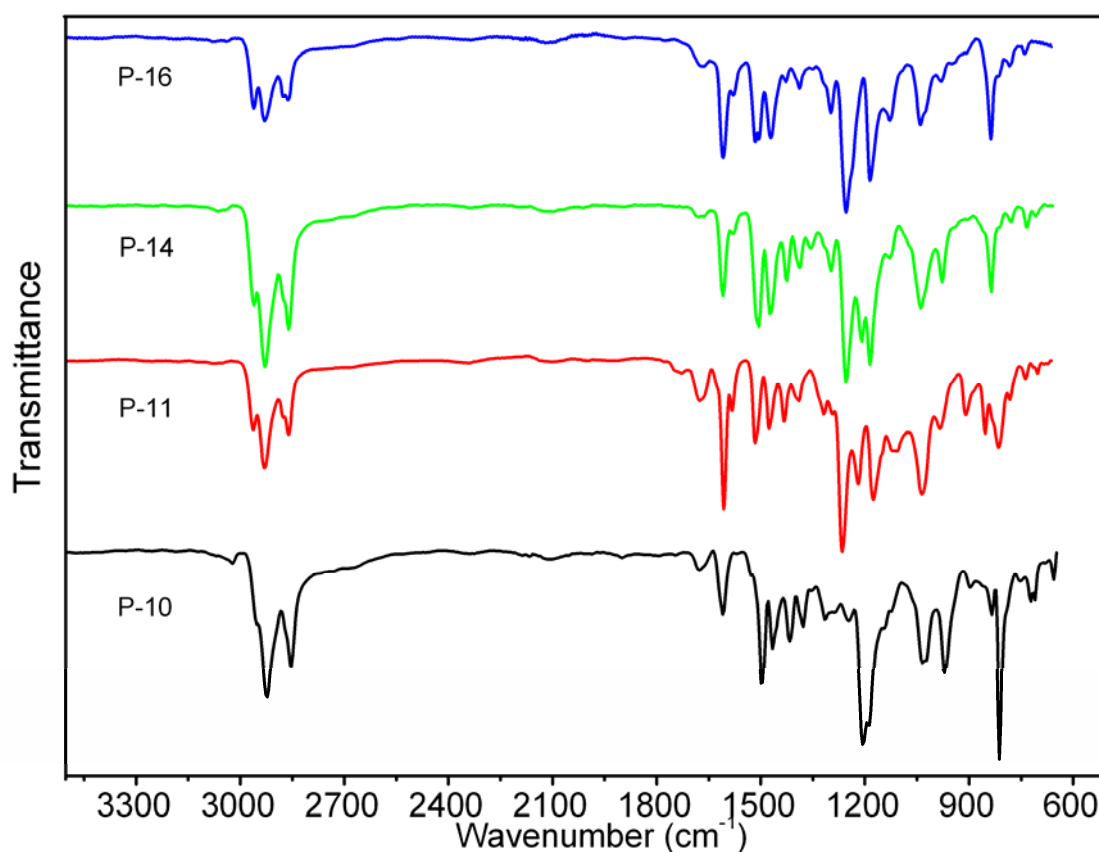
Figure 3.44. FT-IR of polymers **P-10, P-11, P-14** and **P-16**.

An absorption peaked at ~965 cm^{-1} was clearly visible for all polymers, while no signals could be found at 875 cm^{-1}, indicating that these predominantly contains a *trans*-CH=CH group under Horner and Gilch conditions. Therefore, it is concluded that both Horner and Gilch reactions are suitable for developing polymers with regular molecular configurations.

3.2.5 Optical Properties

The photophysical characteristics of the new monomers, model compounds and polymers were investigated by UV-vis absorption and photoluminescence in dilute chloroform solution as well as in solid state. The optical data are summarized in Table 3.8, namely the absorption peak maxima, λ_a, the absorption coefficients at the peak maxima, log ε, the optical band gap energy, E_g^{opt} (calculated from $\lambda_{10\%max}$, wavelength at which the absorption coefficient has dropped to 10% of the peak value),[114] the emission maxima λ_e, and the fluorescence quantum yields, Φ_{fl}. All emission data given here were obtained after exciting at the wavelength of the main absorption band. Figure 3.45 show the absorption and emission spectra of model compounds.
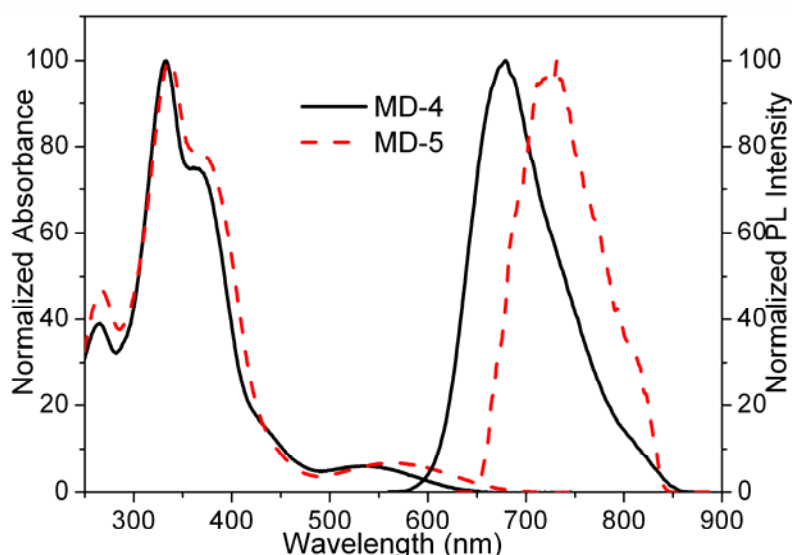
Figure 3.45. Normalized UV-vis and emission spectra of **MD-4** and **MD-5** in solution (Toluene 10^{-7}mol).

The absorption spectra of the monomer (**M-9**) shows two peaks located in the UV and visible region at 307 nm due to the presence of tolyl group and at 503 nm due to thieno(3,4-b)pyrazine system. Similarly two peaks in the absorption spectra of the monomer (**M-15**) are located at 347 nm due to presence of electron donor alkoxy phenyl groups adjacent to thienopyrazine moiety (5,7 position) and 621 nm attributed to the effective chromophore system. This indicates that the presence of strong donor groups at 5 and 7 position of thieno[3,4-*b*]pyrazine lead to a red shift in absorption spectra. The absorption maxima of model compounds **(MD-4-MD-5)** are red shifted relative to monomers (**M-13-M-14**) (Table 3.8). Obviously, increase in conjugation length is the reason for this red shift. In comparison

to monomers and model compounds, the respective polymers (**P-10-P-16**) show a little or no change in the first absorption band (~330 nm), a blue shift is observed in the second absorption band originated from the π-π^* absorption of conjugated main chain.

Table 3.8. Optical Data of Polymers **P-10-P-16** and Model Compounds **MD-4-MD-5** in Dilute Toluene Solution (~ 10^{-7} M) and in Solid State.[b]

Poly mer	UV-vis λ_{max}, nm				E_g opt. eV[c]		PL[d] λ_{em}, nm		% ϕ_{fl}	
	Toluene (log ε)[a]	$\lambda_{0.1max}$ (nm)	film[b]	$\lambda_{0.1max}$ (nm)	Toluene	film	Toluene	film	Toluene	film
P-10	338, 440 (4.4)(4.3)	573	444	590	2.16	2.10	560	618	12	1
P-11	300, 420 (4.3)(4.0)	549	484	604	2.26	2.05	706	-	02	-
P-12	341, 405 (4.5)(4.4)	516	427	651	2.40	1.90	508	-	02	0
P-13	300, 457 (4.4)(4.0)	599	467	605	2.07	2.05	-	-	-	-
P-14	312, 476 (4.4)(4.2)	615	488	605	2.01	2.05	-	-	-	-
P-15	321, 540 (4.3)(3.3)	600	325, 545	602	2.06	2.06	694	-	05	0
P-16	337, 530 (4.5)(3.5)	627	338, 530	630	1.97	1.96	665	680	44	1
MD-4	361, 538 (4.6)(3.5)	633	340	615	1.96	2.01	676	-	13	0
MD-5	363, 565 (4.6)(3.6)	678	397	620	1.82	2.00	728	-	02	0

[a]Molar absorption coefficient. Molarity is based on the repeating unit. [b]Spin coated from chlorobenzene solution. [c]$E_g^{opt} = hc /\lambda_{0.1max}$. [d]Photoluminescence data.
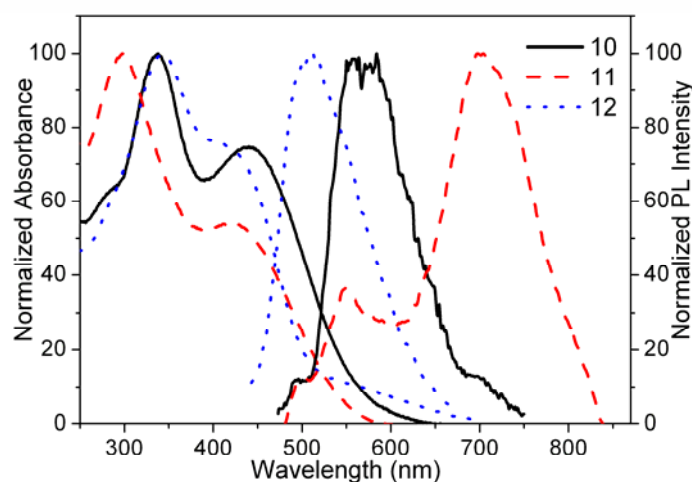
Figure 3.46. Normalized UV-vis and emission spectra of **P-10**, **P-11** and **P-12** in solution (Toluene 10^{-7} mol).

The thieno(3,4-*b*)pyrazine unit is attached to the PPV such that the polymer backbone is kinked, thereby shortening conjugation lengths. The blue shift especially in the absorption maxima of alternating copolymers suggests increased disruption of conjugation caused by increased amount of bent 5,7-disubstituted thieno(3,4-*b*)pyrazine linkages in the polymer backbone. The incorporation of such kinked linkages in polymer backbones has been used successfully in poly(*p*-phenylenevinylene) backbones to control the conjugation length of the polymer and tune the emission colors.[142] The absorption maxima of homopolymers (**P-15** and **P-16)** show a bathochromic shift (λ_{max} 530-540 nm) relative to other copolymers probably due to the absence of steric hinderance caused by long alkoxy side chains.
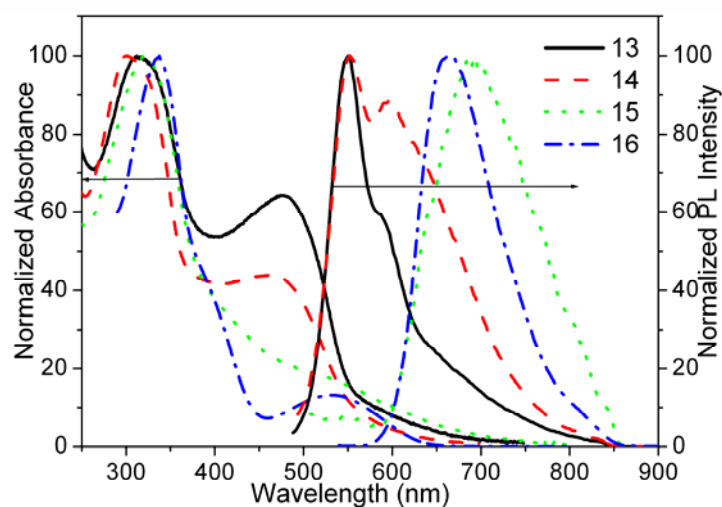
Figure 3.47. Normalized UV-vis and emission spectra of **P-13**, **P-14, P-15** and **P-16** in solution (Toluene 10^{-7} mol).

Figure 3.48 shows the normalized optical absorption spectra of thin films of copolymers and homopolymers (**P-10-P-16**) are almost similar to those of the absorption spectra in dilute solution. The distinct similarity between the thin film absorption spectra and the dilute solution spectra suggests comparable groundstate electronic structures of the polymers with no significant aggregation in the condensed state.
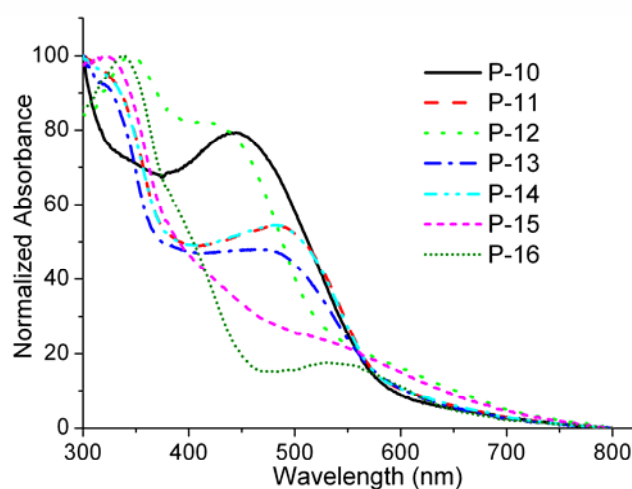
Figure 3.48. Normalized UV-vis spectra of **P-10, P-12** and **P-16** in solid state. (film from chlorobenzene)

This again confirms that the bent 5,7-disubstituted thieno[3,4-*b*]pyrazine linkages introduce disorder in the polymer backbones and thus prevent ordered intrachain conformations. The optical band gaps derived from the absorption edge of the thin film spectra gave values of 1.9-2.1 eV for (**P-10-P-16**).

The PL emission spectra of model Compounds, homo and the copolymers in dilute toluene solution are shown in Figures 3.45, 3.46 and 3.47. All emission data given were obtained by the excitation at the maximum absorption peaks. The emission maximum of **MD-4** in dilute toluene solution is at $\lambda_{max,em}$ =676 nm, while the emission curve of **MD-5**, showing its maximum at $\lambda_{max,em}$ = 728 nm. The fluorescence quantum yields were found to be around 2 and 13% for **MD-4** and **MD-5** respectively. In dilute solutions, the polymers (**P-10-P-16**) only show one emission peak ranging between 508 to 706 nm. The fluorescence quantum yields were found to be around 2 and 44% for **P-10-P-16**. Large Stokes shift between 75-286 nm were observed in these polymers. The emission maximum of **P-10** in solid film is located at $\lambda_{max,em}$ = 618 nm leading to Stokes shift of 174 nm, and a lower fluorescence quantum yield of 1%. We assumed that thienopyrazine moiety serves as a quenching channel (both radiative and non-radiative) in these polymers.

Table 3.9. Optical Data of **P-17-P-19** and monomer **M-15** in Dilute Toluene Solution ($\sim 10^{-7}$ M) and in Solid State.[a]

Poly mer	UV-vis λ_{max}, nm				E_g opt. eV[b]		PL[c] λ_{em}, nm	% ϕ_{fl}
	Toluene (log ε)[a]	$\lambda_{0.1max}$ (nm)	film[b]	$\lambda_{0.1max}$ (nm)	Toluene	film	Toluene	Toluene
P-17	358, 612 (4.9)(3.7)	735	361, 621	755	1.68	1.64	746	2
P-18	353, 399, 611 (4.4) (4.1)(3.0)	680	358, 612	725	1.82	1.71	491, 745	5, 3
P-19	360, 382, 402,613 (4.0)(4.0)(4.1)(2.2)	620	378, 399, 636	715	2.00	1.73	436, 746	7, 2
M-15	347, 621 (4.8) (3.8)	745	-	-	1.66	-	-	-

[a]Spin coated from chlorobenzene solution. [b]$E_g^{opt} = hc / \lambda_{0.1max}$. [c]Photoluminescence data.

However, the emission of all the polymers (**P-10-P-16**) remains blue as compared to emission of model compounds (**MD-4-MD-5**) with simultaneous loss in vibronic structure of the emission spectra. This loss of the well-resolved structure of the emission spectra in the copolymers suggests lack of intrachain ordering due to the many kinks in the polymer backbone.
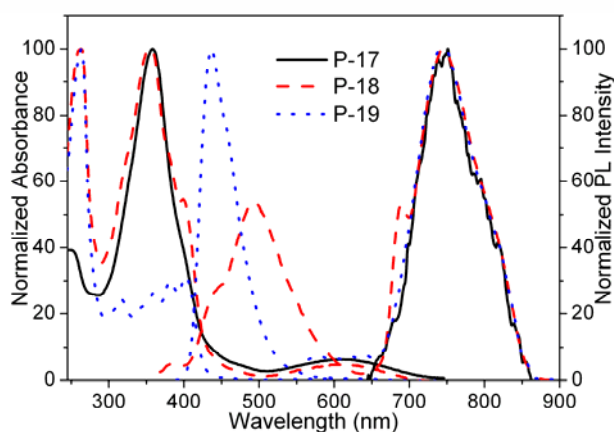
Figure 3.49. Normalized UV-vis and emission spectra of **P-17**, **P-18** and **P-19** in solution (Toluene 10^{-7}mol).

Polymer **P-17** show two absorption peaks in UV-vis region similar to that of monomer (**M-15**), at ~ 358 and 612 nm respectively. The statistical polymers P-18 and P-19 showed many peaks in range of ~350-400 nm, mainly due to presence of anthracene and fluorene moities. The band due to monomer **M-15** was present at longer wavelength around ~ 615 nm. Although in these copolymers conjugated system is retained, because thienopyrazine moiety is present as a pendant group, so the intensity of the band at longer wavelength is lower in intensity as compared to those polymers, where thienopyrazine moiety was present in main chain.

The polymers **P-17** exhibit emission peak at ~ 746 nm, while in case of **P-18** and **P-19** two emission peaks were observed, one in blue region at ~ 491 and ~ 436 nm respectively, second similar to that of **P-17** at ~ 745 nm. In case of **P-19**, the PL intensity of first emission (7%) is greater than the intensity of second emission peak (2%).

Polymer **P-17** shows the normalized optical absorption spectra of thin film similar to those of the absorption spectra in dilute solution.
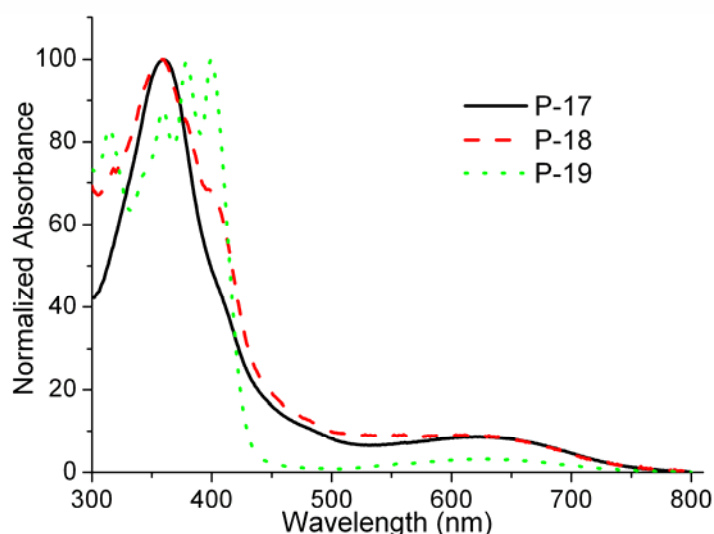
Figure 3.50. Normalized UV-vis spectra of **P-17, P-18** and **P-19** in solid state. (film from chlorobenzene)

3.2.6 Thermal Annealing Effect of P-10 and P-17 Films

To get information about the molecular packing and effect of thermal annealing on polymer films, we performed thermal annealing of polymer films being prepared from a chlorobenzene solution at different temperatures. At each temperature gradient the polymer film was annealed for 10 minutes, cooled to room temperature and UV absorption was measured.

As mentioned above, the visible absorption spectra of **P-10** and **P-17** films show no change in comparison with their solution. Very interestingly, the visible absorption peak of the polymer **P-10** film was slightly blue-shifted after annealing for 10 minutes at 80 ^{0}C, and intensity of the absorption peak was lowered. Further annealing did not bring any change in absorption spectrum of polymer **P-10**.
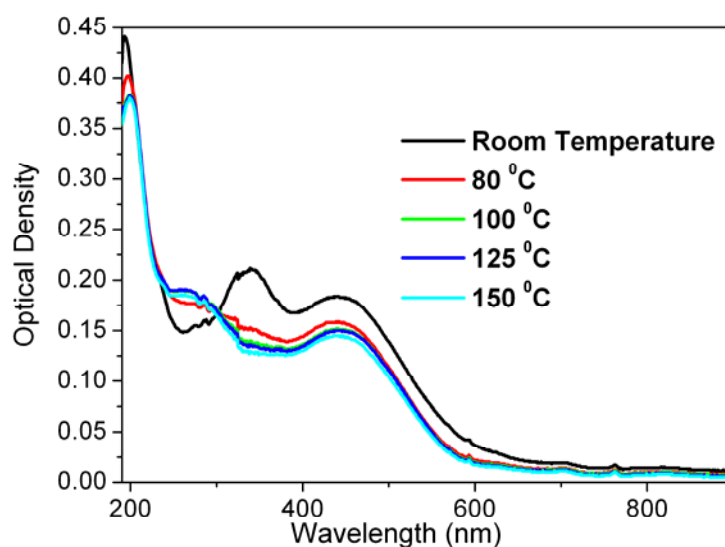
Figure 3.51. UV-vis spectra of **P-10** in solid state at different temperatures. (film from chlorobenzene)

In case of polymer **P-17**, the visible absorption peak was slightly red-shifted further to 632 nm for after the films were treated at 150 °C for 10 min, as shown in Figure 3.45. After the thermal annealing, the band gap of the polymers calculated from the absorption edge is 1.63 eV. This phenomenon was also observed in some other polythiophene derivatives. For example, when the film of regioregular poly- [3-(4-octylphenyl)thiophene] (P3OPT) was thermally annealed or treated in chloroform vapor, its band gap reduced from 2.1 to 1.85 eV, along with significant increase of structure ordering.[121] When the film was thermally annealed, the macromolecular chains of the polymer could realign, and then the conjugation effect could be enhanced. So the band gap of the polymers, which determines the absorption of the π-π* transition of the main chain, could be decreased after the thermal annealing.
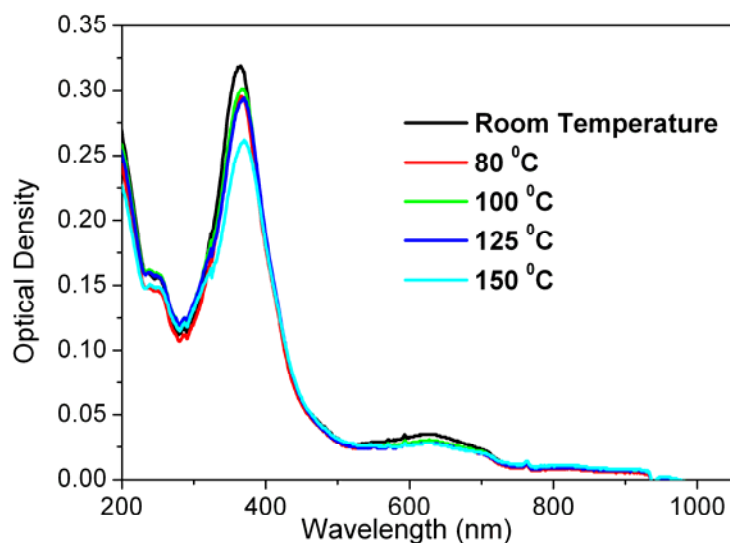
Figure 3.52. UV-vis spectra of **P-17** in solid state at different temperatures. (film from chlorobenzene)

3.2.7 Electrochemical Studies

The electrochemical behavior of the copolymers was investigated by cyclicvoltametry (CV), a useful method for measuring electrochemical behaviors and evaluation of the relative HOMO, LUMO energy levels and the band gap of a polymer. The solution of polymers (**P-10, P-12, P-15, P-16, P-17,** and **P-18**) was prepared in dichloromethane (5 mg/mL). The DPP(Differential pulse polarography) of polymers was carried out in dichloromethane at a potential scan rate of 15 mV/s. Ag/AgCl served as the reference electrode; it was calibrated with ferrocene ($E^{1/2}_{\text{ferrocene}}$ = 0.52 V vs Ag/ AgCl). The supporting electrolyte was tetrabutylammonium hexafluorophosphate (n-Bu$_4$NPF$_6$) in acetonitrile (0.1 M). Several ways to evaluate HOMO and LUMO energy levels from the onset potentials, $E^{\text{ox/onset}}$ and $E^{\text{red/onset}}$, have been proposed in the literature.[123-130] HOMO and LUMO energy levels were estimated here on the basis of the reference energy level of ferrocene (4.8 eV below the vacuum level) according to the following equation:

$$E^{\text{HOMO/LUMO}} = [\text{-}(E_{\text{onset (vs. Ag/AgCl)}} - E_{\text{onset (Fc/Fc+ vs. Ag/AgCl)}})] - 4.8 \text{ eV}.$$

The onset and the peak potentials, the electrochemical band gap energy, and the estimated position of the upper edge of the valence band (HOMO) and of the lower edge of conduction band (LUMO) are listed in Table 3.9. As shown by the cyclic voltammogramms in Figure

3.53, the polymer **P-10** showed reversibility in n-doping processes and irreversibility for their p-doping processes. The electrochemical reduction (or n-doping) of **P-10** starts at about -1.01 V Ag$^+$/Ag and gives n-doping peak at -1.31 V vs Ag$^+$/Ag. The reduction CV traces of the **P-12** show peak at -0.87 V vs Ag$^+$/Ag (onset at -0.76 V). Similarly the reduction of **P-17** and **P-18** starts at about -0.98 and -0.82 V Ag$^+$/Ag and gives n-doping peaks at –1.17 and –0.91 V Ag$^+$/Ag, respectively. However, oxidation of the polymers **P-17** and **P-18** was irreversible with peaks at 1.28 and 1.16 V, respectively. Such irreversibility in the electrochemical processes has been reported for several other π-conjugated polymers.[143] These moderately negative reduction potentials have been attributed to the electron withdrawing effects of thieno[3,4-*b*]pyrazine moiety.[60]
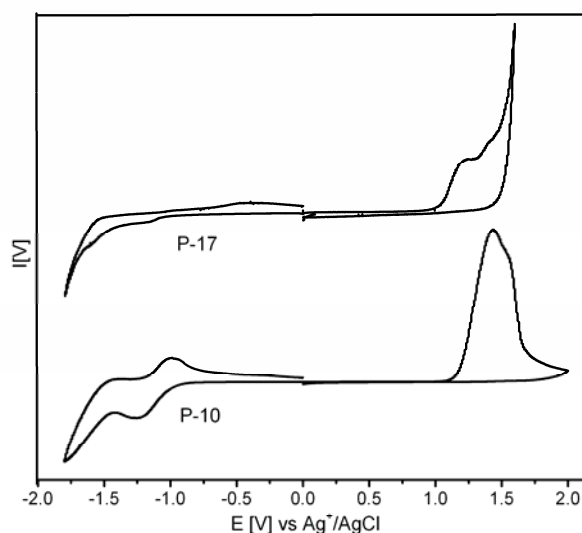
Figure 3.53. Cyclic voltammetry-curves of polymers (**P-10** and **P-17**) in 0.1M TBAPF$_6$/CH$_3$CN at 25 ^{0}C.

Table 3.10. Electrochemical Potentials and Energy Levels of the Polymers **P-10, P-12** and **P-15-P-18**.

Polymer	Oxidation Potential		Reduction Potential		Energy Levels[b]		Band Gap	
	E_{ox}[a]	$E_{onset, Ox}$	E_{red}[a]	$E_{onset, Red}$	HOMO	LUMO	E_g^{ec}	E_g^{opt}
	(V vs Ag/Ag$^+$)		(V vs Ag/Ag$^+$)		(eV)	(eV)		
P-10	1.42	1.18	-1.31	-1.01	-5.47	-3.28	2.19	2.10
P-12	1.28	1.10	-0.87	-0.76	-5.39	-3.53	1.86	2.18
P-15	1.22	1.12	-0.88	-0.76	-5.41	-3.53	1.88	2.06
P-16	1.11	1.03	-1.05	-0.83	-5.32	-3.46	1.86	1.96
P-17	1.28	1.04	-1.17	-0.98	-5.33	-3.31	2.02	1.69
P-18	1.16	1.01	-0.91	-0.82	-5.30	-3.47	1.83	1.83

[a]Reduction and oxidation potential measured by cyclic voltammetry. [b]Calculated from the reduction and oxidation potentials assuming the absolute energy level of ferrocene/ferrocenium to be 4.8 eV below vacuum.
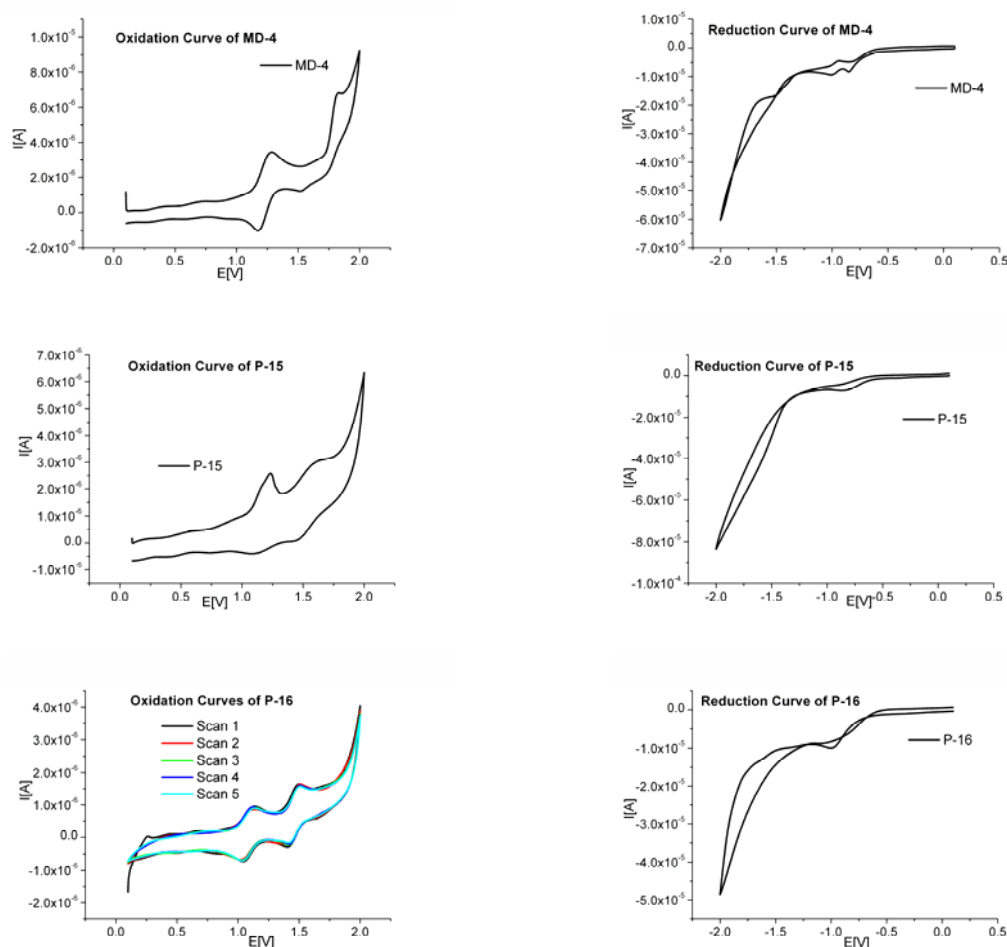
Figure 3.54. Cyclic voltammetry-curves of Model Compound (**MD-4**), Polymers **P-15** and **P-16** in 0.1M TBAPF$_6$/CH$_3$CN at 25 ^{0}C.

4   Experimental

4.1   Instrumentation

Melting Point. Melting points were obtained by a melting point apparatus *Melting Point B-540 of Büchi.*

NMR Spectroscopy. ^{1}H NMR and ^{13}C NMR spectra were recorded using a Bruker DRX 400 and a Bruker AC 250. The ^{1}H NMR was checked by using 250 MHz and 400 MHz while ^{13}C NMR by using 62 MHz and 400 MHz. The deuterated solvents used were $CDCl_3$, Acetone-D_6 and DMSO-D_6. Chemical shifts (δ values) are given in parts per million with tetramethylsilane as an internal standard.

Elemental Analysis. The C-H-N-S was measured on a CHNS-932 Automat Leco. While the Bromine was measured by potentiometric titration.

FT-IR. Infrared spectroscopy was recorded on a Nicolet Impact 400.

Thermogravimetric Analysis (TGA). A NETZSCH apparatus served for the thermogravimetric measurements.

Vapour Pressure Osmometry (VPO). The measurements were performed in chloroform in a Knauer Osmometer.

Gel Permeation Chromatography (GPC). The GPC measurements were performed on a set of Knauer using THF as eluent and polystyrene as a standard.

UV/Vis-Spectroscopy. The absorption spectra were recorded in dilute chloroform solution (10^{-5}-10^{-6} M) on a Perkin-Elmer UV/vis-NIR spectrometer Lambda 19.

Luminescence Spectroscopy. Quantum-corrected emission spectra were measured in dilute chloroform solution (10^{-6} M) with an LS 50 luminescence spectrometer (Perkin-Elmer). Photoluminescence quantum yields were calculated according to Demas and Crosby[144] against quinine sulfate in 0.1 N sulfuric acid as a standard ($\phi_{fl} = 55\%$). The solid-state absorption and emission were measured with a Hitachi F-4500. The films were cast from chlorobenzene. The quantum yield in the solid state was determined against a CF_3P-PPV (poly{1,4-phenylene-[1-(4-trifluoromethylphenyl)ethenylene]-2,5-dimethoxy-1,4-phenylene-[2-(4-trifluoromethylphenyl)ethenylene]}) copolymer reference that has been measured by integrating sphere as 0.43.

Cyclic Voltammetry. For study on electrochemical behavior, a polymer thin film was prepared on a platinum wire as a working electrode, using a platinum wire as the counter

electrode and Ag/Ag+ as the reference electrode in a solution of tetrabutylammonium hexafluorophosphate (0.1 M) in acetonitrile. The reference electrode potential vs normal hydrogen electrode (NHE) is 0.2223 V.[145] The cyclic voltammogram was recorded on a computer-controlled EG&G potentiostat/galvanostat model 283. The lowest unoccupied molecular orbital (LUMO) and the highest occupied molecular orbital (HOMO) energy levels of the polymers were converted from the onset reduction and oxidation potentials, respectively, with the assumption that the energy level of ferrocene/ferrocenium (Fc) is 4.8 eV below vacuum.

Differential Scanning Calorimetry (DSC). The glass transition temperature Tg was measured by DSC. For the measurements an instrument *Perkin-Elmer-DSC 2C*.

4.2 Pi-conjugated polymers containing thieno[3,4-*b*]pyrazine unit incorporated in backbone chain.

Materials. All starting materials including thiophene, glyoxal, hydroquinone, 2-methylbenzene-1,4-diol were purchased from commercial suppliers (Fluka, Merck, and Aldrich). Toluene, tetrahydrofuran and diethyl ether were dried and distilled over sodium and benzophenone. Diisopropylamine was dried over KOH and distilled. If not otherwise specified, the solvents were degassed by sparkling with argon or nitrogen 1 h prior to use. 1,4-dihexyloxy benzene (**1**),[104] 1,4-dihexyloxy-2,5-dibromo benzene (**2**),[105] 4-bromo-2,5-bis-dihexyloxy-benzaldehyde (**3**),[106] 4-formylphenylboronic acid (**6**),[146] 4-bromo-(2-ethyl-hexyloxy)benzene (**7**),[104] 1-(2-ethylhexyloxy)-4-ethynylbenzene (**9**),[147] 2,5-dibromo thiophene (**12**),[109a] 2,5-dibromo-3,4-dinitro thiophene (**13**),[109d] 3,4-diaminothiophene hydrochloride (**14**),[109d] 3,4-dihexylthiophene (**21**)[122] [4-(diethoxy-phosphorylmethyl)-2,5-bis-octyloxy-benzyl]-phosphonic acid diethyl ester (**M-5**),[104] [4-(diethoxy-phosphorylmethyl)-2,5-bis-(2-ethyl-hexyloxy)-benzyl]-phosphonic acid diethyl ester (**M-6**),[104] (4-cyanomethyl-2,5-bis-octyloxy-phenyl)-acetonitrile (**M-8**),[110] were prepared according to known literature procedures.

4.2.1 Synthesis of Monomer Precursors

2-(4-Bromo-2,5-bis-hexyloxy-phenyl)-[1,3]dioxane (4). To a solution of 4-bromo-2,5-bis-dihexyloxy-benzaldehyde (**3**) (10g, 25.95 mmol) and propane-1,3-diol (2.2g, 28.8mmol) in toluene (30 mL) was added BF$_3$•OEt$_2$ (3-4 drops). This mixture was refluxed for 6-7 h in a Dean Stark apparatus to remove the theoretical amount of water. The solution was washed with 1 M aq. NaHCO$_3$ and then with water, dried over MgSO$_4$ and concentrated in vacuum to give **5** (10.8g, 94 %) as a white solid, which was sufficiently pure to be employed in the next step.

4-Formyl-2,5-bis(hexyloxy)phenylboronic acid (5). A 2.5M solution of *n*-butyllithium (11.3mL, 28.4 mmol) was added to an argon-purged solution of 2-(4-Bromo-2,5-bis-hexyloxy-phenyl)-[1,3]dioxane (**4**) (10.5g, 23.7mmol) in anhydrous THF (50mL) at -78 °C using a syringe. The solution was then stirred for 2 h. Trimethyl borate (3g, 28.4mmol) was added with a syringe. The resulting mixture was allowed to come to room temperature and stir for 24 h. Then it was cooled to 0°C, 2N HCl (43mL) was added and the mixture was at room temperature for an additional 20 h. The organic layer was separated and the aqueous layer was

extracted with (3x50 mL) diethyl ether. The combined ether layers were washed twice with 50 mL of water, brine and dried over magnesium sulfate. After filtration, solvent was then removed under reduced pressure. The crude product was purified by recrystallization from hexane to give a light yellow powder. Yield: 6.3g (76%). ^{1}H NMR (250 MHz, CDCl$_3$): δ = 10.50 (s, 1H), 7.50 (s, 1H), 7.32 (s, 1H), 6.46 (bs, 2H), 4.09 (t, 2H), 3.95 (t, 2H), 2.16-0.88 (m, 22H), ^{13}C NMR (62 MHz, CDCl$_3$): δ = 190.33, 157.74, 155.88, 127.23, 121.27, 108.89, 69.29, 31.65, 31.57, 29.32, 29.27, 25.86, 25.77, 22.70, 22.64, 14.13, 14.08. Elemental analysis calculated for **C$_{19}$H$_{31}$BO$_5$** (350.26 g/mol): C, 65.15; H, 8.92. Found: C, 65.28; H, 9.09.

1,1′-Ethyne-1,2-diyl-bis[4-(2-ethyl-hexyloxy)benzene] (10) To a degassed solution of diisopropylamine (40 ml) and toluene (50 ml) were added 1-Bromo-4-(2-ethyl-hexyloxy) benzene (**7**) (6.19g, 21.7mmol),1-(2-Ethyl-hexyloxy)-4-ethynylbenzene (**9**) (5g, 21.7mmol), bis(triphenylphosphine)-palladium(II)chloride([Pd(PPh$_3$)$_2$]Cl$_2$) (420 mg, 0.6 mmol) and copper(I)iodide(CuI) (114 mg, 0.6 mmol). The reaction mixture was stirred at 80 °C for 12 h under inert gas atmosphere (argon). After cooling, the ammonium bromide precipitates were filtered off and washed with hexane. The solvent was removed under reduced pressure, and the residue was chromatographed over a silica gel column with n-hexane:10% Toluene as eluent to obtain desired product as light yellow liquid. Yield: 7.1g (51%). ^{1}H NMR (250 MHz, CDCl$_3$): δ = 7.38-7.32 (d, 4H), 6.80-6.76 (d, 4H), 3.77-3.71 (d, 4H), 2.27-0.85 (m, 30H), ^{13}C NMR (62 MHz, CDCl$_3$): δ = 158.19, 131.76, 114.43, 113.50, 86.93, 69.54, 38.33, 29.49, 28.06, 22.83, 22.02, 13.05, 10.08.

1,2-Bis-[4-(2-ethyl-hexyloxy)-phenyl]-ethane-1,2-dione (11) To a mixture of (**10**) (5g, 11.5mmol), acetone (120mL), and distilled water (40mL) KMnO$_4$ (9.1g, 58.2mmol) was slowly added and stirred at room temperature for 4 h. After the reaction was completed, black MnO$_2$ solids were removed by filtration. The concentrated filtrate was extracted with 500 mL of ethyl acetate. The organic layer was washed several times with water, brine and dried over anhydrous MgSO$_4$. After the solvent was removed under reduced pressure, the product was purified by chromatography (solvent, dicholomethane:hexane,2:1). Yield: 4.2g (79%) yellow oil. ^{1}H NMR (250 MHz, CDCl$_3$): δ = 7.88-7.82 (d, 4H), 6.91-6.85 (d, 4H), 3.85-3.83 (d, 4H), 1.71-0.75 (m, 30H), ^{13}C NMR (62 MHz, CDCl$_3$): δ = 192.58, 163.70, 131.31, 125.04, 113.71, 69.88, 38.20, 29.40, 28.00, 22.76,2197, 13.03, 10.04.

Thieno[3,4-*b*]pyrazine (15). 3,4-diaminothiophene hydrochloride (**14**) (5g, 26.7mmol) was added to 5% Na_2CO_3 (100 mL). Glyoxal (1.7g, 29.4mmol) was then added as an aqueous solution prepared by diluting 4.25g of a 40% glyoxal solution to 5 mL with water. This mixture was stirred at room temperature for one hour and then extracted repeatedly with ether. The combined ether fractions were washed with water, dried with anhydrous Na_2SO_4, and concentrated by rotary evaporation without heating to give light brown oil. Analytical samples were prepared by dissolving the oil in a minimal amount of CH_2Cl_2 and purified by chromatography using ether as the eluting solvent to give 2.4g of a light tan solid (66%). M.p. 47.3-48.1 °C (lit.[1] 46.5 °C); ^{1}H NMR (250 MHz, $CDCl_3$): δ = 8.46 (s, 2H), 8.01 (s, 2H). ^{13}C NMR (62 MHz, $CDCl_3$): δ = 144.4, 142.8, 118.4. Elemental analysis calculated for $C_6H_4N_2S$ (136.18 g/mol): C, 52.92; H, 2.96; N, 20.57. Found: C, 53.03; H, 3.28; N, 20.23.

2,3-Diphenylthieno[3,4-*b*]pyrazine (16). 3,4-diaminothiophene hydrochloride (**14**) (5g, 26.7mmol) and Benzil (5.62g, 26.7mmol) were combined in 100 mL absolute ethanol. Triethyl amine (5.76g, 56mmol) was added and mixture stirred overnight in dark and then concentrated by rotary evaporation without heating to give a solid residue. The residue was washed repeatedly with petroleum ether; the combined petroleum ether washes were dried with anhydrous Na_2SO_4, and then concentrated by rotary evaporation to give a light tan product. The product was purified further by chromatography (solvent, dichloromethane) to give light yellow-tan needles. Yield: 5.16 g (67 %). M.p. 169.1-171.0 ºC. ^{1}H NMR (250 MHz, $CDCl_3$): δ = 7.30-7.45 (m), 8.05 (s), ^{13}C NMR (62 MHz, $CDCl_3$): δ = 116.54, 127.13, 127.82, 128.60, 138.12, 140.59, 152.33. Elemental analysis calculated for $C_{18}H_{12}N_2S$ (288.37 g/mol): C, 74.97; H, 4.19; N, 9.71. Found: C, 74.64; H, 4.36; N, 9.65.

2,3-Bis-[4-(2-ethylhexyloxy)-phenyl]-thieno[3.4-*b*]pyrazine (17). Same procedure was followed as mentioned above for **16**. 3,4-diaminothiophene hydrochloride (**14**) (1.4g, 75mmol) and 1,2-Bis-[4-(2-ethylhexyloxy)-phenyl]-ethane-1,2-dione (**11**) (3.5g, 75mmol). Yield: 2.45g (60%). ^{1}H NMR (250 MHz, $CDCl_3$): δ =7.85 (s, 1H), 7.32-7.28 (d, 4H), 6.76-6.72 (d, 4H), 3.77-3.74 (d, 4H), 1.68-0.79 (m, 30H), ^{13}C NMR (62 MHz, $CDCl_3$): δ = 159.02, 152.04, 140.58, 130.52, 130.05, 115.77, 113.21, 69.60, 38.30, 29.47, 28.06, 22.82, 22.0, 13.06, 10.08. Elemental analysis calculated for $C_{34}H_{44}N_2O_2S$ (544.79 g/mol): C, 74.96; H, 8.14; N, 5.14. Found: C, 74.81; H, 8.23; N, 5.03.

5,7-Dibromo-thieno[3,4-*b*]pyrazine (18). To Compound (**15**) (2g, 14.7mmol) in chloroform/ acetic acid (1:1) 60mL was added NBS (5.75g, 32.3mmol) in dark and stirred overnight under argon. The reaction mixture was diluted with equal amount of water; the chloroform layer was separated and washed once with KOH solution and once with water, dried over MgSO$_4$. The organic layer was concentrated by rotary evaporation without heating to give a solid residue. The product was further purified by chromatography using Hexane: dichloromethane (1:1) to give greenish yellow solid. Yield: 2.85g (66%). ^{1}H NMR (250 MHz, CDCl$_3$): δ = 8.70 (s, 2H). ^{13}C NMR (62 MHz, CDCl$_3$): δ = 154.4, 152.8, 108.4. Elemental analysis calculated for **C$_6$H$_2$Br$_2$N$_2$S** (293.97): C, 24.51; H, 0.69: N, 9.53; Br, 54.36. Found: C, 24.30; H, 0.60: N, 9.24; Br, 54.20.

5,7-Dibromo-2,3-diphenylthieno[3,4-*b*]pyrazine (19). Same procedure was followed as mentioned above for **18**. Compound (**16**) (3g, 10.4mmol), NBS (2.28g, 22.8 mmol). Yield: 3.4g (74%). M.p. 169.1-171.0 ºC. ^{1}H NMR (250 MHz, CDCl$_3$): δ = 7.44-7.32 (m). ^{13}C NMR (62 MHz, CDCl$_3$): δ = 154.63, 139.29, 138.23, 130.25, 129.86, 129.37, 128.49. Elemental analysis calculated for **C$_{18}$H$_{10}$Br$_2$N$_2$S** (446.16 g/mol): C, 48.46; H, 2.26; N, 6.28; Br, 35.82. Found: C, 48.36; H, 2.08; N, 6.24; Br, 35.60.

5,7-Dibromo-2,3-bis-[4-(2-ethylhexyloxy)-phenyl]-thieno[3.4-*b*]pyrazine (20) In the absence of light, a solution of NBS (1.3g, 7.4mmol) in DMF (10mL) was slowly and dropwise added to a solution of 2,3-Bis-[4-(2-ethylhexyloxy)-phenyl]-thieno[3.4-*b*]pyrazine (**17**) (2g, 3.67mmol) in DMF (20 mL), and the mixture was stirred at -25 ^{0}C for 3h, poured onto ice, and extracted several times with diethyl ether. The organic phases were combined, washed with water, and dried over sodium sulfate. Evaporation of the solvent and chromatography (solvent, dichloromethane: hexane (2:1)) yielded 5,7-Dibromo-2,3-Bis-[4-(2-ethylhexyloxy)-phenyl]-thieno[3.4-*b*]pyrazine (**14**) (1.6g, 62%) as a yellowish liquid. ^{1}H NMR (250 MHz, CDCl$_3$): δ = 7.39-7.36 (d, 4H), 6.78-6.74 (d, 4H), 3.79-3.77 (d, 4H) 1.68-0.75 (m, 30H), ^{13}C NMR (62 MHz, CDCl$_3$): δ = 159.6, 153.3, 138.22, 130.40, 129.63, 113.23, 103.02, 69.63, 38.29, 29.48, 28.06, 22.82, 22.02, 13.06, 10.08. Elemental analysis calculated for **C$_{34}$H$_{42}$Br$_2$N$_2$O$_2$S** (702.58 g/mol): C, 58.12; H, 6.03; N, 3.99; Br, 22.75. Found: C, 58.06; H, 6.10; N, 3.90; Br, 22.65.

4.2.2 Monomers Synthesis

General Procedure for Synthesis of Monomers (M-1, M-2, M-3 and M-4):

Under an argon atmosphere, 5,7-dibromo-2,3-disubsituted thieno[3,4-*b*]pyrazines (**18, 19, 20**) (5 mmol) and 4-formyl-2,5-bis(substituted)phenylboronic acids (**5, 6**) (12.5 mmol) were added to degassed aqueous solution of potassium carbonate 16 mL (2.0 M), toluene and THF 40 mL (1:1, volume ratio). After 30 minutes degassing 3 mol% (173mg, 0.15mmol) of Pd(PPh₃)₄ was added. The mixture was stirred vigorously at 80-90 °C for 24 h under an argon atmosphere. The reaction mixture was cooled to room temperature, followed by the addition toluene and water. The organic layer was separated and washed with water, brine and dried over MgSO₄. After evaporation of solvent, the product was further purified by chromatography (solvent, toluene). Finally, pure product can be obtained by recrystallization from hexane.

2,3-Diphenyl-thieno[3,4-*b*]pyrazine-5,7-diyl-bis(2′,5′-dihexyloxy-4′-benzaldehyde) (M-1): 5,7-Dibromo-2,3-diphenylthieno[3,4-*b*]pyrazine (**19**) (2.24g, 5mmol) and 4-formyl-2,5-bis(hexyloxy)phenylboronic acid (**5**) 4.38g, 12.5mmol). Yield: 2.5g (57%).^{1}H NMR (250 MHz, CD₂Cl₂): δ = 10.54 (s, 2H), 9.23 (s, 2H), 7.58-7.31 (m, 12H), 4.27-4.13 (m, 8H), 2.02-0.87 (m, 44H). ^{13}C NMR (62 MHz, CDCl₃): δ = 190.64, 157.95, 153.51, 151.23, 142.21, 141.64, 139.99, 131.99, 131.47, 131.03, 130.47, 130.14, 125.28, 117.34, 113.16, 111.66, 72.06, 71.32, 33.76, 33.64, 31.49, 31.08, 27.97, 27.34, 24.77, 24.51, 15.95, 15.88. FAB MS: *m/z* 896 (M⁺). Elemental analysis calculated for **C₅₆H₆₈N₂O₆S** (897.22 g/mol): C, 74.97; H, 7.64; N, 3.12; S, 3.57. Found: C, 74.96; H, 7.52; N, 3.08; S, 3.46.

Thieno[3,4-*b*]pyrazine-5,7-diyl- bis(2′,5′-dihexyloxy-4′-benzaldehyde) (M-2):

5,7-Dibromo-thieno[3,4-*b*]pyrazine (**18**) (1.47g, 5mmol) and 4-formyl-2,5-bis(hexyloxy)phenylboronic acid (**5**) (4.38g, 12.5mmol). Yield: 1.7g (68%). ^{1}H NMR (250 MHz, CDCl₃): δ = 10.44 (s, 2H), 8.57 (s, 4H), 7.40 (s, 2H), 4.15-3.96 (m, 8H), 1.85-0.72 (m, 44H). ^{13}C NMR (62 MHz, CDCl₃): δ = 188.40, 155.15, 148.49, 142.52, 140.65, 128.63, 127.97, 122.97, 115.15, 109.20, 69.09, 68.46, 30.83, 30.75, 28.42, 28.38, 25.06, 24.99, 21.85, 21.75, 13.27, 13.17. FAB MS: *m/z* 744.4 (M⁺). Elemental analysis calculated for **C₄₄H₆₀N₂O₆S** (745.025 g/mol): C, 70.94; H, 8.12; N, 3.76; S, 4.30. Found: C, 71.20; H, 8.26; N, 3.54; S, 4.28.

2,3-Bis-[4-(2-ethylhexyloxy)-phenyl]-thieno[3.4-*b*]pyrazine-5,7-diyl-bis(2´,5´-dihexyloxy-4´-benzaldehyde) **(M-3):** 5,7-Dibromo-2,3-bis-[4-(2-ethylhexyloxy)-phenyl]-thieno[3.4-*b*]pyrazine (**20**).(1.4g, 2mmol) and 4-formylphenylboronic acid (**6**) (1.16g, 5mmol). Yield: 0.8g (56%). ^{1}H NMR (250 MHz, CDCl$_3$): δ = 10.04 (s, 2H), 8.51 (d, 4H), 7.98 (d, 4H), 7.55 (d, 4H), 6.92 (d, 4H),3.92 (d, 4H), 1.78-0.86 (m, 30H). ^{13}C NMR (62 MHz, CDCl$_3$): δ = 191.41, 160.61, 153.30, 150.78, 140.26, 138.96, 135.11, 131.37, 130.23, 129.46, 127.91, 114.33, 70.72, 39.39, 31.92, 30.55, 29.68, 29.11, 23.88, 23.03, 23.01, 22.67, 14.06, 14.04, 11.12. FAB MS: *m/z* 752 (M$^+$). Elemental analysis calculated for **C$_{48}$H$_{52}$N$_2$O$_4$S** (753.0 g/mol): C, 76.56; H, 6.96; N, 3.72; S, 4.26. Found: C, 76.25; H, 7.26; N, 3.77; S, 4.18.

2,3-Diphenyl-thieno[3,4-*b*]pyrazine-5,7-diyl-bis(4´-benzaldehyde) **(M-4):** 5,7-Dibromo-2,3-diphenylthieno[3,4-*b*]pyrazine (**19**).(1.34g, 3mmol) and 4-formylphenylboronic acid (**6**) (1.12g, 7.5mmol). Yield: 0.94g (63%).^{1}H NMR (250 MHz, CDCl$_3$): δ = 10.06 (s, 2H), 8.52 (d, 2H), 8.00 (d, 2H), 7.58-7.34 (m, 10H). FAB MS: *m/z* 496.1 (M$^+$). M.p. 324-325 ^{0}C. Elemental analysis calculated for **C$_{32}$H$_{20}$N$_2$O$_2$S** (496.12 g/mol): C, 77.40; H, 4.06; N, 5.64; S, 6.46. Found: C, 77.21; H, 4.09; N, 5.49; S, 6.38.

2,5-Bis(bromomethyl)-3,4-dihexylthiophene (22). Compound (**21**) (10.0g, 39.6mmol) and paraformaldehyde (2.84g, 94.6mmol) were dissolved in 5 mL of acetic acid and HBr solution (30% in acetic acid, 95mmol, 20 mL). The reaction was stirred at room temperature under argon overnight. The reaction was diluted with 200 mL of ethyl ether washed with water, saturated NaHCO$_3$ solution and brine. After the solvent removal, 13 g of light brown oil was obtained (75% yield), which was sufficiently pure for next step reaction.

3,4-Dihexyl-2,5-bis(methylenediethylphosphate)-thiophene (M-7). Compound (**22**) (8.76 g, 20mmol) reacted with triethyl phosphite (10 g, 60mmol) at 120 °C for 4 h. The crude product was purified by column chromatography on silica gel using acetone-hexane (25:75) as an eluent to give 8.8 g of light yellow oil (80% yield). ^{1}H NMR (250 MHz, CDCl$_3$): δ = 4.14-4.01 (m, 8 H), 3.26-3.21 (m, 4 H), 2.46 (t, 4 H), 1.42-0.86 (m, 34 H). ^{13}C NMR (62 MHz, CDCl$_3$): δ = 139.98, 124.53, 62.26, 31.64, 30.58, 29.53, 27.25, 25.86, 22.59, 16.37, 16.05, 14.01.

4.2.3 Model Compounds Synthesis

MD-1: Dialdehyde **M-1** (0.5 g, 0.56 mmol) and diethyl benzylphosphonate (0.28 g, 1.2 mmol) were dissolved in dried THF (7 mL) while stirring vigorously under argon at 0 ^{0}C. Potassium-*tert*-butoxide (1M in THF, 1 mL, 1.8 mmol) was added dropwise and the solution was stirred for further 2 h at room temperature. The reaction was quenched by addition of water and aqueous layer was extracted with diethyl ether (25mL) three times. The ether layer was washed with water, brine and dried over anhydrous MgSO$_4$. After the solvent was removed under reduced pressure, the product was purified by chromatography (solvent, dicholomethane:hexane,2:1). Yield: 0.42g (73%) dark violet solid. ^{1}H NMR (400 MHz, CDCl$_3$): δ = 8.97 (s, 2H), 7.61-7.20 (m, 26H), 4.27-4.15 (m, 8H), 2.04-0.87 (m, 44H). ^{13}C NMR (400 MHz, CDCl$_3$): δ = 150.98, 150.56, 149.48, 139.87, 139.01, 138.09, 129.88, 128.84, 128.62, 128.52, 127.89, 127.53, 127.33, 126.52, 125.68, 123.69, 123.45, 114.91, 110.48, 70.11, 69.20, 31.65, 29.57, 29.46, 25.98, 25.86, 22.67, 22.60, 14.03. FAB MS: *m/z* 1044.6 (M$^+$).UV-Vis (CHCl$_3$): λ$_{max}$/nm (ε/(1·mol^{-1}·cm^{-1})) 370(45800), 398(45300), 564(16000). Elemental analysis calculated for **C$_{70}$H$_{80}$N$_2$O$_4$S** (1045.46 g/mol): C, 80.42; H, 7.71; N, 2.68; S, 3.07. Found: C, 80.64; H, 8.03; N, 2.29; S, 2.84.

MD-2: Dialdehyde **M-1** (0.5g, 0.56 mmol) and (**25**) (0.61g, 1.2 mmol). Yield: 0.42g (71%) dark green solid. ^{1}H NMR (400 MHz, CDCl$_3$): δ = 8.94 (s, 2H), 7.63-7.32 (m, 16H), 7.14 (s, 2H), 6.76 (s, 2H), 4.26-3.97 (m, 16H), 2.27 (s, 6H), 2.04-0.86 (m, 104H). ^{13}C NMR (400 MHz, CDCl$_3$): δ = 151.60, 150.77, 150.53, 150.44, 149.93, 138.91, 129.89, 128.47, 127.86, 127.58, 127.54, 126.70, 125.36, 123.90, 122.97, 122.51, 116.22, 114.90, 110.29, 109.34, 70.03, 69.78, 69.17, 68.84, 31.88, 31.83, 31.68, 31.65, 29.58, 29.47, 29.42, 29.33, 29.30, 26.20, 25.97, 25.89, 22.70, 22.66, 22.60, 16.43, 14.07, 14.01**.** FAB MS: *m/z* 1586 (M$^+$). UV-Vis (CHCl$_3$): λ$_{max}$/nm (ε/(1·mol^{-1}·cm^{-1})) 411(68900), 574(23500). Elemental analysis calculated for **C$_{104}$H$_{148}$N$_2$O$_8$S** (1586.36 g/mol): C, 78.74; H, 9.40; N, 1.77; S, 2.02. Found: C, 78.68; H, 9.34; N, 1.72; S, 1.93.

MD-3: Dialdehyde **M-1** (0.5g, 0.56 mmol) and phenyl acetonitrile (0.14g, 1.2 mmol). Yield: 0.48g (79%) dark green solid. ^{1}H NMR (400 MHz, CDCl$_3$): δ = 9.17 (s, 2H), 8.09-7.31 (m, 20H), 4.36-4.11 (m, 16H), 2.36 (s, 6H), 2.07-0.86 (m, 104H). ^{13}C NMR (400 MHz, CDCl$_3$): δ = 150.06, 148.95, 147.07, 137.87, 137.76, 134.31, 133.29, 128.01, 127.13, 127.08, 126.84, 126.32, 126.07, 124.68, 124.02, 119.79, 117.01, 112.13, 109.28, 107.62, 68.15, 67.29, 29.75, 29.72, 27.53, 27.40, 24.03, 23.93, 23.91, 20.73, 12.11, 12.06. FAB MS: *m/z* 1094 (M$^+$). UV-

Vis (CHCl$_3$): λ_{max}/nm (ε/(1·mol^{-1}·cm^{-1})) 329(31300), 431(44700), 564(28900). Elemental analysis calculated for **C$_{72}$H$_{78}$N$_4$O$_4$S** (1095.48 g/mol): C, 78.94; H, 7.18; N, 5.11; S, 2.93. Found: C, 78.70; H, 7.20; N, 5.02; S, 2.76.

4.2.4 Synthesis of Polymers

General Procedure for Horner-Wadsworth-Emmons polycondensation

Dialdehyde (0.56 mmol) and corresponding phosphonate derivative (0.56 mmol) were dissolved in dried toluene (10 ml) while stirring vigorously under argon and heating under reflux. The polycondensations was started by adding potassium-*tert*-butoxide (2.23 mmol) and the solution refluxed for further 3.5 h. After cooling to room temperature toluene (15 ml) and an excess of dilute HCl were added. The organic layer was separated and extracted several times with distilled water until the water phase became neutral (pH = 6 – 7). A Dean-Stark apparatus was used to dry the organic layer. The hot (50-60°C) toluene solution was filtered, the filtrate was concentrated to the minimum by using a rotary evaporator and then precipitated in vigorously stirred methanol (300 ml). The polymer was extracted (soxhlet extractor) 12 h with methanol, acetone and finally with diethyl ether to remove oligomers, dried under vacuum. The polymer yields are mentioned after purification.

P-1: Dialdehyde **M-1** (0.5g, 0.56 mmol) and **M-5** (0.35g, 0.56 mmol). Yield: 0.49g (0.401 mmol, pertaining of the repeating unit) of dark green polymer were obtained. Yield: 491mg (72%). **^{1}H NMR** (400 MHz, CDCl$_3$): δ = 9.00 (bs, 2H), 7.63-7.26 (m, 16H), 6.89 (bs, 2H), 4.29-4.15 (m, 12H), 2.06-0.93 (m, 74H). **^{13}C NMR** (400 MHz, CDCl$_3$): δ = 151.04, 150.56, 150.44, 149.67, 148.86, 140.03, 139.07, 129.92, 128.49, 127.89, 127.37, 127.22, 126.73, 126.09, 125.53, 125.19, 123.74, 123.53, 123.41, 116.39, 115.12, 114.41, 110.92, 110.56, 70.19, 69.94, 69.73, 69.32, 31.89, 31.69, 31.49, 29.63, 29.55, 29.48, 29.34, 26.29, 25.98, 25.72, 22.66, 14.02. **GPC** (THF): $\overline{M}$w = 65100 g/mol, $\overline{M}$n = 32100; PDI = 2.0; $\overline{P}$n = 26. **UV-Vis** (CHCl$_3$): λ_{max}/nm (ε/(1·mol^{-1}·cm^{-1})) 446 (32300), 589 (20000). Elemental analysis calculated for **(C$_{80}$H$_{106}$N$_2$O$_6$S)$_n$** (1223.8)$_n$: C, 78.52; H, 8.71: N, 2.29; S, 2.62; Found: C, 77.35; H, 8.74,: N, 2.13; S, 2.53.

P-2: Dialdehyde **M-1** (0.5g, 0.56 mmol) and 1,4-bis(2-ethylhexyloxy)-2,5-di(methylenediethylphosphate)-benzene **(M-6)** (0.31g, 0.56 mmol). Yield: 0.48g (70%) green polymer. **^{1}H NMR** (400 MHz, CDCl$_3$): δ = 8.99 (bs, 2H), 7.63-7.26 (m, 16H), 6.88 (bs, 2H), 4.28-4.01 (m, 12H), 2.04-0.72 (m, 74H). **^{13}C NMR** (400 MHz, CDCl$_3$): δ = 150.56, 150.41,

149.70, 148.86, 140.03, 139.05, 129.91, 128.48, 127.88, 127.63, 127.15, 126.78, 126.13, 125.58, 125.11, 123.34, 123.14, 122.91, 122.64, 116.40, 115.22, 114.37, 110.11, 110.02, 71.95, 71.83, 71.65, 70.06, 69.35, 69.15, 68.79, 39.92, 39.78, 39.40, 31.66, 30.95, 30.76, 30.63, 29.57, 29.25, 28.92, 25.94, 25.72, 24.38, 24.11, 23.11, 22.89, 22.66, 22.60, 14.02, 13.95. **GPC** (THF): $\bar{M}w$ = 53100 g/mol, $\bar{M}n$ = 33500; PDI = 1.50; $\bar{P}n$ = 27. **UV-Vis** (CHCl$_3$): λ_{max}/nm (ε/(1·mol^{-1}·cm^{-1})) 446 (47000), 592 (29100). Elemental analysis calculated for **(C$_{80}$H$_{106}$N$_2$O$_6$S)$_n$** (1223.8)$_n$: C, 78.52; H, 8.73: N, 2.29; S, 2.62; Found: C, 78.15; H, 8.83,: N, 2.26; S, 2.62.

P-3: Dialdehyde **M-2** (0.5g, 0.67 mmol) and **M-5** (0.43g, 0.67 mmol). 0.43g (0.440 mmol, pertaining of the repeating unit) of dark green polymer were obtained. Yield: 65%. **^{1}H NMR** (400 MHz, CDCl$_3$): δ = 8.57 (bs, 2H), 8.42 (bs, 2H), 7.59 (bs, 2H), 7.34-6.87 (m, 6H), 4.2-4.12 (m, 12H), 1.93-0.88 (m, 74H). **^{13}C NMR** (400 MHz, CDCl$_3$): δ = 151.25, 150.89, 149.77, 142.63, 140.48, 128.36, 127.62, 127.35, 123.80, 123.37, 122.54, 115.72, 114.29, 110.73, 110.38, 69.97, 69.63, 69.46, 31.89, 31.72, 31.62, 29.61, 29.46, 29.35, 26.30, 25.99, 25.90, 22.67, 22.58, 14.07, 13.98. **GPC** (THF, polystyrene): $\bar{M}w$ = 64600 g/mol, $\bar{M}n$ = 29200; PDI = 2.2; $\bar{P}n$ = 27. **UV-Vis** (CHCl$_3$): λ_{max}/nm (ε/(1·mol^{-1}·cm^{-1})) 326 (18200), 437 (33300), 552 (23400). Elemental analysis calculated for **(C$_{68}$H$_{98}$N$_2$O$_6$S)$_n$** (1071.58)$_n$: C, 76.22; H, 9.22: N, 2.61; S, 2.99. Found: C, 75.40; H, 9.36; N, 2.43; S, 2.54.

P-4: Dialdehyde **M-3** (0.5g, 0.66 mmol) and **M-5** (0.42g, 0.66 mmol) Yield: 0.39g (54%) dark red polymer. **^{1}H NMR** (400 MHz, CDCl$_3$): δ = 8.40-6.87 (m, 22H), 4.10-3.90 (m, 8H), 1.96-0.91 (m, 60H). **^{13}C NMR** (400 MHz, CDCl$_3$): δ = 160.17, 153.17, 150.09, 139.83, 137.99, 132,87, 131.42, 130.27, 129.54, 128.78, 127.65, 126.40, 125.45, 124. 67, 116.78, 115.97, 115.30, 112.34, 111.68, 70.84, 69.91, 69.76, 69.33, 39.44, 36.61, 31.71, 30.57, 29.26, 29.11, 26.08, 23.91, 22.99, 22.60, 18.68, 13.99, 11.08. **GPC** (THF): $\bar{M}w$ = 34200 g/mol, $\bar{M}n$ = 15600; PDI = 2.1; $\bar{P}n$ = 14. **UV-Vis** (CHCl$_3$): λ_{max}/nm (ε/(1·mol^{-1}·cm^{-1})) 422 (47800), 553 (21000). Elemental analysis calculated for **(C$_{72}$H$_{90}$N$_2$O$_4$S)$_n$** (1079.56)$_n$: C, 80.10; H, 8.40: N, 2.59; S, 2.97; Found: C, 79.38; H, 8.17,: N, 2.31; S, 2.81.

P-5: Dialdehyde **M-1** (0.5g, 0.56 mmol) and **M-7** (0.31g, 0.56 mmol) Yield: 0.34g (54 %) green polymer. **^{1}H NMR** (250 MHz, CDCl$_3$): δ = 9.02 (s, 2H), 7.63-7.18 (m, 14H), 4.27-4.21 (m, 8H), 2.71 (t, 4H), 2.05-0.94 (m, 66H). **^{13}C NMR** (62 MHz, CDCl$_3$): δ = 151.30, 150.61, 149.68, 141.51, 140.30, 139.15, 136.50, 129.91, 128.48, 127.90, 127.65, 126.91, 126.11,

124.42, 123.73, 123.18, 122,47, 114.88, 112.02, 70.28, 69.24, 31.69, 31.39, 29.66, 29.57, 29.26, 27.33, 25.91, 25.54, 22.67, 14.04, 13.97. **GPC** (THF): $\bar{M}w$ = 13300 g/mol, $\bar{M}n$ = 1000; PDI = 1.50; $\bar{P}n$ = 9. **UV-Vis** (CHCl$_3$): λ_{max}/nm (ε/(1·mol^{-1}·cm^{-1})) 465 (31100), 615 (30300). Elemental analysis calculated for **(C$_{74}$H$_{96}$N$_2$O$_4$S$_2$)$_n$** (1141.7)$_n$: C, 77.85; H, 8.48: N, 2.45; S, 5.62; Found: C, 77.24; H, 8.11,: N, 2.40; S, 5.29.

P-6: Dialdehyde **M-2** (0.5g, 0.67 mmol) and **M-7** (0.37g, 0.67 mmol) Yield: 0.33g (50%) blue polymer. **^{1}H NMR** (400 MHz, CDCl$_3$): δ = 8.57 (bs, 2H), 8.45 (bs, 2H), 7.56-7.52 (d, 2H), 7.25-7.21 (d, 2H), 7.17 (bs, 2H), 4.2 (m, 8H), 2.69 (t, 4H), 2.00-0.83 (m, 66H). **^{13}C NMR** (400 MHz, CDCl$_3$): δ = 151.18, 149.73, 142.58, 141.53, 140.55, 136.40, 128.35, 126.88, 123.57, 122.45, 122.17, 115.72, 111.84, 70.16, 69.48, 31.68, 31.58, 31.35, 29.51, 27.30, 25.92, 25.84, 22.63, 22.53, 13.99, 13.88. **GPC** (THF): $\bar{M}w$ = 19200 g/mol, $\bar{M}n$ = 13300; PDI = 1.40; $\bar{P}n$ = 13. **UV-Vis** (CHCl$_3$): λ_{max}/nm (ε/(1·mol^{-1}·cm^{-1})) 458 (31000), 585 (33100). Elemental analysis calculated for **(C$_{62}$H$_{88}$N$_2$O$_4$S$_2$)$_n$** (989.5)$_n$: C, 75.26; H, 8.96: N, 2.83; S, 6.48; Found: C, 74.30; H, 8.41,: N, 2.50; S, 6.07.

General Procedure for Knoevenagel Polycondensation

Tetrabutylammonium hydroxide (62 µL, 1.0 M in methanol) was added into the degassed mixture solution of the dinitrile (0.56 mmol), the dialdehyde (0.56 mmol), THF (5 mL), and *tert*butyl alcohol (3 mL). The reaction mixture was heated to 50 °C while stirring under nitrogen atmosphere. After stirring for 2 h, the dark mixture was poured into methanol (150 mL), and the precipitate was collected by filtration. The crude polymer was Soxhlet extracted 12 h with methanol, acetone and finally with diethyl ether to remove oligomers, dried under vacuum. The polymer yields are mentioned after purification.

P-7: Dialdehyde **M-1** (0.5g, 0.56mmol) and **M-8** (0.23g, 0.56 mmol) Yield: 0.5g (71%) green polymer. **^{1}H NMR** (400 MHz, CDCl$_3$): δ = 9.17 (s, 2H), 8.19 (s, 2H), 7.61-7.18 (m, 14H), 4.41-4.15 (m, 12H), 2.08-0.87 (m, 74H). **^{13}C NMR** (400 MHz, CDCl$_3$): δ = 151.94, 151.43, 150.79, 149.27, 140.82, 140.19, 139.80, 129.88, 129.44, 128.70, 128.33, 127.92, 126.93, 126.51, 123.18, 122.25, 118.88, 115.30, 114.78, 114.25, 112.91, 111.72, 110.09, 106.97, 71.25, 70.23, 70.02, 69.23, 31.79, 31.58, 29.38, 29.30, 29.22, 26.12, 25.87, 25.79, 22.59, 13.94. **GPC** (THF): $\bar{M}w$ = 279000 g/mol, $\bar{M}n$ = 50200; PDI = 5.0; $\bar{P}n$ = 39. **UV-Vis** (CHCl$_3$): λ_{max}/nm (ε/(1·mol^{-1}·cm^{-1})) 434 (29500), 573 (17400). Elemental analysis calculated

for $(C_{82}H_{104}N_2O_6S)_n$ $(1273.8)_n$: C, 77.32; H, 8.23: N, 4.40; S, 2.52; Found: C, 76.92; H, 8.26,: N, 4.15; S, 2.19.

P-8: Dialdehyde **M-2** (0.5g, 0.67 mmol) and dinitrile **M-8** (0.28g, 0.67 mmol) Yield: 0.50g (67 %) green polymer. **^{1}H NMR** (400 MHz, CDCl$_3$): δ = 8.65 (bs, 2H), 8.19-8.16 (m, 4H), 7.18 (bs, 2H), 7.05 (s, 2H), 4.33-3.75 (m, 12H), 2.00-0.82 (m, 74H). **^{13}C NMR** (400 MHz, CDCl$_3$): δ = 151.86, 150.81, 149.22, 142.80, 141.12, 140.91, 128.67, 126.33, 125.81, 122.87, 118.76, 114.82, 111.85, 107.02, 70.14, 70.04, 69.42, 31.89, 31.77, 31.57, 29.30, 29.19, 26.10, 25.81, 22.57, 13.90. **GPC** (THF): $\overline{M}$w = 140000 g/mol, $\overline{M}$n = 42200; PDI = 3.3; $\overline{P}$n = 37. **UV-Vis** (CHCl$_3$): λ$_{max}$/nm (ε/(1·mol^{-1}·cm^{-1})) 432 (29000), 550 (31600). Elemental analysis calculated for $(C_{70}H_{96}N_4O_6S)_n$ $(1121.62)_n$: C, 74.96; H, 8.63: N, 5.00; S, 2.86; Found: C, 74.53; H, 8.50,: N, 4.89; S, 2.59.

P-9: Dialdehyde **M-3** (0.5g, 0.66 mmol) and **M-8** (0.27g, 0.66 mmol) Yield: 0.44g (57%) **brownish red** polymer. **^{1}H NMR** (400 MHz, CDCl$_3$): δ = 8.50-6.89 (m, 20H), 4.06-3.90 (m, 8H), 1.76-0.94 (m, 60H). **^{13}C NMR** (400 MHz, CDCl$_3$): δ = 160.48, 153.00, 150.29, 148.33, 145.99, 139.93, 135.02, 133,07, 131.32, 130.22, 129.94, 129.38, 127.85, 126.40, 125.45, 118.28, 117.47, 114.60, 114.34, 113.08, 70.79, 69.96, 69.66, 69.15, 39.44, 36.61, 31.71, 30.57, 29.26, 29.11, 26.08, 23.91, 22.99, 22.60, 18.68, 13.99, 11.08. **GPC** (THF): $\overline{M}$w = 14000 g/mol, $\overline{M}$n = 10500; PDI = 1.90; $\overline{P}$n = 9. **UV-Vis** (CHCl$_3$): λ$_{max}$/nm (ε/(1·mol^{-1}·cm^{-1})) 387 (25100), 511 (7950). Elemental analysis calculated for $(C_{74}H_{88}N_4O_4S)_n$ $(1129.58)_n$: C, 78.68; H, 7.85: N, 4.96; S, 2.84; Found: C, 77.94; H, 8.06,: N, 4.44; S, 2.45.

4.3   Pi- conjugated polymers containing thieno[3,4-*b*]pyrazine as pendant group

Materials. All starting materials including 4,4′-dimethylbenzil, 4-bromophenol, 1,4-dibromo-butane-2,3-dione, phenanthrene-9,10-dione, anthracene, benzaldehyde, 4-tolyl boronic acid (**29**), terephthalaldehyde (**M-16**), and 9,10-dibromoanthracene (**M-18**) and were purchased from commercial suppliers (Fluka, Merck, and Aldrich). Toluene, tetrahydrofuran and diethyl ether were dried and distilled over sodium and benzophenone. Diisopropylamine was dried over KOH and distilled. If not otherwise specified, the solvents were degassed by sparkling with argon or nitrogen 1 h prior to use., 1,4-dioctyloxy benzene,[104] 1-(2-ethylhexyloxy)-4-bromobenzene (**28**),[105] 4-(2-ethylhexyloxy)phenyl boronic acid (**30**),[133] 1,2-bis(4-(bromomethyl)phenyl)ethane-1,2-dione (**27**),[132] 2,7-dioxaborolan-9,9-didecylfluorene (**M-17**)[139] and 1,4-bis(bromomethyl)2,5-bis(octyloxy)benzene (**M-19**)[104] were prepared according to known literature procedures.

4.3.1   Synthesis of Monomer Precursors

2,7-dibromophenanthrene-9,10-dione (**26**): Phenanthrene-9,10-dione (2g, 9.6 mmol) was placed in a round bottom flask under nitrogen. Triflouromethanesulphonic acid (8.4ml, 96 mmol) was added to the flask followed by cooling to 0°C. N-bromosuccinimide (3.4g, 19.2mmol) was added slowly over 5 min and the reaction was allowed to gradually warm to room temperature. After 6 h at room temperature the reaction was poured onto ice, filtered and dried. Recrystallized from toluene to afford (**26**) in 85% yield as a bright orange crystals. ^{1}H NMR (CDC1$_3$): δ = 7.97 (d, J = 2.0 Hz, 2H), 7.66 (dd, J = 8.5 Hz, 2H), 7.03 (d, J = 8.4 Hz, 2H). ^{13}C NMR (CDCl$_3$): δ = 170.34, 139.71, 134.62, 130.49, 129.24, 127.94, 89.35. Elemental analysis calculated for **C$_{14}$H$_6$Br$_2$O$_2$** (366.0 g/mol): C, 45.94; H, 1.65; Br, 43.66. Found: C, 45.66; H, 1.59; Br, 43.48.

3,4-dinitro-2,5-di*p*-tolylthiophene (31): Under an argon atmosphere, 2,5-dibromo-3,4-dinitro-thiophene (**13**) (6g, 18mmol) and *p*-tolyl boronic acid (**29**) (6.12g, 45.1mmol) were added to degassed aqueous solution of potassium carbonate 50mL (2M), toluene and THF 100 mL (1:1, volume ratio). After 30 minutes degassing 3mol% (624mg, 0.54mmol) of Pd(PPh$_3$)$_4$ was added. The mixture was stirred vigorously at 80-90 °C for 24 h under an argon atmosphere. The reaction mixture was cooled to room temperature, diluted with toluene and water. The organic layer was separated and washed with water, brine and dried over MgSO$_4$.

After evaporation of solvent, the product was purified by column chromatography on silica gel using a hexane/dichloromethane mixture (2:1) to yield 4.5g,(70 %) of the title compound as a pale yellow solid. ^{1}H NMR (CDCl$_3$): δ = 7.34 (d, J = 8.7 Hz, 4H, Ph), 7.18 (d, J = 8.9 Hz, 4H, Ph), 2.31 (s, 6H, CH$_3$). ^{13}C NMR (CDCl$_3$): δ = 141.32, 140.77, 129.92, 128.89, 125.24, 124.84, 21.45. Elemental analysis calculated for **C$_{18}$H$_{14}$N$_2$O$_4$S** (354.39 g/mol): C, 61.01; H, 3.98; N, 7.90; S, 9.05. Found: C, 60.97; H, 3.95; N, 7.88; S, 8.95.

2,5-bis[4-(2-ethylhexyloxy)phenyl]-3,4-dinitrothiophene (32): Same procedure was followed as mentioned above for (**31**). 2,5-dibromo-3,4-dinitro-thiophene (**13**) (6g, 18mmol) and 1-borohydroxy-4-(2-ethylhexyloxy)benzene (**30**) (11.26g, 45mmol). Yield 6.5 g (62 %) of the title compound as a lemon yellow crystals. ^{1}H NMR (CDCl$_3$): δ = 7.38 (d, J = 8.8 Hz, 4H, Ph), 6.92 (d, J = 9.2 Hz, 4H, Ph), 3.82 (t, 4H, OCH$_2$), 1.70-0.83 (m, 26H, CH$_2$CH$_3$). ^{13}C NMR (CDCl$_3$): δ = 161.40, 140.68, 136.25, 130.52, 119.90, 115.25, 70.65, 39.26, 30.45, 29.03, 23.80, 23.00, 14.04, 11.06. Elemental analysis calculated for **C$_{32}$H$_{42}$N$_2$O$_6$S** (582.76 g/mol): C, 65.95; H, 7.26; N, 4.81; S, 5.50. Found: C, 65.81; H, 7.23; N, 4.67; S, 5.39.

2,5-di*p*-tolylthiophene-3,4-diamine (33): The dinitro-compound (**31**) (4g, 11.3mmol) was suspended in absolute ethanol (80mL) and treated with anhydrous stannous chloride (21.4g, 113mmol) dissolved in 45 mL conc. HCl and subsequently heated at reflux overnight. The homogeneous solution was poured into ice water and made alkaline by treating with aqueous sodium hydroxide. The solids formed were collected by filtration and dried under vacuum. The off white solid was recrystallized from a dichloromethane/hexane mixture to yield an analytically pure sample. Yield 2.7 g (82 %) ^{1}H NMR (CDCl$_3$): δ = 7.58 (d, J = 8.6 Hz, 4H, Ph), 7.17 (d, J = 8.7 Hz, 4H, Ph), 3.34 (bs, 4H, NH$_2$), 2.30 (s, 6H, CH$_3$). ^{13}C NMR (CDCl$_3$): δ = 136.44, 132.90, 131.49, 129.81, 127.54, 116.18, 21.21. Elemental analysis calculated for **C$_{18}$H$_{18}$N$_2$S** (294.42 g/mol): C, 73.43; H, 6.16; N, 9.51; S, 10.89. Found: C, 73.50; H, 5.97; N, 9.27; S, 11.01.

2,5-bis[4-(2-ethylhexyloxy)phenyl]thiophene-3,4-diamine (34): Same procedure was followed as mentioned above for (**33**).
2,5-bis[4-(2-ethyl-hexyloxy)phenyl]-3,4-dinitrothiophene (**32**) (5g, 8.6mmol), absolute ethanol (60mL), anhydrous stannous chloride (16.3g, 86 mmol) dissolved in 34 mL conc. HCl.The title compound was obtained as thick yellow liquid. Yield 3.4g (76 %) ^{1}H NMR (CDCl$_3$): δ = 7.21 (d, J = 8.7 Hz, 4H, Ph), 6.85 (d, J = 9.2 Hz, 4H, Ph), 5.1(bs, 4H, NH$_2$) 3.76

(t, 4H, OCH$_2$), 1.67-0.82 (m, 26H, CH$_2$CH$_3$). ^{13}C NMR (CDCl$_3$): δ = 160.34, 135.56, 129.43, 124.15, 121.96, 115.60, 70.62, 39.26, 30.46, 29.04, 23.81, 23.02, 14.05, 11.08. Elemental analysis calculated for **C$_{32}$H$_{46}$N$_2$O$_2$S** (522.78 g/mol): C, 73.52; H, 8.87; N, 5.36; S, 6.13. Found: C, 73.31; H, 8.69; N, 5.23; S, 6.05.

2,5-Dioctyloxy-1,4-phenylenemethylene diacetate (35): 1,4-bis(bromomethyl)2,5-bis(octyloxy)benzene (**M-19**) (4g, 7.7mmol), sodium iodide (2.3g, 15.4mmol), anhydrous sodium acetate (3.8g, 46.3mmol) and DMF (70ml) were charged in a round-bottom flask. The mixture was heated to 140 °C for 2 days with stirring. After cooling to room temperature, the mixture was poured into 200 mL of water and extracted with ethyl acetate three times (25 mL each). The organic phase was washed with water and brine and then dried with anhydrous MgSO4. After decolorization with active charcoal, the solvent was evaporated by rotary evaporation, and the residue was purified by recrystallization in ethyl acetate to afford 3.6g (97 %) of white crystals. ^{1}H NMR (CDCl$_3$): δ = 6.89 (s, 2H, Ph), δ = 5.37 (s, 4H, CH$_2$), δ = 3.94 (t, *J*=6.2, 4H, OCH$_2$), δ = 2.12 (s, 6H, Ac), δ = 1.46-1.39 (m, 24H, Alk), δ = 0.83-0.79 (t, 6H, CH$_3$). ^{13}C NMR (CDCl$_3$): δ = 174.93, 157.88, 128.36, 114.58, 69.22, 63.05, 35.75, 31.39, 28.18, 25.32, 22.35, 13.92. Elemental analysis calculated for **C$_{28}$H$_{46}$O$_6$** (478.66 g/mol): C, 70.26; H, 9.69. Found: C, 70.11; H, 9.75.

2,5-Dioctyloxy-1,4-bishydroxymethylbenzene (36): Compound (**35**) (3.45g, 7.2mmol) was added into 200 mL of mixed solvent of ethanol-water (1:1) containing sodium hydroxide (3.5g). The mixture was refluxed for 4 h with stirring. After cooling to room temperature, ethanol was evaporated through a rotary evaporator. The residue was extracted with ethyl acetate, and the organic layer was washed with water and brine and then dried by anhydrous MgSO4. After the solvent was evaporated, the crude product was purified by recrystallization from ethyl acetate to give 2.2g (82 %) of white crystals. ^{1}H NMR (CDCl$_3$): δ = 6.67 (s, 2H, Ph), δ = 4.92 (d, 4H, CH$_2$), δ = 4.79 (s, 4H, OH), δ = 3.84 (d, 4H, OCH$_2$), δ = 1.37-1.33 (m, 24H, Alk), δ = 0.83 (t, 6H, CH$_3$). ^{13}C NMR (CDCl$_3$): δ =154.33, 131.62, 113.49, 69.20, 63.16, 31.41, 28.17, 25.32, 22.36, 13.92. Elemental analysis calculated for **C$_{24}$H$_{42}$O$_4$** (394.6 g/mol): C, 73.05; H, 10.73. Found: C, 74.91; H, 10.81.

4.3.2 Monomers Synthesis

2,3-bis(bromomethyl)-5,7-di*p*-tolylthieno[3,4-b]pyrazine (M-9): The diamine (**33**) (2.5 g, 8.5 mmol) and 1,4-dibromo-butane-2,3-dione (2.07g, 8.5mmol) were dissolved in dry chloroform (75 mL) and a catalytic amount of p-toluene sulfonic acid was added to effect the

reaction. The mixture was stirred overnight at room temperature. After the volatiles were driven off, the violent red residue was adsorbed onto silica gel and subjected to column chromatography. The desired product was eluted with hexane/dichloromethane mixture (1:2). Yield: 3g (71%). ^{1}H NMR (CDCl$_3$): δ = 7.98 (d, J = 8.04 Hz, 4H, Ph), 7.20 (d, J = 8.03 Hz, 4H, Ph), 4.80 (s, 4H, CH$_2$Br), 2.34 (s, 6H, CH$_3$). ^{13}C NMR (CDCl$_3$): δ = 149.25, 138.29, 138.11, 132.44, 129.93, 129.62, 127.97, 31.79, 21.34. Elemental analysis calculated for **C$_{22}$H$_{18}$N$_2$Br$_2$S** (502.26 g/mol): C, 52.61; H, 3.61; N, 5.58; S, 6.38; Br, 31.82. Found: C, 52.57; H, 3.60; N, 5.56; S, 6.13; Br, 31.90.

2,3-bis(bromomethyl)-5,7-bis[4-(2-ethylhexyloxy)phenyl]thieno[3,4-b]pyrazine (M-10): Same procedure was followed as mentioned above for **M-9**.

Compound (**34**) (3g, 5.7mmol), 1,4-dibromo-butane-2,3-dione (1.4g, 5.7mmol) were dissolved in dry chloroform (50 mL). The violet product was eluted with hexane/dichloromethane mixture (3:2). Yield: 3.2g (76%). ^{1}H NMR (CDCl$_3$): δ = 8.08 (d, J = 8.8 Hz, 4H, Ph), 7.03 (d, J = 8.8 Hz, 4H, Ph), 4.87(s, 4H, CH$_2$Br) 3.93 (t, 4H, OCH$_2$), 1.80-0.90 (m, 26H, CH$_2$CH$_3$). ^{13}C NMR (CDCl$_3$): δ = 159.53, 148.93, 137.62, 131.67, 129.25, 125.92, 114.98, 70.62, 39.33, 31.90, 30.90, 29.06, 23.85, 23.04, 14.07, 11.09. Elemental analysis calculated for **C$_{36}$H$_{46}$O$_2$N$_2$Br$_2$S** (730.64 g/mol): C, 59.18; H, 6.35; N, 3.83; S, 4.39; Br, 21.87. Found: C, 59.43; H, 6.28; N, 3.73; S, 4.16; Br, 21.60.

2,3-bis[4-(bromomethyl)phenyl]-5,7-di _p_-tolylthieno[3,4-_b_]pyrazine (M-11): Same procedure was followed as mentioned above for **M-9**.

Compound (**33**) (3g, 10.2mmol), 1,2-bis(4-(bromomethyl)phenyl)ethane-1,2-dione (**27**) (4g, 10.2mmol) were dissolved in dry chloroform (50 mL). The violet red product was eluted with hexane/dichloromethane mixture (1:2). Yield: 4.5g (69%).^{1}H NMR (CDCl$_3$): δ = 8.17 (d, J = 8.04 Hz, 4H, Ph), 7.53 (d, J = 8.03 Hz, 4H, Ph), 7.37 (d, J = 8.04 Hz, 4H, Ph), 7.31 (d, J = 8.03 Hz, 4H, Ph), 4.50 (s, 4H, CH$_2$Br), 2.41 (s, 6H, CH$_3$). ^{13}C NMR (CDCl$_3$): δ = 151.29, 149.97, 144.71, 139.40, 138.35, 137.80, 130.49, 130.25, 129.59, 128.81, 127.65, 32.98, 21.32. Elemental analysis calculated for **C$_{34}$H$_{26}$Br$_2$ N$_2$S** (654.5 g/mol): C, 62.40; H, 4.00; N, 4.28; S, 4.90; Br, 24.42. Found: C, 62.34; H, 4.13; N, 4.12; S, 4.79; Br, 24.27.

2,3-bis[4-(bromomethyl)phenyl]-5,7-bis[4-(2-ethyl-hexyloxy)phenyl]thieno[3,4-b]pyrazine (M-12): Same procedure was followed as mentioned above for **M-9**.

Compound (**34**) (3g, 5.7mmol), 1,2-bis(4-(bromomethyl)phenyl)ethane-1,2-dione (**27**) (2.3g,

5.7mmol) were dissolved in dry chloroform (50 mL). The deep violet product was eluted with hexane/dichloromethane mixture (3:2). Yield: 3.6g (72%). ^{1}H NMR (CDCl$_3$): δ = 8.10 (d, J = 8.04 Hz, 4H, Ph), 7.44 (d, J = 8.03 Hz, 4H, Ph), 7.28 (d, J = 8.04 Hz, 4H, Ph), 6.94 (d, J = 8.03 Hz, 4H, Ph), 4.43 (s, 4H, CH$_2$Br), 3.84 (t, 4H, OCH$_2$), 1.71-0.81 (m, 26H, CH$_2$CH$_3$). ^{13}C NMR (CDCl$_3$): δ = 157.34, 149.14, 137.60, 136.36, 135.92, 128.74, 128.35, 127.13, 126.91, 124.00, 113.10, 68.75, 37.45, 31.15, 28.63, 27.18, 21.97, 21.17, 12.21, 9.22. Elemental analysis calculated for **C$_{48}$H$_{54}$O$_2$N$_2$Br$_2$S** (882.8 g/mol): C, 65.30; H, 6.17; N, 3.17; S, 3.63; Br, 18.10. Found: C, 65.21; H, 6.28; N, 3.03; S, 3.46; Br, 17.97.

[3-(Diethoxy-phosphorylmethyl)-5,7-di*p*-tolylthieno[3,4-*b*]pyrazin-2-ylmethyl]-phosphonic acid diethyl ester (M-13): A mixture of **M-9** (2g, 3.9mmol) and excess triethylphosphite (2.1g, 12.7mmol) was heated slowly to 150-160 [0]C, and the evolving ethyl bromide was distilled off simultaneously. After 4 h, vacuum was applied for 30 min at 160 [0]C to distil off the excess of triethyl phosphite. The resulting oil was allowed to cool to room temperature to form a deep red solid, which was recrystallized from diethyl ether yielding 2.1g (85%) of pure substance. ^{1}H NMR (CDCl$_3$): δ = 8.03 (d, J = 8.03 Hz, 4H, Ph), 7.20 (d, J = 7.65 Hz, 4H, Ph), 4.06 (m, 8H, OCH$_2$), 3.83 (s, 2H, CH$_2$), 3.74 (s, 2H, CH$_2$), 1.18 (t, 12H, CH$_3$). ^{13}C NMR (CDCl$_3$): δ = 147.34, 138.32, 137.72, 130.74, 130.38, 129.40, 127.68, 62.49, 35.72, 33.60, 21.29, 16.30, 16.20. Elemental analysis calculated for **C$_{30}$H$_{38}$N$_2$O$_6$P$_2$S** (616.65 g/mol): C, 58.43; H, 6.21; N, 4.54; S, 5.20. Found: C, 58.41; H, 6.14; N, 4,53; S, 4.94.

{3-(Diethoxy-phosphorylmethyl)-5,7-bis[4-(2-ethyl-hexyloxy)-phenyl]thieno[3,4-*b*]pyrazin-2-ylmethyl}-phosphonic acid diethyl ester (M-14): Same procedure was followed as mentioned above for **M-13**. Compound (**M-10**) (2g, 2.7mmol), triethyl phosphite (1.45g, 8.7mmol) Yield:1.9g dark purple solid (82%) ^{1}H NMR (CDCl$_3$): δ = 8.14 (d, J = 8.7 Hz, 4H, Ph), 7.01 (d, J = 8.8 Hz, 4H, Ph), 4.18 (m, 8H, OCH$_2$) 3.93 (t, 4H, OCH$_2$), 3.89 (s, 2H, CH$_2$), 3.83 (s, 2H, CH$_2$) 1.79-0.90 (m, 26H, CH$_2$CH$_3$). ^{13}C NMR (CDCl$_3$): δ = 159.21, 147.19, 137.85, 129.96, 128.99, 125.85, 114.84, 70.70, 62.43, 39.40, 35.38, 34.06, 31.91, 30.55, 29.34, 29.10, 23.90, 23.05, 22.67, 16.30, 16.08,14.06, 11.11. Elemental analysis calculated for **C$_{44}$H$_{66}$N$_2$O$_8$P$_2$S** (845.02 g/mol) : C, 62.54; H, 7.87; N, 3.32; S, 3.79. Found: C, 62.60; H, 8.01; N, 3.09; S, 3.70.

1,3-bis[4-(2-ethylhexyloxy)phenyl]-6,11-dibromodibenzo[*a,c*]thieno[3,4-*b*]quinoxaline (M-15): The diamine (**34**) (2.5 g, 4.8 mmol) and 2,7-dibromophenanthrene-9,10-dione (**26**)

(1.7g, 4.8 mmol) were dissolved in dry chloroform (75 mL) and a catalytic amount of p-toluene sulfonic acid was added to effect the reaction. The mixture was stirred overnight 40°C. After the volatiles were driven off, the bluish green residue was adsorbed onto silica gel and subjected to column chromatography using chloroform as an eluent. Yield: 2.8g (69%). ^{1}H NMR (CDCl$_3$): δ = 9.18 (s, 2H, quinoxaline), 8.40 (d, J = 8.79 Hz, 2H, quinoxaline), 8.06 (d, J = 9.18 Hz, 2H, Ph), 7.05 (d, J = 8.79 Hz, 2H, quinoxaline), 6.97 (d, J = 9.18 Hz, 2H, phenazine), 3.91 (s, 4H, OCH$_2$), 1.49-0.85 (d, 30H, CH$_2$CH$_3$). Elemental analysis calculated for **C$_{46}$H$_{48}$ Br$_2$N$_2$O$_2$S** (852.76 g/mol): C, 64.79; H, 5.67; N, 3.29; S, 3.76; Br, 18.74. Found: C, 64.61; H, 5.80; N, 3.13; S, 3.64; Br, 18.66.

2,5-Dioctyloxy-1,4-diformylbenzene   (M-20): Compound (**36**) (4g, 10.1mmol), pyridium chlorochromate (8.7g, 40.4mmol), freshly dried 4Å molecular sieves (1.75g) ,silica gel (1.75g) and 77mL of dry methylene chloride were charged into a 150 mL round-bottom flask. The mixture was cooled to 0 °C in an ice bath and stirred for 4 h, warmed to room temperature, and stirred for another 24 h. TLC monitoring indicated the diol compound had been completely converted to diformyl product. The mixture was run through a reduced pressure silicon gel column eluted with hexane. After the solvent was evaporated, yellow crystals 3.2g (81%) were obtained. ^{1}H NMR (CDCl$_3$): δ = 10.13 (s, 2H, CHO), δ = 6.97 (s, 4H, Ph), δ = 4.20 (t, 4H, OCH$_2$), δ = 1.30- 1.19 (m, 24H, Alk), δ = 0.84 (t, 6H, CH$_3$). ^{13}C NMR (CDCl$_3$): δ = 174.93, 157.88, 128.36, 114.58, 69.22, 63.05, 35.75, 31.39, 28.18, 25.32, 22.35, 13.92. Elemental analysis calculated for **C$_{24}$H$_{38}$O$_4$** (390.56 g/mol): C, 73.81; H, 9.81. Found: C, 73.69; H, 9.75.

4.3.3   Model Compounds Synthesis

2,3-distyryl-5,7-di*p*-tolylthieno[3,4-*b*]pyrazine (MD-4): Compound (**M-13**) (308mg, 0.5 mmol) and benzaldehyde (117mg, 1.1 mmol) were dissolved in dried THF (7 mL) while stirring vigorously under argon at 0 ^{0}C. Potassium-*tert*-butoxide (1M in THF, 1 mL, 1.8 mmol) was added dropwise and the solution was stirred for further 2 h at room temperature. The reaction was quenched by addition of water and aqueous layer was extracted with diethyl ether (25mL) three times. The ether layer was washed with water, brine and dried over anhydrous MgSO$_4$. After the solvent was removed under reduced pressure, the product was purified by chromatography (solvent, dicholomethane:hexane,2:1). Yield: 213mg (82%) dark violet solid. **^{1}H NMR** (400 MHz, CDCl$_3$): δ = 8.17 (d, 4H), 7.90 (d, 2H), 7.65 (d, 2H) 7.52-7.39 (m, 10H), 7.29 (d, 4H), 2.44 (s, 6H). **^{13}C NMR** (400 MHz, CDCl$_3$): δ = 159.89, 153.03,

139.11, 134.75, 131.96, 131.10, 130.41, 129.51, 129.43, 129.36, 127.96, 127.83, 127.77, 127.66, 127.54, 127.29, 117.58, 114.22, 22.56. FAB MS: m/z 520.2 (M^+).**UV-Vis** (CHCl$_3$): λ_{max}/nm (ϵ/(1·mol^{-1}·cm^{-1})) 265(20500), 333(52700), 361(39500), 538(3150). Elemental analysis calculated for **C$_{36}$H$_{28}$N$_2$S** (520.69 g/mol): C, 83.04; H, 5.42; N, 5.38; S, 6.16. Found: C, 82.93; H, 5.55; N, 5.27; S, 6.00.

5,7-bis-[4-(2-ethylhexyloxy)phenyl]-2,3-distyrylthieno[3,4-*b*]pyrazine   (MD-5):   M-14 (422mg, 0.5mmol) and benzaldehyde (117mg, 1.1 mmol) Yield: 295mg (79%) dark green solid. . **^{1}H NMR** (400 MHz, CDCl$_3$): δ = 8.21 (d, 4H), 7.92 (d, 2H), 7.67 (d, 2H) 7.56-7.36 (m, 10H), 7.04 (d, 4H), 3.96-3.95 (m, 4H, OCH$_2$), 1.82-0.93 (m, 30H). **^{13}C NMR** (400 MHz, CDCl$_3$): δ = 159.10, 147.88, 145.72, 138.34, 137.15, 136.83, 136.34, 133.14, 129.55, 129.04, 128.84, 128.78, 127.67, 127.60, 126.41, 123.26, 114.96, 114.22, 70.79, 39.51, 30.63, 29.15, 23.98, 23.05, 14.03, 11.13. FAB MS: m/z 748.2 (M^+). **UV-Vis** (CHCl$_3$): λ_{max}/nm (ϵ/(1·mol^{-1}·cm^{-1})) 266(26800), 336(57300), 363(45300), 565(3830). Elemental analysis calculated for **C$_{50}$H$_{56}$N$_2$O$_2$S** (749.06 g/mol): C, 80.17; H, 7.54; N, 3.74; S, 4.28. Found: C, 80.00; H, 7.45; N, 3.80; S, 4.20.

4.3.4 Synthesis of Polymers

General Procedure for Horner-Wadsworth-Emmons polycondensation

Dialdehyde (0.8mmol) and corresponding phosphonate derivative (0.8mmol) were dissolved in dried toluene (10 ml) while stirring vigorously under argon and heating under reflux. The polycondensations was started by adding potassium-*tert*-butoxide (3.2 mmol) and the solution refluxed for further 3.5 h. After cooling to room temperature toluene (15 ml) and an excess of dilute HCl were added. The organic layer was separated and extracted several times with distilled water until the water phase became neutral (pH = 6 – 7). A Dean-Stark apparatus was used to dry the organic layer. The hot (50-60°C) toluene solution was filtered, the filtrate was concentrated to the minimum by using a rotary evaporator and then precipitated in vigorously stirred methanol (300 ml). The polymer was extracted (soxhlet extractor) 12 h with methanol, acetone and finally with diethyl ether to remove oligomers, dried under vacuum. The polymer yields are mentioned after purification.

P-10: **M-13** (493mg, 0.8mmol) and 2,5-bis(octyloxy)benzene-1,4-dialdehyde (**M-20**) (312mg, 0.8mmol) Yield: 72%. **^{1}H NMR** (400 MHz, CDCl$_3$): δ = 8.26-7.20 (m, 14H), 4.15-3.95 (m, 4H), 2.47 (s, 6H), 1.87-0.79 (m, 30H). **^{13}C NMR** (400 MHz, CDCl$_3$): δ = 152.28, 149.09, 139.11, 137.19, 133.38, 131.11, 129.46, 127.83, 113.30, 69.72, 31.78, 29.23, 26.27, 22.54,

21.28, 13.95. **GPC** (THF, polystyrene): $\overline{M}$w = 14800 g/mol, $\overline{M}$n = 8800; PDI = 1.68; $\overline{P}$n = 13. **UV-Vis** (CHCl$_3$): λ_{max}/nm (ε/(1·mol^{-1}·cm^{-1})) 338 (28200), 440 (2100). Elemental analysis calculated for **(C$_{46}$H$_{54}$N$_2$O$_2$S)$_n$** (699.0)$_n$: C, 79.04; H, 7.79; N, 4.01; S, 4.59. Found: C, 78.40; H, 7.63,: N, 3.95; S, 4.21.

P-11: **M-14** (676 mg, 0.8mmol) and 2,5-bis(octyloxy)benzene-1,4-dialdehyde (**M-20**) (312mg, 0.8mmol) Yield: 65%. **^{1}H NMR** (400 MHz, CDCl$_3$): δ = 8.12-7.89 (m, 6H), 7.53-7.51 (m, 4H), 6.97-6.94 (m, 4H) 3.95-3.90 (m, 4H), 1.92-0.85 (m, 60H). **^{13}C NMR** (400 MHz, CDCl$_3$): δ = 163.77, 153.28, 152.19, 150.78, 140.30, 136.32, 133.15, 132.42, 131.52, 129.94, 128.78, 127.01, 124.61, 122.19, 116.74, 115.42, 114.14, 71.97, 70.84, 69.52, 68.79, 42.93, 39.35, 37.45, 37.09, 32.76, 31.77, 30.51, 29.65, 29.06, 27.60, 27.06, 26.06, 24.45, 23.87, 22.96, 22.57, 22.06, 20.88, 20.09, 19.64, 19.17, 13.96. **GPC** (THF, polystyrene): $\overline{M}$w = 7600 g/mol, $\overline{M}$n = 6000; PDI = 1.26; $\overline{P}$n = 6. **UV-Vis** (CHCl$_3$): λ_{max}/nm (ε/(1·mol^{-1}·cm^{-1})) 300 (21400), 420 (11600). Elemental analysis calculated for **(C$_{60}$H$_{82}$N$_2$O$_4$S)$_n$** (927.37)$_n$: C, 77.71; H, 8.91: N, 3.02; S, 3.46. Found: C, 77.08; H, 8.64; N, 3.02; S, 3.28.

P-12: **M-14** (676mg, 0.8mmol) and terephthalaldehyde (**M-16**) (107mg, 0.8mmol) Yield: 64%. **^{1}H NMR** (400 MHz, CDCl$_3$): δ = 8.23-7.95 (m, 4H), 7.65-7.53 (m, 6H), 7.12-6.95 (m, 6H), 3.97-3.86 (m, 4H), 1.85-0.98 (m, 30H). **^{13}C NMR** (400 MHz, CDCl$_3$): δ = 159.05, 147.53, 138.29, 128.98, 127.82, 126.42, 123.65, 114.87, 70.80, 39.50, 30.61, 29.16, 23.96, 23.06, 14.04, 11.14. **GPC** (THF, polystyrene): $\overline{M}$w = 10800 g/mol, $\overline{M}$n = 7400; PDI = 1.45; $\overline{P}$n = 11. **UV-Vis** (CHCl$_3$): λ_{max}/nm (ε/(1·mol^{-1}·cm^{-1})) 341 (33000), 405 (25000).Elemental analysis calculated for **(C$_{44}$H$_{50}$N$_2$O$_2$S)$_n$** (670.95)$_n$: C, 78.77; H, 7.51: N, 4.18; S, 4.78. Found: C, 78.03; H, 7.61; N, 3.93; S, 4.48.

General Procedure for Gilch polymerization

2,3-bis(bromomethyl)-5,7-disubstituted thieno[3,4-b]pyrazine (0.8mmol) was dissolved in 10 mL of anhydrous tetrahydrofuran, and 3 mL of potassium *t*-butoxide (1 M in THF) was slowly added dropwise to the solution under argon atmosphere. The reaction was let to proceed for 48 hours at room temperature. The reaction mixture was slowly added to an excess amount of methanol while stirring it. The crude polymer was precipitated two times in methanol for removal of low-molecular weight products. The polymer was extracted for 24 h with methanol and dried under vacuum.

P-13: **M-9** (402mg, 0.8mmol) and 1,4-bis(bromomethyl)2,5-bis(octyloxy)benzene (**M-19**) (416mg, 0.8 mmol)Yield: 70%. **^{1}H NMR** (400 MHz, CDCl$_3$): δ = 8.16-7.01 (m, 14H), 4.10-3.73 (m, 4H), 2.41 (s, 6H), 1.90-0.90 (m, 30H). **^{13}C NMR** (400 MHz, CDCl$_3$): δ = 151.24, 137.40, 129.38, 127.67, 123.51, 114.59, 110.86, 69.67, 68.84, 31.87, 29.61, 29.45, 29.32, 26.30, 22.63, 21.24, 14.00. **GPC** (THF, polystyrene): $\overline{M}$w = 25200 g/mol, $\overline{M}$n = 6100; PDI = 4.2; $\overline{P}$n = 9. **UV-Vis** (CHCl$_3$): λ$_{max}$/nm (ε/(1·mol^{-1}·cm^{-1})) 300 (24500), 457 (45200), 552 (10700). Elemental analysis calculated for **(C$_{46}$H$_{54}$N$_2$O$_2$S)$_n$** (699.0)$_n$: C, 79.04; H, 7.79; N, 4.01; S, 4.59. Found: C, 78.48; H, 6.95,: N, 3.94; S, 4.36; Br, 1.07.

P-14: **M-10** (584mg, 0.8mmol) and 1,4-bis(bromomethyl)2,5-bis(octyloxy)benzene (**M-19**) (416 mg, 0.8 mmol) Yield: 58%. **^{1}H NMR** (400 MHz, CDCl$_3$): δ = 8.05-7.62 (m, 6H), 7.49-7.46 (m, 4H), 6.76-6.72 (m, 4H) 3.84-3.81 (m, 4H), 1.90-0.86 (m, 60H). **GPC** (THF, polystyrene): $\overline{M}$w = 70500 g/mol, $\overline{M}$n = 11600; PDI = 6.1; $\overline{P}$n = 13. **UV-Vis** (CHCl$_3$): λ$_{max}$/nm (ε/(1·mol^{-1}·cm^{-1})) 312 (25000), 476 (16000) Elemental analysis calculated for **(C$_{60}$H$_{82}$N$_2$O$_4$S)$_n$** (927.37)$_n$: C, 77.71; H, 8.91: N, 3.02; S, 3.46. Found: C, 76.41; H, 9.00; N, 2.84; S, 3.28; Br, 0.84.

P-15: **M-10** (584 mg, 0.8 mmol) Yield: 67%. **^{1}H NMR** (400 MHz, CDCl$_3$): δ = 8.02-7.95 (m, 4H), 7.08-6.95 (m, 8H), 3.96-3.91 (m, 4H), 1.78-0.96 (m, 30H). **^{13}C NMR** (400 MHz, CDCl$_3$): δ = 159.11, 138.45, 130.45, 129.01, 128.20, 125.28, 114.87, 70.70, 39.47, 30.60, 29.12, 23.02, 21.38, 14.01, 11.09. **GPC** (THF, polystyrene): $\overline{M}$w = 5000 g/mol, $\overline{M}$n = 4200; PDI = 1.2; $\overline{P}$n = 7. **UV-Vis** (CHCl$_3$): λ$_{max}$/nm (ε/(1·mol^{-1}·cm^{-1})) 321 (22900), 540 (2000). Elemental analysis calculated for **(C$_{36}$H$_{44}$N$_2$O$_2$S)$_n$** (568.8)$_n$: C, 76.02; H, 7.80: N, 4.92; S, 5.64. Found: C, 75.48; H, 7.30; N, 4.79; S, 4.95; Br, 0.93.

P-16: **M-12** (706 mg, 0.8 mmol) Yield: 69%. **^{1}H NMR** (400 MHz, CDCl$_3$): δ = 8.25-8.22 (m, 4H), 7.59-7.33 (m, 10H), 7.05-7.01 (m, 4H) 3.95-3.94 (m, 4H), 1.80-0.95 (m, 30H). **^{13}C NMR** (400 MHz, CDCl$_3$): δ = 159.17, 151.74, 141.04, 138.01, 130.31, 129.82, 129.02, 126.76, 126.24, 115.03, 70.80, 39.46, 30.61, 29.11, 23.96, 23.04, 14.02, 11.10. **GPC** (THF, polystyrene): $\overline{M}$w = 19400 g/mol, $\overline{M}$n = 11500; PDI = 1.68; $\overline{P}$n = 16. **UV-Vis** (CHCl$_3$): λ$_{max}$/nm (ε/(1·mol^{-1}·cm^{-1})) 336 (32500), 530 (3570). Elemental analysis calculated for

(C$_{48}$H$_{52}$N$_2$O$_2$S)$_n$ (721.0)$_n$: C, 79.96; H, 7.27: N, 3.89; S, 4.45. Found: C, 78.55; H, 7.49,: N, 3.56; S, 4.02; Br, 1.26.

General Procedure for Polymerization (Suzuki Coupling). Under an argon atmosphere, dibromo monomers (**M-15**) (0.8 mmol)**,** 2,7-dioxaborolan-9,9-didecylfluorene (**M-17**) (0.8 mmol) and 9,10-dibromoanthracene (**M-18**) (0 mmol) were mixed together with 1.0-1.5% (0.012 mmol) of Pd(PPh$_3$)$_4$ in a small flask. Degassed aqueous solution of potassium carbonate 10 mL (2.0 M) and toluene 20 mL (1:2, volume ratio) were added to the flask. The mixture was stirred vigorously at 80-90 °C for 72h under an argon atmosphere. The resulting solution was added dropwise into stirring methanol to precipitate the polymer. The fibrous solid was collected by filtration and washed with methanol and water. The material was washed continuously with methanol and acetone for 2 days in a Soxhlet extractor to remove the oligomers and catalyst residues. The product was dried under reduced pressure overnight.

P-17: **M-15** (682mg, 0.8mmol) and 2,7-dioxaborolan-9,9-didecylfluorene (**M-17**) (469mg, 0.8 mmol) Yield: 71%. **^{1}H NMR** (400 MHz, CDCl$_3$): δ = 9.57 (s, 2H), 8.25-7.63 (m, 14H), 7.10-7.06 (m, 4H), 4.01 (bs, 4H, OCH$_2$), 2.17-0.78 (m, 72H). **^{13}C NMR** (400 MHz, CDCl$_3$): δ = 164.04, 159.19, 152.11, 151.07, 141.08, 140.62, 139.34, 133.35, 132.04, 131.07, 129.23, 128.77, 126.61, 124.16, 123.58, 121.66, 120.43, 115.07, 114.31, 70.94, 55.53, 40.40, 39.56, 39.42, 31.84, 30.59, 30.02, 29.66, 29.25, 24.01, 23.14, 23.02, 22.57, 14.11, 13.97, 11.23. **GPC** (THF, polystyrene): $\bar{M}$w = 25500 g/mol, $\bar{M}$n = 14000; PDI = 1.8; $\bar{P}$n = 12. **UV-Vis** (CHCl$_3$): λ$_{max}$/nm (ε/(1·mol^{-1}·cm^{-1})) 358 (79400), 612 (5000). Elemental analysis calculated for **(C$_{79}$H$_{96}$N$_2$O$_2$S)$_n$** (1137.68)$_n$: C, 83.40; H, 8.51; N, 2.46; S, 2.82. Found: C, 84.08; H, 8.40,: N, 2.25; S, 2.87; Br, 1.03.

P-18: **M-15** (341mg, 0.4mmol); 2,7-dioxaborolan-9,9-didecylfluorene (**M-17**) (469mg, 0.8 mmol) and and 9,10-dibromoanthracene (**M-18**) (134mg, 0.4mmol) Yield: 73%. **^{1}H NMR** (400 MHz, CDCl$_3$): δ = 9.61 (s, 2H), 8.49-7.15 (m, 26H), 4.04 (bs, 4H, OCH$_2$), 2.19-0.78 (m, 72H). **^{13}C NMR** (400 MHz, CDCl$_3$): δ = 159.26, 151.97, 151.31, 142.48, 140.49, 139.19, 138.03, 137.71, 132.28, 131.46, 130.23, 129.21, 127.13, 126.64, 126.41, 125.07, 124.18, 123.71, 122.94, 121.11, 120.39, 119.82, 115.13, 70.89, 55.62, 40.55, 39.59, 31.86, 30.69, 30.14, 29.56, 29.25, 24.01, 23.09, 22.59, 14.00, 11.20. **GPC** (THF, polystyrene): $\bar{M}$w = 28800 g/mol, $\bar{M}$n = 18600; PDI = 1.5; $\bar{P}$n = 42. **UV-Vis** (CHCl$_3$): λ$_{max}$/nm (ε/(1·mol^{-1}·cm^{-1}))

353 (25100), 399 (12600), 611 (1000). Elemental analysis calculated for $(C_{31.5}H_{40}N_{0.5}O_{0.5}S_{0.25})_n$ $(441.67)_n$: C, 85.66; H, 9.139; N, 1.58; S, 1.48. Found: C, 85.33; H, 8.88,: N,1.34; S, 1.48; Br, 1.10.

P-19: **M-15** (68mg, 0.08mmol); 2,7-dioxaborolan-9,9-didecylfluorene (**M-17**) (469mg, 0.8 mmol) and and 9,10-dibromoanthracene (**M-18**) (242mg, 0.72mmol) Yield: 67%. **¹H NMR** (400 MHz, CDCl$_3$): δ = 9.71 (s, 2H), 8.52-7.25 (m, 26H), 4.06 (bs, 4H, OCH$_2$), 2.12-0.90 (m, 72H). **¹³C NMR** (400 MHz, CDCl$_3$): δ = 159.41, 151.31, 142.45, 140.51, 139.21, 138.03, 137.73, 131.55, 130.23, 129.24, 127.13, 126.64, 126.42, 125.07, 124.18, 123.81, 122.95, 121.11, 119.82, 115.18, 70.89, 55.54, 40.54, 39.59, 31.88, 30.69, 30.14, 29.56, 29.25, 24.33, 24.03, 23.08, 22.61, 14.02, 11.18. **GPC** (THF, polystyrene): $\overline{M}w$ = 26800 g/mol, $\overline{M}n$ = 18300; PDI = 1.5; $\overline{P}n$ = 54. **UV-Vis** (CHCl$_3$): λ$_{max}$/nm (ε/(1·mol^{-1}·cm^{-1})) 360 (10000), 382 (10000), 402 (12600), 613 (200). Elemental analysis calculated for $(C_{25.1}H_{32}N_{0.1}O_{0.1}S_{0.05})_n$ $(338.3)_n$: C, 89.1; H, 9.53; N, 0.41; S, 0.47. Found: C, 88.93; H, 9.50,: N, 0.39; S, 0.39; Br, 1.07.

5   Zusammenfassung in Thesen

Polymere mit konjugierten Doppelbindungen besitzen auf Grund des ausgedehnten Pi-Bindungs-Systems unter anderem eine langwellige Lichtabsorption im sichtbarem Spektralbereich, und sie zeigen nach Dotierung elektrische Leitfähigkeit bzw. Photoleitfähigkeit. Sie sind in den gebräuchlichen organischen Lösungsmitteln löslich und filmbildend.

Konjugierte Polymere sind potentiell interessant für die "Molekular Elektronik" sie werden bereits eingesetzt in OLEDs , und weltweit wird ihre Verwendung als aktive Schicht in Polymersolarzellen untersucht. Hierbei werden das stereoreguläre Poly(3-hexylthiophen) und Poly(phenylenvinylen)e besonders intensiv untersucht. Insbesondere wünschenswert und verbesserungswürdig sind die langwellige breitbandige Lichtabsorption(größer als 600 nm, niedrige Band Gap Energie) und eine verbesserte Beständigkeit gegenüber Luftsauerstoff.

Anliegen der vorliegenden Untersuchungen war es, einen Beitrag zur Lösung dieser beiden Probleme zu liefern. Hierzu wurden neue Polyarylen(heteroarylen)vinylene synthetisiert, die als Chromophor Thienopyrazin enthalten, das als Akzeptor mit elektronenreichen Aromaten (Alkoxyphenylen, Alkylthiophen) alternierend verbunden ist.

In der Arbeit werden insbesondere Polymere mit zwei unterschiedlichen Primärstrukturen synthetisiert und charakterisiert:

Polyarylen(heteroarylen)vinylene mit (3,4-*b*)Pyrazin

    a) in der Hauptkette

    b) als Seitengruppe.

In die Untersuchungen werden die niedermolekularen Modellverbindungen mit einbezogen. Zur Synthese der Polymere und der Modellverbindungen sind die Suzuki-Kopplung und die Horner -Wittig Reaktion besonders geeignet.

Im Folgenden sind die Ergebnisse dieser Arbeit in Thesen zusammengefasst.

1. Schlüsselsubstanz für die Synthese der Polyarylen(heteroarylen)vinylene ist die 4-Formyl-2,5-bis(alkoxy)phenylboronsäure**(5)**, die unter Suzuki-Bedingungen mit 5,7-Dibrom-2,3-disubstituiertenThieno(3,4-b)Pyrazinen zum entsprechenden Dialdehyd führt (**M-1/M-2/M-3**).

2. die Dialdehyd-Monomere **M-1,M-2,M-3** lassen sich unter Standardbedingungen der Horner-Reaktion zu den tieffarbigen Polymeren **P-1-P-3** umsetzen.

3. Kondensation mit 3,4-Dihexyl-2,5-bis(methylendiethylphosphat)-thiophen (**M-7**) ergibt in sehr guten Ausbeuten die Polymere **P-5** und **P-6**.


P-5 R = phenyl
P-6 R = H
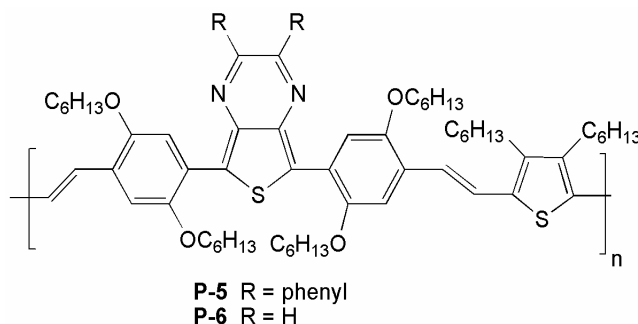
4. Der Polymerisationsgrad der Polymere **P-1-P-3** und **P-5-P-8** ist hoch (13 bis 39), die zahlenmittleren Molmassen betragen zwischen 29 000 und 42 000 g/mol.Sie zeigen eine enge Molmassenverteilung. Die Polymer sind gut löslich und bilden transparente farbige Filme.

5. Tabelle 3.3 der Dissertation gibt die exakten UV/Vis- Daten der Polymere **P-1-P-9** in Lösung sowie im Film an. Die daraus errechnete Band Gap Energie beträgt in Lösung 1.80 eV; im Film ist sie deutlich niedriger (1.6 eV).

6. Für eine potentielle Anwendung in Polymersolarzellen spielt die thermische Belastung (thermal annealing) im Film eine wesentliche Rolle. Die Untersuchungen zeigen, dass die Polymere mit linearen Seitengruppen (z.B. **P-1, P-5**) bis 150 ^{0}C ihr UV/Vis Spektrum nicht verändern (Fig. 3.21), verzweigte großvolumige Reste dagegen zu einem irreversiblen Abbau der Farbbande (650 nm) führen.
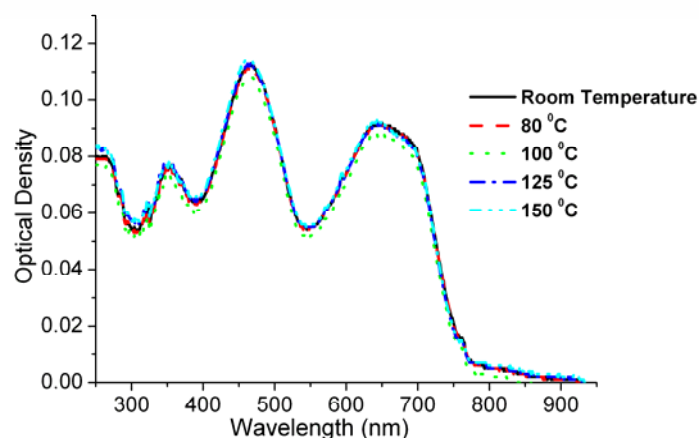

Figure 3.21. UV-vis spectra of **P-1** in solid state at different temperatures. (film from chlorobenzene)

7. Die neuen Polymere aggregieren in Lösung bei Zugabe von Methanol (nonsolvent). Das Absorptionsmaximum verschiebt sich dabei bathochrom (Abb. 3.24/3.25) und entspricht dem im Film (Abb.3.18).
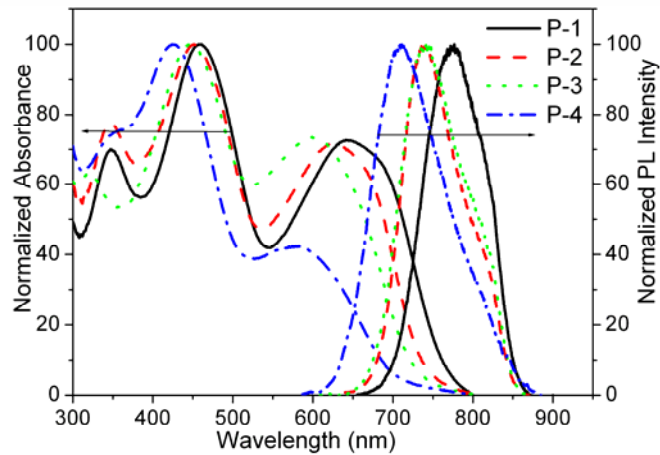
Figure 3.18. Normalized UV-vis and emission spectra of **P-1**, **P-2, P-3** and **P-4** in solid state. (film from chlorobenzene)

8. CV-Messungen zeigen, dass die Polymere reversibel oxidierbar und reduzierbar sind.

9. **Im zweiten Teil der Arbeit** werden konjugierte Polymere beschrieben, die als Chromophor Thieno(3,4-b)pyrazin als Seitengruppe tragen. Es werden zwei unterschiedliche Polymer-Typen synthetisiert, einmal solche vom Polyarylen-Typ mit Thienopyrazin als Seitengruppe (**P-17,P-18,P-19**) und alternativ solche mit "unterbrochener" Konjugation (**P-10,P-11,P-12**). Das folgende Bild gibt die für die Polymersynthese essentiellen Monomere und deren Preparation an .
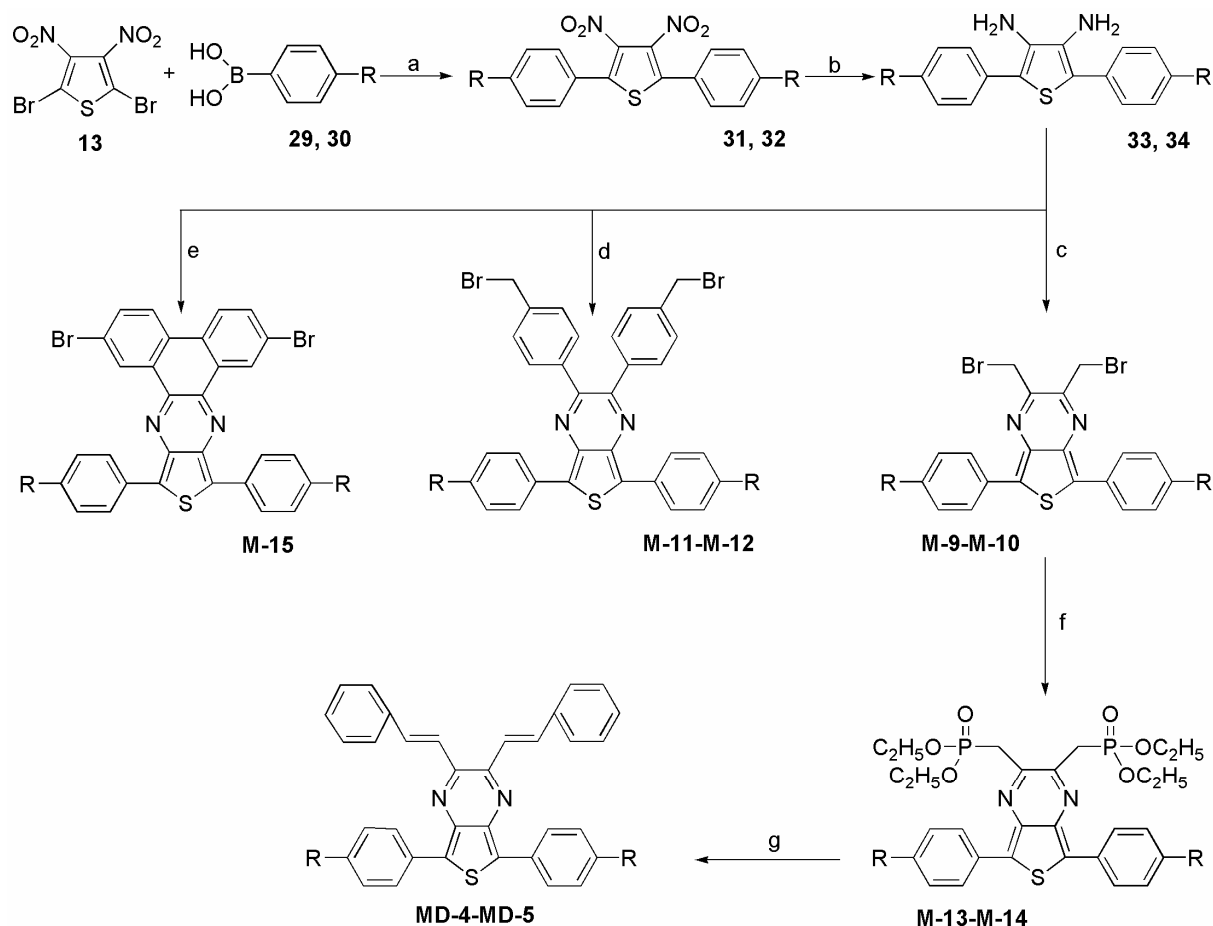
Reagents and conditions: (a) toluene, THF, aq. K_2CO_3 (2M), $Pd(PPh_3)_4$, 80 ^{0}C, 12 h; (b) ethanol, $SnCl_2$ (anhydrous), conc. HCl, reflux, overnight; (c) 1,4-dibrom-2,3-butandione, $CHCl_3$, p-toluenesulfonic acid, room temperature 12 h; (d) 1,2-bis(4-(bromomethyl)phenyl)ethane-1,2-dione, $CHCl_3$, p-toluenesulfonic acid, room temperature 12 h; (e) 2,7-dibromophenanthrene-9,10-dione, $CHCl_3$, p-toluenesulfonic acid, room temperature 12 h (f) triethyl phosphite, 160 ^{0}C, 4 h; (g) benzaldehyde, THF, t-BuOK, 0 ^{0}C to room temperature 3 h.

Scheme 3.10. Synthesis of Monomers **M9-M-15** and Model Compounds **MD-4-MD-5**.

10. Die Polymersynthese gelingt durch HWE Reaktion, Die Gilch Methode liefert nach ersten Versuchen schlechtere Ergebnisse (niedrige Molmassen, hohe Polydispersität).

11. Eine Copolymerisation ergibt hochmolekulare Polymere (PDI 1,5).
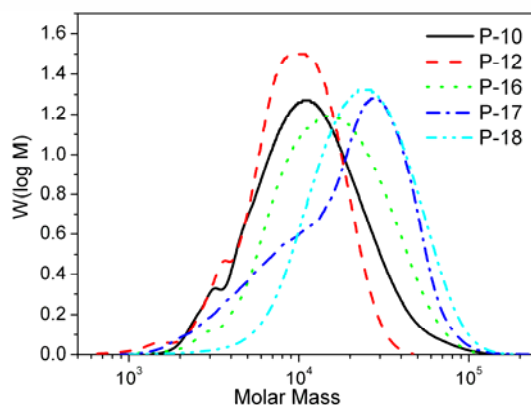
Figure 3.41. GPC curves of polymers **P-10, P-12, P-16, P-17** and **P-19**.

Table 3.7. GPC data of polymers **P-10-P-19.**

Polymer	$\bar{M}$n (g/mol)	$\bar{M}$w (g/mol)	PDI	$\bar{P}$n	Yield (%)
P-10	8800	14800	1.68	13	72
P-11	5800	8400	1.46	07	65
P-12	7400	10900	1.46	11	64
P-13	6100	25200	4.2	09	70
P-14	11600	70500	6.05	13	58
P-15	4200	5000	1.2	07	67
P-16	11500	19400	1.7	16	69
P-17	14000	25500	1.8	12	71
P-18	18600	28800	1.5	42	73
P-19	18300	26800	1.5	54	67

Mn, GPC (polystyrene standards).

12. Die elektrochemischen Untersuchungen zeigen für die Polymere eine reversible Reduktion (n-doping processes) und irreversible Oxidation (p-doping processes).

13. Mit den Polymeren **P-1, P-2, P-5** und PCBM wurden auf Polyesterfolien Solarzellen gefertigt und vermessen. In nicht optimierten Versuchen ergab sich eine Effizienz von 1,57% und eine Stromdichte kleiner 4mA/cm^2. Diese Werte entsprechen den bisher besten Werten der Literatur, die mit Low Band Gap Polymeren erreicht worden sind.

6   References

(1)   Skotheim, T. A.; Elsenbaumer, R. L.; Reynolds, J.; Eds. *Handbook of Conducting Polymers*, 2nd ed.; Marcel Dekker: New York, **1998**.

(2)   Kraft, A.; Grimsdale, A. C.; Holmes, A. B. *Angew. Chem.* **1998**, *37*, 402.

(3)   Hide, F.; Diaz-Garcia, M. A.; Schwartz, B. J.; Heeger, A. J. *Acc. Chem. Res.* **1997**, *30*, 430.

(4)   Yu, G.; Gao, J.; Hummelen, J. C.; Wudl, F.; Heeger, A. J. *Science* **1995**, *270*, 1789.

(5)   (a) Jenekhe, S. A.; Osaheni, J. A. *Science* **1994**, *265*, 765. (b) Brédas, J. L.; Beljonne, D.; Coropceanu, V.; Cornil, J. *Chem. Rev.* **2004**, *104*, 4971.

(6)   Ball, P. Made to Measure: *New Materials for the 21st Century*; Princeton University Press: Princeton, NJ, **1997**.

(7)   (a) Seminario, J. M.; Zacarias, A. G.; Tour, J. M. *J. Am. Chem. Soc.* **1999**, *121*, 411. (b) Tour, J. M.; Kozaki, M.; Seminario, J. M. *J. Am. Chem. Soc.* **1998**, *120*, 8486.

(8)   Chang, S. C.; Liu, J.; Bharathan, J.; Yang, Y.; Onohara, J.; Kido, J. *Adv. Mater.* **1997**, *11*, 734.

(9)   Sensors Special Issue. *Acc. Chem. Res.* **1998**, *31* (5).

(10)   Chiang, C. K.; Park, Y. W.; Heeger, A. J.; Shirakawa, H.; Louis, E. J.; MacDiarmid, A. G. *Phys. Rev. Lett.* **1977**, *39*, 1098.

(11)   Roncali, J. *Chem. Rev.* **1992**, *92*, 711.

(12)   Mertz, A. *Topics in Current Chemistry*; Springer-Verlag: Berlin, **1990**, *152*, 49.

(13)   Deronzier, A.; Moutet, J. C. *Acc. Chem. Res.* **1989**, *22*, 249.

(14)   Burroughes, J. H.; Bradey, D. D. C.; Brown, A. R.; Marks, R. N.; Mackay, K.; Friend, R. H.; Burns, P. L.; Holmes, A. *Nature* **1990**, *347*, 539.

(15)   (a) Enkelmann, V. *Adv. Polym. Sci.* **1984**, *63*, 91. (b) Wegner, G. *Z. Naturforsch.* **1969**, *24B*, 824.

(16)   Scherf, U. *Top. Curr. Chem.* **1999**, *201*, 163.

(17)   (a) Schlüter, A. D.; Wegner, G. *Acta Polym.* **1993**, *44*, 59. (b) Schlüter, A. D. *Adv. Mater.* **1991**, *3*, 282.

(18)   (a) Gorman, C. B.; Ginsburg, E. J.; Grubbs, R. H. *J. Am. Chem. Soc.* **1993**, *115*, 1397. (b) Sailor, M. J.; Ginsburg, E. J.; Gorman, C. B.; Kumar, A.; Grubbs, R. H.; Lewis, N. S. *Science* **1990**, *249*, 1146.

(19)   Intergovernmental Panel on Climate Change (IPCC), " Third Assessment Report of Working Group I - Summary for policy makers", **2001**, Web page: http://www.ipcc.ch/

(20)   Hatfield, C. B. *Nature* **1997**, *387*, 121.

(21)   Campbell, C. J. **2001**, *19*, 117-133.

(22)   Shaheen, S. E.; Brabec, C. J.; Sariciftci, N. S.; Padinger, F.; Fromherz, T.; Hummelen, J. C. *Appl. Phys. Lett*. **2001**, *78*, 841-843.

(23)   Granstrom, M.; Petritsch, K.; Arias, A. C.; Lux, A.; Andersson, M. R.; Friend, R. H. *Nature* **1998**, *395*, 257.

(24)   (a) Li, G.; Shrotriya, V.; Yao, Y.; Yang, Y. *J. Appl. Phys*. **2005**, *98,* 043704. (b) Li, G.; Shrotriya, V.; Huang, J. S.; Yao, Y.; Moriarty, T.; Emery, K.; Yang, Y. *Nat. Mater.* **2005**, *4*, 864.

(25)   Peumans, P.; Forrest, S. R. *Appl. Phys. Lett.* **2002**, *80,* 338-338.

(26)   Huynh, W. U.; Dittmer, J. J.; Alivisatos, A. P. *Science* **2002**, *295*, 2425-2427.

(27)   Ago, H.; Shaffer, M. S. P.; Ginger, D. S.; Windle, A. H.; Friend, R. H.; *Phys. Rev. B* **2000,** *61*, 2286-2290.

(28)   Chen, L.; Godovsky, D.; Inganäs, O.; Hummelen, J. C.; Janssen, R. A. J.; Svensson, M.; Svensson, M. R. *Advanced Materials* **2000,** *12*, 1367.

(29)   Brabec, C. J.; Cravino, A.; Meissner, D.; Sariciftci, N. S.; Rispens, M. T.; Sanchez, L.; Hummelen, J. C.; Fromherz, T. *Thin Solid Films* **2002**, *403-404*, 368-372.

(30)   Shaheen, S. E.; Radspinner, R.; Peyghambarian, N.; Jabbour, G. E. *Appl. Phys. Lett.* **2001**, *79,* 2996-2998.

(31)   Tour, J. M. *Chem. Rev.* **1996**, *96*, 537-553.

(32)   Roncali, J. *Chem. Rev.* **1997**, *97*, 173-205.

(33)   van Mullekom, H. A. M.; Vekemans, J. A. J. M.; Meijer, E. W. *Chem. Eur. J.* **1998**, *4*, 1235-1243.

(34)   Martin, R. E.; Diederich, F. *Angew. Chem., Int. Ed. Engl.* **1999**, *38*, 1350-1377.

(35)   van Mullekom, H. A. M.; Vekemans, J. A. J. M.; Havinga, E. E.; Meijer, E. W. *Mater. Sci. Eng.* **2001**, *32*, 1-40.

(36)   Ajayaghosh, A. *Chem. Soc. Rev.* **2003**, *32*, 181-191.

(37)   Sonmez, G.; Meng, H.; Wudl, F. *Chem. Mater.* **2003**, *15*, 4923-4929.

(38)   Chen, M.; Perzon, E.; Andersson, M. R.; Marcinkevicius, S.; Jönsson, S. K. M.; Fahlman, M.; Berggren, M. *Appl. Phys. Lett.* **2004**, *84*, 3570.

(39)   Shaheen, S. E.; Brabec, C. J.; Sariciftci, N. S.; Padinger, F.; Fromherz, T.; Hummelen, J. C. *Appl. Phys. Lett.* **2001**, *78*, 841.

(40)   Hoppe, H.; Sariciftci, N. S. *J. Mater. Res.* **2004**, *19*, 1924.

(41)   Wang, F.; Luo, J.; Yang, K. X.; Chen, J. W.; Huang, F.; Cao, Y. *Macromolecules* **2005**, *38*, 2253.

(42)   Kim, Y.; Cook, S.; Tuladhar, S. M.; Choulis, S. A.; Nelson, J.; Durrant, J. R.; Bradley, D. D. C.; Giles, M.; Mcculloch, I.; Ha, C. S.; Ree, M. *Nat. Mater.* **2006**, *5*, 197.

(43)   Reyes-Reyes, M.; Kim, K.; Carrolla, D.L. *Appl. Phys. Lett.* **2005**, 87**,** 083506.

(44)   Ma, W.; Yang, C.; Gong, X.; Lee, K.; Heeger, A.J. *Adv. Funct. Mater.* **2005**, 15**,** 1617.

(45)   Winder C.; Sariciftci, N. S. *J. Mater. Chem.* **2004**, 14**,** 1077.

(46)   Wang, X.; Perzon, E.; Delgado, J. L.; de la Cruz, P.; Zhang, F.; Langa, F.; Anderson, M. R.; Inganas, O. *Appl. Phys. Lett.* **2004**, *85*, 5081.

(47)   Schimmel, T.; Schwoerer, M.; Naarmann, H. *Synthetic Metals* **1990**, *37*, 1.

(48)   Farchioni, R.; Grosso, G.; Eds. *Organic electronic materials – conjugated polymers and low molecular weight organic solids*, Springer-Verlag, Berlin Heidelberg, **2001**.

(49)   Eklund, P.C.; Rao, A.M.; Eds. *Fullerene polymers and fullerene polymer composites*, Springer-Verlag, Berlin Heidelberg, **2000**.

(50)   Sariciftci, N. S.; Smilowitz, L.; Heeger, A. J.; Wudl, F. *Science***1992**, *258*, 1474.

(51)   Kraabel, B.; McBranch, D.; Sariciftci, N. S.; Moses,D.; Heeger, A. J. *Phys. Rev. B* **1994**, *50*, 18543.

(52)   Halls, J. J. M.; Pichler, K.; Friend, R. H.; Moratti, S. C.; Holmes, A. B. A*ppl. Phys. Lett.* **1996,** *68*, 3120.

(53)   Brabec, C. J.; Sariciftci, N. S.; Hummelen, J. C. *Adv. Funct. Mater.* **2001**, 11**,** 15.

(54)   Zhang, F.; Perzon, E.; Wang, X.; Mammo, W.; Anderson, M. R.; Inganas, O. *Adv. Funct. Mater.* **2005**, *15*, 745.

(55)   Wienk, M. M.; Turbiez, R.; Struijk,M. P.; Fonrodona, M.; Janssen, R. A. J. *Appl. Phys. Lett.* **2006**, *88*, 153511.

(56)   Campos, L. M.; Tontcheva, A.; Günes, S.; Sonmez, G.; Neugebauer, H.; Sariciftci, N. S.; Wudl, F. *Chem. Mater.* **2005**, *17*, 4031.

(57)   Wang, X.; Perzon, E.; Langa, F. F.; Admassie, S.; Anderson, M. R.; Inganas, O. *Adv. Funct. Mater.* **2005**, *15*, 1665.

(58)   Schneller, S.W.; Clough, F.W.; Skancke, P.N. *J. Heterocyclic Chem.* **1976**, *13*, 581.

(59)   Thomas, K. R. J.; Lin, J. T.; Tao, Y. T.; Chuen, C. H. *Adv. Mater.* **2002**, *14*, 822.

(60)   Kitamura, C.; Tanaka, S.; Yamashita, Y. *J. Chem. Soc., Chem. Commun.* **1994**, 1585. (b) Kitamura, C.; Tanaka, S.; Yamashita, Y. *Chem. Mater.* **1996,** *8*, 570.

(61)   Ashraf, R. S.; Hoppe, H.; Shahid, M.; Gobsch, G.; Sensfuss, S.; Klemm, E. *J. Polym Sci: Part A: Polym Chem.* **2006**, DOI: 10.1002/pola.21645.

(62)   Ashraf, R. S.; Shahid, M.; Klemm, E.; Al-Ibrahim, M.; Sensfuss, S. *Macromol. Rapid Commun.* **2006**, *27,* 1454.

(63)   Laue, T.; Plagens, A. *Named Organic Reactions;* 2nd ed. John Wiley & Sons **2005**; p 293.

(64)   Wittig, G.; Geissler, G. *Liebigs Ann.* **1953**, *580*, 44.

(65)   Horner, L.; Hoffmann, H. M. R.; Wippel, H. G. *Chem. Ber.* **1958**, *91*, 61.

(66)   Wadsworth, W. S.; Emmons, W. D. *J. Org. Chem.* **1961**, *83*, 1733.

(67)   Horner, L.; Hoffmann, H. M. R.; Wippel, H. G.; Klahre, G. *Chem. Ber.* **1959**, *92*, 2499.

(68)   Larsen, R. O.; Aksnes, G. *Phosphorus Sulfur* **1983**, *15*, 219.

(69)   Corey, E. G. ; Kwiatkowski, G.T. *J. Am. Chem. Soc.* **1966**, *88*, 5654.

(70)   Lefeˊbvre, G.; Seyden-Penne, J. *J. Chem. Soc. Chem. Comm.* **1970**, 1308.

(71)   Thomson, S. K.; Heathcock, C. H. *J. Org. Chem.* **1990**, *55*, 3386.

(72)   (a) Knoevenagel, E. *Berichte* **1898**, *31*, 2585. (b) Jones, G. *Org. React.* **1967**, *15*, 204..

(73)   (a) Knoevenagel, E. *Ber.* **1894**, *27*, 2346. (b) Knoevenagel, E. *Ber.* **1896**, *29*, 172.

(74)   (a) Bigi, F.; Chesini, L.; Maggi, R.; Sartori, G. *J. Org. Chem.* **1999**, *64*, 1033. (b) Yu, N.; Aramini, J. M.; Germann, M. W.; Huang, Z.;*Tetrahedron Lett.* **2000**, *41*, 6993.

(75)   Boucard, V. *Macromolecules* **2001,** *34,* 4308.

(76)   Hann, A. C. O.; Lapworth, A. *J. Chem. Soc*. **1904**, *85*, 46.

(77)   Shriner, R. L. *Org. React*. **1942**, *1*, 1.

(78)   Gilch, H. G.; Wheelwright, W. L. *Polym. Sci., Part A: Polym. Chem.* **1966**, *4*, 1337.

(79)   Parekh, B. P.; Tangonan, A. A.; Newaz, S. S.; Sanduja, S. K.; Ashraf, A. Q.; Krishnamoorti, R.; Lee, T. R. *Macromolecules* **2004,** *37,* 8883.

(80)   Issaris, A.; Vanderzande, D.; Gelan, J. *Polymer* **1997**, *38*, 2571.

(81)   Wessling, R. A. *J. Polym. Sci., Polym. Symp.* **1985**, *72*, 55.

(82)   Hsieh, B. R.; Yu, Y.; Forsythe, E. W.; Schaaf, G. M.; Field, W. A. *J. Am. Chem. Soc.* **1998**, *120*, 231.

(83)   (a) Hsieh, B. R.; Yu, Y.; VanLaeken, A. C.; Lee, H. *Macromolecules* **1997**, *30*, 8094. (b) Hsieh, B. R.; Yu, Y.; Forsythe, E. W.; Schaaf, G. M.; Feld, W. A. *J. Am. Chem. Soc.* **1998**, *120*, 231.

(84)   Neef, C. J.; Ferraris, J. P. *Macromolecules* **2000**, *33*, 2311.

(85)   (a) Wessling, R. A. *J. Polym. Sci.: Polym. Symp.* **1985**, *72*, 55. (b) Denton, F. R., III.; Lahti, P. M.; Karasz, F. E. *J. Polym. Sci.: Polym. Chem.* **1992**, *30*, 2223. (c) Cho, B. R.; Kim, Y. K.; Han M. S. *Macromolecules* **1998**, *31*, 2098.

(86)   Hontis, L.; Vrindts, V.; Vanderzande, D.; Lutsen, L. *Macromolecules* **2003,** *36,* 3035.

(87)   Miyaura, N.; Yanagi, T.; Suzuki, A. *Synth. Commun.* **1981,** *11*, 513.

(88)   (a) Suzuki, A. *Pure Appl. Chem.* **1985**, *57*, 1749. (b) Suzuki, A. *Pure Appl. Chem.* **1991,** *63*, 419.

(89)   Martin, A. R.; Yang, Y. *Acta Chem. Scand.* **1993,** *47*, 221.

(90)   Suzuki, A. *Pure Appl. Chem.* **1994,** *66*, 213.

(91)   Miyaura, N.; Suzuki, A. *Chem. Rev.* **1995,** *95*, 2457.

(92)   Stanforth, S. P. *Tetrahedron* **1998,** *54*, 263.

(93)   Miyaura, N. *Advances in Metal-organic Chemistry*; Libeskind, L. S., Ed.; Jai: London, **1998**; Vol. *6*, pp 187–243.

(94)   Suzuki, A. *J. Organomet. Chem.* **1999,** *576*, 147.

(95)   Suzuki, A. *In Organoboranes for Syntheses.* ACS Symposium Series 783; Ramachandran, P. V.; Brown, H. C., Eds.; American Chemical Society: Washington, DC, **2001**; pp 80–93.

(96)   Rehahn, M.; Schlüter, A. D.; Wegner, G.; Feast, W. J. *Polymer* **1989**, *30*, 1054.

(97)   Rehahn, M.; Schlüter, A. D.; Wegner, G. *Macromol. Chem.* **1990**, *191*, 1991.

(98)   Remmers, M.; Schulze, M.; Wegner, G. *Macromol. Rapid Commun.* **1996**, *17*, 239.

(99)   Miyaura, N.; Yamada, K.; Suginome, H.; Suzuki, A. *J. Am. Chem. Soc.* **1985**, *107*, 972.

(100)   Saito, S.; Sakai, M.; Miyaura, N. *Tetrahedron Lett.* **1996**, *37*, 2993.

(101)   Casalnuovo, A. L.; Calabrese, J. C.; *J. Am. Chem. Soc*. **1990**, *112*, 4324.

(102)   Kotha, S.; Lahiri, K.; Kashinath, D. *Tetrahedron* **2002**, *58*, 9633.

(103) Cowie, J. M. G. *Polymers: Chemistry and Physics of Modern Materials*, International Textbook Company Ltd., London, **1973**.

(104) Egbe, D. A. M.; Tillmann, H.; Birckner, E.; Klemm, E. *Macromol. Chem. Phys.* **2001**, *202,* 2712.

(105) Maruyama, S.; Kawanishi,Y. *J. Mater. Chem.* **2002**, *12*, 2245.

(106) Wright, M. E.; Mullick, S.; Lackritz, H. S.; Liu, L. Y. *Macromolecules* **1994**, *11,* 3009.

(107) Sonogashira, K.; Tohda, Y.; Hagihara, N. *Tetrahedron Lett.* **1975**, *16*, 4467.

(108) Younus, M.; Kohler, A.; Cron, S.; Chawdhury, N.; Al-Mandhary, M. R. A.; Khan, M. S.; Lewis, J.; Long, N. J.; Friend, R. H.; Raithby, P. R. *Angew. Chem. Int. Ed.* **1998**, *37,* 3036.

(109) (a) Keegstra, M. A.; Brandsma, L. *Synthesis* **1988**, *11,* 890. (b) Mozingo, R.; Harris, S. A.; Wolf, D. E.; Hoffhine, C. E.; Easton, N. R.; Folkers, K. *J. Am. Chem. Soc.* **1945**, *67*, 2902. (c) Outurquin, F.; Paulmier, C. *Bull. Soc. Chim. Fr., II* **1983**, 159. (d) Don, D. K.; Kari, A. M.; Tessa, R. C.; Melanie, R. F.; Daniel, J. S.; Seth, C.R. *J. Org. Chem.* **2002**, *67,* 9073.

(110) Martinez-Ruiz, P.; Behnisch, B.; Schweikart, K.-H.; Hanack, M.; Lüer, L.; Oelkrug, D. *Chem. Eur. J.* **2000**, *8*, 1294.

(111) Niazimbetova, Z. I.; Christian, H. Y.; Bhandari, Y.; Beyer, F. L.; Galvin, M. E. *J. Phys. Chem. B,* **2004**, *108,* 8675.

(112) Drury, A.; Maier, S.; Rüther, M.; Blau, W.J. *J. Mater. Chem.* **2003**, *13*, 485.

(113) Egbe, D. A. M.; Kietzke, T.; Carbonnier, B.; Mühlbacher, D.; Hörhold, H. H.; Neher, D.; Pakula, T. *Macromolecules* **2004**, *37,* 8863.

(114) Egbe, D. A. M.; Bader, C.; Nowotny, J.; Günther, W.; Klemm, E. *Macromolecules* **2003**, *36*, 5459.

(115) Wagner, M.; Nuyken, O. *Macromolecules* **2003**, *36*, 6716.

(116) Apperloo, J. J.; Janssen, R. A. J.; Malenfant, P. R. L.; Frechet, J. M. J. *Macromolecules* **2000**, *33*, 7038.

(117) (a) Hernandez, V.; Castiglioni, C.; DelZoppo, M.; Zerbi, G. *Phys. Rev. B* **1994**, *50*, 9815. (b) *Conjugated Polymers*: *The Novel Science and Technology of Highly Conducting and Nonlinear Optically Active Materials*; Bredas, J. L., Silbey, R., Eds.; Kluwer: Dordrecht, The Netherlands, 1991. (c) Bredas, J. L.; Cornil, J.; Heeger, A. J. *Adv. Mater.* **1996**, *8*, 447.

(118) McBranch, D. W.; Sinclai, M. B. *"The Nature of The Photoexcitations in Conjugated Polymers"*, Sariciftci, N. S. Ed., World Scientific Publishing, Singapore **1997**, Chapter 20, p. 608.

(119) Rothberg, L. J.; Yan, M.; Papadimitrakopoulos, F.; Galvin, M. E.; Kwock, E. W.; Miller, T. M. *Synth. Met* **1996**, *80*, 41.

(120) Peng, Z. *Polym. News* **2000**, *25*, 185.

(121) (a) Ruseckas, A.; Namdas, E. B.; Ganguly, T.; Theander, M.; Svensson, M.; Andersson, M. R.; Inganas, O.; Sundstrom, V. *J. Phys. Chem. B*. **2001**, *105*, 7624. (b) Fell, H. J.; Samuelsen, E. J.; Andersson, M. R.; Als-Nielsen, J.; Gru¨bel, G.; Mardalen, J. *Synth. Met.* **1995**, *73*, 279.

(122) Ashraf, R.S.; Klemm, E. *J. Polym Sci: Part A: Polym Chem.* **2005**, *43*, 6445.

(123) Mühlbacher, D. Diploma thesis, Linz, Austria, **2002**.

(124) Bredas, J. L.; Silbey, R.; Boudreux, D. S.; Chance, R. R. *J. Am. Chem. Soc.* **1983**, *105*, 6555.

(125) deLeeuw, D. M.; Simenon, M. M. J.; Brown, A. B.; Einerhand, R. E. F. *Synth.Met.* **1997**, *87*, 53.

(126) Liu, M. S.; Jiang, X.; Liu, S.; Herguth, P.; Jen, A. K.-Y. *Macromolecules* **2002**, *35*, 3532.

(127) Liu, Y.; Liu, M. S.; Jen, A. K.-Y. *Acta Polym.* **1999**, *50*, 105.

(128) Gerischer, H., Tobias, C. W., Eds. *Advances in Electrochemistry and Electrochemical Engineering;* John Wiley: New York, **1977**; Vol. *10*, p 213.

(129) Gomer, R. J.; Tryson, G. *J. Chem. Phys.* **1977**, *66*, 4413.

(130) Kötz, R.; Neff, H.; Müller, K. *J. Electroanal. Chem.* **1986**, *215*, 331.

(131) Wienk, M. M.; Struijk,M. P.; Janssen, R. A. J. *Chem. Phys. Lett.* **2006**, *422*, 488.

(132) Krieg, B. *Chem. Ber.* **1969**, *102,* 371.

(133) Zheng, M.; Ding, L.; Lin, Z.; Karasz, F.E. *Macromolecules* **2002,** *35,* 9939.

(134) Thomas, K.R.J.; Lin, J. T.; Tao, Y.T.; Chuen, C. -H. *Adv. Mater.* **2002**, *14,* 822.

(135) Arbuzow , B. A.; *Pure Appl. Chem.* **1964**, *9*, 307.

(136) Ciszek, J. W. Tour, J. M. *Tetrahedron lett.* **2004,** *45,* 2801.

(137) Hörhold, H. -H.; Opfermann, J. *Makromol. Chem.* **1970**, *131*, 105;

(138) Hörhold, H. -H.; *Z. Chem.* **1972**, *12*, 41; (b) Hörhold, H. -H.; Helbig, M. *Makromol. Chem., Macromol. Symp.* **1987**, *12*, 229.

(139) Ranger, M.; Rondeau, D.; Leclerc, M. *Macromolecules* **1997**, *30*, 7686.

(140) Chen, Z.-K., Meng, H., Lai, Y.-H., and Huang, W. *Macromolecules* **1999**, *32*, 4354.

(141) Fan, Q. -L.; Lu, S.; Lai, Y. –H. ; Hou, X.-Y. ; Huang, W. *Macromolecules* **2003,** *36,* 6976.

(142) Kulkarni, A. P.; Zhu, Y.; Jenekhe, S. A. *Macromolecules* **2005**, *38, 1553.

(143) Shiraishi, K.; Yamamoto, T. *Synth. Met.* **2002**, *130*, 139.

(144) Demas, J. N.; Crosby, G. A. *J. Phys. Chem.* **1971**, *75*, 991.

(145) Milazzo, G.; Caroli, S. *Tables of Standard Electrode Potentials*; Wiley-Interscience: New York, **1977**.

(146) Park, K.; Yoshino, K.; Tomiyasu, H. *Synthesis* **1999**, *12*, 2041.

(147) Mitschke, U.; Bäuerle, P. *J. Mater. Chem.* **2000**, *10*, 1471-1507.

7   Appendix

7.1 ^{1}H and ^{13}C NMR Spectra
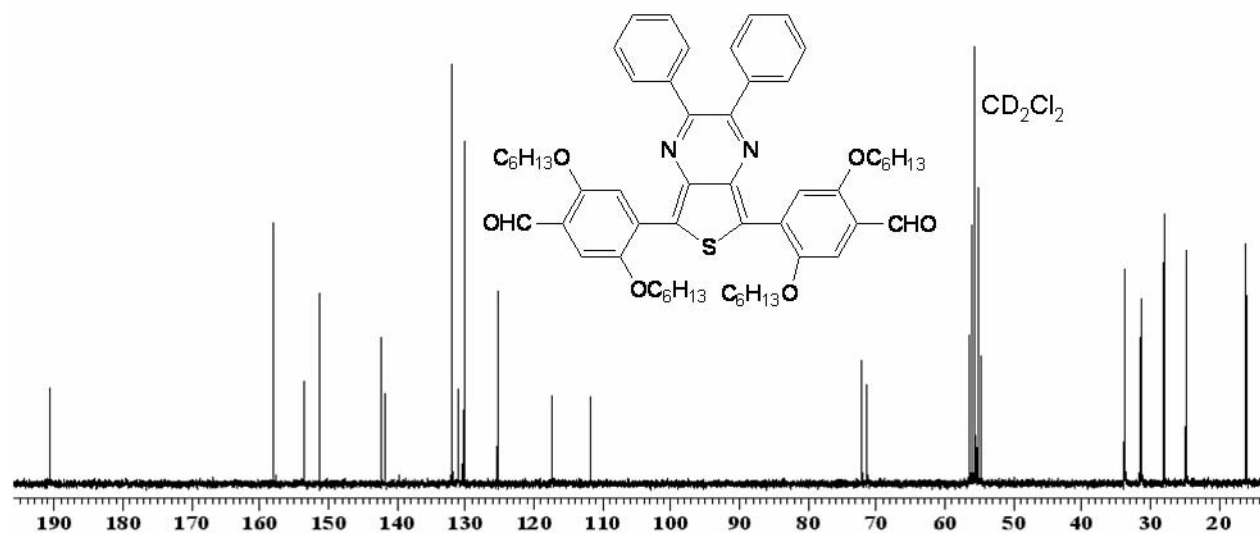
Figure 1. ^{13}C NMR of **M-1**.
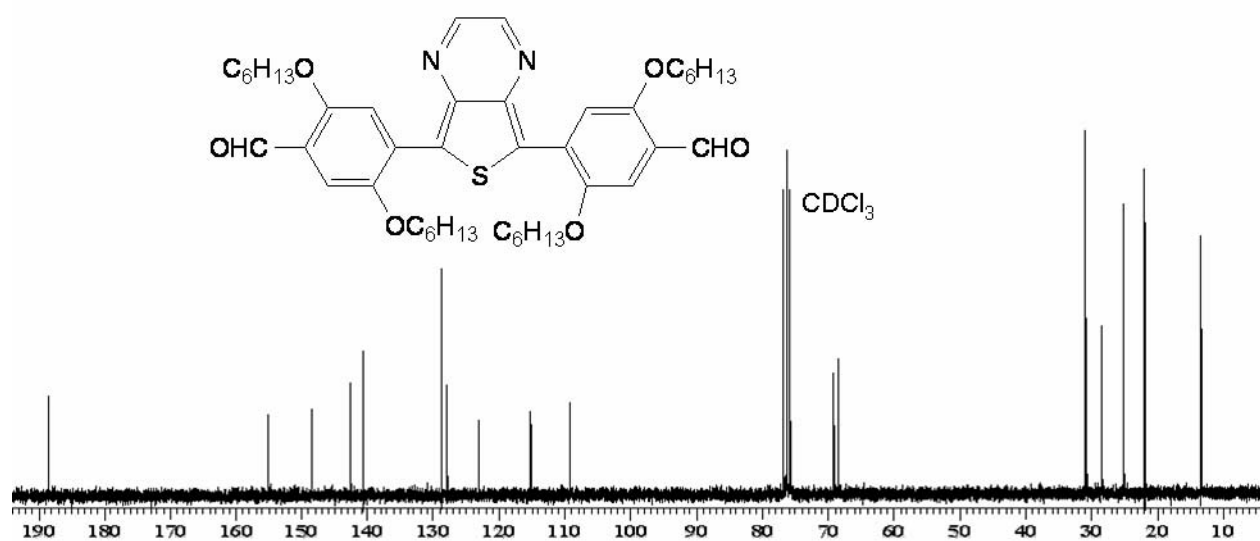
Figure 2. ^{13}C NMR of **M-2**.
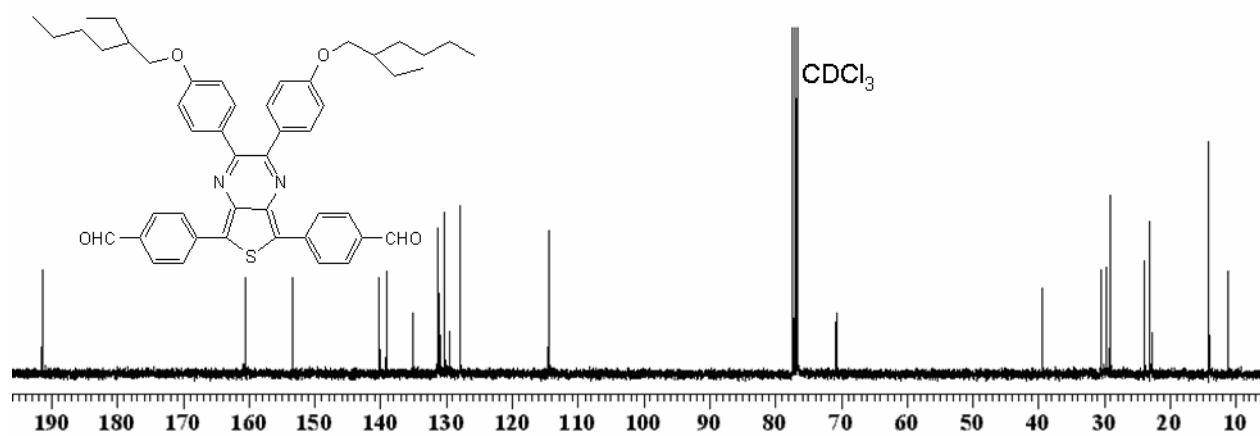
Figure 3. ^{13}C NMR of **M-3**.
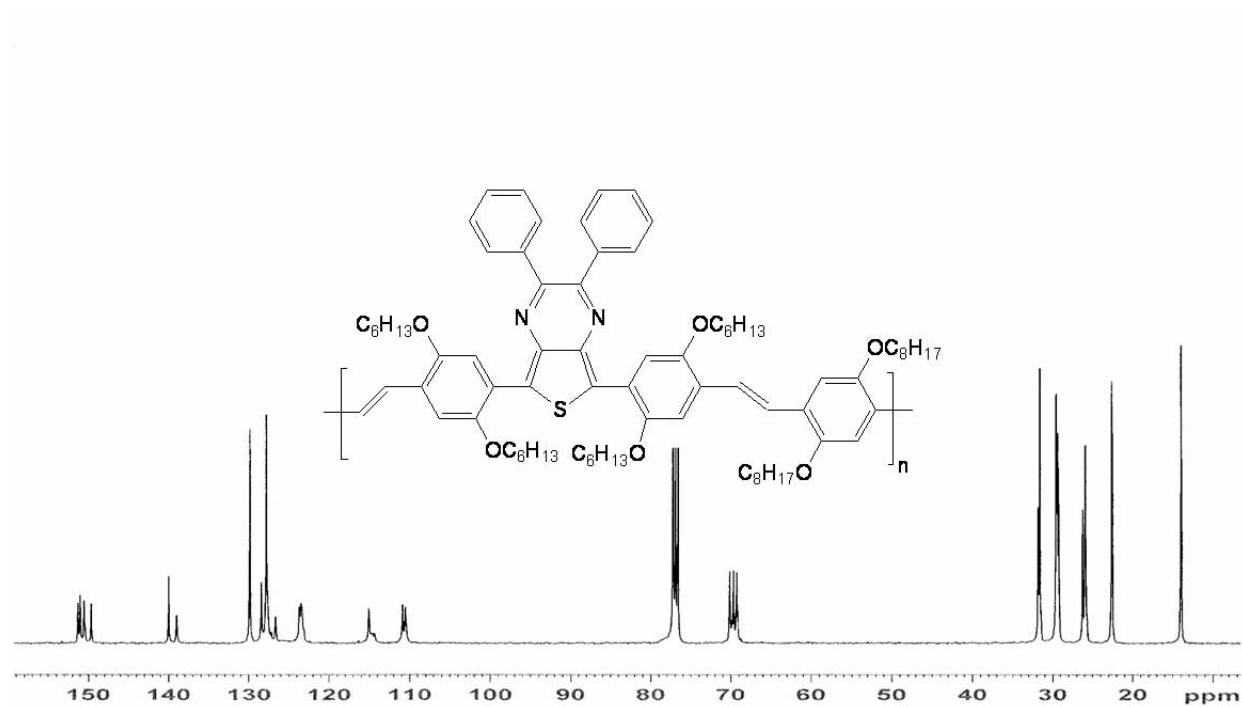
Figure 4. ^{13}C NMR of **P-1**.
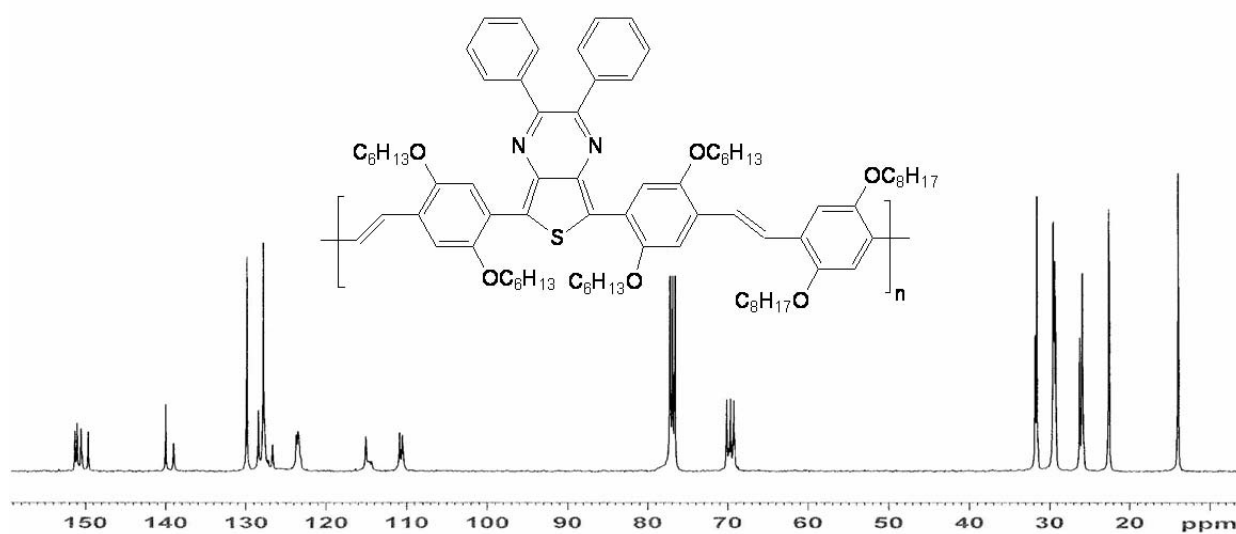
Figure 5. ^{13}C NMR of **P-1**.
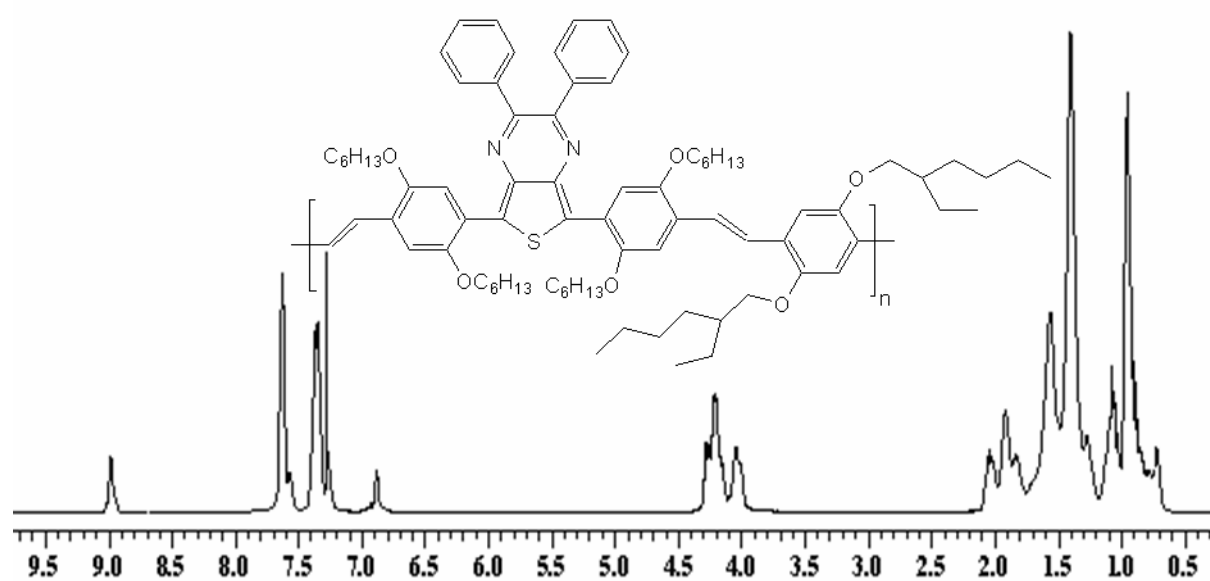
Figure 6. ^{1}H NMR of **P-2**.
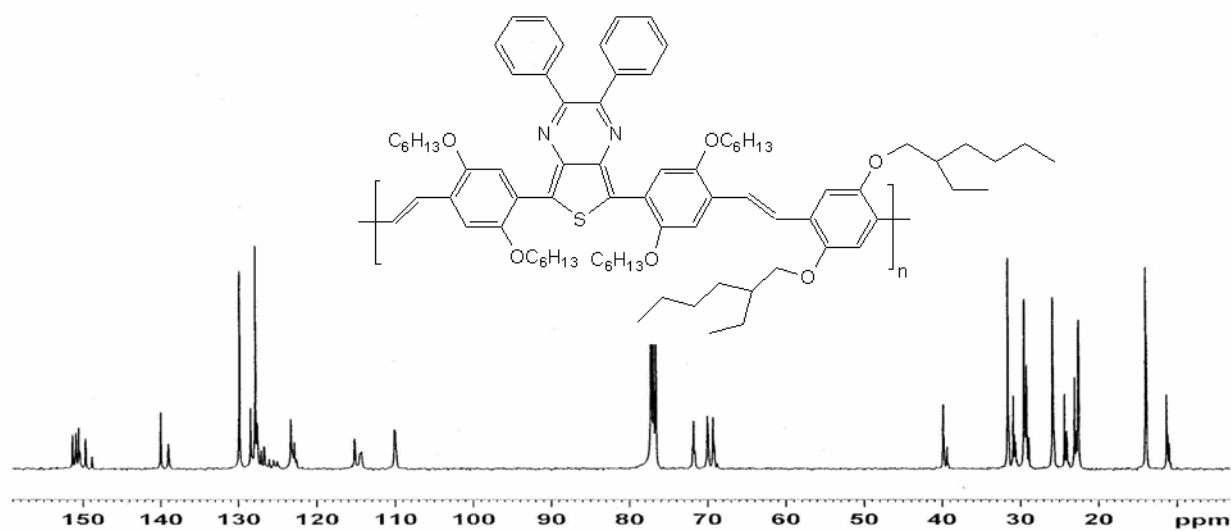
Figure 7. ^{13}C NMR of **P-2**.
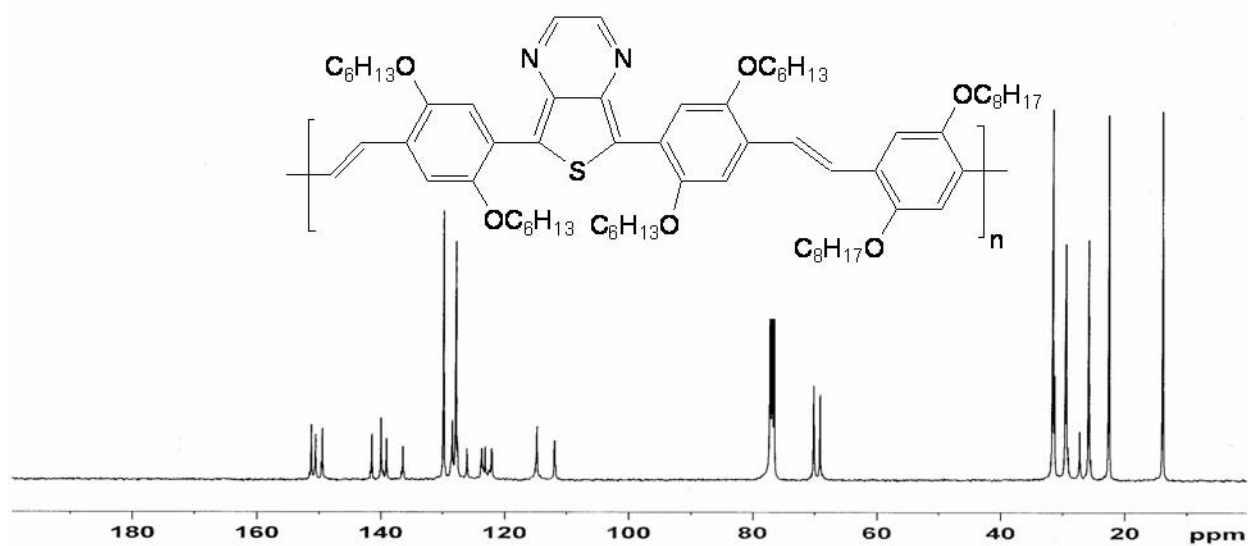
Figure 8. ^{13}C NMR of **P-3**.
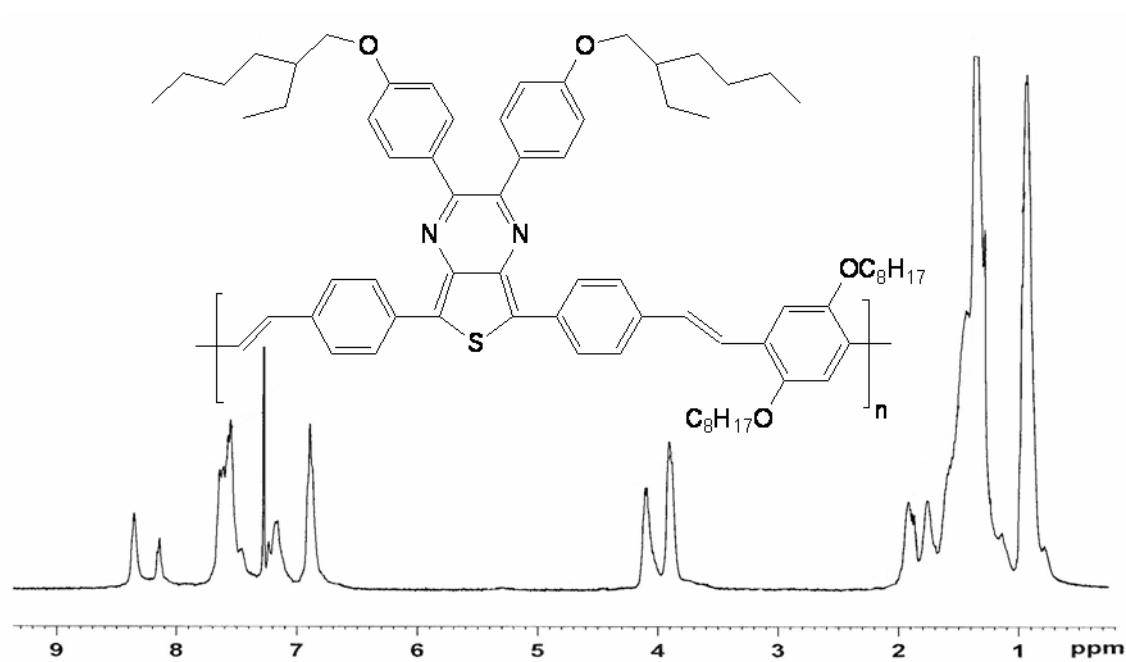
Figure 9. ^{1}H NMR of **P-4**.
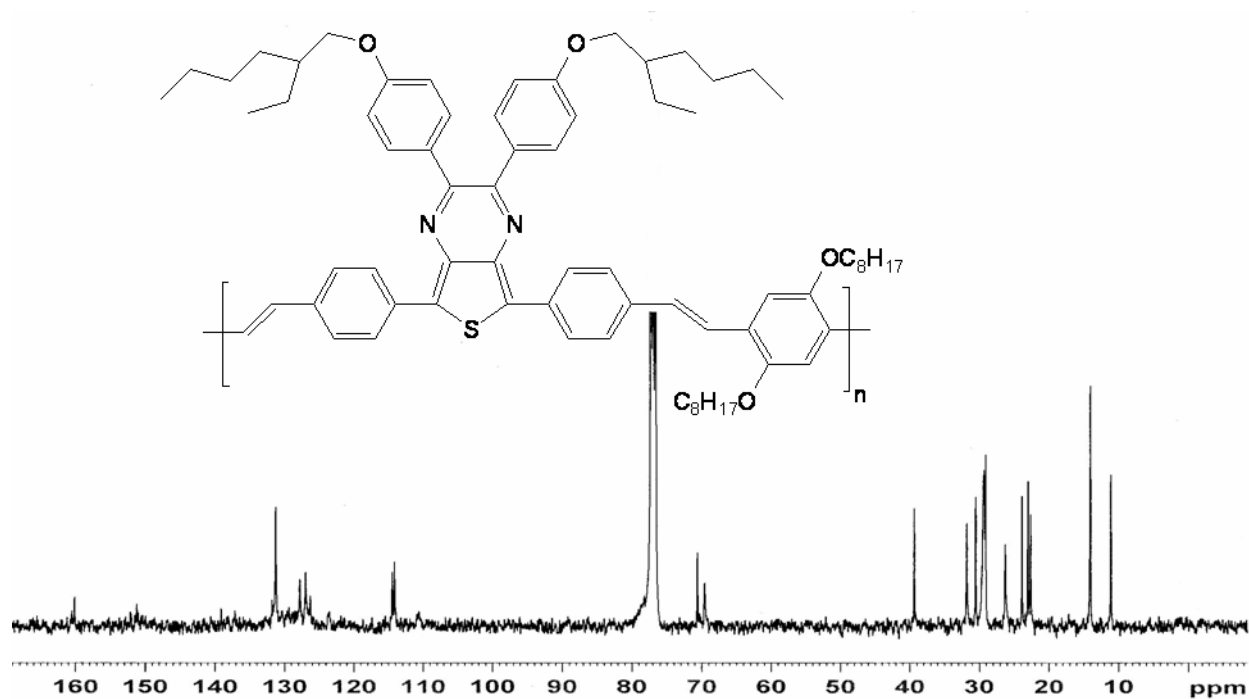
Figure 10. ^{13}C NMR of **P-4**.
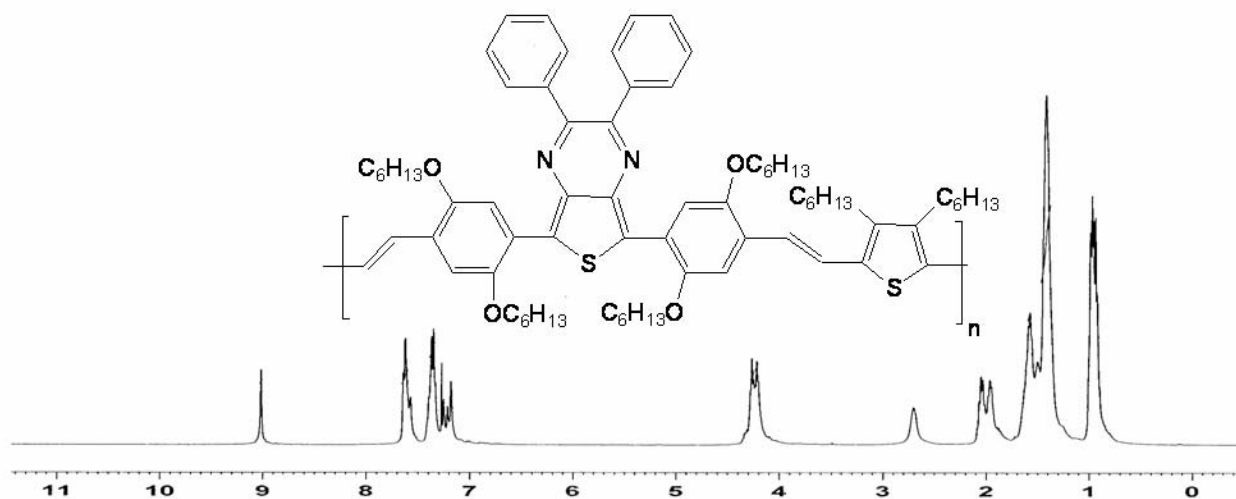
Figure 11. ^{1}H NMR of **P-5**.
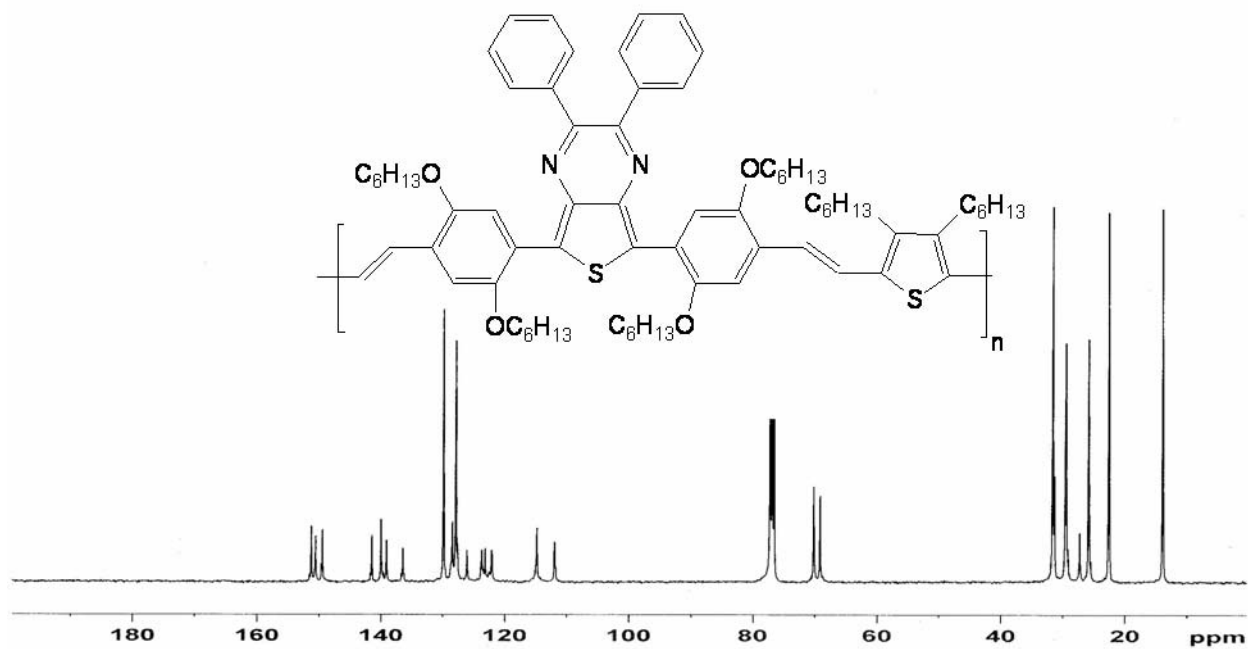
Figure 12. ^{13}C NMR of **P-5**.
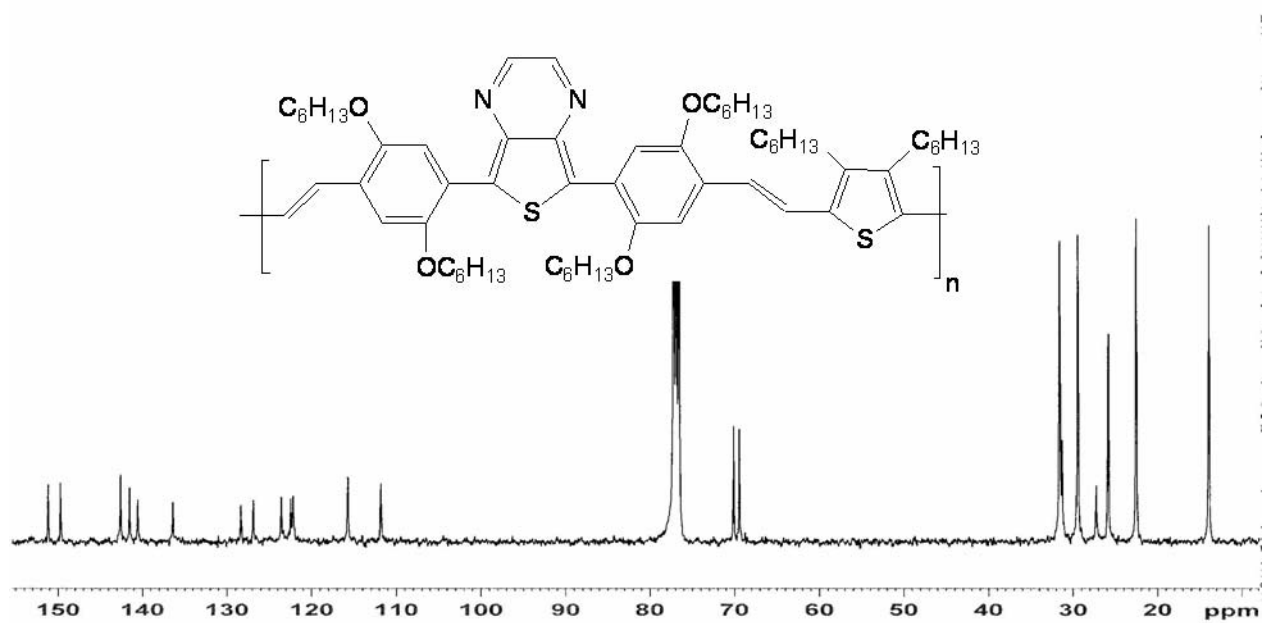
Figure 13. ^{13}C NMR of **P-6**.
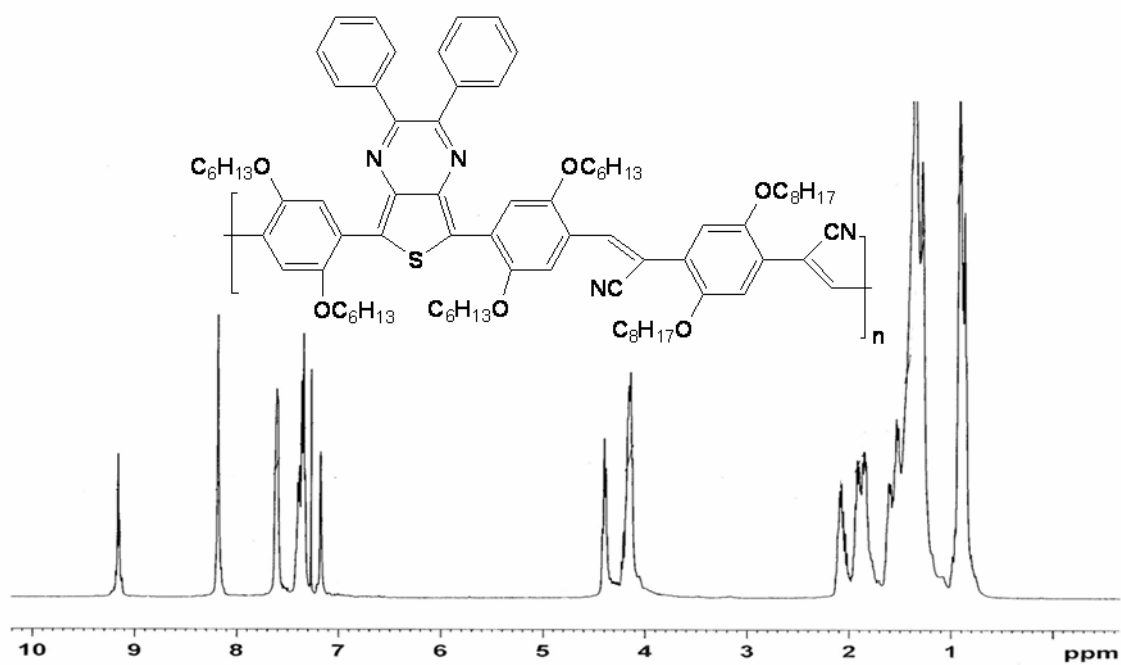
Figure 14. ^{1}H NMR of **P-7**.
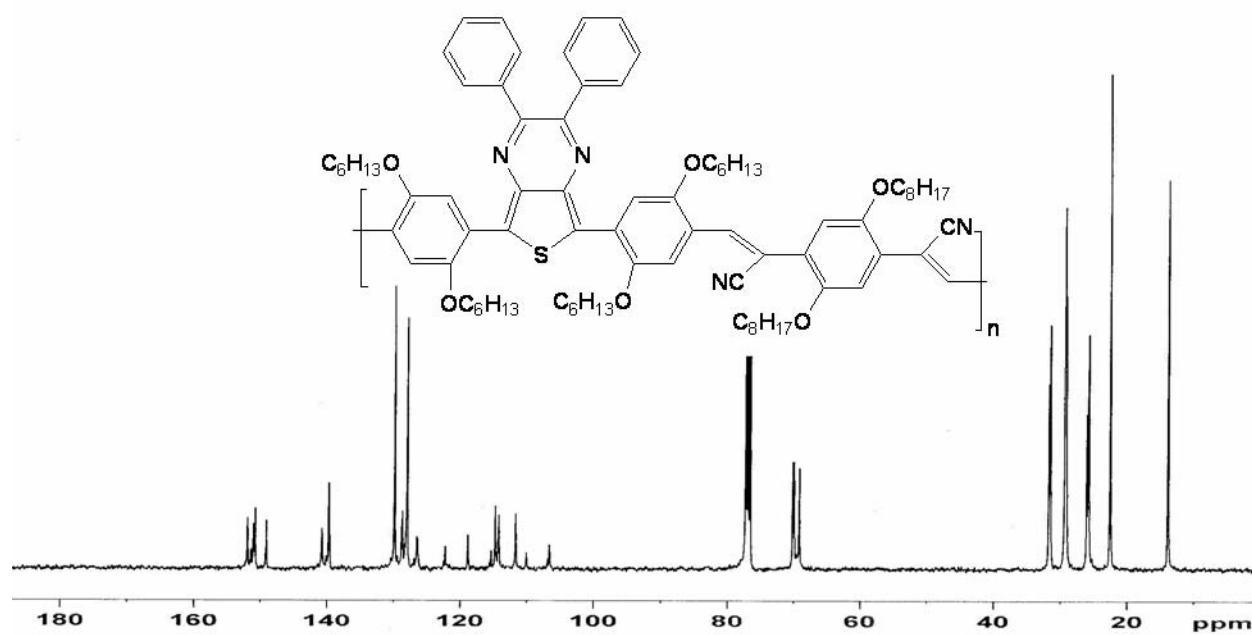
Figure 15. ^{13}C NMR of **P-7**.
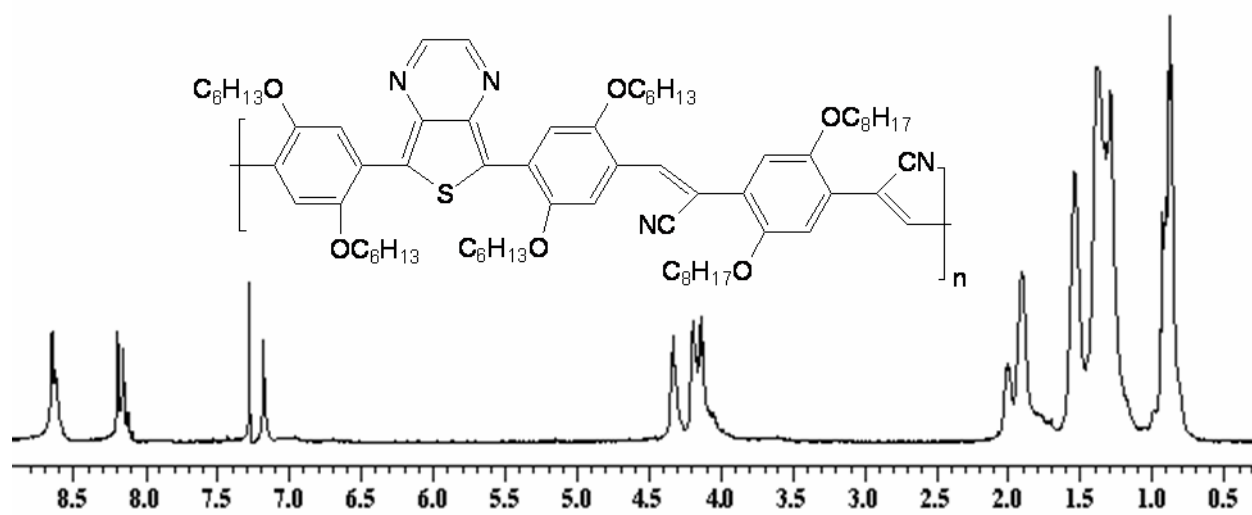
Figure 16. ^{1}H NMR of **P-8**.

Figure 17. ^{13}C NMR of **P-8**.

Figure 18. ^{1}H NMR of **P-9**.
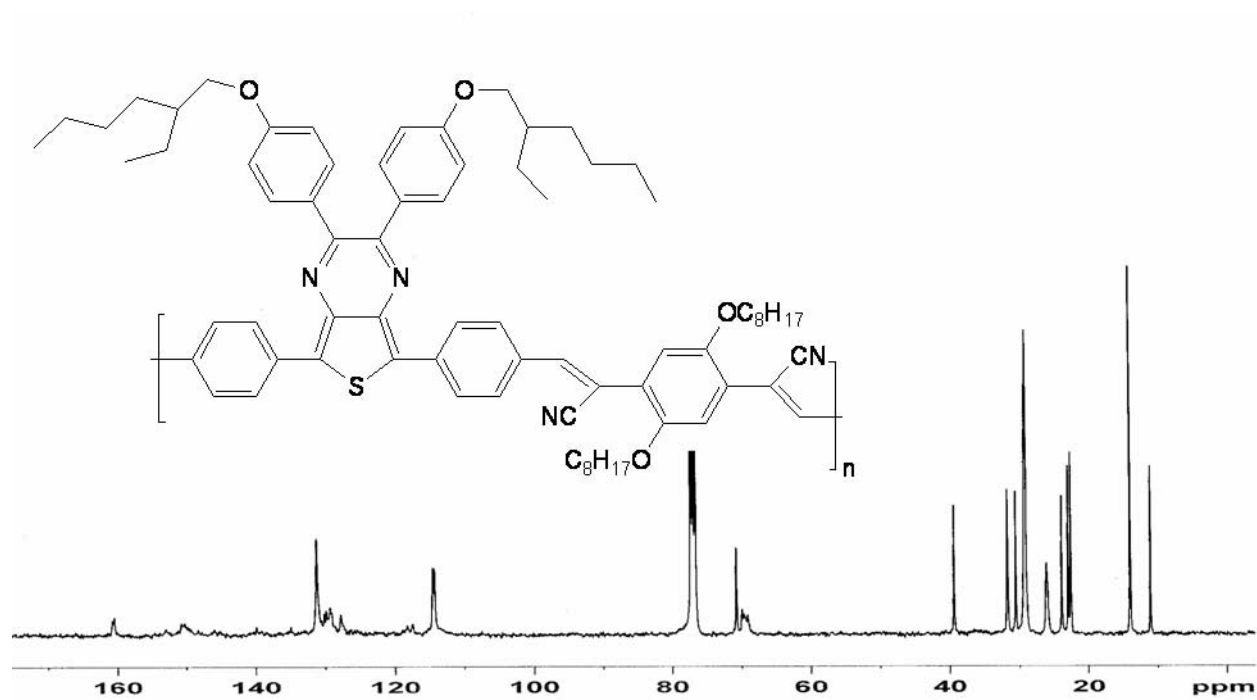
Figure 19. ^{13}C NMR of **P-9**.

7.2   Molecular Formulae

Structures of Model Compounds
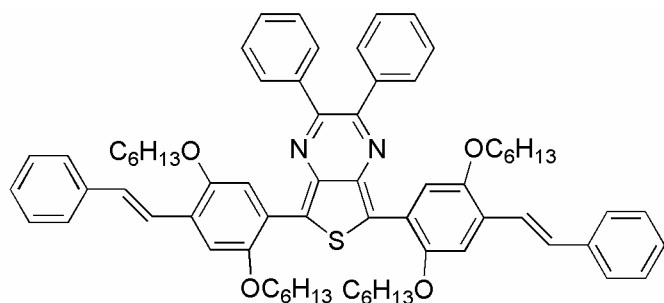
MD-1 (MSD-1)
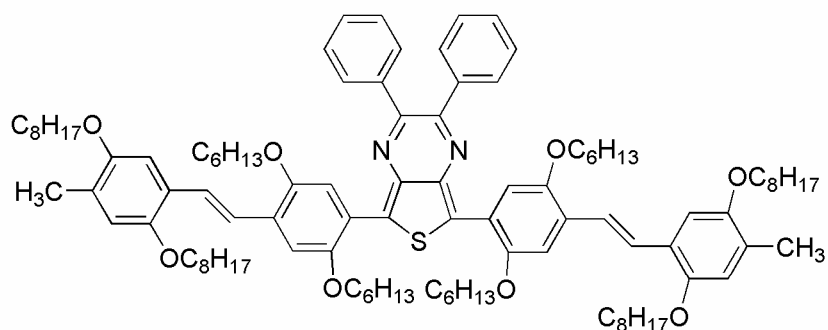
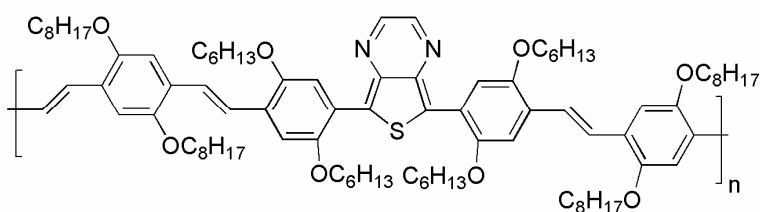MD-2 (MSD-2)
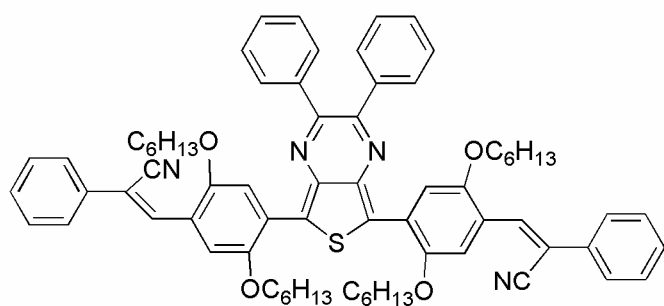
MD-3 (MSD-3)
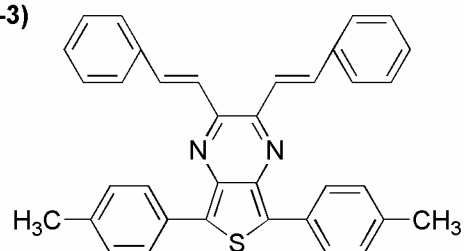
MD-4 (MSD-11)
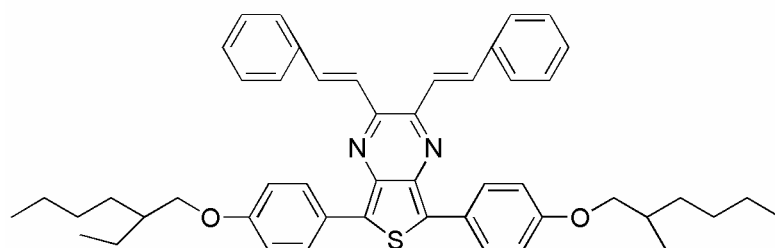
MD-5 (MSD-12)

Structures of Polymers
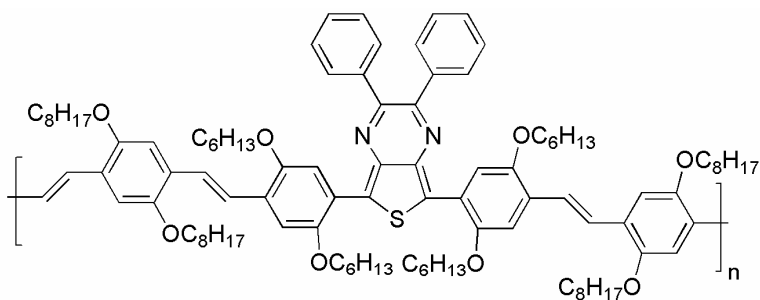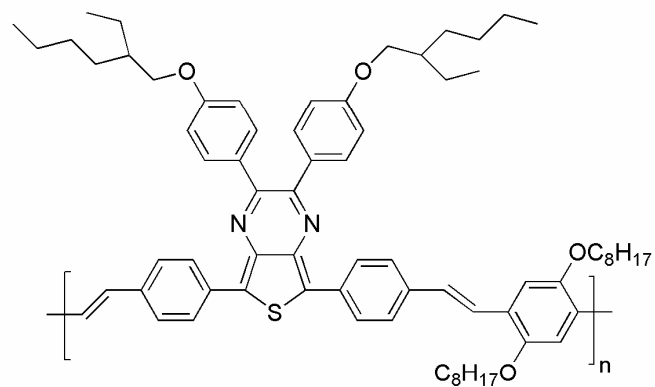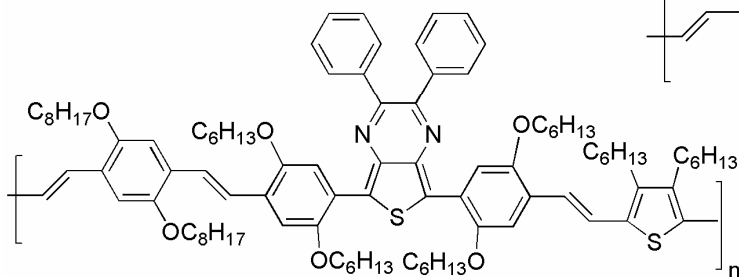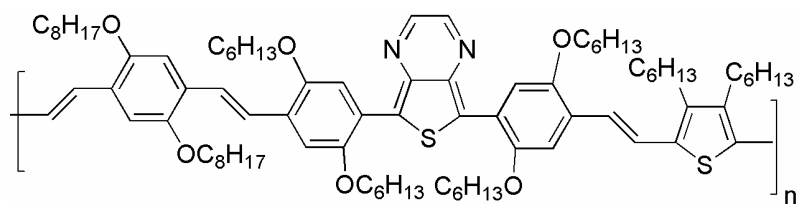

P-1 (PM-19)
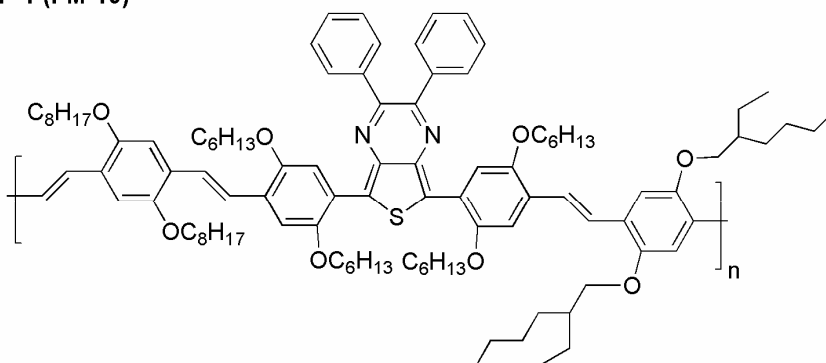
P-2 (PM-20

P-3 (PM-8)

P-4 (PM-35)

P-5 (PM-18)

P-6 (PM-17)
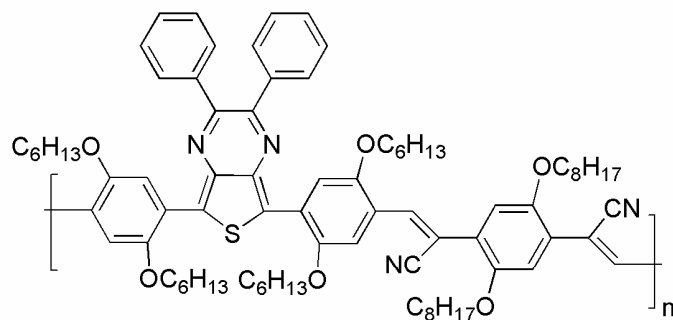
P-7 (PM-26)

P-8 (PM-13)
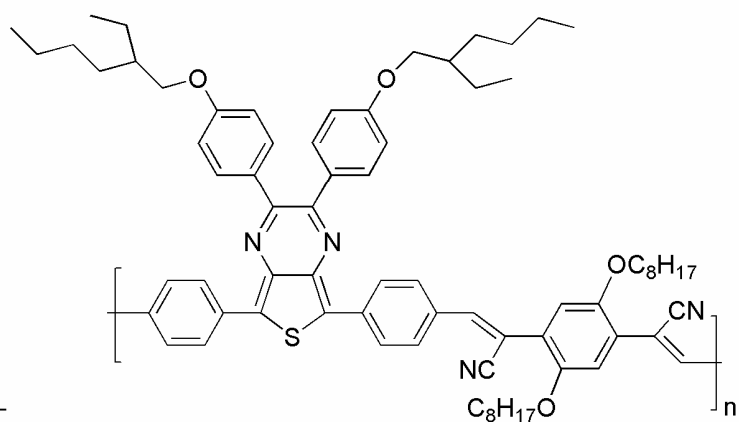
P-9 (PM-36)
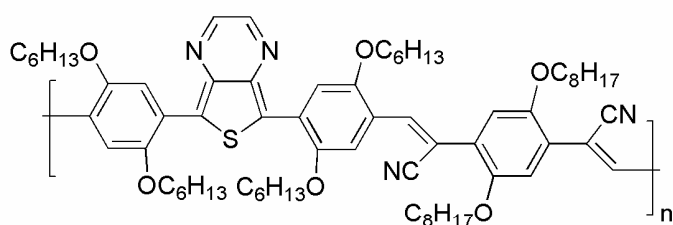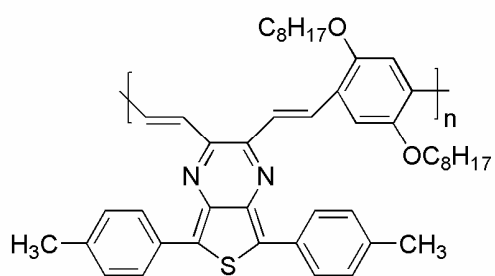

P-10 (PM-12)
P-13 (PM-32)
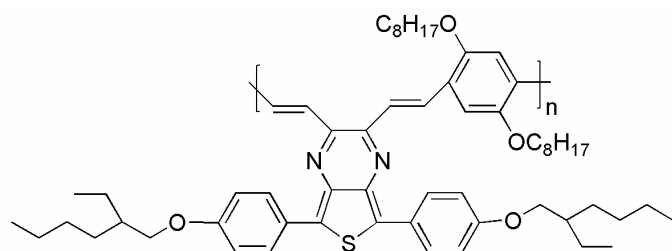
P-11 (PM-25)
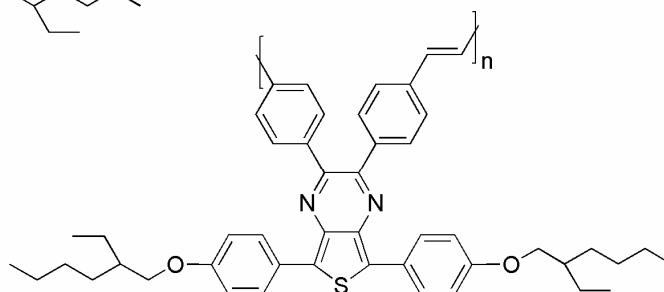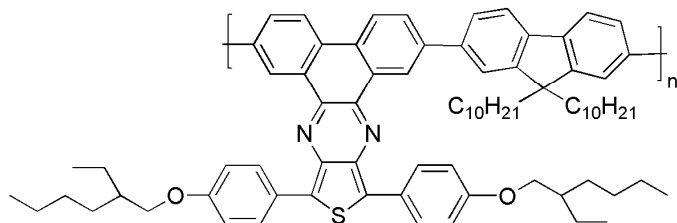P-14 (PM-31)
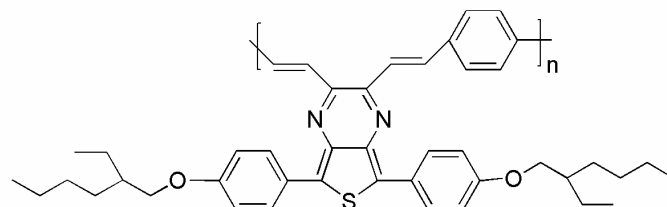
P-12 (PM-14)
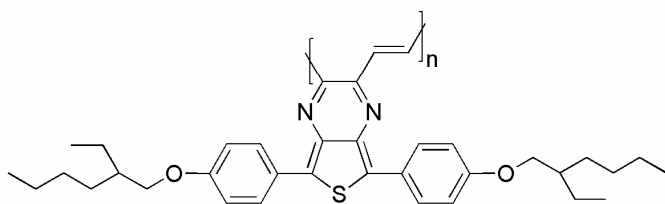
P-15 (PM-16)

P-16 (PM-15)

P-17 (PM-7)
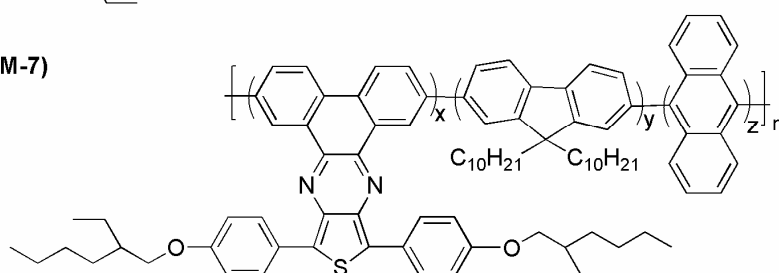
P-18 (PM-21) X=25, Y=50, Z=25
P-19 (PM-22) X=25, Y=50, Z=25

7.3   Abbreviations

BuLi	Butyl lithium
$CDCl_3$	Deutrated chloroform
$CHCl_3$	Chloroform
CuI	Copper(I)-iodide
CV	Cyclic voltammetry
DMF	Dimethyl formamide
DMSO	Dimethyl sulfoxide
DSC	Differential scanning calorimetry
E_g	Band gap energy
E_g opt.	Optical band gap energy
E_g ec	Electrochemical band gap energy
E_{ox}	Oxidation potential
E_{red}	Reduction potential
eV	Electron volt
ε	Molar absorption coefficient
Φ_{fl}	Quantum luminescence yield
g	Gram
GPC	Gel permeation chromatography
H_2O	Water
HOMO	Highest occupied molecular orbital (valence band)
K	Kelvin
K_2CO_3	Potassium carbonate
LUMO	Lowest unoccupied molecular orbital (conduction band)
OLEDs	Organic light emitting diodes
$LiPF_6$	Lithium hexafluoro phosphate
λ_{max}	Wavelength at maximum absorption
$\lambda_{0.1max}$	Wavelength at longer wave length
$\lambda_{max, em}$	Wavelength at maximum emission
m	Meta
mg	Milligram
MHz	Mega Hertz
mL	Milliliter

$\overline{M}_n$	Number-average molecular weight
$\overline{M}w$	Weight-average molecular weight
M.P.	Melting point
n	Number of repeating units in polymer
Na_2CO_3	Sodium Carbonate
NaOH	Sodium hydroxide
NMR	Nuclear magnetic resonance
o	ortho
p	para
PDI	Poly dispersity index
$\overline{P}n$	Number-average degree of polymerization
PAE	Poly(aryleneethynylene) and poly(heteroaryleneethynylene)
PL	Photoluminescence
ppm	Part per million
PPP	Poly(*para*-phenylene) and Poly(heterophenylene)
PPV	Poly(*para*-phenylenevinylene)
RT	Room temperature
TGA	Thermogravimetric analysis
T_g	Glass transition temperature
THF	Tetrahydrofuran
UV/Vis	Ultraviolet/visible
VPO	Vapour pressure osmometry

Curriculum Vitae

Personal Data

Name	Munazza Shahid
Date of Birth	26-01-1975
Place of Birth	Sargodha (Punjab)
Marital Status	Married
Nationality	Pakistani
Languages	English, Urdu, Punjabi, Deutsch

Qualifications

1990	S.S.C. (Secondary School Certificate)
1990-1992	H.S.S.C. (Higher Secondary School Certificate)
1993-1995	B.Sc. Punjab University, Pakistan
1996-1998	M.Sc. in Chemistry, Punjab University, Pakistan
1999-2001	M.Phil in Organic Chemistry (Synthesis and Characterization of Some Novel Amides and Related Compounds) Quaid-i-Azam University, Pakistan
07/2003-2006	Doktorandin, FSU-Jena, Germany

Jena, 22-08-2006   ....

                                                                                Munazza Shahid

List of Publications

1) Shahid, M.; Ashraf, R. S.; Klemm, E.; Sensfuss, S. "Synthesis and Properties of Novel Low Band Gap Thienopyrazine Based Poly(heteroarylenevinylene)s" *Macromolecules,* **2006**, accepted.

2) Ashraf, R. S.; Shahid, M.; Klemm, E.; Al-Ibrahim, M.; Sensfuss, S. "Thienopyrazine based low band gap poly(heteroaryleneethynylene)s for photovoltaic devices" *Macromol. Rapid Commun.* **2006**, 27, 1454.

3) Ashraf, R. S.; Hoppe, H.; Shahid, M.; Gobsch, G.; Sensfuss, S.; Klemm, E. "Synthesis and Properties of Fluorene based Polyheteroarylenes for Photovoltaic Devices" *J. Polym Sci: Part A: Polym Chem.* **2006**, DOI: 10.1002/pola.21645.

Poster Presentations

1) Raja Shahid Ashraf, Munazza Shahid, Elisabeth Klemm, Lars Blankenburg, Steffi Sensfuss, "Novel polyheteroaryleneethynylene)s for photovoltaic devices", *European Conference on Hybrid and Organic Solar Cells - ECHOS06*, Paris, France, **2006**.

2) Raja Shahid Ashraf, Harald Hoppe, Munazza Shahid, Gerhard Gobsch, Steffi Sensfuss, Elisabeth Klemm, "Synthesis and properties of polyheteroarylenes for photovoltaic devices", *Technologies for Polymer Electronics - TPE 06*, TITK Rudolstadt, Germany, **2006**.

3) Munazza Shahid, Raja Shahid Ashraf, Elisabeth Klemm, Lars Blankenburg, Steffi Sensfuss, "Synthesis and properties of thienopyrazine based novel low band gap poly(heteroarylenevinylene)s", *Technologies for Polymer Electronics - TPE 06*, TITK Rudolstadt, Germany, **2006**.

Patent

1. Verwendung von Thieno[3,4-b]pyrazin-Copolymeren und Verfahren zu deren Herstellung

   Erfinder: Elisabeth Klemm, Raja Shahid Ashraf, Munazza Shahid, Steffi Sensfuss, Maher Al-Ibrahim, Lars Blankenburg; (Registry number 10 2006 014172.5).

Acknowledgement

My name appearing alone on the first page of this work does not reflect the enormous contributions of the following individuals, both directly and indirectly, to the very existence of this manuscript. Most important is the thanks I owe to my supervisor, ***Prof. Dr. Elisabeth Klemm***, for her help and advice during the last three years. Her generous support allowed me to spend most of my time on research and also to travel to interesting conferences. She has always been willing to let me go my way, giving me a significant degree of freedom on my research. Her advice and suggestions were most valuable to understand the obtained results and to determine the next steps for the research presented in this thesis.

My experience in the laboratory has been particularly enriching due to several exceptional individuals willing to share their knowledge and time. I would like to thank all the students and post-doc that came and went throughout my Ph. D. for their brief friendships, which have made my time here in Germany an enjoyable and worthwhile experience. Special thanks go to *Cornila Bader, Kathrin Schmidt* and *Friedricke Kramer* for being great lab fellows. It had been an absolute pleasure to work with. They were always nice to talk whenever I had to cope with my German.

I ought to submit my thanks to *Dr. S. Sensfuss* who contributed to a great extent directly to the electrochemical and photovoltaic studies presented here.

I am much grateful to all coworkers of research group of the *Prof. Dr. Elisabeth Klemm* for their cooperation and moral support.

I am obliged to express my heart full thanks to *Frau G. Sentis* (UV/Vis measurements), *Dr. W. Günther* and *B. Friedrich* (NMR measurements), *E. Arnold* (GPC measurements), *H. Schönfeld* and *B. Lentvogt* (Elemental analysis), *J. Nowotny* (Photoluminescence and UV-Vis measurements), *Dr. E. Birkner* and *E. Kielmann* (fluorescence measurements), *A. Kuse* (electrochemistry), *Dr. Flammersheim* and *P. Weiß* (DSC measurements) and our secretary *R. Klausnitzer* for their cooperation and help.

I extend my cordial thanks to my dear friends, who remember me in their prayers and hearts.

Finally, my appreciation goes to my family for the love I was always surrounded with.

I want to thank my husband, ***Shahid***. His love and support helped me tremendously. I could always count on his cheering me up during the frustrating times that are inevitable during the long process of getting your Ph.D. He encourages me to discover my potential and make the most of it; he is always there when I need him. Without that I never would have made it this far- your love is my greatest privilege. I owe my heartful gratitude to my *parents* -I love you

beyond words*,* my *parents in law* whose affection and prayers encourage me throughout my work, dear and precious brothers *Sarmad, Abrar, Nadeem, Mudassir, Israr, Shehzad* and *Shehbaz* who never cease to share love, understanding, advice, and support.

Selbständigkeitserklärung

Ich erkläre, dass ich die vorliegende Arbeit selbständig und nur unter Verwendung der angegebenen Hilfsmittel und Literatur angefertigt habe.

Jena, 22.08.2006   ....

                                                         Munazza Shahid